DEFORMATION OF THE PANNONIAN LITHOSPHERE AND RELATED TECTONIC TOPOGRAPHY: A DEPTH-TO-SURFACE ANALYSIS

Endre Dombrádi

UTRECHT STUDIES IN EARTH SCIENCES
No. 019

Members of the dissertation committee

Prof. Dr. J.-P. Brun	Université de Rennes 1, France
Prof. Dr. C. Faccenna	Università Roma Tre, Italy
Prof. Dr. F. Horváth	Eötvös University, Budapest, Hungary
Dr. E. Willingshofer	Utrecht University, The Netherlands
Prof. Dr. R. Wortel	Utrecht University, The Netherlands

The research on which thesis is based on was carried out at:

The Netherlands Research Centre for Integrated Solid Earth Science (ISES),
The Netherlands

Dept. of Geophysics and Space Sciences, Institute of Geography and Earth Sciences,
Eötvös University, Budapest, Hungary.

ISBN: 978-90-6266-304-0

Printed by Ipskamp Drukkers B.V., Amsterdam / Enschede

Cover: Topography of the Pannonian basin and the surrounding orogens (SRTM database) with the summary figure of the main results of 2D analogue tectonic experiments, modelling the folding of the weak lithosphere and its related subsidence and uplift pattern (Dombrádi et al., 2010).

Deformation of the Pannonian lithosphere and related tectonic topography: a depth-to-surface analysis

Deformatie van de lithosfeer onder het Pannoonse bekken

en zijn expressie in de tektonische topografie:

een analyse van de diepere aarde tot het aardoppervlak

(met een samenvatting in het Nederlands)

Proefschrift

ter verkrijging van de graad van doctor aan de Universiteit Utrecht op gezag van de rector magnificus, prof.dr. G.J. van der Zwaan, ingevolge het besluit van het college voor promoties in het openbaar te verdedigen op dinsdag 6 november 2012 des middags te 4.15 uur

door

Endre Dombrádi

geboren op 15 november 1979

Boedapest, Hongarije

Promotoren:	Prof. Dr. S.A.P.L. Cloetingh
	Prof. Dr. D. Sokoutis
Co-promotoren:	Dr. L. Matenco
	Dr. G. Bada

This thesis was accomplished with financial support from:

The Netherlands Research Centre for Integrated Solid Earth Sciences (ISES), The Netherlands

Hungarian National Science Fund (OTKA) project NK60445: "TECTOP-Hungary" conducted by the Dept. of Geophysics and Earth Sciences, Eötvös University, Budapest, Hungary

TABLE OF CONTENTS

Acknowledgement

It is late night again. One of the stolen hours these days dedicated to complete this thesis. Writing these lines marks the end of a long journey, though not a final destination. This journey consisted of several shorter and longer trips to the Netherlands. My persistent companion during these trips was an interesting research topic. These trips, however, offered a constant opportunity to have more and more companions throughout the whole journey, whom I can call friends. And last but not at all least, there is a third group of companions, who backed me from home. Now, it is time to thank all of you for being my companion. In doing so, I try to recall some memorable moments that we shared.

First of all, I would like to thank my promotors and co-promotors for making this research become reality, eventually formulated in this very thesis: Prof. Dr. Sierd Cloetingh, Prof. Dr. Dimitrios Sokoutis, Dr. Liviu Matenco and Dr. Gábor Bada.

In a strict chronological order from my perspective it all started with Gábor. After some easy talks in the kitchen of the Dept. of Geophysics in Budapest he proposed that I could do my PhD studies in the Netherlands instead of flying overseas. I admit I liked the idea very much. Our collaboration and friendship dates back to this decision point and has been continuous. Though in a different working environment, we keep on doing so. Thank you, Gábor.

My first meeting with Sierd was in Budapest, at the TOPO-EUROPE kick-off meeting. Ever since, you have given me tremendous support, guidance and motivation. You were always open for discussion, even in not the most conventional environments for scientific discussion. I wish that you find a new Pannonian guy soon. Thank you, Sierd.

Soon I met Liviu. You were among of the first ones, who helped me to find my way in a new environment in Amsterdam. You were standing by me in both good and hard times. I could always turn to you with my questions; let it be on the Carpathians or about everyday life. Thank you, Liviu.

It was a great moment when I was introduced to the General of the TecLab, Dimi. I have not only learned the ins and outs of analogue modelling under your command but spent a jolly, great time together. Often during the weekends we found themselves bending over a model, trying to find out what it wants to say. Yes, I know... Thank you, Dimi.

I have to express my gratitude to the members of the reading committee, who have dedicated time and attention to read the thesis and made suggestions to improve it: Prof. Dr. Jean-Pierre Brun, Prof. Dr. Claudio Faccenna, Prof. Dr. Frank Horváth, Dr. Ernst Willingshofer and Prof. Dr. Rinus Wortel.

During my stays in Amsterdam and now in Utrecht, I got to know many people at or around the Tectonics Dept. I do thank you all for your friendship, help (in various ways), or simply the great time we had together: Anna, Ernst, Fred, Anco, Ron, Giovanni, Randell, Ronald, Marlies, Magdala, Karen, Maarten, Erik, Susan, Arno, Nico, Jeroen, Sandra, Diana, Andrei, Stefan, Javier, John, Tadashi, Nynke, Andrea, Melody, Mohammed, David, Marten, Ward, Inge, yet another Andrea, Ioan, Elisa and all of you whom I have forgotten to mention... I will never forget the big table soccer tournaments after lunch.

During the thesis and defence preparation I received great help from Utrecht University as well. I thank Ria van der Linden, Jacqueline Landsheer and Margot Stoete for shepherding me through the administrative machinery.

I am indebted to the staff at the Dept. of Geophysics in Budapest for the beautiful 5 years we could spend together as colleagues and friends. I thank all of you. Special thanks to Frank, who involved me into fantastic research topics since I was a student and started my career. And for all the inspiring discussions over a glass of nice wine.

I also have to thank my colleagues and friends at Falcon-TXM, who helped me and let me finish this thesis.

I am grateful to my parents, who, since my early childhood, always helped and encouraged me to achieve my goal to become an astronomer and were not too disappointed when I eventually ended up as a geophysicist. Thank you for all your support.

Finally, I thank my Love, Ágica and our daughter, Zsófi for their continuous love throughout these years, which was the most solid background that I could wish. I dedicate this thesis to you.

Here comes the B part...

Summary

The Pannonian-Carpathian region has always been at the forefront of tectonic studies. The concept of tectonic topography (i.e. the manifestation of tectonic processes on the surface) has been recognised and investigated in this area at an early stage. The importance of recent crustal deformation, substantial differential vertical movements and neotectonic processes that have taken place during the Late Neogene-Quaternary has previously been demonstrated. Better understanding the 3D deformation pattern of the Pannonian basin in space and time is obviously an essential component to reconstruct related landscape evolution.

The investigations discussed in this thesis follow a depth-to-surface approach.

First, the focus was on the large-scale characteristics of differential vertical movements, directly linked to the deformation of the Pannonian lithosphere being under Pliocene to recent compression. The back-arc lithosphere beneath the Pannonian basin has been extended, significantly stretched and heated up during the Miocene and, thus became extremely weak from a rheological point of view. From Pliocene times onward the rheologically stratified, i.e. "crème brûlée" type of lithosphere (with strength concentrated in the upper crust) has been subject to compressional stresses and, albeit at low strain rate, continuously shortened. Field data and numerical models suggested lithospheric folding as a primary mode of intraplate deformation resulting co-existence of subsiding and uplifting areas. Complementing previous studies and addressing new perspectives, analogue tectonic models were performed, which enabled simulation of the physical properties of the Pannonian lithosphere under laboratory conditions. These targeted to record the style of deformation under various boundary conditions, starting with simple set-ups and moving towards more complicated scenarios. The experiments gave insight into the mode of intraplate deformation during the Quaternary uplift and subsidence history of the Pannonian basin. Spatial and temporal changes in topography were recorded, analysed, quantified and compared to field data for model validation.

The model results support that far-field tectonic and gravitational stresses could trigger folding of the low-strength Pannonian lithosphere. The amplitude of folding was comparable to the order of the observed amount of Pliocene-Quaternary subsidence and uplift. The dominant wavelength of folding was ~400 km in all experiments. However, shorter wavelength modes of folding were also detected and found to be amplified by initial thickness variations of the brittle crust. This multi-wavelength behaviour of the folding is in line with geological data and recent numerical predictions. It also emphasises that the uneven basement morphology, generated by the heterogeneous Miocene extension of the basin, played a dominant role in the subsequent deformation of the basin.

3D analogue models shed light on the strain partitioning between lithospheric folding and activation of strike-slip zones in the upper crust. Horizontal shortening was absorbed by the folding of the ductile lithosphere and distributed among multiple shear zones. As a

consequence of the "crème brûlée" rheological structure, the low strain rate and the number of fault zones, the individual seismoactive surface is reduced and only low slip rates can occur. These observations readily explain the recorded low seismicity in the basin interior.

The 2D and 3D analogue models gave an independent verification of the concept that folding of the weak Pannonian lithosphere controls basin inversion and moulds topography.

Surface and shallow subsurface expressions of the folding are presented in a case study from the western part of the basin, where inversion has the most pronounced imprints on the landscape. Various theories have been put forward for the origin of topographic highs and lows in this region. This particular series of investigations focused on landforms that had originally been thought to be pre-defined by brittle tectonics. The main scientific question addressed here was to what extent (neo)tectonic processes have controlled the investigated morphologic features and in how far other forces, mainly climate related, have contributed to their formation.

In doing so, a discussion on the various hypotheses is presented, including the latest neotectonic analyses around Lake Balaton. This is followed by a case study, which focuses on a ridge-and-valley system in southwestern Hungary, where subsurface data were hitherto very sparse. To this aim, previous concepts, mainly based on geomorphologic reasoning, put forward to explain the formation of the topographic highs and lows, were tested with shallow geophysical data.

Revision of the hypotheses was accomplished by the interpretation of high-resolution, near-surface geophysical data that have proven to be particularly advantageous in this context. Geophysical imaging of the sub-surface provided further evidence for the folding of young deposits on a more local scale. In addition, instead of the long-lived scientific concept of fault control, a combination of aeolian erosion and small-scale folding was found to play a key role in the formation of the analysed morphology.

Finally, a geomorphologic and geostatistical approach is presented. Rivers and streams are elements of the surface that are sensitive recorders of differences in subsidence or uplift rates. The effects of crustal movements on drainage network development were investigated in a feasibility study. The catchment area of the Carpathian hinterland was analysed by means of various fractal measures. The results evidenced that stochastic behaviour of erosional processes has been overprinted by alterations related to differences in the uplift history. Fractal dimensions reflected trends that correlated to different amounts of uplift. The results demonstrated that the fractal properties of the drainage, combined with other morphologic tools, can be an effective proxy to extract tectonic imprints on the surface.

In summary, a close relationship between lithospheric to crustal deformation and surface processes has been established affecting many aspects of the Pliocene to recent evolution of the Pannonian basin system.

Samenvatting

Het Pannoonse bekken en de Carpaten boog zijn altijd een belangrijk onderwerp geweest van tektonisch onderzoek. In dit gebied werd het concept van tektonische topografie – de manifestatie van tektonische processen aan het aardoppervlak – al vroeg onderkend en onderzocht. Het belang van recente korstdeformatie, substantiële variaties in verticale bewegingen en neotektonische processen tijdens het laat Neogeen-Kwartair zijn inmiddels aangetoond. Om de topografische evolutie van het Pannoons bekken te reconstrueren is een beter begrip van het 3D deformatie patroon, zowel in ruimte als tijd, noodzakelijk.

In het in dit proefschrift presenteerde onderzoek wordt telkens een benadering gevolgd vanuit de diepte naar het aardoppervlak.

De focus van dit onderzoek ligt in eerste instantie op grootschalige karakteristieken van de variaties in verticale bewegingen van de lithosfeer. Deze verticale bewegingen zijn direct gekoppeld aan de deformatie van de Pannoonse lithosfeer, die sinds het Plioceen onder horizontale compressie staat. Voorafgaand aan deze fase, heeft de lithosfeer onder het Pannoonse bekken tijdens het Mioceen extensie ondergaan. Daarbij is de lithosfeer sterk opgerekt, verdund en opgewarmd, met als gevolg dat deze, rheologisch gezien, extreem zwak is geworden. Sinds het Plioceen is de rheologisch gelaagde "crème brûlée" type lithosfeer met zijn sterkte geconcentreerd in de bovenkorst, onderworpen aan compressie en met een lage vervormingsnelheid continu verkort. Veldgegevens en numerieke modellen suggereren dat plooiing van de lithosfeer het primaire mechanisme is van intraplaat deformatie, hetgeen resulteert in het naast elkaar bestaan van gebieden met bodemdaling en opheffing. In aanvulling op voorgaande studies en om nieuwe inzichten te onderzoeken, zijn analoge tektonische modellen gemaakt die het simuleren van de fysische eigenschappen van de Pannoonse lithosfeer onder laboratorium condities mogelijk maken. Met deze modellen kan de wijze van vervorming onder verschillende randvoorwaarden – van simpele opstellingen tot complexe scenario's – gekwantificeerd worden. De experimenten geven inzicht in de rol van intraplaatdeformatie bij de opheffing en bodemdaling in het Pannoonse bekken tijdens het Plioceen-Kwartair. Om de modellen te kunnen valideren werden veranderingen in topografie -zowel in ruimte als in tijd- gemeten, geanalyseerd, gekwantificeerd en vergeleken met veldgegevens.

De resultaten van deze modelstudie ondersteunen de hypothese dat tektonisch geinduceerde spanningen en het effect van topografie op het spanningveld plooiing in de Pannoonse lithosfeer kunnen veroorzaken. De orde van grootte van de amplitude van de plooiing is vergelijkbaar met de geschatte hoeveelheid bodemdaling en opheffing in het Plioceen-Kwartair. De dominante golflengte van de lithosfeerplooiing was ~400km in alle experimenten. Daarnaast zijn ook kortere golflengten van de plooiing waargenomen. Deze werden versterkt door variaties in de initiële dikte van de brosse korst. De plooiing met meerdere golflengten is consistent met geologische gegevens en recente numerieke voorspellingen. Dit benadrukt verder dat de ongelijkmatige morfologie van de basis van het

sedimentaire bekken systeem, ontstaan door de heterogene extensie van het bekken, een overheersende rol in de daaropvolgende deformatie van het bekken heeft gespeeld.

Analoge 3D modellen versschaffen nieuwe inzichten in de verdeling van de vervorming tussen lithosferische plooiing en de activering van zones met laterale verschuivingen in de bovenkorst. Horizontale verkorting wordt opgevangen door de plooiing van de ductiele lithosfeer en verdeeld over meerdere schuifzones. Ten gevolge van de "crème brûlée" structuur, de lage vervormingsnelheid en het grote aantal breukzones wordt het individuele seismisch actieve oppervlak verkleind zodat alleen nog lage schuifsnelheden kunnen voorkomen. Dit verklaart tevens de lage seismiciteit in het centrale deel van het Pannoonse bekken.

Dat plooiing van de zwakke Pannoonse lithosfeer de inversie en de topografie in het bekken beheerst, is onafhankelijk bevestigd door de 2D en 3D analoge modellen.

Voorbeelden van plooiingen aan de oppervlakte en op geringe diepte worden in een detail studie van het westelijk deel van het bekken gepresenteerd. Hier heeft de inversie namelijk de duidelijkste sporen in het landschap achtergelaten. Er zijn in het verleden verschillende theorieën geponeerd over de herkomst van de differentiele topografie in deze regio. De hier gepresenteerde serie onderzoeken concentreert zich op morfologieën waarvan men aanvankelijk dacht dat ze door brosse tektoniek bepaald zijn. De hoofdvraag is tot op welke hoogte (neo)tektonische processen de onderzochte morfologische kenmerken hebben bepaald en in hoeverre andere, voornamelijk klimaatgerelateerde, processen een bijdrage hebben geleverd aan hun vorming.

Hierbij zijn verschillende hypothesen in aanmerking genomen, waaronder inzichten vanuit de meest recente neotektonische analyses rond het Balatonmeer. Vervolgens is er een detail studie gepresenteerd van een topografisch systeem in zuidwest Hongarije, waar tot nu toe weinig gegevens over de structuur onder het aardoppervlak beschikbaar waren. Oudere hypothesen hadden tot doel de topografische verschillen te verklaren en waren voornamelijk gebaseerd op geomorfologische aspecten. Deze concepten zijn in deze studie getest met gebruik making van ondiepe geofysische gegevens.

Herziening van deze hypothesen is mogelijk gemaakt door de interpretatie van hoge resolutie geofysische gegevens van de structuur dicht onder het oppervlak, die uitstekend geschikt bleken voor dit doel. Het geofysisch in kaart brengen van de ondergrond leverde ook evidentie voor het plooiien op lokale schaal van jonge afzettingen. Daarnaast is aangetoond dat een combinatie van eolische erosie en kleinschalige plooiing een sleutelrol speelt in het ontstaan van de geanalyseerde morfologie, in plaats van het tot dusverre gangbare idee dat deze door breuken bepaald wordt.

Tot slot volgt een discussie over de geomorfologische en geostatistische analyse van afwatering systemen. Bodemdaling en opheffing worden geregistreerd door rivieren en beken aan het aardoppervlak. Deze effecten van korstbewegingen op de ontwikkeling van

het afwaterings netwerk zijn onderzocht in een haalbaarheidsonderzoek. Het stroomgebied van het achterland van de Carpaten boog is geanalyseerd door middel van een aantal fractale methoden. Dit liet zien dat het signaal van wijzigingen ten gevolge van verschillen in opheffingsgeschiedenis gesuperponeerd wordt op het stochastische signaal van erosieprocessen. Fractale dimensies weerspiegelen trends die correleren met verschillende hoeveelheden opheffing. Deze resultaten tonen aan dat fractale eigenschappen van het stroomgebied, samen met andere geomorfologische gegevens, een bruikbare indicator kunnen geven voor het herkennen van tektonische bijdragen aan de morfologie van het aardoppervlak.

Kort samengevat, een aantal nieuwe aspecten van de evolutie van het Pannoonse bekken systeem bevestigen de nauwe verbinding tussen deformatie van de lithosfeer en de korst enerzijds en oppervlakte processen anderzijds.

Chapter 1

Introduction

1.1 Tectonic topography in the Carpathian-Pannonian region

Tectonic topography is a collective term for landscape development that is controlled by tectonic processes. Fingerprints of deep-seated and usually large-scale deformation mechanisms and lithosphere dynamics are often recognised on the surface as well. Beyond climatic effects, these geologic factors can profoundly influence topographic evolution, drainage organisation and mass transport, which in turn entail various aspects of natural hazard concerns. The importance of linking processes acting on various scales ranging from deep lithospheric ones to those moulding the topography has been addressed in numerous research projects and studies. Elements of the complex interaction within this multi-scale geologic environment have already been revealed and investigated in a great number of natural laboratories. Successful application of such an approach demands interdisciplinary research efforts (see Topo-Europe research programme, Cloetingh et al., 2007). Albeit, vast datasets have been utilised from various fields of earth sciences and an arsenal of methodologies, research techniques and modelling tools have been employed, there is still room for more process-oriented as well as site-related studies in the framework of tectonic topography research.

Results obtained so far have demonstrated the importance of recent crustal deformation, substantial differential vertical movements and neotectonic processes that have taken place during the late-stage (Late Neogene-Quaternary) evolution of the Pannonian-Carpathian region. Horváth and Cloetingh (1996) established the importance of Late Pliocene through Quaternary compression in the Carpathians–Pannonian system, explaining its anomalous Quaternary uplift and subsidence pattern by lithospheric folding.

Bada et al. (2007) presented a compilation of present-day stress data within the Pannonian basin and the surrounding orogens (i.e., Alps and Dinarides). Through utilisation of direct stress field measurements and inversion of earthquake focal mechanisms the horizontal stress field has been reconstructed and the lateral changes in the tectonic regimes mapped. Primary source of the compressional stresses acting on the Pannonian basin and controlling the basin inversion was found to be the counterclockwise rotation of the Adriatic microplate. In addition, lateral extrusion of crustal flakes from the axis of the Alpine orogen has a significant role in the stress and strain pattern, particularly in the western Pannonian basin.

A great number of studies discussing the coupling between lithospheric and surface processes at various locations within the Pannonian-Carpathian is available (see review in Cloetingh et al. 2005a). These data provided direct and reliable link between lithospheric and surface processes on various scales.

Utilising outcrop studies, interpretation of industrial seismic sections with borehole control and integrating topographic data Fodor et al. (2005) demonstrated that the reactivation of inherited Miocene structures plays a significant role in the evolution of landforms and drainage systems in the central and western part of the Pannonian basin. Typical structures controlling landscape development were found to be folds, blind reverse faults and transpressional strike-slip faults. Their review also underlined that the tectonic origin of morphologic features showing strikingly linear configuration in many cases cannot be proven.

Microtectonic, morphotectonic and sedimentary analyses of outcrops south of Lake Balaton in the area of Somogy hills, western Hungary again suggested a compressionally active neotectonics (Magyari et al., 2005). Three distinct compressional events with alternating stress field could be detected by the field observations. These events manifested in folds and fold related faulting as well as tens or hundred metres offset strike-slip faults. The identified three phases of compression had a detectable impact on the spatial arrangement of the valleys and low-altitude crests in the Somogy hills. The structures observed on outcrop- and micro-scale could directly be connected with the underlying subsurface structures. Interpreted seismic lines constrained by data from hydrocarbon exploration wells revealed reactivated antiformal sedimentary packages above thrust faults and flower structures in this hilly landscape (Csontos et al., 2005). The Late Miocene basin fill covering the entire study area was found to be heavily folded. The Quaternary stress directions deduced from outcrop deformation pattern coincided with the main directions of shortening directions derived from structural seismic interpretation.

By means of the integration of shallow geological and deep geophysical data the late stage evolution of the SE Carpathian foreland has been studied (Matenco et al., 2007). Two major deformation phases have been inferred affecting the evolution of the region. The late Miocene-Pliocene subsidence and subsequent Quaternary folding is an interplay of the pull-down of the slab beneath the Carpathian chain and the inversion of the whole Carpathian-Pannonian systems. These processes generated pronounced vertical and horizontal movements, which are reflected by the basin architecture, the overlying topography and disequilibrium in the river network.

Qualitative as well as quantitative analyses of the Late Pliocene to Quaternary uplift have been done in several locations within the Pannonian-Carpathian region. In contrast with the quantification of subsidence by analysis of the basin fill sediments, uplifted areas are more difficult to study since most of the sediments have been eroded. The integration of geomorphologic markers and isotope geochemistry can provide important constraints in order to better assess the amount of uplift. Such studies have been elaborated in the central part of the Pannonian basin, in the Transdanubian Range (Ruszkiczay-Rüdiger et al., 2005a,b). Here river terrace levels and associated travertine deposits data were used to quantify the incision rates and in turn quantify the young tectonic processes. In the framework of the research, these geomorphologic indicators have been dated by

cosmogenic isotopes, which yielded remarkably consistent uplift rates for the last few hundred thousand years. Similar techniques were applied on cave rafts in the karst system of the Buda hills, in the direct vicinity of the city of Budapest and corroborated continuous uplift for the past 300,000 years (Szanyi et al., 2009). Geomorphologic and structural investigations of river terraces at the western flank of the Focsani basin, SE Carpathians, documented several episodes of uplift (Necea et al., 2005). Quantitative results of these works are presented in detail in Chapter 2.

1.2 Research objectives

Building on the available geological information on the tectonic topography of the Pannonian basin system the following research objectives are addressed in this thesis.

- The proposed lithospheric folding has been investigated by numerical models (Horváth & Cloetingh, 1996). The adjacent subsiding and uplifting areas generated by the models were in close correlation with field observations. However, they yielded only moderate amplitudes. Thus, an alternative modelling tool was selected to reconstruct the subsidence and uplift history of the Pannonian basin during the last 3.5 My. 2D analogue models utilised the down-scaled physical properties of the lithosphere and the geometric and kinematic boundary conditions. The simulations sought answer to the question whether the Pannonian lithosphere is indeed prone to folding and can explain the bulk of the Pleistocene-Quaternary vertical movements.
- 2D analogue models also concentrated at heterogeneities at the upper crustal level. These inherited structures were expected to control the major parameters of folding (i.e. wavelength and amplitude) and explain the existence of folding on various scales as documented by the field observations.
- 3D reconstructions were also done by means of the analogue tectonic models. These, on one hand, incorporated an additional source of compressional stresses exerted on the northern part of the basin and investigated its role in the development of the structures. Secondly, the strain partitioning between lithospheric folding and activation of multiple strike-slip zones was addressed.
- A number of recent geophysical data acquisition campaigns targeted to unravel the formation of various landforms in the western Pannonian basin. During the interpretation the main focus was set on the interaction of neotectonic (controlled by folding to a major extent) and surface processes. The ultimate aim was to better constrain the key factors contributing to the formation and evolution of these morphologic elements. The results were expected to provide important added value, particularly in an area where hitherto only limited geological information was available.

- Differences in the vertical crustal movements and related topographic boundary conditions may significantly alter the configuration of the drainage network. Having an extensive dataset on the streams and rivers draining the hinterland of the Carpathians, spatial indicators were sought by multidimensional fractal analysis that may reflect the changes in the uplift history of individual tectonic domains.

1.3 Thesis outline

Chapter 2 gives an extensive overview of the formation of the Pannonian basin and its late-stage (~Late Pleistocene-Quaternary) deformation history, which comprises the most recent concepts of basin evolution as well as enlists alternative explanations or questions yet unresolved. Our present knowledge on the physical properties of the lithosphere and the tectonic boundary conditions is summarised.

In Chapter 3 results of the analogue tectonic models are described, which aimed at simulating the behaviour of a mechanically extremely weak lithosphere and its control on basin inversion. In doing so, several parameters have been analysed including crustal and/or mantle heterogeneities, 3D configuration of tectonic blocks and role of crustal and mantle strength. Inferences derived from the models are discussed in the context of available information on lithosphere dynamics presented in Chapter 2 and related tectonic topography.

Carefully scaled 2D analogue experiments simulating the behaviour of the hot and weak Pannonian lithosphere demonstrated that far-field tectonic and additional gravitational stresses can trigger folding of the weak Pannonian lithosphere. In agreement with previous numerical studies and first-order vertical crustal motions in the area, folding with 400 km wavelength folding was inferred as the most dominant large-scale deformation. Geological and geophysical data, in addition to the result of numerical models, invoke the possibility of multi-wavelength mode of folding. These modes were confirmed by analogue experiments as well. The results indicate that the heterogeneous basement morphology after basin extension may account for the amplification of smaller wavelength deformations and the existence of irregular folds.

Principal sources of compression acting on the Pannonian basin were taken into account in 3D analogue tectonic models. Besides lithospheric folding, the change in the geometric boundary conditions resulted in strain localisation and thrust development with complex internal structure and additional shear components. Despite the simplified 3D set-up, the localised shortening controlled by the folding could directly be correlated to the natural laboratory. The pop-up systems that developed in the models are representative of the Quaternary evolution of the Dinaric orogen, the Sava fold belt and Transdanubia and the SW part of the Pannonian basin.

Quasi-3D conceptual models confirmed the possible co-activity of lithosphere folding and deformation along shear zones in the interior of the Pannonian basin. In spite of the simplifications in the model, a reasonable reconstruction of the first-order structural development of the natural prototype was achieved in terms of both brittle and ductile tectonics.

Chapter 4 presents a case study from the western part of the Pannonian basin, where basin inversion has the most pronounced imprints on the landscape. The investigation was focusing on landforms that have been associated with near-surface tectonic activity and/or their origin could not be determined unambiguously. The area provided an excellent opportunity to apply the recent inferences on the deformation mechanism and to observe the interplay with surface processes. Revision of the hypotheses on the formation of these morphologic elements has been accomplished by application of advanced, high-resolution geophysical data acquisition techniques and also by embedding the theories into the neotectonic framework of the inversion of the Pannonian basin system. The presented results illustrated how the overall folded character of Transdanubia is preserved by near surface sediments. The new findings underline the importance of aeolian processes overprinting the effects of small-scale folding in Transdanubia. The advantage of high-resolution geophysical methods examining the uppermost subsurface region was also well demonstrated.

Chapter 5 focuses on the effects of differential vertical crustal movements on the self-organisation of drainage networks. The spatial organisation of drainage networks due to differential vertical crustal movements was investigated. The catchment area, which comprised the Apuseni Mts., Transylvanian basin and the western margin of the Eastern Carpathians, was analysed by fractal dimension estimators. In the form of a kind of feasibility study, description and applicability of various multi-scale parameterisation approaches are given. The set of fractal measures was then correlated to the differences in the uplift history of distinct tectonic domains.

Each selected method demonstrated a non-space filling spatial configuration of the river network, suggesting the influence of geological processes on drainage development. Comparison of the determined fractal dimensions and spectra showed coherent values for the streams draining the Transylvanian basin, while the adjacent mountain chains (Apuseni Mts. and Eastern Carpathians) exhibited slight, yet systematic deviations from these trends. Consequently, stochastic behaviour of erosional processes has been overprinted by alterations related to crustal deformation to such an extent, which is detectable in the spatial organisation of the drainage network. Differences in the bedrock lithology have been found to play only a secondary role and, thus, areal variations in the multifractal dimensions reflect the varying rates of surface uplift independent of the types of rocks exposed on the surface.

Chapter 6 is the synthesis of the entire depth-to-surface analysis. Major inferences on the interaction of lithosphere dynamics, crustal- and basin-scale tectonics and topography development are highlighted and summarised and a forward look is given.

Chapter 2

Formation and deformation of the Pannonian basin: tectonic setting, deformation pattern and observational data[1]

2.1 Formation of the back-arc type Pannonian basin

The Pannonian basin, one of the hottest basins in continental Europe, is surrounded by the Alpine, Dinaric and Carpathian mountain belts (*Fig. 2.1*). The formation and extension of this back-arc basin commenced in Early Miocene times (~20 Ma, Horváth, 1993). Collision between Adria and the European continent led to the gravitational instability and eventually collapse of the eastern Alpine orogen and induced lateral, E-NE directed, extrusion of crustal blocks (Horváth, 1988; Ratschbacher et al., 1991; Tari et al., 1999, Horváth et al., 2006a). The extrusion and extension was facilitated or actively governed by the coeval retreating subduction in the Carpathian realm (Royden & Horváth, 1988; Horváth, 1993; Bada & Horváth, 2001).

The ALCAPA (ALpine-CArpathian-PAnnonian) wedge of Alpine origin was directly driven by the lateral extrusion in response to the N-S oriented shortening in the Alpine orogen and made up the northern part of the Pannonian basement (Csontos & Nagymarosy, 1998, *Fig. 2.2*). The complex kinematic history of the southern unit, the Tisza-Dacia terrane was far less known (Csontos & Vörös, 2004). Paleomagnetic data (Márton, 2001) and structural analyses (Fodor et al., 1999) suggest strong deformation, rotation of the terranes during the Tertiary. Recent palinspastic reconstructions (Ustaszewski et al., 2008) corroborate that extension in the ALCAPA domain and shortening in the Carpathian thrust belt was not only coeval but the calculations of the restoration yield similar magnitudes. These results support the concept of the retreating Carpathian subduction zone causing extension in the Pannonian domain. For the ALCAPA and Tisza-Dacia blocks counter-clockwise and clockwise rotations were inferred, respectively. Rotation of ALCAPA appears to be controlled by the combined effect of slab retreat and its collision with the advancing and oppositely rotating Tisza-Dacia unit to the south. The authors also highlight that besides subduction rollback, rotation and northward translation of Adria could also act as a driving force on the complex kinematics of ALCAPA and Tisza-Dacia. By the Early Miocene, when the formation of the Pannonian basin started, however, the two terranes were already juxtaposed (Csontos et al., 1992). The present-day contact of the two blocks is marked by the Mid-Hungarian Shear Zone (see *Fig. 2.2*).

[1] The chapter is partly based on the book chapter: Horváth, F., Dombrádi, E., 2007. Interpretation of the Carpathian-Pannonian region from a plate tectonic perspective, *Geography of the Carpathian-Pannonian region*, Akadémiai Kiadó, Budapest, in press

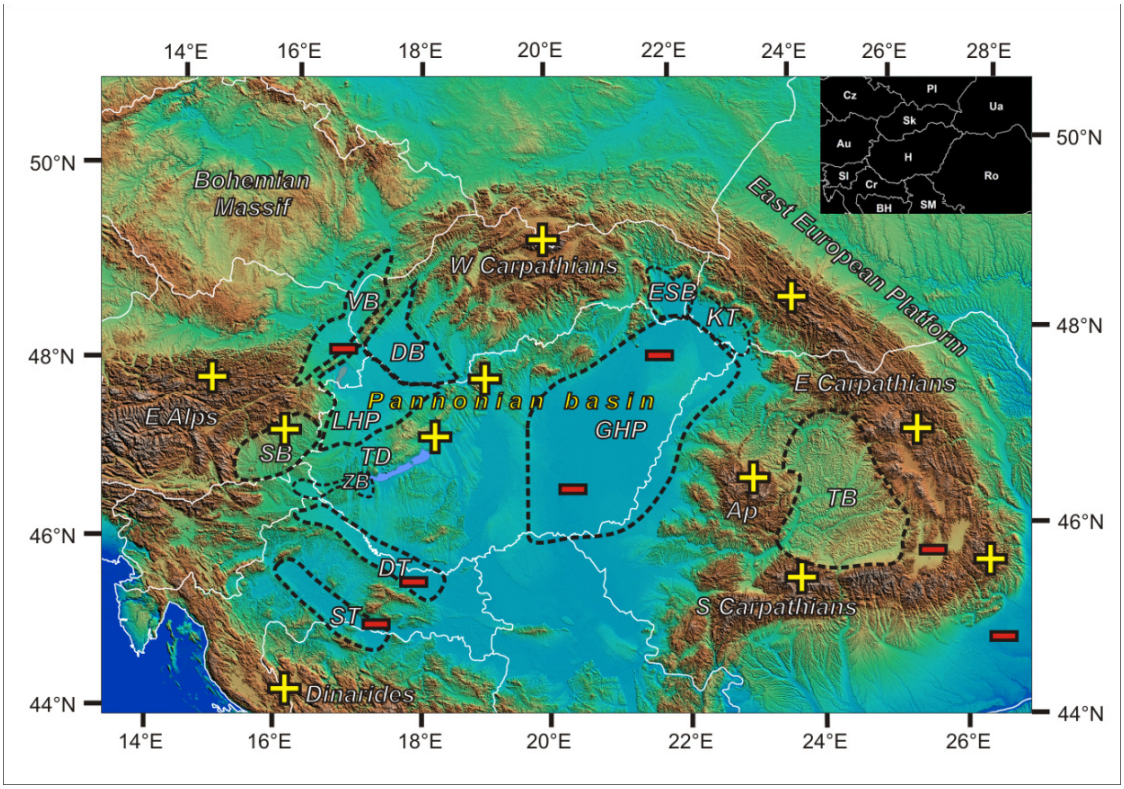

Figure 2.1 *Geographical setting of the Pannonian basin and the surrounding orogens. Digital elevation model was compiled using SRTM database. Black dashed lines contour major sub-basins within the region. The used abbreviations stand for as follow: VB=Vienna basin, DB=Danube basin, LHP=Little Hungarian Plain, SB=Styrian basin, TD=Transdanubian Range, ZB=Zala basin, DT=Drava trough, ST=Sava trough, GHP=Great Hungarian Plain, ESB=East Slovakian basin, KT=Kárpátalja trough, Ap=Apuseni Mts., TB=Transylvanian basin. Plus and minus signs illustrate trends of present-day vertical surface motions (uplift vs. subsidence, respectively) based on geodetic measurements, structural and stratigraphic interpretations of seismic sections, basin analysis results and complemented by data from isotope geochemistry methods. Top right inset map shows the political boundaries.*

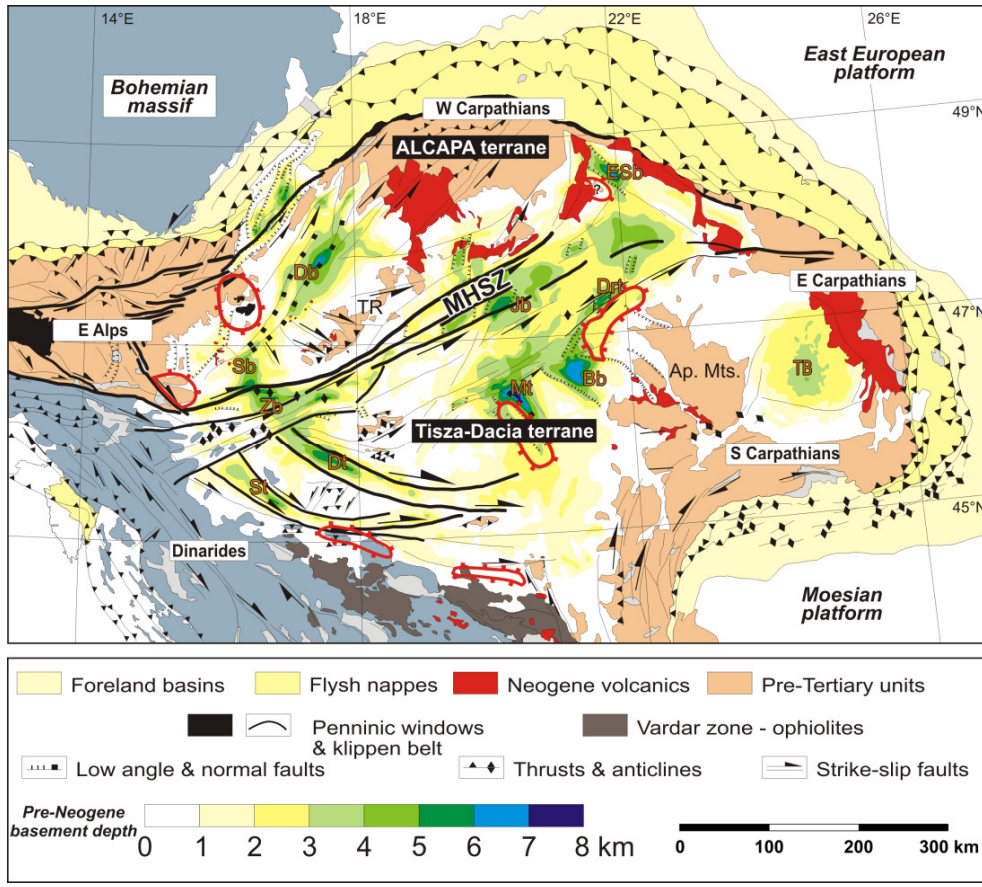

Figure 2.2 *Geodynamic setting of the Alpine-Pannonian-Carpathian region. The main structural elements are displayed on the map of Pre-Neogene basement depths. ALCAPA and Tisza-Dacia terranes are shown. Their contact zone is manifested in a wide shear zone, the Mid-Hungarian Shear Zone (MHSZ). Deepest troughs are also labelled. Db=Danube basin, Sb=Styrian basin, Zb=Zala basin, Dt=Drava trough, St=Sava trough, Mt=Makó trough, Bb=Békés basin, Drt=Derecske trough, Jb=Jászság basin, ESb=East Slovakian basin, TB=Transylvanian basin. Besides the tectonic elements, tectonic windows of the Alpine Tethys units (black spots), distribution of Neogene volcanic (red areas) and locations of identified metamorphic core complexes (red contours) are displayed on the map. After Horváth et al., 2006a.*

The Pannonian basin was amongst the first natural laboratories to test thermomechanical model of basin evolution (McKenzie, 1978; Royden & Horváth, 1988). Input data of the models comprised the lithological columns determined from hydrocarbon exploration wells and industrial seismic sections, surface heatflow values and constraints on the thickness of the crust and the lithosphere. According to the interpretation of this dataset, the initial phase of extension in the basin took place in the Early Miocene (Eggenburgian-Ottnangian), peaked during the Middle Miocene (Badenian) and finally the syn-rift sedimentation was gradually waning by the end of the Sarmatian. Hence, from Sarmatian times on, the Pannonian basin has entered the thermal, post-rift phase (*Fig. 2.3*). More recent studies relying on industrial data challenge these interpretations and put forward larger time-span and a more gradual manner of extension (e.g. Magyar et al., 2006; Matenco & Radivojević, 2012). Further development of these investigations may alter our

view on the general mechanism of extension allow more accurate reconstruction of the modes of extension and the subsequent post-rift evolution especially in the case of the Tisza-Dacia terrane. The following paragraphs therefore confine to the latest geodynamic synthesis on the Pannonian basin, which is certainly not exempt of open questions.

Concerning the thickness of accumulated sedimentary pile, the various sub-basins of the Alpine-Pannonian-Carpathian region exhibit profound differences. Basins located at the periphery of the Pannonian basin (e.g. Vienna basin, Transylvanian basin, *Fig. 2.1*) are filled with relatively thicker Karpatian-Sarmatian successions and limited thickness of Pannonian and younger sediments is observed. In addition, compared to the Pannonian sub-basins, the Vienna and Transylvanian basins are cold (50-70 mW/m^2 and 30-40 mW/m^2, respectively, Dövényi & Horváth, 1988). The surface heatflow values are below the continental average. The sub-basins in the interior of the Pannonian basin system (e.g. Little Hungarian Plain, Zala basin, Great Hungarian Plain, *Figs. 2.1 & 2.2*), however, are characterised by thick Pannonian and Pliocene to Quaternary sedimentary sequences and the surface heatflow (90-120 mW/m^2) exceeds the continental average in all cases.

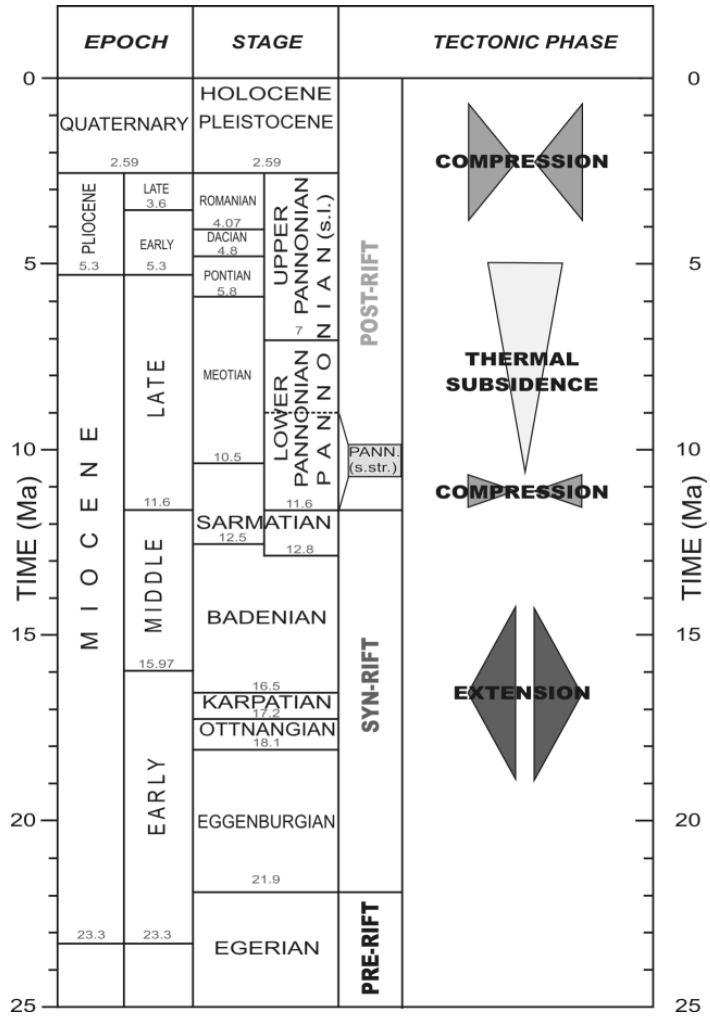

Figure 2.3 *Time chart of the syn-rift and post-rift evolution of the Pannonian basin and the major tectonic phases (modified after Horváth & Tari, 1999). For the sake of correlation, besides the units of standard international stratigraphic chart, the stages are shown both in Central and Eastern Paratethys terms. The boundaries of the stages in the latter case are after Vasiliev et al. (2004).*

The comparison of observed accumulation of sediments and the theoretical subsidence curves derived from thermomechanical model results made obvious that the concept of homogeneous extension cannot be applied to the basins in the interior of the Pannonian basin (Horváth et al., 1988). Considering the high heat flows, a crustal thinning factor larger than two should be concluded and in turn would demand a 9-11 km thick basin fill deposited dominantly in the initial syn-rift phase (see also Lenkey, 1999). It contradicts to the main observation on the sedimentary architecture of the basin-fill that is composed of only a few hundreds of metres of syn-rift and several kilometres of post-rift sediments.

The obvious contradiction could be resolved by implementing a heterogeneous extension model, which incorporated the extreme thinning of the lower lithosphere (δ=5-50, in certain cases vanishing of the entire mantle lithosphere, Horváth et al., 1988). The effects

of heterogeneous extension are also reflected by the present-day first-order inferences on morphology. Around the midmountains and inselbergs, the amount of crustal extension was not significant (β~1.0-1.2). In contrast, where deep basins (h>3 km) are located beneath the plains, extension had decreased the crustal thickness to almost the half of the original amount (β~1.6-2.0). At the flanks of the basin system, due to the vicinity of eroding source areas (particularly the continuously uplifting Carpathians), the depocentres provided sufficient accommodation space and were filled up by large amount of sediments during the syn-rift period, whereas the central sinks were practically 'starving basins'. These latter were characterised by gradually increasing water depth, which could reach or even excess 1000 m (Mattick et al., 1988) and their fill-up up took place during the post-rift subsidence phase by the Early Pliocene. Since the Pliocene times on, dominantly alluvial sediments accumulated in these basins, or in certain cases, erosion occurred.

Recently, an alternative mechanism for the extension of the Pannonian basin and simultaneous shortening and thrusting in the Carpathians has been put forward by Houseman and Gemmer (2007). This model proposes gravitational instability of the mantle lithosphere, which leads to the downwelling of the mantle lithosphere and its replacement by hot asthenospheric material. Presented numerical models provide an explanation for the existence of different stretching factors in the crust and the mantle. In addition, the arcuate shape of the Carpathian orogenic belt could be reconstructed by the models. However, to date this mechanism could not provide a satisfactory reconstruction for the complex kinematics of the tectonic blocks constituting the Pannonian basement. It is to be noted that the authors do not exclude the possibility of simultaneous subduction in certain parts of the Carpathian system.

As for the structural style of extensional basin evolution, the essential tectonic elements are the low angle, often listric normal faults, usually situated at the flank of the deep basins and the steeper normal fault planes (e.g. Horváth & Rumpler, 1984; Rumpler & Horváth, 1988, *Fig. 2.4*). In addition, strike-slip faults occur as transform faults, mostly concentrated in the contact zone of the ALCAPA and Tisza-Dacia terranes accommodating differential motion generated by the extension of the two terranes (see also *Fig. 2.7*). Transform faulting was also often accompanied by the formation of pull-apart basins.

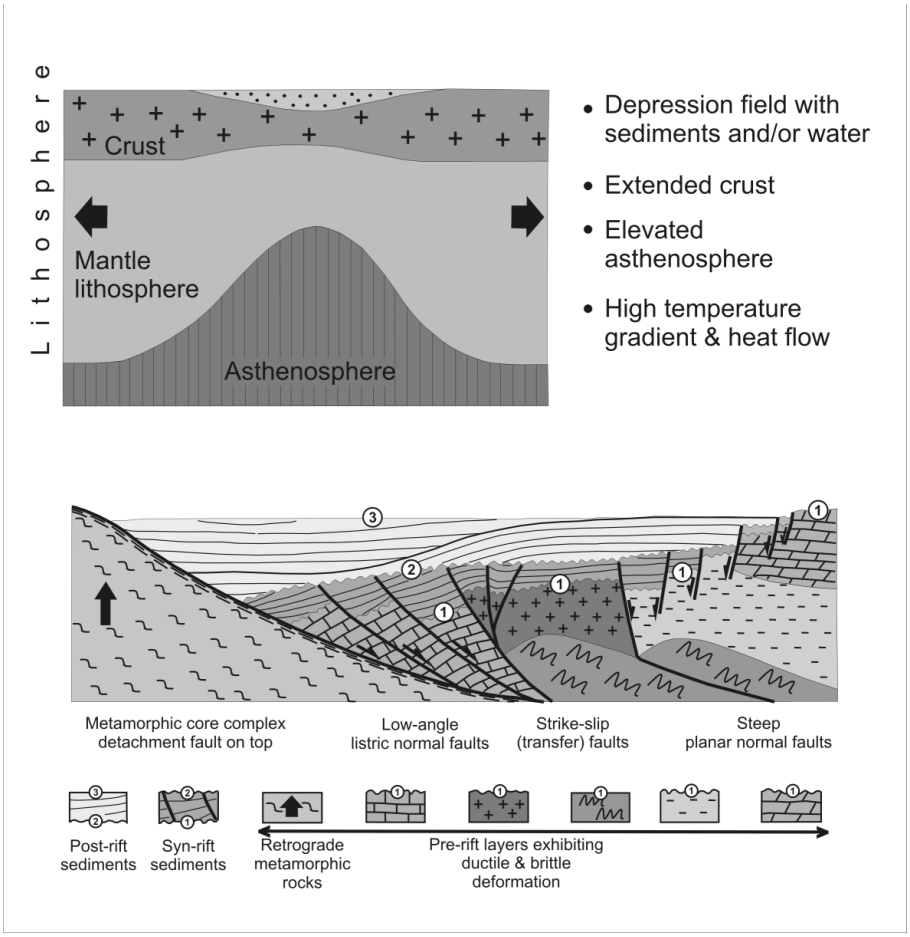

Figure 2.4 *Cartoon illustrating geodynamic setting after extension and the prime associated structural elements in the Pannonian basin. For further explanation see text (modified after Horváth, 2007).*

Understanding the mechanism of metamorphic core complexes has also contributed to the reconstruction of the evolution of Alpine and Pannonian region. Metamorphic core complexes characteristically consist of greenschist and amphiboltic rock domains with mylonitic fabrics that have undergone a retrograde metamorphosis (Crittenden et al., 1980; Lister et al., 1984). They are formed during extension due to the updoming of the ductile central part (10-20 km depth) of the continental crust. The overlying brittle crust is then fragmented and downthrown so that the metamorphic core is exhumed (Lister & Davies, 1989).

Thermochronological studies and structural analyses have corroborated that the tectonic windows of Alpine Tethys origin at the western margin of the Pannonian basin are metamorphic core complexes (Ratschbacher et al., 1990; Tari et al., 1992; Dunkl & Demény, 1997; Dunkl et al., 1998; *Fig. 2.2*). According to the measurements, green- and blueschist facies retrograde metamorphic rocks exposed in the Rohonc tectonic window (and smaller exposures in its vicinity) are originating from a 10-12 km depth and their fastest exhumation occurred in the Early Miocene (22-17 Ma). Beneath the basin fill in the

western Pannonian basin, brittle Austroalpine nappe units can be found that moved eastwards along detachment faults above the ductile Alpine Tethys block (Horváth, 1993).

Deep seismic data (Posgay et al., 1996; Tari et al., 1999; *Fig. 2.5*) in the basin interior revealed metamorphic blocks with structures that resembled core complexes buried by the Neogene basin fill (Horváth, 2007; *Fig. 2.2*). These metamorphic basement highs are accompanied by normal faults and non-metamorphic rocks (usually Mesozoic carbonates) in their footwalls. They are generally overlain by asymmetric lower and middle Miocene sedimentary strata. These areas provide excellent hydrocarbon reservoirs thus they have been well explored by boreholes. The detailed studies of these provinces in terms of the metamorphic evolution and structural development, mineralogy of fracture fills altogether corroborated that prior to Miocene times these present-day structural highs had been covered by thick series of Mesozoic sediments. In various hydrocarbon fields in the eastern part of the Great Hungarian Plain zircon fission track data put forward a middle Miocene age for the gradual exhumation (based on unpublished data and a summary given by Horváth et al. (2006b).

In summary, the prevalent style of extension in the Pannonian basin was rifting with transform faults connecting the various extended parts. In addition, build-up of metamorphic core complexes may have contributed to the extension.

The significant stretching of the lithosphere was accompanied (or according to some interpretations facilitated) by pronounced asthenospheric updoming. As a result, the hot and thinned lithosphere became extremely weak and prone to subsequent tectonic reactivation during the subsequent basin inversion (Cloetingh et al., 2005b; Bada et al., 2007a,b, *Fig. 2.6*).

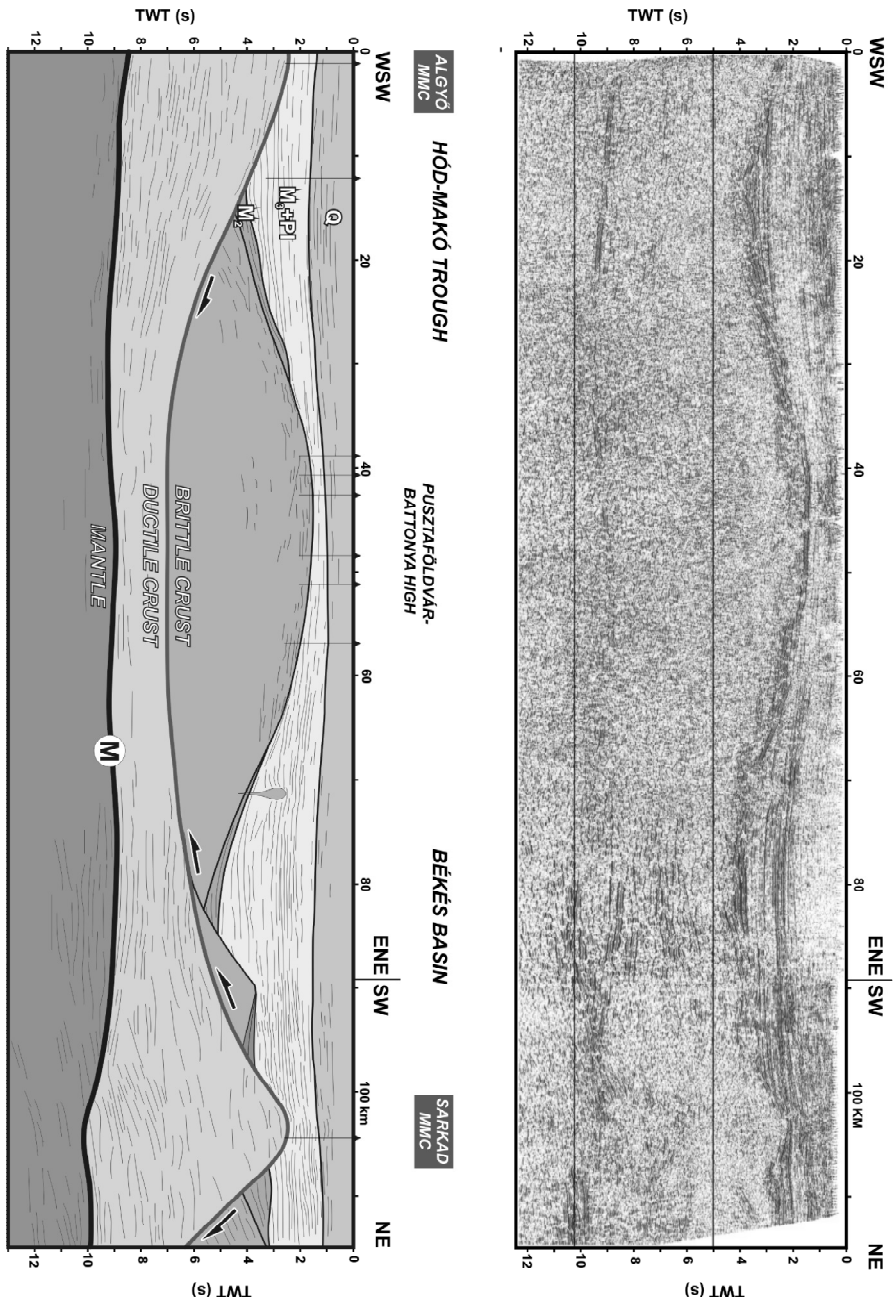

Figure 2.5 *Deep penetration reflection seismic section (PGT-4; modified after Posgay et al., 1996; Tari et al., 1999) that traverses the Great Hungarian Plain and its line drawing interpretation. Two metamorphic core complexes (MCC) can be identified according to the interpretation and supplementary unpublished thermochronological data (Horváth, 2007).*

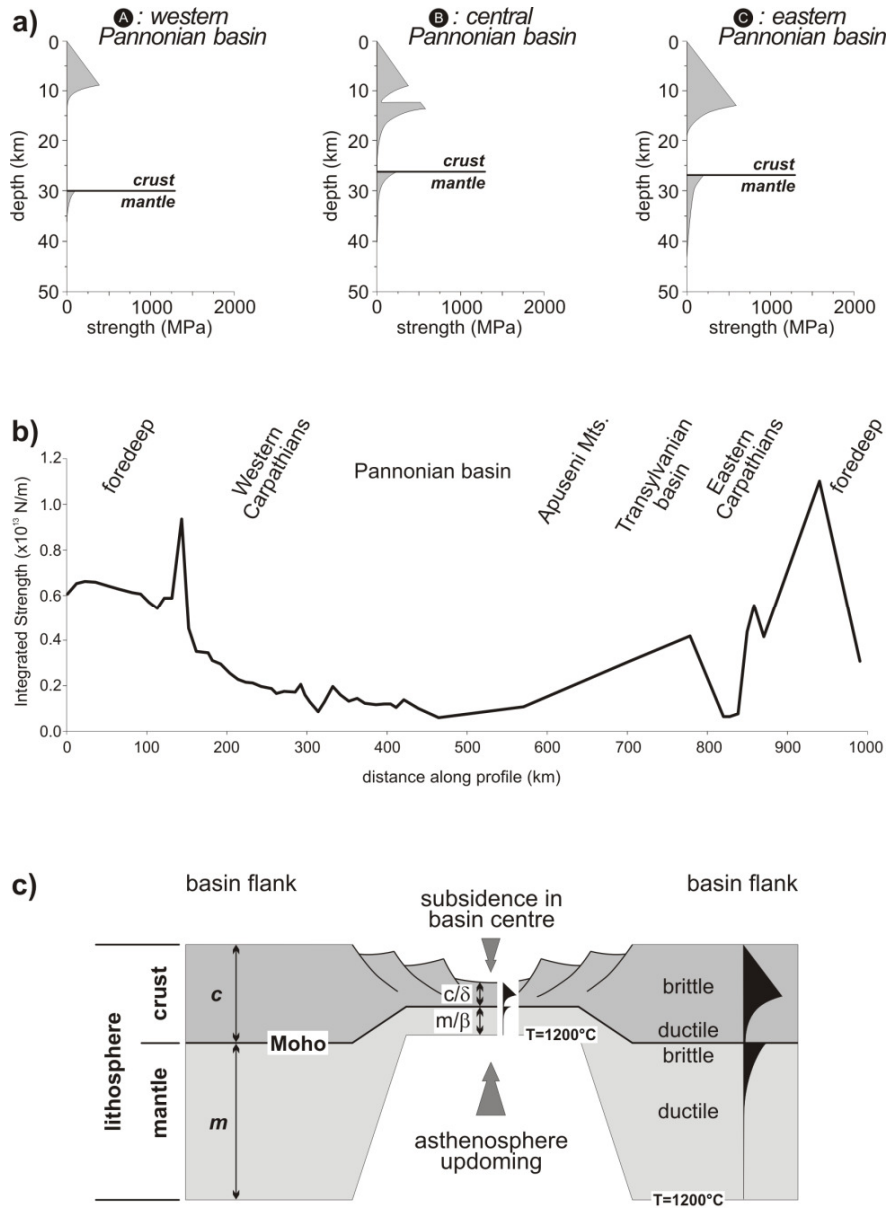

Figure 2.6 *a) Strength envelopes derived for the western (A), central (B) and eastern (C) part of the Pannonian basin based on lithospheric structure, heat flow, strain rate and stress regime data (Lankreijer et al., 1997; Sachsenhofer et al., 1997; Lenkey et al., 2002). b) Total integrated lithospheric strength (TIS) along a regional profile through the Pannonian–Carpathian system. c) Cartoon illustrating the heterogeneous stretching of the Pannonian lithosphere and its effect on rheology (Cloetingh et al., 2006).*

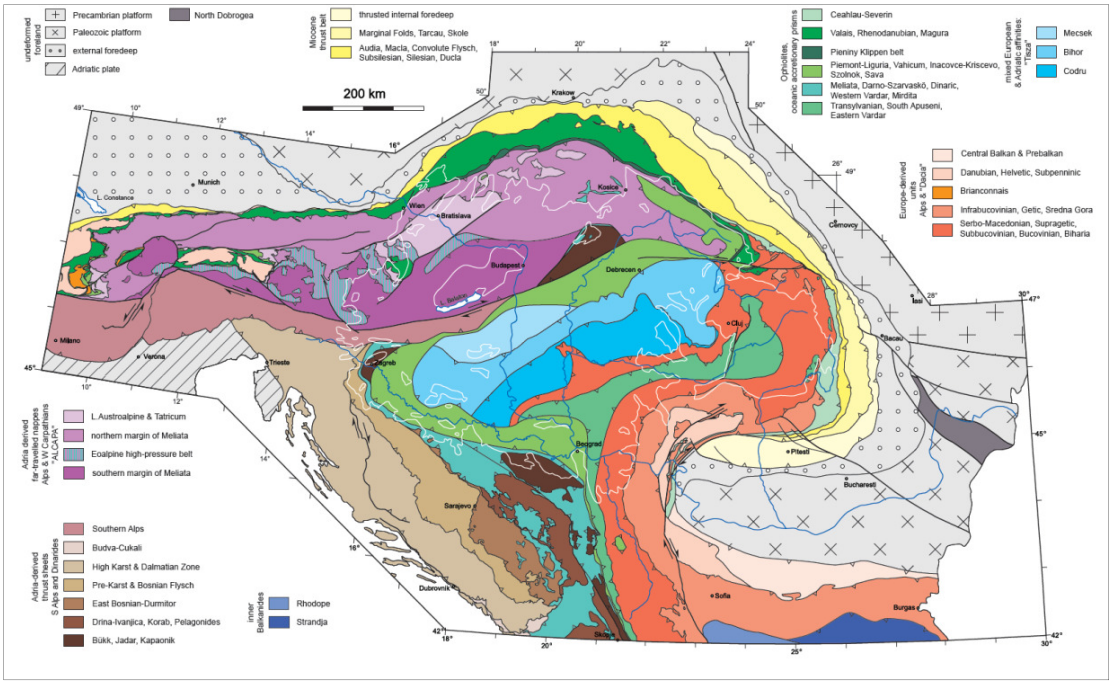

Figure 2.7 *Overview map of major tectonic units in the Alpine-Dinaridic-Pannonian-Carpathian realm (Schmid et al., 2008).*

2.2 Deformation of the Pannonian basin: Quaternary basin inversion

The structural development predicted by the extensional basin formation model proposed by Horváth et al. (1988) is in line with the results of seismic interpretation of the deep zones of the Little and Great Hungarian Plains (*Fig. 2.2*). Other localities in the Pannonian basin, particularly in the western part of the basin, however, display much more complicated geometries (*Figs. 2.8 & 2.9*). It is primarily manifested in the geometry of the synrift/postrift boundary that is often upwarped and according to stratigraphic interpretations, indicates remarkable stratigraphic hiatus. These basement highs are also characterised by the absence of Sarmatian sediments, locally, thickness of the Badenian deposits can also be restricted and the Lower Pannonian strata are neither fully evolved. These observations led to the conclusion that the Pannonian basin underwent a compressional event around the end of the Sarmatian (approximately 12 Ma), resulting in the inversion of the formerly extended halfgrabens (*Fig. 2.3*).

The basin has gradually entered another compressional phase during late Pliocene times (~3.5 Ma, *Fig. 2.3*) that is still ongoing and exhibits lateral as well as temporal changes across the basin system. This can be considered the neotectonic period of the basin evolution. Basin inversion is manifested in the sedimentary architecture of postrift sediments as well as in surface morphology. Significant thickness of Quaternary sediments (max. 1000 m) only occurs in the central part of the Great Hungarian Plain. On either side of it, hills and midmountains appear (the Transdanubian Range and Styrian basin to the west, and the Apuseni Mts. and the Transylvanian basin to the east) where only negligible amount or absolutely no Quaternary sediments are observed. This scenario can be explained by the continuous uplift and erosion of the present-day elevated terrains and coeval subsidence of the area of Little and Great Hungarian Plains in Pliocene to Quaternary times. These observed differential vertical crustal movements are due to gradual shift towards compressional stresses.

In general, basin inversion is related to changes in the regional stress field (Ziegler et al., 1995, 2002) from tension controlling basin formation and subsidence to compression resulting in contraction and flexure of the lithosphere, often associated with differential vertical movements. Such major changes in the stress fields from extension, governing Miocene basin formation, to compression, controlling Pliocene to Quaternary neotectonic deformation of the Pannonian basin have been recognised (Horváth & Cloetingh, 1996; Fodor et al., 1999; Bada et al., 2001, 2007a; Fodor et al., 2005; Horváth et al., 2006a).

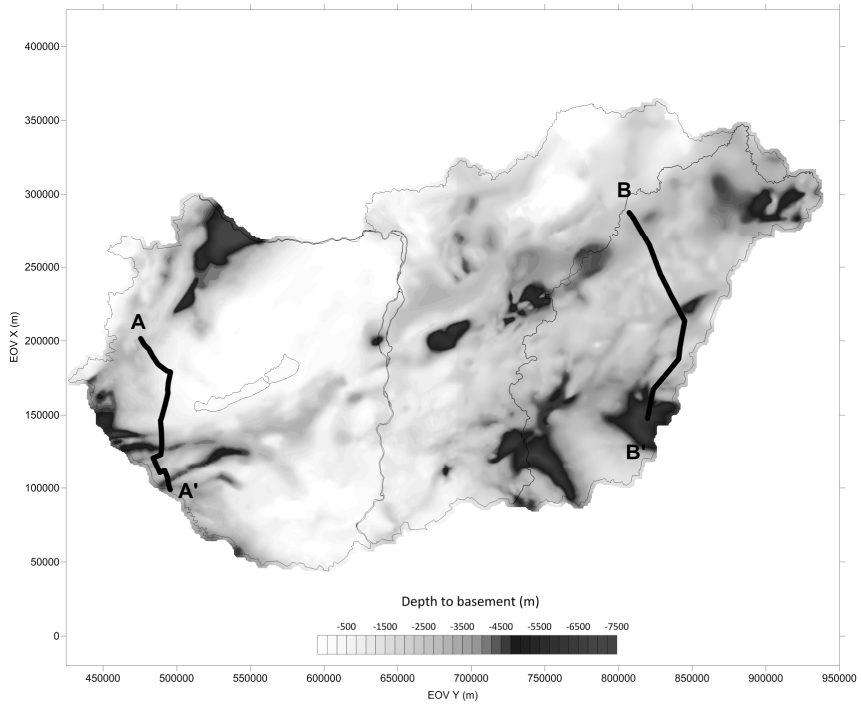

Figure 2.8 *Location map of regional scale composite reflection seismic sections to illustrate the effect of inversion on the architecture of syn- and post-rift sediments and tectonics. The greyscale shading indicates pre-Neogene basement depth values (see scale in metres).*

Figure 2.9 *a) Composite seismic line across the Transdanubian region (Fig. 2.8, AA'). The leftmost side of the section displays the metamorphic units related to the extension. Geometry of the unconformity between of syn- and post-rift sediments is indicative of inversion. In addition, erosional truncation of the post-rift sedimentary pile and intensive folding in the region of Zala basin can be observed. Note also the lateral thickness variation of the syn-rift deposits. b) The seismic section from the Great Hungarian Plain (Fig. 2.8, BB') reveals thick postrift deposits evidencing continuous subsidence. However, areas subjected to multiple uplift events can also be identified (see architecture of sedimentary infill). An example of the typical strike-slip neotectonic (sometimes even active) faults bordering the Derecske trough is also imaged (central part of the section).*

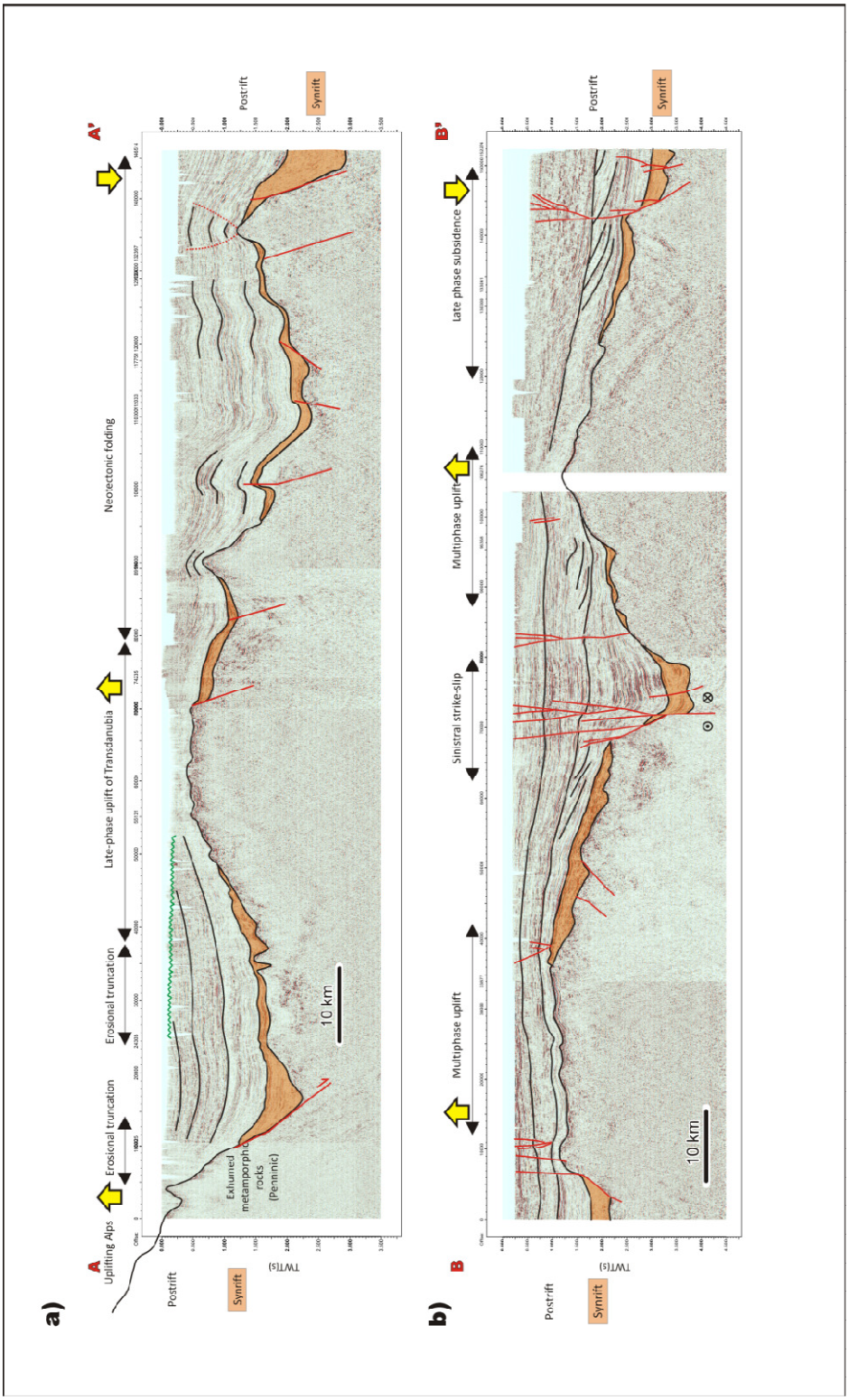
a)
A
Uplifting Alps
Erosional truncation
Erosional truncation
Late-phase uplift of Transdanubia
Neoectonic folding
A'
Postrift
Synrift
Exhumed metamorphic rocks (Pennnic)
10 km
TWT[s]
b)
B
Multiphase uplift
Sinistral strike-slip
Multiphase uplift
Late phase subsidence
B'
Postrift
Synrift
10 km
TWT[s]

Consequently, positive structural inversion of the basin is in progress and accompanied by fault reactivation, related seismicity and development of tectonic topography (Horváth & Cloetingh, 1996; Bada et al., 1999; Gerner et al., 1999; Cloetingh et al., 2005a,b; Bada et al., 2007a). The late-stage evolution of the Pannonian basin is intimately linked to the continuous indentation of the Adriatic microplate (Bada et al., 2001; Horváth et al., 2006a). The complete consumption of subducted lithosphere of the European foreland and, hence, the absence of forces driving extension (Horváth, 1993) led to a completely landlocked position of the basin constrained by rigid plate boundaries on all sides. Thus, gradual build-up of intraplate compressional stresses in the Pannonian lithosphere has been taking place since the Pliocene onwards. According to numerical stress field modelling results (Bada et al., 1998), the main source of compression is the ongoing Adriatic indentation. However, additional intraplate forces associated with density variations may also significantly influence the observed stress pattern (Bada et al., 2001).

2.2.1 Present-day stress field and neotectonics

In recent years, a Pannonian stress field database comprising on borehole breakout analyses, earthquake focal mechanism solutions and in-situ stress measurements has been established (see latest data in Bada et al., 2007a). The area exhibits remarkable lateral changes in the stress field reflected by the spatial distribution of different tectonic regimes. The dominant style of deformation at the margins of Adria is thrusting, often in combination with strike-slip faulting (transpression), arguing for convergence between Adria and the Alps-Dinarides. Towards the basin centre and the north-eastern regions strike-slip faulting is dominant (Bada et al., 2007a). Results of the stress field analysis suggest that intraplate stresses are transmitted across the Pannonian lithosphere resulting in the propagation of shortening as far as the NE Carpathians.

The presence of compressive tectonic stress during Pliocene-Quaternary times can explain the coexistence of rapidly subsiding and uplifting areas (*Fig. 2.9*). Both observational data (Horváth, 1995; Horváth et al., 2006a) and modelling results (Horváth & Cloetingh, 1996; Cloetingh et al., 2006) appear to confirm that compressive stresses can cause a considerable amount of differential vertical movements influencing topography (Cloetingh et al., 2005a). The present-day deep sub-basins of the area (e.g. Sava and Drava troughs, sub-basins of the Great Hungarian Plain, Little Hungarian Plain *Figs. 2.1 & 2.3*) have been continuously subsiding ever since the onset of basin formation in the Early Miocene, and are covered on the top by Quaternary alluvial sequences of 300-1000 m thickness. In contrast, the periphery of the basin system, as well as the Transdanubian Range has been uplifting and significantly eroded since late Miocene-Pliocene times (Horváth & Cloetingh, 1996; Bada et al., 1999, 2001; Cloetingh et al., 2005b). Inferences from the neotectonic development of the area (Fodor et al., 1999, 2005) and the architecture of the sediment in-fill (e.g. Nádor et al., 2003; Horváth et al., 2006a) provide further information on the Quaternary uplift and subsidence history. Associated landscape-forming processes, particularly drainage development as a sensitive recorder of changes in topography, enable

both qualitative and quantitative analysis of the vertical surface movements (e.g. Ruszkiczay-Rüdiger et al., 2005a,b; Timár, 2003; Timár et al., 2005; Dombrádi et al., 2007).

The high level of intraplate stresses (up to >100 MPa) in the brittle part of the lithosphere is close to the integrated strength of the system (Bada et al., 1999; Cloetingh & Lankreijer, 2001). This may lead to whole lithospheric failure in the form of large-scale folding and intense shallow brittle faulting (Horváth & Cloetingh, 1996). The general structural inversion and the observed late-stage deformation pattern can be explained in terms of stress-induced lithospheric deflection. Integrated geological and geophysical data argue for a large wavelength lithospheric buckling beneath the Pannonian basin system (Horváth & Cloetingh, 1996; Cloetingh et al., 2005a, *Fig. 2.10*).

It is to be emphasised that besides lithospheric folding other geodynamic or sedimentary mechanisms may also contribute to the observed vertical displacements. Uplift can partially be driven by isostatic rebound of the lithosphere due to the termination of roll-back manifested in dynamic topography (Horváth et al., 2011). Small-scale mantle convection is assumed to have facilitated the formation and extension of the Pannonian basin (Horváth & Faccenna, 2011). Mantle dynamics, however, could have influenced the post-rift evolution as well in the form of plume activity or supposedly plume-folding interaction (Burov & Cloetingh, 2009). It is to be noted that the downward deflection of the 660 km discontinuity almost everywhere beneath the Pannonian-Carpathian region is evidenced by seismic tomography and inversion of receiver function data. This fact suggests less likelihood for a lower mantle-seated plume affecting the thermal history of the Pannonian basin (Hetényi et al., 2009). Recent studies deal with the revision of early post-rift subsidence history and point out that compaction trends in the light of new data from hydrocarbon exploration wells must be re-evaluated in order to better quantify rate of tectonic subsidence (Horváth et al., 2012).

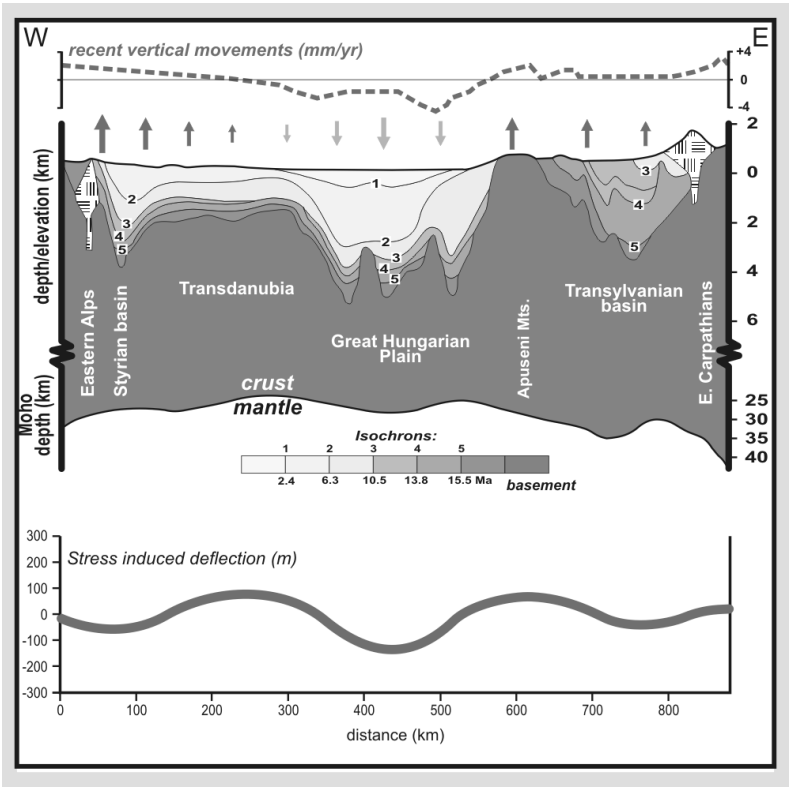

Figure 2.10 *Compilation of deep lithospheric structure, stratigraphic data (isopach horizons 1-5) and recent vertical motions (indicated by the arrows) along a profile running across the Pannonian basin from the Eastern Alps to the Eastern Carpathians (Fig. 2.1). Extent of lithospheric folding accounting for the spatial distribution of uplifted and subsided areas is illustrated relying on observational data and numerical modelling (Horváth & Cloetingh, 1996; Cloetingh et al., 1999, 2005b).*

2.2.2 Constraints on the neotectonic activity

Besides the differential crustal movements the most important signature of neotectonic activity is the formation of regional scale fault zones (*Figs. 2.2 & 2.8b*). These fault zones generally consist of ENE-WSW striking left-lateral strike-slip faults. Influence of active tectonics can be documented, for instance, in the seismicity of the basin and its surroundings, by means of space geodetic measurements and via in-situ stress measurements. In the following paragraphs the observations of these methods are lined up together with their implications on the neotectonic activity.

2.2.2.1 Seismicity

Seismicity in the Pannonian basin and its wider environment is spatially rather heterogeneous (*Fig. 2.11*).

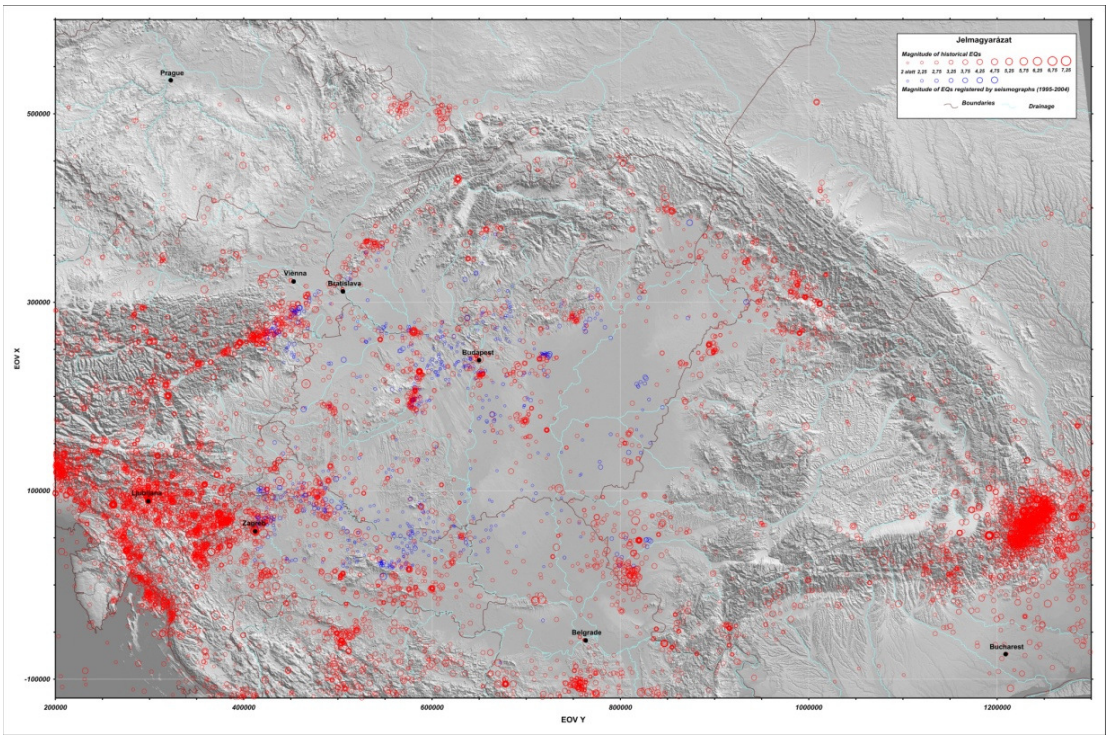

Figure 2.11 *Seismicity map of the Pannonian-Carpathian-Dinarides area. Red circles represent instrumental data, blue circles historical earthquakes events, respectively. The size of circles is proportional to the magnitude of the earthquake (after Tóth et al., 2004). The map was compiled in the framework of the OTKA project entitled 'Atlas of the present-day geodynamics of the Pannonian basin: euroconform map series and explanatory text' (project reg. no.: T034928). http://geophysics.elte.hu/atlas/atlas_geodin.htm*

The Vrancea zone (SE Carpathians), the Southern Alps and the Dinarides are characterised by intensive earthquake activity and frequent occurrence of large magnitude events (M≥6). On the other hand, the basin interior is moderately active in terms of seismicity. Earthquakes of M=6 are expected every 100 years, while M=5 events may happen average 20-30 years (Tóth et al., 2004). It is also to be noted that events in the Pannonian basin as well as in the Eastern Alps are almost exclusively restricted to the upper crust (max. 20 km depth) and intermediate mantle earthquakes (70-200 km) are observed only in the South Carpathian bend, more precisely in the Vrancea zone (Wenzel et al., 2002). As for the spatial distribution of the earthquakes in the basin interior, a fairly disperse pattern can be inferred. Although some clusters of events do appear (*Fig. 2.11*), clearly defined seismoactive tectonic elements are not detectable except for maybe the so-called Zagreb line and its Hungarian continuation. The explanation for this phenomenon is the overall low

seismicity of the entire region that also yields a relatively higher error level in the determination of the epi- and hypocentres.

2.2.2.2 Constraints on the horizontal movements

Present-day velocity of horizontal crustal movements can be determined by repeated space geodetical measurements with sufficiently high precision. Advance towards more accurate constraints on the recent kinematics of the Pannonian region has been accomplished during the past decade owing to the operation of the Central European GPS network and numerous campaigns. Adria is converging with an average 4-5 mm/y velocity relative to a stable European continent in a NNW direction (Grenerczy et al., 2005). Due to this convergence, the Adriatic microcontinent is rotating in a counter-clockwise manner (*Fig. 2.12*).

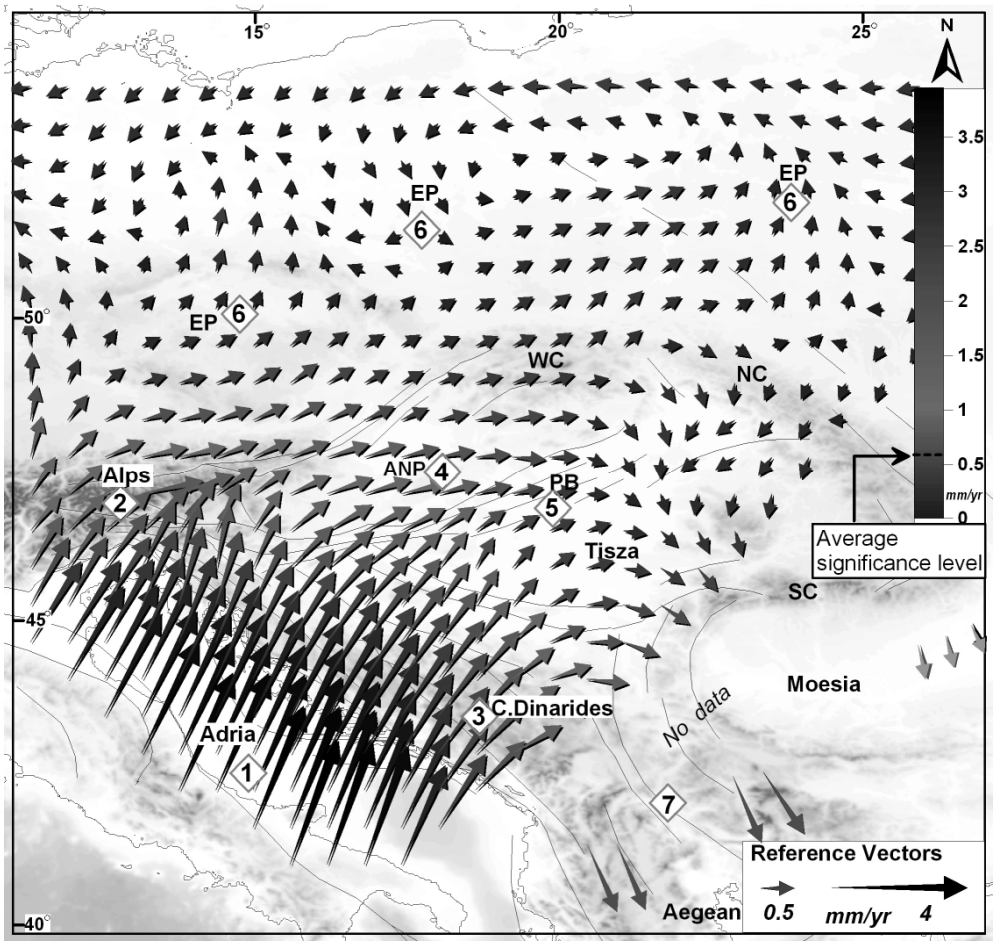

Figure 2.12 *Interpolated GPS velocity vectors displaying the present-day strain field of the PANCARDI region. The indentation of the Adriatic microplate imposes considerable compressional stress to the area. The horizontal motion is transferred towards the Carpathian orogen with gradually decreasing values across the Pannonian basin (Grenerczy et al., 2005).*

The angular velocity is about 0.3-0.4°/My, which in the central part of Adria means a roughly 3-4.5 mm/y and 2-3 mm/y translation to the NNE towards the Dinarides and perpendicular to the main strike of the Eastern and Southern Alps, respectively. It is concluded that this counter-clockwise rotation of Adria directly controls the actual kinematics of the region and accounts for the compressional setting of the Pannonian basin (*Fig. 2.12*, Bada et al., 1998). As for the interior of the Pannonian basin, approximately 1-1.5 mm/y contraction can be derived from the measurements. In addition, distance between individual GPS stations located in Hungary is regularly measured with high precision. These so called baseline measurements yield a direct measure of the total shortening and confirm the amount of contraction provided by the entire GPS network (Grenerczy & Bada, 2005).

2.2.2.3 Constraints on the vertical movements

By means of basin analysis, the subsidence curves for depocentres in the basin system can be derived and hence the subsidence history can be traced through time. In contrast, in areas of uplift and continuous erosion (e.g. Transdanubia) it is difficult to assess the rates of vertical surface motions. Albeit, the cutting-edge space geodetic technology based on regular radar measurements (InSAR, PSInSAR, etc.) allows the millimetre scale reconstruction of vertical displacements, the time-span since such methodologies are applied is still rather short to provide sufficient dataset for the reliable determination of the slow vertical crustal motions. Indirect ways of the assessment of uplift rates can rely on geomorphologic studies (e.g. Pécsi, 1959), paleontological data (Scheuer & Schweitzer, 1988) and isotope geochemistry (Ruszkiczay-Rüdiger et al., 2005a,b). Various techniques are valid for different time spans, therefore, only certain periods of the young deformation history have been reconstructed in terms of uplift rates. These data reveal variability in the velocity of the uplift. Exposure ages determined for the Transdanubian Range show temporal as well as spatial variations. At the northeaster flank (Visegrád hills) thermochronolgical data show moderate uplift in the early stages then acceleration up to 1.6 mm/y (Ruszkiczay-Rüdiger et al., 2005b). The Buda hills reveals a sequential uplift history in the last 0.5 My. From 500 to 320 ka a relatively stagnant period is put forward. Dating calcite precipitations by means of U-Th series in caves of the hill yield 0.16 mm/y uplift rate for the period 320-70 ka (Szanyi et al., 2009), that is in line with results of dated travertines (0.18 mm/y) and strath terraces (0.14 mm/y) in the area (Ruszkiczay-Rüdiger et al., 2005a). Thermochronological studies carried out on Triassic carbonates exposed in the Hungarian Midmountains (Bükk hills) provided an assessment that 5 Ma they were buried ca. 1 km deep, which indicates an average 0.2-0.3 mm/y Neogene uplift. Sequence stratigraphy data of the Békés basin show 800 m subsidence in the central part of the depocentre, however at its flanks the eroded column could have totalled ca. 600 m in the last 3 My, which means 0.2 mm/y uplift rate.

Chapter 3

Modelling the deformation of the weak Pannonian lithosphere: lithospheric folding and tectonic topography[2]

3.1 Modelling objectives

The Pannonian-Carpathian region is regarded as a key natural laboratory for studying the interaction between deep lithospheric processes, neotectonic activity and associated topography development (e.g., Cloetingh et al., 2005a; Bada et al., 2006; Fodor et al., 2005). Buckling of the thinned, hot and weak back-arc lithosphere is considered to be an essential form of aseismic deformation. The Pannonian basin is often cited as a natural example of irregular lithospheric folding (Cloetingh et al., 1999), controlling the overall pattern of vertical crustal movements (Horváth & Cloetingh, 1996; Cloetingh et al., 2006; Horváth et al., 2006a; Bada et al., 2007a).

Complementary to numerical modelling approaches, analogue models offer an additional tool to study the complex deformation history of this area. Crustal-scale analogue models were used to investigate fault reactivation during the formation of the Pannonian basin (Windhoffer et al., 2005). They also provided useful information on the neotectonic behaviour of strike-slip faults during basin inversion (Windhoffer & Bada, 2005).

By means of a set of analogue experiments, the focus was on the compression of the whole lithosphere and the consequent subsidence and uplift anomalies observed in the Pannonian region. The geodynamic framework of the extension and subsequent compression of the Pannonian basin has been reviewed in *Chapter 2* with a special emphasis paid to recent vertical motions shaping surface morphology. Hereby an overview on the process of folding in weak intraplate continental lithospheres is given from a general perspective. It is followed by the detailed description of the physical models implemented to tackle the coupling between the deep lithospheric processes and topography. Finally, inferences gained from the analogue approach on the Quaternary to recent evolution of the Pannonian basin are discussed. In doing so, the following topics are addressed: (1) dominant wavelengths and amplitudes of lithospheric folding, (2) related vertical deformation patterns, (3) onset of the positive structural inversion, (4) the role of crustal thickness variation and (5) the influence of indenter geometry in the folding of a previously extended, hot and weak lithosphere.

Basics of the analogue modelling technique are not presented here since extensive descriptions are available on the methodology in the literature. For a most recent summary see Fernandez-Lozano (2012).

[2] This chapter is largely based on the publication: Dombrádi, E., Sokoutis, D., Bada, G., Cloetingh, S., Horváth, F., 2010. Modelling deformation of the Pannonian lithosphere: Lithospheric folding and tectonic topography. *Tectonophysics*, 484:103-118.

Apart from the direct relevance to the evolution of the Pannonian basin, the presented results add scientific value to previous analogue models aiming at general geodynamic processes in compressional setting (Sokoutis et al., 2005) and/or the response of hot and weak lithospheres to deformation (Sokoutis et al., 2007).

3.2 Overview of the models on lithospheric folding

Lithospheric folding appears to be a favourable mechanism to accommodate compressional stresses in continental as well as oceanic lithospheres. The spatial distribution of folds, variations in topography and systematic pattern in the measured gravity anomalies in various continental areas have been associated with the folding or buckling of the lithosphere (e.g. Stephenson & Lambeck, 1985; Martinod and Davy, 1992; Molnar et al., 1993; Burov et al., 1993; Burg et al., 1994).

The concept of linear folding theory (Biot, 1961, Ramberg, 1961), wherein linear differential equations provide an analytical solution for the deformation of a horizontal layer embedded in a less competent medium could be applied to numerous observed cases. However, the linear cases generally involve strong lithospheres, the behaviour of which is less effected by inhomogeneities, surface loads and structural peculiarities (*Fig. 3.1,* Cloetingh et al., 1999).

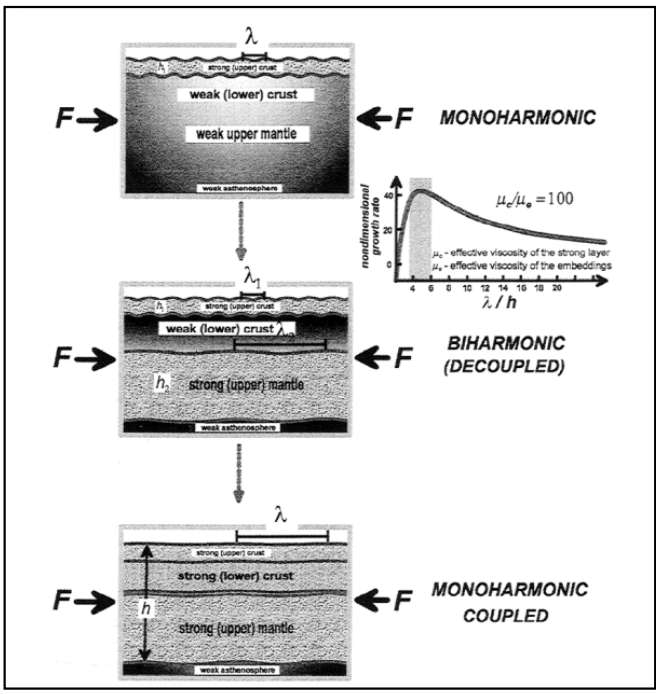

Figure 3.1 *Examples of linear folding in media of various rheological properties subjected to horizontal tectonic forces (F). Top panel illustrates the response of a young and hot lithosphere with weak rheology in the form of monoharmonic folding. Middle panel shows an example of biharmonic folding when the lower crust and upper mantle exhibiting different rheological characteristics behave in a decoupled mode. Finally, in the bottom panel the mechanically strong layers become coupled and the result is again monoharmonic folding of the lithosphere (Cloetingh et al., 1999).*

Several analogue and numerical investigations attempted to unveil and understand the mechanism of lithospheric folding in media characterised by more complex composition or

tectonic setting. This overview is merely concentrated on the results relevant to the weak rheological properties of the Pannonian lithosphere that is the absence of a strong mantle layer.

In the work of Martinod & Davy (1994), the wavelength of folding was analysed as a function of the brittle layer thickness by a set of analogue models, which involved oceanic or weak continental type lithospheres as well. The spacing between the regularly distributed folds proved to be 4-8 times the thickness of the competent layer and fit well to several natural cases. According to their observations, the underlying ductile material had no significant role in the deformation. A large number of analogue experiments have been performed to study tectonic evolution due to large-scale folding in continental areas (e.g. Burg et al., 1994; Sokoutis et al., 2005; Willingshofer et al., 2005). However, less attention has been dedicated to the deformation of weak lithospheres under compression. Recently, Cagnard et al. (2006) modelled the thrust development and the formation of pop-down structures in weak, two-layered systems comparable to Archaean-type lithospheres. Laboratory experiments also suggest the importance of the thin elastic core of the lithosphere in between its brittle and ductile parts, which may control the deformation pattern under shortening (Marques & Podladchikov, 2009). The amount and style of lateral extrusion related to the orogen evolution in the Eastern Alps have also been in the focus of physical modelling (Ratschbacher et al., 1991; Rosenberg et al., 2004). These experiments gave a detailed insight into the geodynamics of the eastern Alpine region. However, the Pannonian area was only involved as a confinement.

The coupled and decoupled behaviour of continental lithospheres generating mono- and biharmonic modes of folding, respectively, have been revealed by a number of numerical studies implementing viscoelastic or viscoelastoplastic media (e.g. Burov et al., 1993; Burov & Molnar, 1998; Cloetingh et al., 1999, 2002; Gerbault et al., 1999; Burg & Podladchikov, 2000; Faccenda et al., 2009). Yet certain areas show remarkable deviations from the theoretically predicted values being classified as examples of irregular folding (Cloetingh et al., 1999). It is to be noted that analogue experiments also successfully tackled the problem of coupled and decoupled modes of deformation and provided implications to orogen building (Willingshofer & Sokoutis, 2009, Sokoutis & Willingshofer, 2011).

The young Pannonian basin belongs to one of these exceptions of the rule. Results of 2D forward modelling of basin stratigraphy during the late-stage shortening implied the existence of a 400 km large wavelength deflection of the lithosphere, a value 25-40 times larger than the thickness of the brittle crust. It is noted that in young basins, such as the Pannonian basin and the North Sea, this large-scale folding is likely to be primarily controlled by the configuration of the rift basin and its associated sedimentary loads prior to the onset of the compression (Horváth & Cloetingh, 1996). Seismic data interpretation and structural analyses document basin inversion on smaller basin-scale as well (Horváth et al., 2006a), implying a multi-wavelength mode of folding during basin inversion (Cloetingh et al., 2005a). Recently, mantle plume and lithosphere interactions have been put forward

to explain the deformation style of several hot intraplate continental lithospheres, including also the Pannonian basin (Burov & Cloetingh, 2009).

3.3 Modelling strategy

The physical modelling technique has been favoured to analyse the process of irregular folding in the Pannonian region. On the one hand, the analogue models were constructed to complement the results of already existing numerical models to study the spectrum of folding and related topographic signals. On the other hand, they provided an alternative tool to test whether the deformation of the weak Pannonian lithosphere can account for the recent anomalous vertical motion pattern recorded in the basin. In comparison with the previous numerical models, the selected analogue materials provided more natural rock properties and realistic brittle faulting. In addition, the effect of the indenter geometry and varying crustal thickness modifying the lithospheric scale folding was investigated.

A series of analogue experiments was performed in the ISES Tectonic Lab. Three types of models were employed to investigate the addressed problems (*see Section 3.1*).

Type-1 models concentrated on the overall signal of lithospheric folding in a uniform, two-layered system that is the rheological equivalent of the weak Pannonian lithosphere. The primary target of this type of models was to compare the obtained dimensions of the large-scale folding with possible values of natural wavelength and amplitude inferred from the available field data and numerical simulations.

Type-2 models aimed at the role of pre-existing thickness variations in the upper brittle crust. As a consequence of the heterogeneous extension of the Pannonian basin, the Moho surface reflects slight, yet not negligible undulations (see deep seismic profile, *Fig. 2.5*). The concept of Type-2 models was to examine how the position of thicker and, thus, stronger units alters the folding parameters. Therefore, models were built with different sequences of alternating thick and thin upper crust units.

Lastly, Type-3 experiments dealt with a different shape of indenter. In the previous experiments (Type-1 & -2) the north-easterly translation of the Adriatic indenter was simulated by the simple plane of a moving wall. The counter-clockwise rotation of the microcontinent was beyond the objective of our models. With respect to the natural geometric boundary conditions, such representation of the eastern margin of Adria that is the Dinaric region is acceptable. However, further to the north, the area of the Eastern Alps suffers N-S directed convergence (e.g. Willingshofer & Cloetingh, 2003). Seismic events clustering along the Mur-Mürz and Lavanttal lines suggest that these faults facilitating the lateral extrusion in Early and Middle Miocene times are still active (Kummerow et al., 2004). It can be assumed, and also deducible from GPS measurements of horizontal movements that eastward escape of the ALCAPA unit has not yet entirely vanished (e.g. Bada et al., 2007a). This direction of horizontal movements was built in Type-3 models, technically by adding an extra, oblique face of indentation. Obviously, it is a major simplification of the Eastern Alpine tectonics but offers an opportunity to examine the deformation of the basin interior under 3D kinematic boundary conditions.

3.3.1 Analogue materials and model set-up

The brittle-ductile stratification of the hot and weak continental lithosphere was based on a plethora of available geological and geophysical data. Seismotectonic data imply a shallow depth range of brittle behaviour, as the seismic events recorded in the Pannonian basin do not exceed 15 km in depth (Tóth et al., 2002; Bada et al., 2007b). An additional essential feature is the noticeable absence of lithospheric strength in the ductile region of the Pannonian lithosphere (i.e. below 15 km). The high heat flow values (Dövényi & Horváth, 1988), as a consequence of an elevated asthenosphere dome below the basin system, are indicative of a close thermal control on the strength of the lithosphere. Inversion of magnetotelluric soundings (Ádám & Wesztergom 2001), campaigns of deep seismic measurements traversing the basin (Posgay et al., 1995, 1996; Tari et al., 1999), together with gravity modelling studies (Szafián et al., 1999; Szafián & Horváth, 2006) were used to constrain the thickness of the Pannonian lithosphere utilised in the analogue experiments.

Rheological modelling results confirm the overall weak rheology of the Pannonian basin system, also demonstrating that brittle behaviour is restricted to the uppermost crustal layer (Lankreijer et al., 1999). Low effective elastic thicknesses (Te<20 km) are inferred for the basin mostly depending on the thickness of the mechanically strong upper crust, whereas the contribution from the lower crust was found to be negligible (Tesauro et al., 2009). In the light of the presented inferences, the hot and weak Pannonian lithosphere can be simulated as a two-layer system, the ductile lower crust and mantle lithosphere overlain by the thin upper brittle crust.

The rheological structure of continental lithospheres has been in the foreground of scientific debates. One concept, referred to as "crème brûlée", argues that most of the strength is restricted for the brittle crust and the mantle lithosphere is generally characterised by ductile behaviour (Jackson, 2002; Jackson et al., 2008). The "jelly sandwich" model allows more than one brittle and ductile layer within the lithosphere and puts forward a mechanically more stable structure (Burov & Watts, 2006). It is also stated that there may be certain areas, which differ from this structure and the "crème brûlée" model may be more suitable, particularly, in the case of young hot rifts (Burov, 2009). Thus, the Pannonian region is likely to belong to these few exceptions. Any of the two models proves to be true for the general structure of the Earth's lithospheres; the two-layered model of the Pannonian basin appears to be adequate.

In selection of the materials used in the experiments of the lithospheric composition extrapolation of laboratory experiments was taken into consideration (Kirby, 1983, 1985; Carter & Tsenn, 1987; Ranalli, 1995, 1997). The analogue experiments represent the modelled Pannonian lithosphere floating above a high-density fluid asthenosphere. The rheological stratification of the models was reproduced by using dry K-feldspar sand simulating the brittle crust, while a mixture of Rhodorsil Gomme CSIR (Rhône Poulenc, France) silicone putty, barium sulphate powder and oleic acid was designed to model the

ductile part of the lithosphere with quasi-Newtonian behaviour. *Table 3.1* documents the properties of the selected materials. The models were built in a plexiglas tank with lubricated walls, which is a satisfactory standard to reduce friction for this sort of experiments (e.g., Davy & Cobbold, 1991; Sokoutis et al., 2000, 2005). Displacing a rigid vertical Plexiglas wall at a constant velocity induced progressive shortening, simulating the ongoing NE-directed indentation of the Adriatic plate. The opposite fixed glasswall represented the western margin of the East European Platform. An illustration of the model set-up is given in *Fig. 3.2*, displaying the comparison of model to nature scaling parameters.

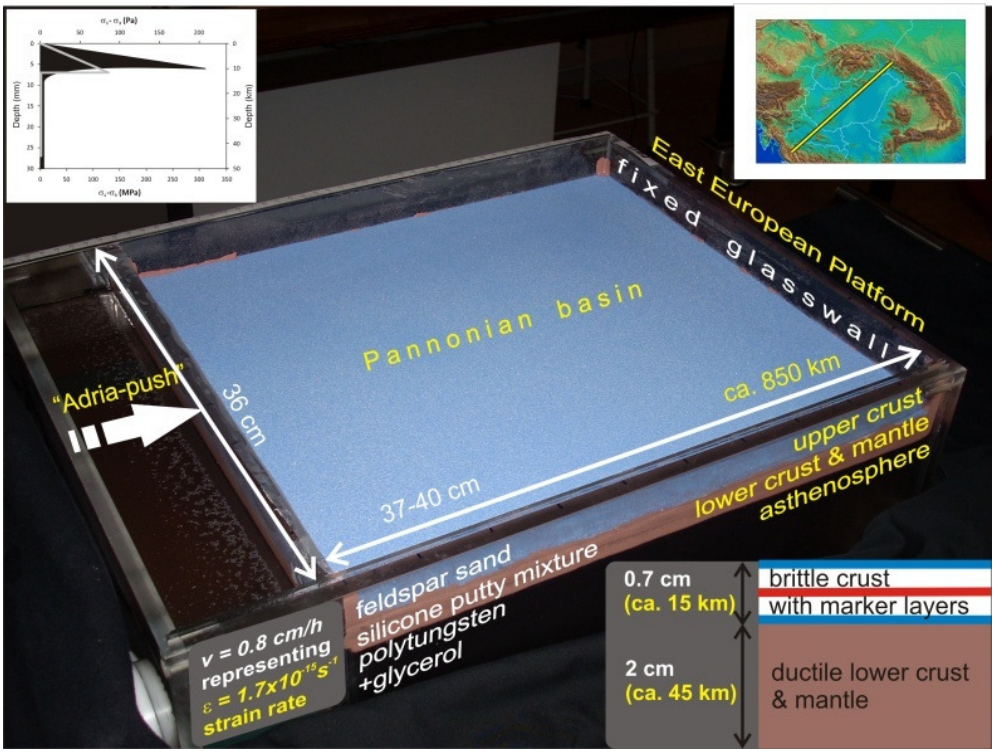

Figure 3.2 *Image of the plexiglas tank with the sand-silicone layers inside, floating on a dense fluid. The figure shows the set-up for Type-1 models and the basic parameters both in the analogue model (white text) and in the natural prototype (yellow text). The strength profiles, given in the upper left corner (model – light grey; nature – black), represent the very initial stage of deformation of a crème brûlée type of lithosphere. Top right inset maps show the main direction of principal stress field originating from the motion of the Adriatic microplate. This direction is considered as the orientation of the 2D analogue models.*

Materials/Parameters		Model	Nature	Dimensionless ratios (model/nature)
upper crust (K-Feldspar sand)	thickness	0.7 cm	15 km	$4.67 \cdot 10^{-7}$
	density	1300 kgm^{-3}	2700 kgm^{-3}	0.48
	coeff. internal friction	0.85	0.75	1.1
	cohesion	15 Pa	$6 \cdot 10^{7}$ Pa	$2.5 \cdot 10^{-7}$
	strength	77 Pa	$3.3 \cdot 10^{8}$ Pa	$2.3 \cdot 10^{-7}$
lower crust & mantle (silicone mixture)	thickness	2 cm	45 km	$4.44 \cdot 10^{-7}$
	density	1424 kgm^{-3}	3200 kgm^{-3}	0.45
	viscosity	10^{4} Pa s	10^{21} Pa s	10^{-17}
	strength	0.08 Pa	$3.58 \cdot 10^{5}$ Pa	$2.3 \cdot 10^{-7}$
	n-value	1.2		
length		~38 cm	~850 km	$4.47 \cdot 10^{-7}$
strain rate		$2.06 \cdot 10^{-4}$ s^{-1}	$8.95 \cdot 10^{-17}$ s^{-1}	$2.3 \cdot 10^{10}$
time		1 s	$2.25 \cdot 10^{10}$ s	$4.44 \cdot 10^{-11}$
bulk shortening		2 cm		15-20 km
Smoluchowski number (S_m)		4.09	4.21	0.97
Ramberg number (R_m)		13670	15780	0.866

Table 3.1 *Summary of the model parameters and their natural equivalents. Brittle and ductile strengths were calculated according to the formulae in Michon & Merle (2000), Michon & Sokoutis (2005) and Sokoutis & Willingshofer (2011).*

After deformation, the models were soaked in water, frozen and cut parallel to the direction of compression to expose cross sections for photographs of the internal structures. This technique provides information only on the very last episode of the deformation history. Therefore, during the model run, photos were regularly taken from above to analyse the first-order geological structures and the evolution of surface topography. High-resolution images of the model surface via laser scans record the subtle variations of topography, which are often invisible for the naked eye or hardly detectable on regular top-view photos. At this resolution even very low angle tilt of the laser scanner device has significant impact on the surfaces under examination In order to correct for this 3D distortion in a non-laborious and user-friendly manner, a semi-automatic processing routine has been developed, which was applied on each and every scan.

3.3.2 Scaling procedure

The models were scaled following the principles of geometric and dynamic-rheologic similarity (Hubbert, 1937; Ramberg, 1981; Weijermars & Schmeling, 1986). Geometric similarity was achieved by reducing lengths in the models by a factor of $2.25 \cdot 10^{6}$ with respect to corresponding lengths in nature. Thus, a 2.7 cm thick model was used to provide the 60 km thick lithosphere. The final distance between the moving and fixed walls (~38 cm) equates 850 km in nature, which closely corresponds to the distance between

the Dinarides and the NE Carpathians in the main direction of compression (*Figs. 2.1 & 3.2*).

Rheologic-dynamic similarity was retained by scaling the gravitational stress $\sigma^*=\rho^*g^*l^*$, where ρ and g are density and gravitational acceleration, respectively, and the asterisk denotes the ratio between model and nature (Sokoutis et al., 2005). Proper scaling was tested by calculations of non-dimensional numbers given by ratios between forces acting on the models (Ramberg, 1981). For the viscous deformation, the ratio between gravitational and viscous stresses (Ramberg number R_m; Weijermars & Schmeling, 1986) is given by:

$$R_m = \frac{\rho_d g h_d}{\eta \dot{\varepsilon}} = \frac{\rho_d g h_d l_d}{\eta v} \qquad (3.1)$$

Density, thickness and length of the ductile layer are denoted by ρ_d, h_d and l_d respectively, g (=9.81 ms^{-2}) is the gravitational acceleration, η is the viscosity and $\dot{\varepsilon}$ is the strain rate given by the ratio between the mean velocity of convergence v and the horizontal extent of the ductile layer l_d.

The velocity of shortening was calibrated according to our present knowledge on the rate of convergence in the Pannonian area. Recent measurements of the GPS network yield approximately 1-1.5 mm/yr overall contraction rate (*Fig. 2.10*, Grenerczy et al., 2005). Contraction inside the Pannonian basin is also evidenced by a systematic shortening of GPS baseline lengths measured directly between GPS stations in the basin system (Grenerczy & Bada, 2005). The applied model shortening rate in all three models, expressed in terms of the displacement velocity of the indenter system, was 0.8 cmh^{-1}.

For scaling brittle deformation, we considered the ratio between gravitational stress and cohesive strength (S_m – Smoluchowski number; Ramberg, 1981):

$$S_m = \frac{\rho_b g h_b}{\tau_c + \mu_c \rho_b h_b} \qquad (3.2)$$

Where, ρ_b and h_b are the density and thickness of the brittle layer, respectively, g (=9.81 ms^{-2}) is the gravitational acceleration, τ_c is the cohesive strength and μ_c is the coefficient of internal friction. For a precise scaling, the prototype and the model must share similar R_m and S_m values. In this work, the ratios between the above dimensionless numbers of the model and nature are very close for both the brittle and ductile part (*Table 3.1*).

The entire scaling procedure and the determination of the dimensionless parameters assume that the inertial forces can be neglected in the analogue models investigating tectonic processes. The validity of such simplification and the relation of the laboratory models to the natural prototype have been recently discussed (Wickham, 2007; Del Ventisette et al., 2007). The argument for this type of simplification is the low value of the Reynolds number.

$$\mathrm{Re} = \frac{\rho v l}{\eta} \tag{3.3}$$

Where ρ stands for the density, v is the velocity of convergence, l is the length and η is the viscosity. The Reynolds numbers are fairly low in both the models and nature (Re=10^{-8} and Re=10^{-21}, respectively). Under such conditions, the inertial forces can be neglected compared to the viscous ones. This fact allows the scaling of the different types of forces to deviate from the strict dynamic similarity, which means that the time and length ratios can be considered as independent variables (for full explanation see Ramberg, 1967). Thus, the time scaling was performed using the length ratio and the corresponding velocities. This yielded a time ratio t*=$4.44 \cdot 10^{-11}$ between the elapsed time from the onset of deformation in the model and the equivalent time period on the geological timescale.

3.3.3 Model simplification and limitations

The geometries and rheologies of analogue models necessarily simplify the complexity of the natural prototype. A major simplification is the homogeneous rheology of analogue materials although the rheology of rocks is known to be strongly temperature dependent and therefore varies with depth (e.g., Ranalli, 1995, 1997). However, representing the mantle by a uniform layer, with depth-invariant properties appears to be an acceptable first-order approximation that has been employed in other previous experiments (e.g., Davy & Cobbold, 1988, 1991; Sokoutis et al., 2005).

A principal limitation of the applied models was the absence of erosion and sedimentation processes. The sedimentary in-fill may not only influence the temporal and spatial evolution of the structures but, as shown by the results of numerical modelling, the wavelength of the folding by reducing the gravitational effects (Cloetingh et al., 1999).

Additionally, the models do not take into account the post-rift thermal relaxation of the lithosphere. Despite these simplifications, our analogue models were able to tackle the problem of irregular folding in the hot and weak Pannonian lithosphere, and trace the large-scale deformation pattern as a response to compression.

3.4 Modelling results

In this section, observations inferred from the three types of models are summarised. First, the style of deformation of the lithosphere in the simplest model (Type-1) is reviewed. In doing so, a description of the major geological structures visible on the final cross sections and their topographic manifestation are given. Then results of Type-2 experiments are presented to analyse the influence of the laterally varying thicknesses of crustal units on the wavelengths and amplitudes of the folding. Finally, Type-3 models are presented, which modelled the combination of indentation of Adria and its direct consequence, the lateral extrusion of ALCAPA wedge.

3.4.1 Type-1: uniform two-layer system

Type-1 models simulated the behaviour of the attenuated lithosphere overlain by a thin brittle crust under compression. Large-scale surface expressions of the advancing deformation could be traced in-situ and were documented by top-view photographs (*Fig. 3.3a*). After 0.5 cm shortening, a back-thrust started to develop close to the moving wall. Later (~1 cm shortening), a fore-thrust appeared in front of the distal wall demonstrating the transfer of strain across the model. In the second half of the total duration, these two thrusts seemed to accommodate a large portion of the strain as their size was continuously increasing until the end of the experiment.

Several sections were cut from the frozen model parallel to the direction of compression allowing 2D interpretation. *Fig. 3.3c* illustrates the main lithosphere-scale structural elements visible in these cross sections. The coloured sand layers made the thrusts more visible and also revealed a gentle, large wavelength buckle ($\lambda \approx$15-18 cm in the model) of the whole lithosphere. The base of the analogue lithospheric mantle was fairly smooth and moderate thickening was noticeable only below the thrusts. Marked uplift occurred in the thrust systems and to a smaller extent above the fold axes, while subsidence was observed on the fold limbs. The amplitude of the folding is in millimetre order. It is to be noted that deformation in the model has reached the level when pop-down structures started to develop (Cagnard et al., 2006).

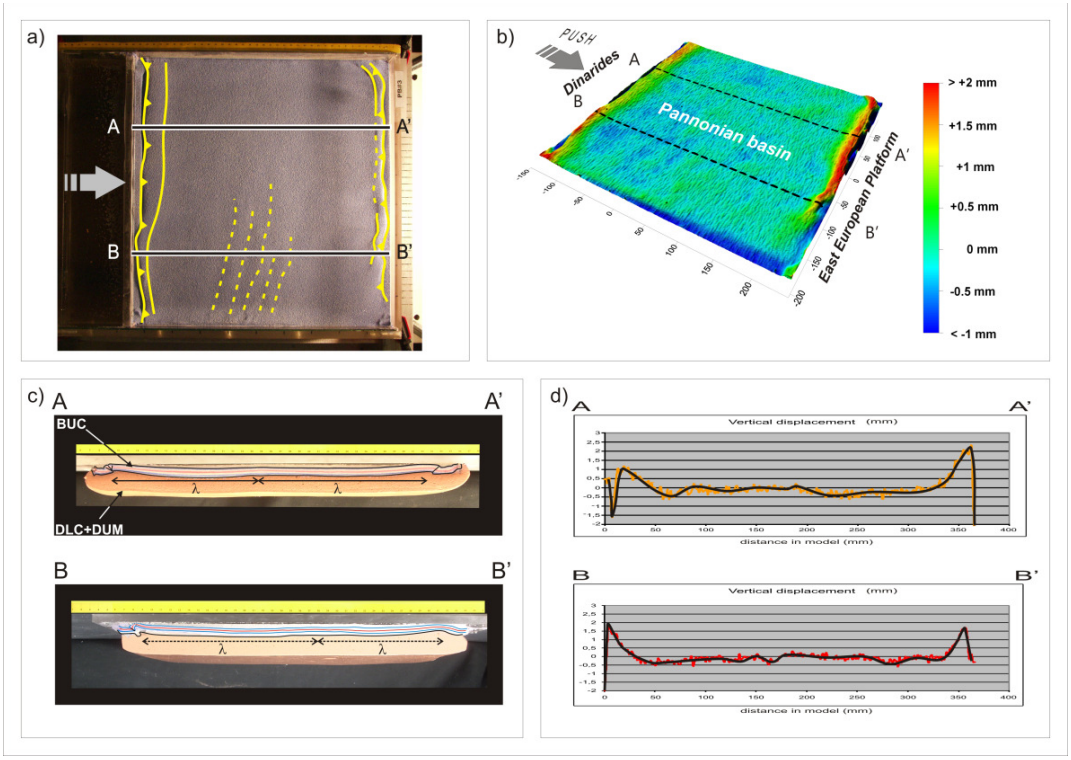

Figure 3.3 *Synthesis of the results of Type-1 models according to a) identified first order structures on top-view photographs, b) laser scan images demonstrating the surface deformation (colour code defined by the amount of vertical surface movement), c) representative cross sections cut from the frozen model depicting the large-scale folding of the lithosphere (λ=350-400 km in nature) and d) diagrams and smoothed trendlines (black solid line) of vertical displacement derived from the surface along the indicated profiles (AA′ and BB′). The results integrating the three sources confirm the influence of the lithospheric deformation on the topography development. Used abbreviations: BUC = brittle upper crust, DLC+DUM = ductile lower crust and upper mantle.*

Detailed analysis of the surface scans (*Fig. 3.3b*) enabled further inferences on the amount of uplift and subsidence. Due to the high density of the fluid, simulating the asthenosphere, and the fixed boundaries confining the deformed model, the expelling of the fluid caused a minor overall uplift in the system. By correcting this effect, the amount of vertical motions could be exactly quantified for the entire length of the experiment. The uplift of the two major thrusts and the subsidence of the related troughs ranged between 1.5 and 2.5 mm. The high-resolution scan images are capable of detecting sub-millimetre variations of the model surface. They revealed a systematic surface undulation in the model interior with alternating uplifting (+0.2-0.3 mm) and subsiding areas (-0.6-0.8 mm). Profiles extracted from the DEM (*Fig. 3.3d*) assisted the visualisation of the topographic features. Additionally, they were used to correlate the vertical surface movements to the dominant wavelength and the amplitude of the large-scale lithospheric folding.

3.4.2 Type-2: incorporated crustal inhomogeneities

Albeit the entire Pannonian basin is characterised by thin upper crust, slight, yet important differences are observable on the map of crustal thickness (Horváth et al., 2006a), for instance, between the western (Transdanubia) and eastern part (Great Hungarian Plain, for locations see *Fig. 2.1*). The pre-Neogene basement depth map (Horváth & Royden, 1981; Horváth et al., 2006a, *see Figs. 2.2 & 2.5*) indicates that the inhomogeneous and laterally varying crustal thinning during the extension of the Pannonian basin resulted in uneven basement morphology.

To study the role of initial crustal inhomogeneities in the weak lithosphere, Type-2 conceptual models were employed by extrapolating the present-day thickness values to the onset of the compression. The models were built up of four units with a difference of 3 mm in thickness (*Fig. 3.4*), thus isostasy assisted to create laterally varying Moho depths. All other parameters of the analogue set-up remained unchanged.

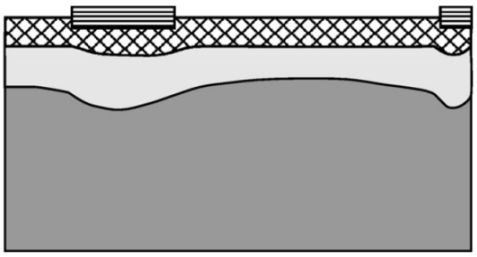

Figure 3.4 *Sketch of the Type-2 model set-up. Thicker, thus, stronger upper crustal units were achieved by placing extra 3 mm thick sand load (hatched blocks) on top of the 7 mm sand layer (chequered layer) used in Type-1 models. The lateral thickness variation in the brittle part also affected the ductile layer (light grey layer). The underlying dark grey domain represents the experimental asthenosphere. The presented layers are out of scale.*

The position of thicker and thinner, and consequently, stronger and weaker, blocks in the first setup was determined to be applicable to the natural case of Transdanubia and the Great Hungarian Plain (*Fig. 3.5a*, thick and thin units denoted from A to D).

At the beginning of the experiment, deformation was localised in the narrow thin crustal unit (A) adjacent to the indenter. The weaker material was significantly squeezed leading to the formation of a major pop-up structure bounded by back- and fore-thrusts. Subsequently, deformation advanced towards the distal margin of the first wide zone of thicker crust (B). Absence of detectable structural features in the more distal part of the model (C and D units) suggests that the extent of strain localisation was much higher compared to Type-1 models, and decreased the amplitude of the folding. Strain localisation was directly reflected by the vertical movements deduced from model morphology and cross sections (*Fig. 3.5b-d*). The observed uplift (2 cm) in the pop-up system next to the moving wall was extremely high compared to the second thrust (~1 mm). The maximum amount of coeval subsidence was found to be also in the millimetre order. Smaller

wavelength (ca. 6 cm) undulations were visible on the surface of the strong crustal unit but totally vanished in blocks C and D. The large-scale folding has been overprinted by the effects of the different crust units and remained hardly detectable in the cross sections. In other words, the wide thick-crusted block appeared to control the style of deformation of the brittle as well as the underlying ductile layer.

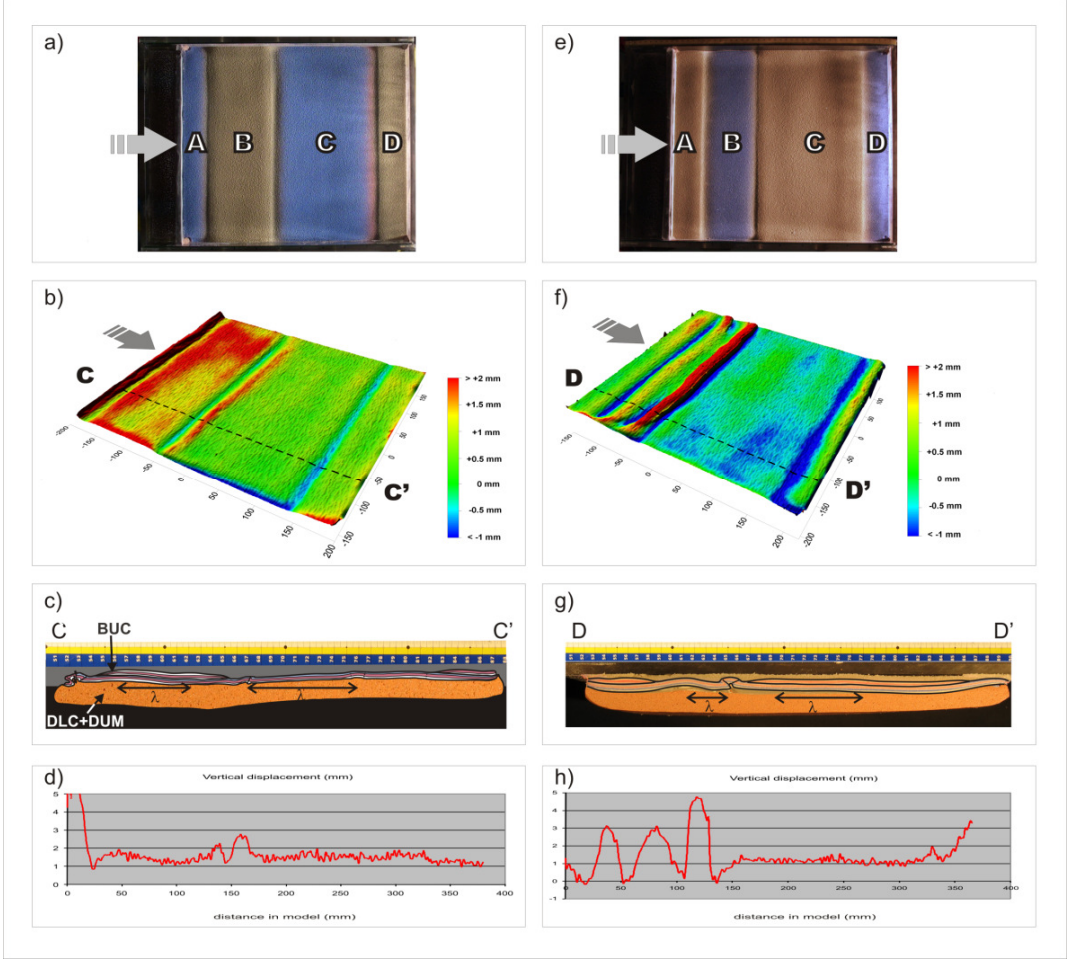

Figure 3.5 *Summary of the results of Type-2 models. a-d) white capital letters are assigned to the weaker and stronger crust units; A: weak, B: strong, C: weak, D: strong and e-h) weak-strong blocks in reverse order. Both the cross sections and the surfaces reveal the changes in brittle as well as in ductile deformation due to the different position of the stronger blocks. Model deformation is illustrated as in Fig. 3.3. Used abbreviations: BUC = brittle upper crust, DLC+DUM = ductile lower crust and upper mantle.*

For conceptual purposes, a different scenario was tested in inverse configuration by simply swapping the position of thin and thick blocks (*Fig. 3.5e*). In this case, concentration of the deformation in the thin brittle crust (B) bounded by the thicker units (A and C) was also evident. The transition between thin and thick crust was marked by thrusting and pop-up at the borders. The DEM (*Fig. 3.5f*) as well as the cross section (*Fig. 3.5g*) demonstrated

that the interior of the basin (C) was folded and deformation occurred even in the end section of the model (D). The amplitude of folding was largely in the same order as observed before. However, the wavelength was strongly controlled by the position of the thick-crusted units and it was again considerably shorter than in Type-1 models (~4 cm in unit B and ~6-7 cm in unit C). In contrast with the previous model, surface uplift in the proximity of the fixed wall was well visible. Though, the weaker crustal units localised a large portion of strain, they did not prohibit the development of gentle undulations in the thicker blocks.

3.4.3 Type-3 models: role of indenter geometry

Type-3 experiments were designed with uniform brittle and ductile layers as in Type-1 models but using an extra, oblique face at the moving wall. In this way an additional source of compression was introduced, which represents the ongoing, yet very low velocity eastward motion of the northern Pannonian block (ALCAPA) into the system. A solid wedge attached to the moving wall represented the Eastern Alpine region, whereas the rest of the Plexiglas wall modelled the Dinaric orogen (*Fig. 3.6*). The angle between the two faces of the advancing wall was chosen conform to the distribution of horizontal motions originating from the "Adria-push" and the extrusion. Apart from the more precise approximation of the indenter geometry, this experiment enabled preliminary investigation of the 3D structural development.

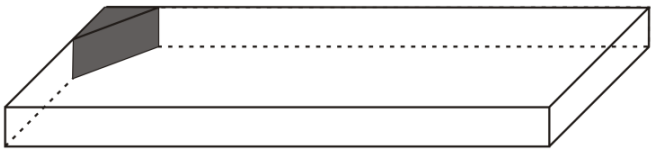

Figure 3.6 *Type-3 models with an additional oblique component of indentation. The grey wedge in the corner represented the lateral extrusion from the Eastern Alps, whereas the moving wall, the compression from the Dinarides.*

During the model run, formation and gradual development of three thrust belts were taking place (*Fig. 3.7a*). First, a doubly-verging thrust appeared in contact with the indenter system, which later fully evolved as a pop-up structure. It was followed by a second thrust zone in a considerable distance from the indenters. Finally, a third pair of thrusts began to develop almost at the centre of the model. The axes of the thrust belts ran roughly parallel to the shape of the indenter. Apparently, deformation of the brittle crust occurred exclusively in the first half of the model, whereas in the vicinity of the fixed wall no major feature developed in the brittle crust.

The frozen model was cut along profiles perpendicular to the two sides of the indenter. This way, in addition to the previous direction, equivalent of a NE-SW orientation in nature, the presented cross sections visualised the structures along an E-W profile as well

(*Fig. 3.7c, e*). In all these profiles, sand layers exhibited the combination of large-scale lithospheric folding (λ≈11-12 cm) and intensive thrust faulting. The three thrust zones exhibited varying internal structure in both directions (*see Fig. 3.7c, e*). From the sidewalls towards the central part, along the axes of the three thrust belts, rapid lateral changes occurred in the vergence of the thrusts. Pop-up and pop-down structures also frequently alternated with single fore- or backthrusts. Minor strike-slip movements accompanied the development of the thrusts, particularly at the contact of thrusts of opposite vergence. The presence of such a shear component is likely to be attributed to the indenter geometry. Instead of brittle faulting, gentle but noticeable folding characterised the upper-crust layers close to the fixed wall. The large-scale folding was decipherable in every cross section with amplitudes comparable to Type-1 models.

Elevated topography and amplified uplift, exceeding 5 mm in the model, characterised the first thrust-system, which then decreased to 2 mm in the second and 1 mm in the last thrust zone. Depressions (1-2 mm depth range) were located between the surrounding thrusts. Sub-millimetre variations of the topography were documented on the laser scan images in the areas unaffected by thrusting (*Fig. 3.7b*).

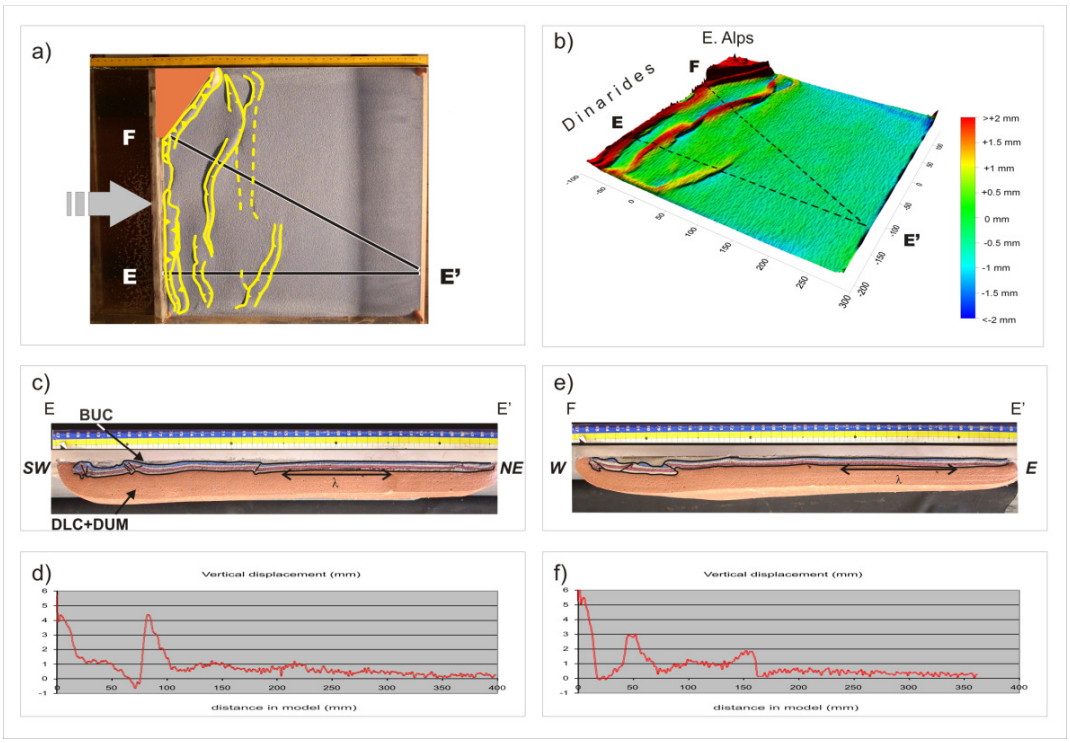

Figure 3.7 *Thrust-belts generated in Type-3 models demonstrated strain localisation. Remarkable lateral changes occurred along the axes of the thrusts in consequence of the indenter geometry (Figs. 3.3 & 3.5 provide a detailed description of data sources obtained from the analogue models and legend).*

3.5 Discussion

The three types of analogue experiments and complementary tests gave valuable insights into the mechanism of the folding of the weak Pannonian lithosphere under various conditions. The successfully reconstructed first-order characteristics of the recent vertical motions and the surface morphology reflect the large-scale deformation of the weak lithosphere. In the following sections, the results are analysed in the light of the processes addressed in the introduction.

3.5.1 Quantification of lithospheric folding and vertical movements

All types of experiments showed the gentle buckling of the weak silicone and the brittle sand layers, which together simulated the Pannonian lithosphere. Converting the periodicity of the folds in Type-1 and Type-3 models to the natural scale, a wavelength of 350-400 km was obtained for lithospheric folds. These values are in good agreement with the findings of Cloetingh et al., (1999) and with the inferences relying on the collected geological and geophysical data in the Pannonian basin (Horváth & Cloetingh, 1996; Cloetingh et al., 2005b; Horváth et al., 2006a).

Using the DEMs of Type-1 model and calculating the power spectrum of the vertical displacements in the model, the characteristic spatial wavelength of the surface deformation was also estimated. According to these calculations, an average 410 km long wavelength component is responsible for the most intensive deformation reflected by the surface (*Fig. 3.8a*). It is in perfect alignment with the long wavelength of folding in numerical models performed by Horváth and Cloetingh (1996). By means of numerical model runs, Jarosinski et al. (2011) have more recently analysed the lithosphere folds accounting for the inversion of the Pannonian basin. They inferred evolution of folds at three distinct wavelengths. The longest one was again in the order of 400 km, the intermediate was found to be at around 100 km and the shortest being 20-30 km. Existence of these modes are supported by a large number of seismic data from the basin interior (for instance visible in regional sections shown in *Fig. 2.7*) and geological observations. Local peaks of the deformation intensity derived from the surface of the analogue experiments are exactly at the above-mentioned three wavelengths (see *Fig. 3.8a*). Type-2 models revealed that intensive deformation occurred at multiple wavelengths due to the position of thicker and, thus, stronger crust units (*Fig. 3.8b-c*).

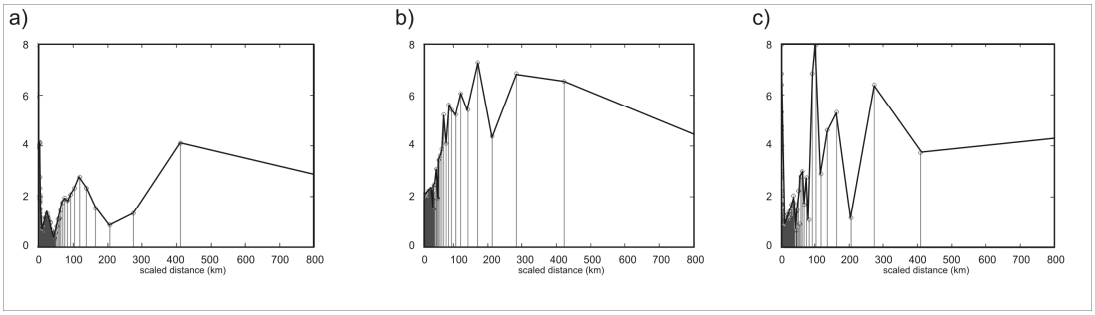

Figure 3.8 *Power spectra illustrate the predominant spatial wavelengths causing the most intensive surface deformation in cases of a) Type-1 and b-c) Type-2 models with weak-strong-weak-strong set-up and reverse configuration, respectively.*

These heterogeneities may as well explain the observed deviations from the overall long wavelength folding and enhance the activity of documented basin-scale or regional folds in the Pannonian basin (Horváth 1995; Horváth et al., 2006a).

The amount of vertical displacements in the orogens derived from the analogue models is between 4 and 5.8 km. These values are in line with the considerations on the Neogene uplift observed in the Dinarides (Ilic & Neubauer, 2005) and with the estimated 2-4 mm/yr Quaternary uplift rate (Marovic et al., 2003). As for the Carpathians, a similarly good agreement was found between previous estimations on the overall amount of uplift and erosion during Pliocene-Quaternary times (Popescu & Lazarescu, 1988; Sanders et al., 1999). However, the derived values misfit with the latest thermochronolgical data from the Carpathians (Merten et al., 2010; Merten, 2011). Time temperature histories evidenced 4-5 km exhumation in the SE Carpathian orogen during the last 2-3 My. The data also suggest that Pliocene-Quaternary exhumation did not affect the eastern part of the Carpathian orogen. These discrepancies highlight that the actual tectonic complexity of the Carpathian orogen was simplified within the 2D analogue experiments.

Concerning the experimental basin interior, folding created moderately deep basins and generated slightly lower amount of coeval uplift. According to statistics performed on the series of laser scan images of Type-1 models, average uplift and subsidence scaled to nature was between 500-700 m and 1.4-1.8 km. Observed apparent asymmetry in the amplitude of folding is assumed to be a result of interference of shorter wavelength folds due to rearrangement of load during deformation. Type-2 models with initially built-in heterogeneities, and consequently uneven distribution of load, exemplify this phenomenon even better.

In this aspect, it is again worth to make a comparison to numerical model results. Finite-element models adopting uniform elastic rheology for the Pannonian basin could successfully generate uplift in the order of few hundred metres (Horváth & Cloetingh, 1996; Cloetingh et al., 1999). On the other hand, these models yielded subdued amount of subsidence compared to the significant Quaternary sedimentary successions having been

deposited in the deep sub-basins. The amplitude of the lithospheric folding that is the amount of recent vertical motion inferred from the analogue models seems to be closer to the estimated values relying on field observations (*Fig. 3.3d*). Ranges for the amount of Quaternary vertical displacement are recalled from *Section 2.2*. The sequence of Pliocene-Quaternary sediment in-fill preserved in the deepest sub-basins of the Great Hungarian Plain reaches or even excesses 1 km compacted thickness (e.g. Juhász et al., 2006). Estimated values on the recent uplift by means of various dating methods applied on mostly young rocks (e.g. Ruszkiczay-Rüdiger et al., 2005a,b) or inferred from geomorphologic studies (Pécsi, 1959) range between 200-600 m, though with temporal changes in the rate (Szanyi et al., 2009).

As demonstrated by Cloetingh et al. (1989), incorporation of a more realistic brittle-ductile rheology can increase the magnitude of stress-induced vertical motions to kilometres. In particular, for a state of stress being close to the integrated lithospheric strength, such as it appears to be the case for the Pannonian lithosphere. The presented results demonstrate that physical tectonic models, perhaps owing to a better representation of load redistribution or the competence contrast can successfully cope with this problem at least for the case of an extremely weak lithosphere. These findings further corroborate the idea that irregular folding of the lithosphere can account for the subsidence and uplift pattern of the Pannonian basin especially in the presence of lateral heterogeneities within the crust. It is needless to say that other mechanisms such as the general post-rift thermal relaxation, isostatic adjustments, perhaps small-scale mantle convection or anomalies in the accumulation and compaction of sediments, have definitely contributed to the late-stage subsidence and uplift history. The outcome of the analogue tectonic model series demonstrates that stress-induced deflection of the weak Pannonian lithosphere is a plausible mechanism to control basin inversion and is capable to produce such amounts of differential vertical movements.

3.5.2 Timing of positive structural inversion due to lithospheric folding

Tectonic regimes in the Pannonian region show significant lateral variations. The style of deformation at the margins of Adria is mostly thrusting, often in combination with strike-slip faulting, reflecting oblique convergence between Adria and the Alps–Dinarides. The dominant style of deformation gradually shifts from transpression in the south and southwest to strike-slip faulting in the more central parts of the basin system. Although contraction is decreasing towards NE, compression is assumed to be transmitted across the entire basin resulting in shortening as far as in the W and NE Carpathians (Bada et al., 2007a, *Fig.3.9*).

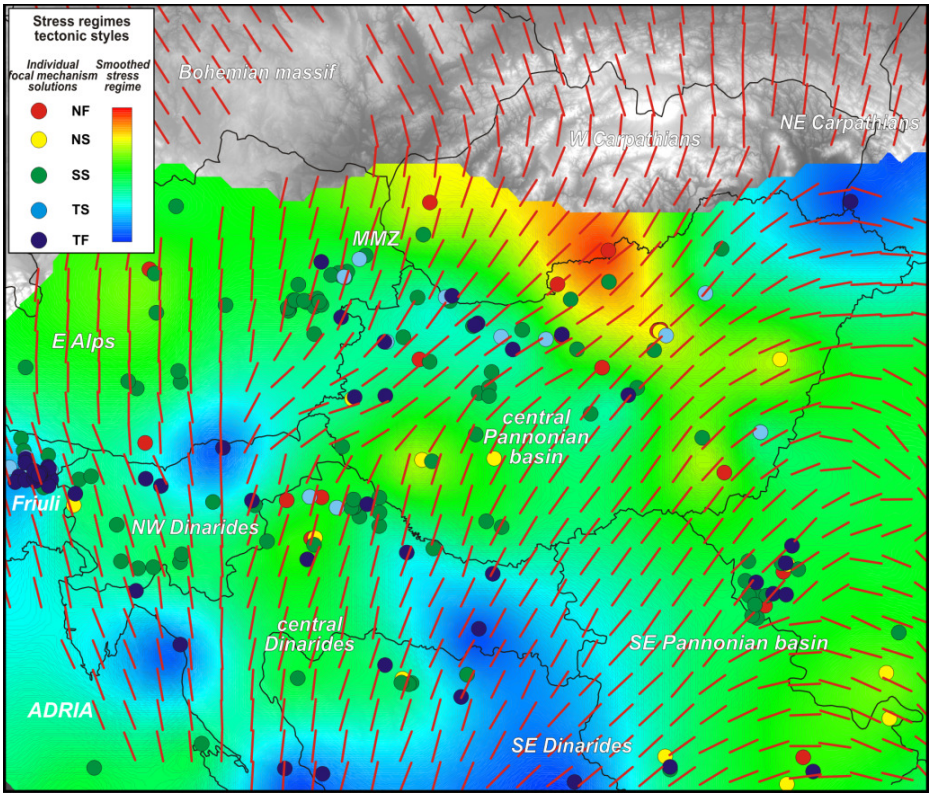

Figure 3.9 *Spatial distribution of tectonic regimes across the Pannonian basin from Bada et al., 2007a. Individual focal mechanism solutions and the derived smoothed regimes are colour-coded. NF = normal faulting, NS = transtension, SS = strike-slip faulting, TS = transpression and TF = thrust faulting. Red sticks represent the smoothed stress trajectories. Note how rare normal faults are in the basin interior and strike-slip faulting being superior to it.*

A rough estimation could be given on how effectively the continuous push from the analogue Adriatic indenter, leading to the folding of the weak lithosphere, is manifested in a recognisable amount of uplift. Using the top-view photos, the structural development at the fixed wall of the plexiglas tank representing the margin of the East European Platform was detected. The first occurrence of the positive structural inversion in Type-1 models was found to appear no more than 5-6 My if scaled up to the natural case (Dombrádi et al., 2008) and could be considered as an upper estimate. Enlarged high-resolution laser scan sections are presented to better illustrate and more accurately assess the time span required for the advance of deformation (*Fig. 3.10*). The prerequisite of the estimation was the time ratio (*see Section 3.3.2 & Table 3.1*) and the moment when the scan image was taken. In this way, it became possible to determine when the first pronounced uplift occurred in the model and convert it back to the geological timescale. According to this method, transmission of strain across the homogeneous two-layer model (Type-1) would be equivalent to 2.8-3.2 My on the geological timescale. It largely corresponds to the generally proposed time-span of the basin inversion ongoing from Pliocene-Quaternary times. The estimation is solely based on the detected surface uplift. It is to be emphasised that the internal deformation could not be documented through time. Therefore, the onset

of inversion in the model may have started earlier without detectable changes on the surface. Interpretation of 2D and 3D industrial seismic data both in the eastern and western parts revealed structures and stratigraphic indicators, which call for inversion starting even in the Late Miocene times.

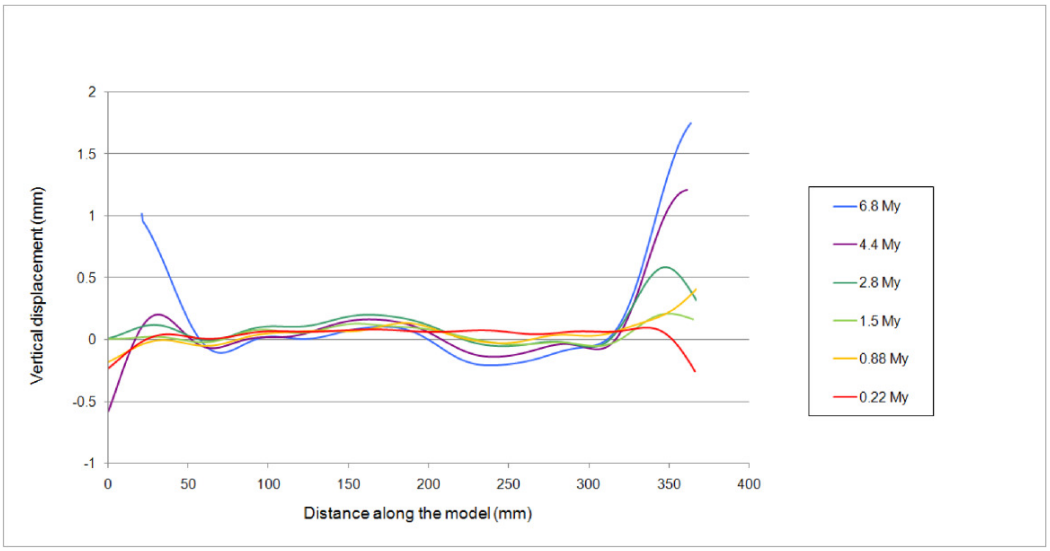

Figure 3.10 *Temporal evolution of the Type-1 models along AA' profile (Fig. 3.3) through certain scaled time-steps demonstrating the gradual appearance of folding. The amount of vertical movements was corrected for the general uplift due to closed model environment. Note that amount of uplift and subsidence is somewhat subdued compared to the values presented in Fig. 3.3 because of larger window of moving average.*

Admittedly, the model also strongly simplifies the complex tectonic scenario and several effects are neglected, which may account for local and/or regional changes in the stress field. Stress field data indicates that the inversion may somewhat be hampered in the eastern Pannonian basin perhaps due to sub-crustal processes and thermal effects resulting from the asthenospheric dome and associated thermal and density perturbations (Bada et al., 2007a). In spite of this simplification, Type-1 models provided a reasonable estimate.

3.5.3 Role of pre-deformation crustal thickness variations

As a general conclusion, the stronger crustal blocks in Type-2 experiments profoundly affected the style of lithospheric folding. In the first case (*Fig. 3.5a*), deformation was mainly localised in the narrow thin-crustal part close to the indenter (A), producing an extensive pop-up system, which in nature would form an unrealistic 40-45 km high mountain belt. The stronger unit (B) was slightly folded with a wavelength in the order of ~120-150 km and a second moderate thrust evolved at the contact of the strong and subsequent weaker part. The remaining two units (C and D) seemed to be rather undeformed with the lack of any significant vertical movement at the distal wall.

A shift to shorter wavelength deformation was more visible in the inverse configuration of the different crustal blocks in Type-2 models. The strong-weak-strong-weak set-up

(*Fig. 3.5e*) favoured the existence of very intensive short wavelength (<100 km in nature) folds in the first weak unit (B) and somewhat larger scaled wavelength (120-150 km) in the subsequent thick-crustal block (C). A significantly slower rate of increase in amplitude, i.e. uplift, was inferred due to the thicker and stronger parts of the lithosphere. Under such circumstances, the onset of observable positive deflection of the modelled area after the start of shortening corresponded to 4.5-4.75 My on the geological timescale. The final amplitude of the folded layers was found fairly similar to the values of Type-1 models in both cases.

It is obvious from the results of Type-2 conceptual models that deformation of the weak and thinned Pannonian lithosphere is fairly sensitive to crustal heterogeneities. It is also likely that multi-scale folding in the basin interior (Cloetingh et al., 2006) can partly be attributed to the lateral variation of crustal thickness, which leads to modified wavelengths of folding and their superposition. Since sedimentation and erosion are absent from these models, the 2D interpretation, at this stage, does not permit a direct comparison to subsidence or uplift history. Instead it is to be considered as a process-oriented study. Nevertheless, the results may be relevant to the actual uplift history of Transdanubia and the late-stage evolution of deep sub-basins in the Great Hungarian Plain, where accelerated rate of subsidence was documented.

3.5.4 Role of indenter geometry, outlook to 3D interpretation

A step towards a more precise simulation of the natural geometric boundaries was taken by adding an oblique component of shortening from the direction of the Eastern Alps and, thus, a simple 3D interpretation. As a first inference, three thrust systems with decreasing size were formed during the advance of deformation. The first pop-up structure has undergone an intensive uplift reaching an equivalent level of 10 km altitude, while the subsequent thrusts were uplifted by 2-4.5 km. It is to be emphasised again that these models are performed in the lack of any erosional processes. Interestingly enough, changing only the indenter geometry and maintaining the homogeneous crustal layer resulted in strain localisation.

Moderate uplift also took place adjacent to the fixed wall with a time-lag compared to the Type-1 model. Calculations yielded a 4.6-6.8 My scaled time interval for the beginning of uplift. The larger time lag observed in the 3D setting compared to that of the 2D Type-1 models is in slight contradiction with widely accepted time of onset of the inversion (i.e. Late Pliocene). Inversion in the Dinarides, however, appears to start in the Late Miocene (Ilic & Neubauer, 2005) and similar ages are put forward for the SW part of Transdanubia (Zala hills) according to results of stratigraphic interpretation (Uhrin et al., 2009).

In the proximity of the indenter, the intensive brittle deformation prevailed over the large-scale folding, which became more dominant towards the distal wall. The observed wavelength was in the order of Type-1 models, whereas the amplitudes were slightly reduced. Due to the indenter geometry, the internal structure of the thrust-belts showed

significant lateral changes, presence of small-scale shear components could be observed within the thrust zones.

In this simple set-up, the development of the first thrust belt can be regarded as the Neogene evolution of the already existing Dinaric orogenic belt, which is characterised by a marked Late Neogene-Quaternary uplift. The second pop-up system is attributed to the Sava fold belts (*Figs. 2.1 & 2.2*), where significant uplift (ca. 700 m) of the Slavonian Mts., bounded by reverse faults, is documented during the Quaternary (Pavelic, 2001). Young folded structures are also reported from the border zone of the Alpine and Dinaric orogens in northern Croatia (Tomljenovic & Csontos, 2001). The initiating third thrust system may be correlated to the pop-up systems in the Mecsek hills and the Fruska Gora Mts. in Serbia (*Fig. 3.11*).

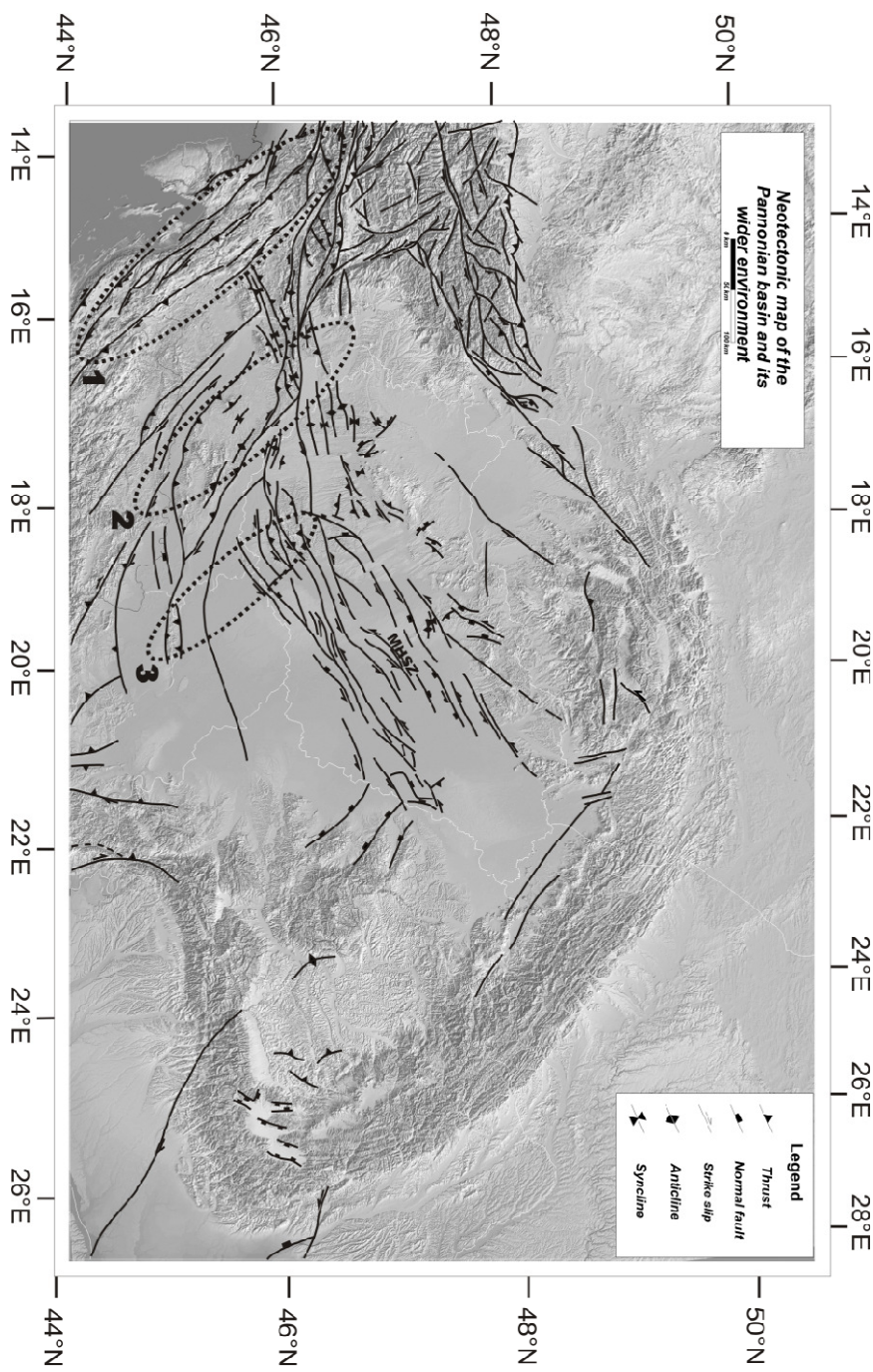

Figure 3.11 *Neotectonic structures in the Alpine-Dinarides-Pannonian basin-Carpathians system. The figure is based on the map compiled in the framework of the OTKA project entitled 'Atlas of the present-day geodynamics of the Pannonian basin: euroconform map series and explanatory text' (project reg. no.: T034928). http://geophysics.elte.hu/atlas/atlas_geodin.htm. MHSZ denotes the Mid-Hungarian Shear Zone. The three numbered ellipses mark the natural equivalents of the pop-up systems developed in Type-3 models.*

Although during the Late Miocene-Quaternary evolution of the Dinarides, structural data indicates reactivation of several reverse faults due to the compressional setting, especially

in the northern parts (Tari & Pamic, 1998), the central region can be characterised as a transpressional tectonic regime. Kinematics of the Alpine-Dinaric domain is controlled by large strike-slip structures such as the Peri-Adriatic Line, Drava Fault or the Lavanntal fault (e.g. Prelogovic et al., 1997; Bada et al., 2007a, *Figs. 2.2 & 3.11*), which were not incorporated into Type-3 models. It is obvious that a more detailed 3D analogue structural reconstruction of the Dinaric region requires implementation of these faults. Similarly, the Mid-Hungarian Shear Zone is a key element in the accommodation of deformation stress data indicates a gradual change to strike-slip regimes towards the basin interior (*Fig. 3.9*, Bada et al., 2007a).

In summary, it is concluded from 2D analogue models of Type-2 and -3 that crustal heterogeneities as well as the indenter geometry may significantly influence the style of lithospheric folding and related tectonic topography. In order to design analogue models capable to target analysis of 3D pattern of recent vertical motions and kinematics in the Pannonian-Carpathian system, further constraints on the spatial distribution of different crust units and incorporation of major inherited structures are necessary. Certainly a full reconstruction cannot be expected from a lithospheric-scale analogue model but the role of the most significant tectonic elements is worth to be tested.

Locally, crustal-scale models provide a solution for the detailed analysis of faults and related kinematics. For instance, recently, the Mur-Mürz line was investigated by a series of crustal-scale analogue models (van Gelder, 2010). Although the experiments focused on the kinematics and dynamics of extrusion, there are interesting conclusions with respect to the inversion phase as well. It was found that fixing the boundary in the Carpathian orogen, which represents the onset of collision, inversion of sub-basins commenced although lateral displacement along strike-slip structures did not vanish but the slip rate significantly decreased. Since the base of the models was of ductile silicone putty, simulating the uppermost 10 km of the lower crust, it points towards potential ductile energy dissipation on a whole lithosphere-scale.

3.5.5 Inferences on the mechanism of folding of the weak lithosphere

The mechanism of topography-induced stresses triggering folding of the weak lithosphere was also investigated. The role of vertical loads exerting horizontal stresses in a weak, two-layer lithosphere system was tested. According to the observations, in absence of the crustal material, the mantle lithosphere underwent only pure thickening regardless of the strain rate. These findings confirm the primary role of the brittle upper crust in initiating the deflection of the whole lithosphere. The importance of gravitational stresses in addition to plate boundary forces in compressional setting has been discussed by several authors (e.g. Fleitout & Froidevaux, 1982; Richardson & Coblentz, 1994; Gölke & Coblentz, 1996). Numerical model calculations confirmed their significance for the case of the Pannonian weak lithosphere (Bada et al., 2001). The sequence of laser scans of Type-1 models evidenced that the folding commenced after the orogens at the indenter and the fixed wall were already formed (*Fig. 3.12*).

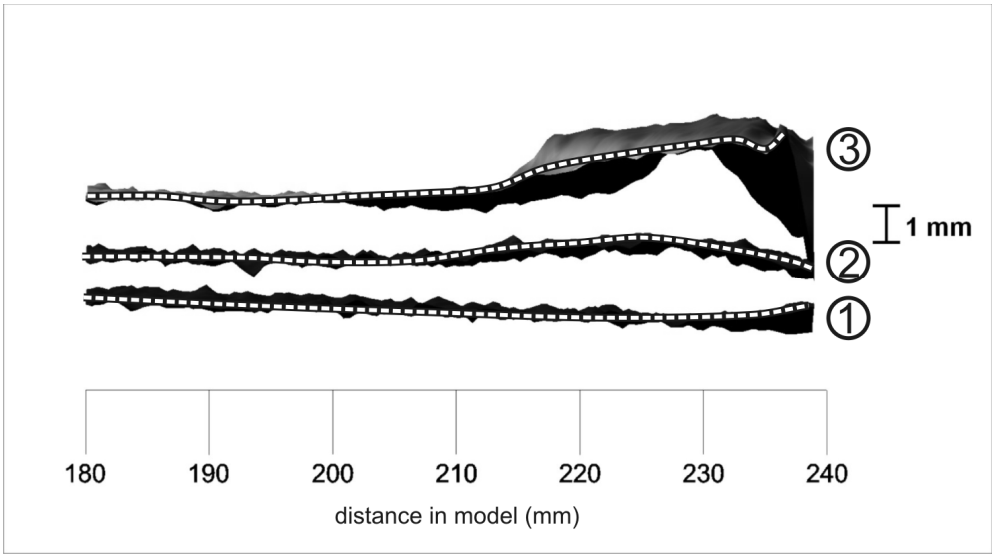

Figure 3.12 *Laser scan surfaces taken in front of the fixed distal wall, representing the East European Platform, to detect the gradual increase of the amplitude of folding and related positive structural inversion. White dashed lines mark the edge of the surface along profile AA', in the vicinity of the fixed wall of the tank (Fig. 3.3). 1: un-deformed model, 2: commence of detectable uplift, 3: developed surface after completing the experiment.*

To track the model evolution due to various vertical loads more precisely, sand wedges of brittle behaviour were deployed at both margins of the model. The extra vertical load of the surrounding orogens represented by these sand wedges easily initiated the folding process. Gentle folding of the lithosphere took place parallel to the orogen development (*see Fig. 3.13*). The recorded wavelengths in these combined experiments align with results of previous analogue models on the folding of the Pannonian lithosphere.

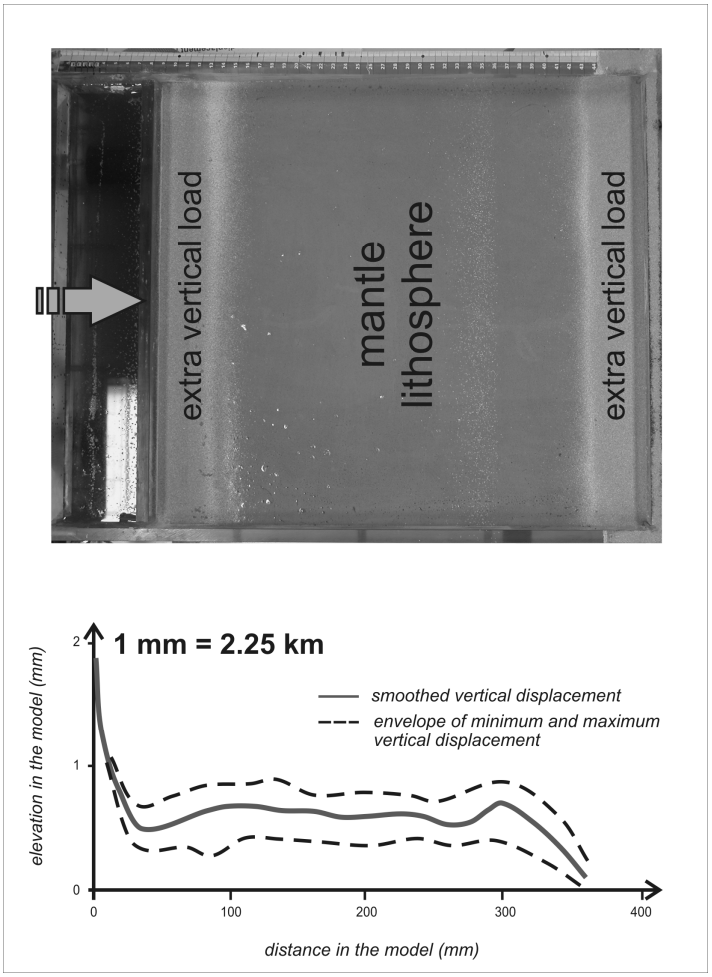

Figure 3.13 *The silicone putty to represent the ductile Pannonian mantle lithosphere was loaded with sand piles at the margins to test the role of the vertical load of the surrounding orogens. The lower panel shows the amount of vertical displacement during the model deformation. The smoothed trendline (solid curve) and the envelope of the data points (black dashed lines) show the difference between the final stage and the undeformed model (the right end of the curve is truncated).*

Consequently, the gravitational forces due to topographic relief differences in the surrounding orogens exert horizontal compression and efficiently contribute to the deformation of the Pannonian lithosphere (Bada et al., 2001; Pascal & Cloetingh, 2009).

3.6 Conceptual models of the shear zones across the Pannonian basin

As pointed out in *Section 3.5.4* and displayed in *Fig. 3.11* several shear zones have been mobilised during the tectonic reactivation of the basin. The largest among them is the Mid-Hungarian Shear Zone. A fully detailed, complete 3D reconstruction is perhaps beyond the possibilities of the analogue modelling technique, especially in terms of scaling, which does not allow investigation of smaller scale structures. Nevertheless, some exploratory work has been done to gain insight into how shear zones modify the results of the previously inferred pattern of folding and thrusting. Main results of two types of conceptual models are presented.

Type-4 models dealt with a wide, oblique weak zone connecting the indenter and the backstop in a set-up same as used in case of Type-3 models. Ultimate goal of these models was to investigate whether folding of the lithosphere still occurs in such a setting and whether parameters of thrust development and/or folding are modified in the presence of the weak zone.

Type-5 models incorporated several weak zones emplaced into the brittle upper crust. The indenter was a single plane but the backstop exhibited differences in geometry and rheology. The scope of the models was to simulate the present-day geodynamic scenario in very simplistic form and to investigate how displacement along the weak zones is distributed in consequence of the different kinematic (and rheologic) boundary conditions. More specifically, the southern Pannonian unit (Tisza-Dacia) can escape towards the SE Carpathians (Vrancea zone), where slab detachment / tear-off is still taking place, whereas the movement of the northern terrane (ALCAPA) is completely blocked. A secondary, but not less important, aspect was to observe the deformation of the brittle crust overlying the implemented weak zones. In the following sub-sections, instead of the very detailed description of the modelling procedure, only the main highlights are presented and briefly discussed.

3.6.1 Type-4 models: oblique shear zone

Except for the thin, weak silicone layer emplaced onto the experimental lithosphere, Type-4 models had exactly the same set-up as Type-3 ones (*Fig. 3.14*). Density and viscosity of the selected material was in the order of that of the model lithosphere but slightly lower. The strike of the weak zone was selected to largely correspond to the actual direction of the Mid-Hungarian Shear Zone.

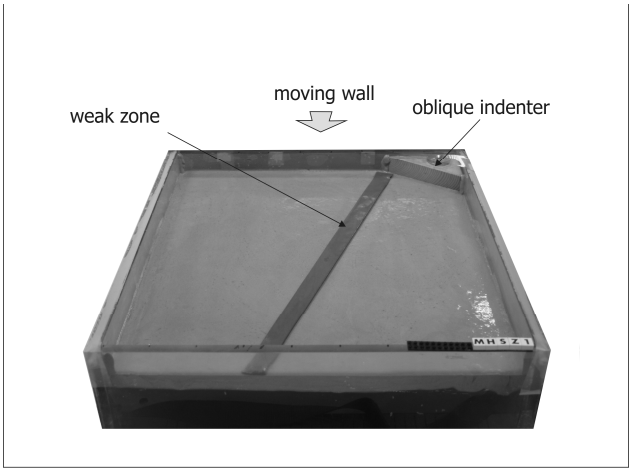

Figure 3.14 *Photo taken before sieving the sand on the model surface to illustrate the structure of model lithosphere for Type-4 models.*

The major contrast in the recorded structural evolution after the same amount of bulk shortening as in Type-3 models was that formation of the thrust belts was restricted to the proximity of the indenters (*Fig. 3.15a*). Apparently, a significant amount of deformation was absorbed in a ductile manner, taken up by the shear zone and transformed into folding of the weak lithosphere. Horizontal displacement along the shear zone is reflected by the central part of the second thrust belt. The central part of the belt is detached and offset from the one in the corner zone and much less developed, indicating strain partitioning.

A DEM of the model surface displayed similar characteristics in terms of large-scale subsidence and uplift pattern as observed before in Type-1 & -2 models (*Fig. 3.15b*). In Type-3 models deformation was localised and intensive thrust building was concentrated in the first half of the model, making folding structures hardly detectable in the distal part. Implementation of the weak zone seems to have resulted in a more widespread folding at least with observable amplitudes compared to results of Type-3 models.

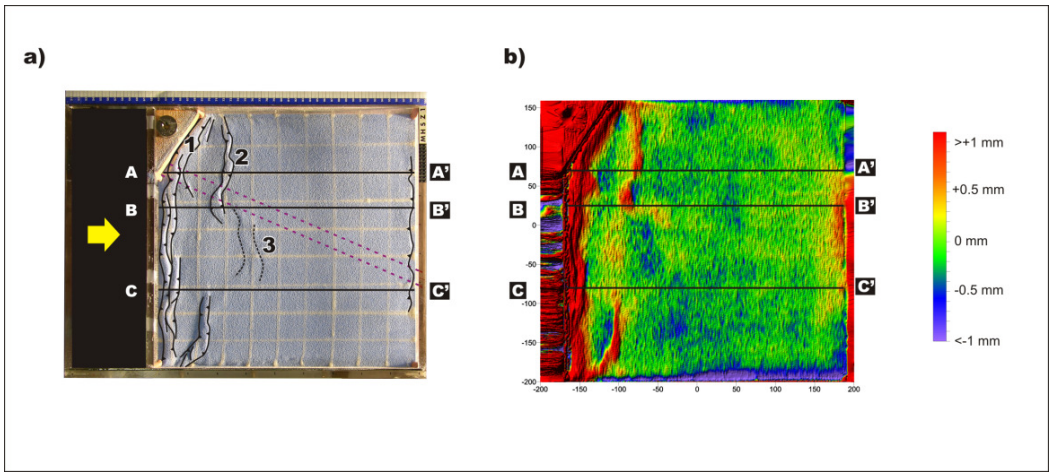

Figure 3.15 *Plan view of the model surface in a) photo with the interpreted first-order structural elements and b) high-resolution laser scan image depicting the relative differences in vertical movements. Yellow arrow marks the direction of the push of the moving wall. Cross-sections and topography of the labelled profiles are shown in Fig. 3.16. Dashed lines indicate the outline of the oblique weak zone. Numbers denote the three generations of uplifted areas within the model.*

Cross-sections cut from the model reveal a combination of thrusting close to the indenter, often transpressional behaviour of the weak zone (e.g. *Fig. 3.16b*) and gentle folding of the lithosphere. Multiple modes of folding can be deduced upon the corresponding topographic profiles derived from the DEM of the model (*Fig. 3.16a-c*). Among the clearly visible wavelengths, on the basis of the scaling ratio of the previous models, the longest equates to $\lambda \approx 400$ km in nature and the $\lambda \approx 100$ km can also be found.

In comparison with Type-3 models, where the most intensive deformation was recorded by thrust building and limited amount of folding, a combination of thrusting, shear movements and general lithospheric folding have been recorded in Type-4 models. In that sense, the models gave a better reconstruction in the vicinity of the indenters even if in a simplified 3D setting. Interpretation of the model results prove the importance of inherited zones of weakness in the brittle crust during basin inversion and put forward the possibility of the deformation along them co-existent with folding of the lithosphere.

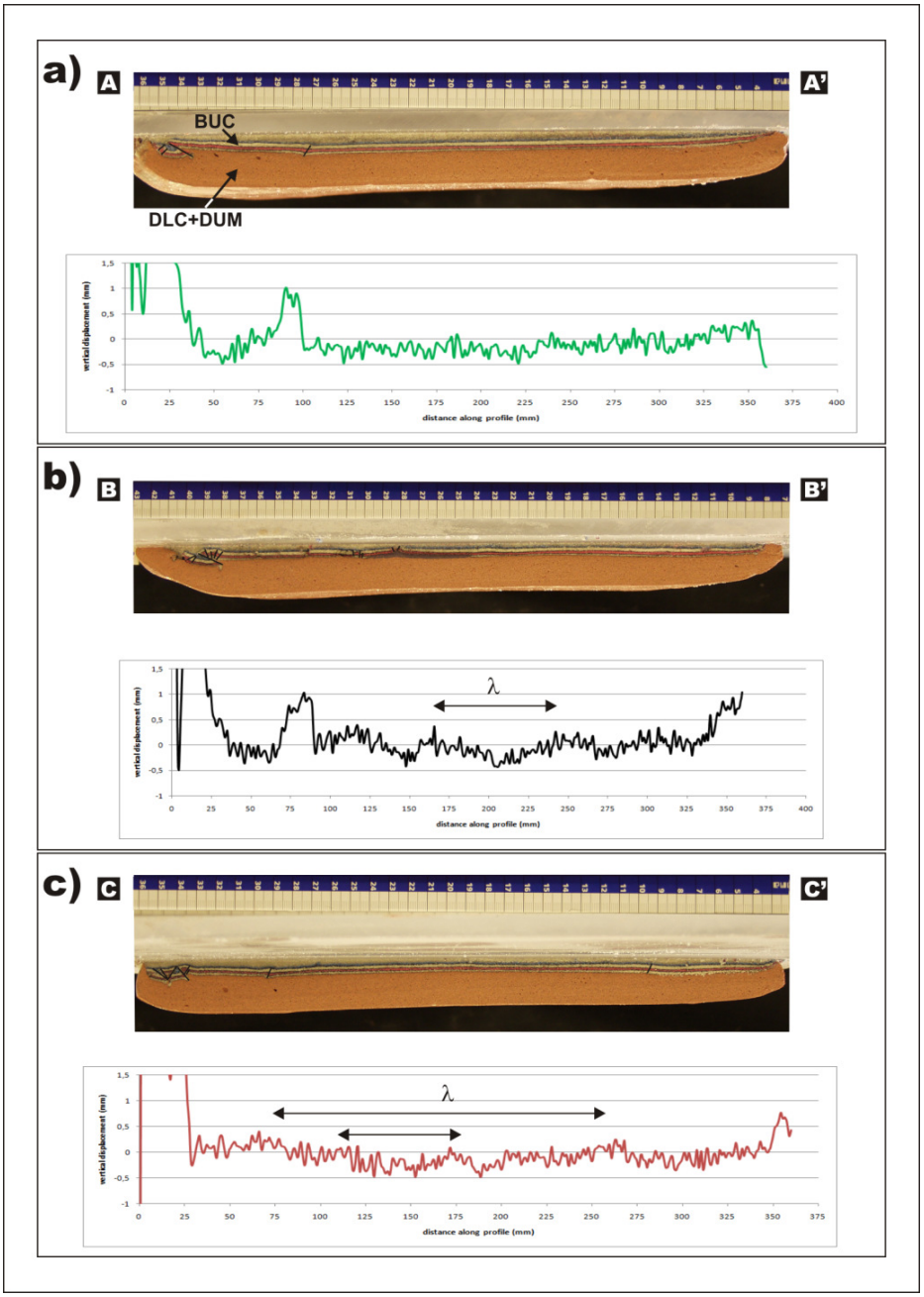

Figure 3.16a-c *Cross-sections cut from the analogue model of Type-4 along the profiles shown in Fig. 3.15. Topographic profiles were sliced from the model surface along the same profiles and converted to relative vertical displacements. Note that the horizontal scale between the model cross-sections and the graphs showing the trends in vertical motion do not always exactly match due to technical difficulties during picture taking. Generally, the two types of data can be well correlated. The profiles exhibit various modes of lithospheric folding: a) very gentle, hardly detectable, b) dominantly short wavelength deformation and c) short wavelength folding superimposed on the longest wavelength folding. BUC and DLC+DUM stand for brittle upper crust and ductile lower crust and mantle, respectively.*

3.6.2 Type-5 models: multiple weak zones in the brittle crust

In addition to the faults belonging to the Mid-Hungarian Shear Zone, mapping of neotectonic structures has revealed several other strike-slip faults in the territory of Hungary and across the border as well (*Fig. 3.17*). The spatial distribution of these faults is fairly consistent within the basin. A set of industrial seismic sections imaging numerous flower structures in the late post-rift strata is given as an example (*Figs. 3.18-3.20*).

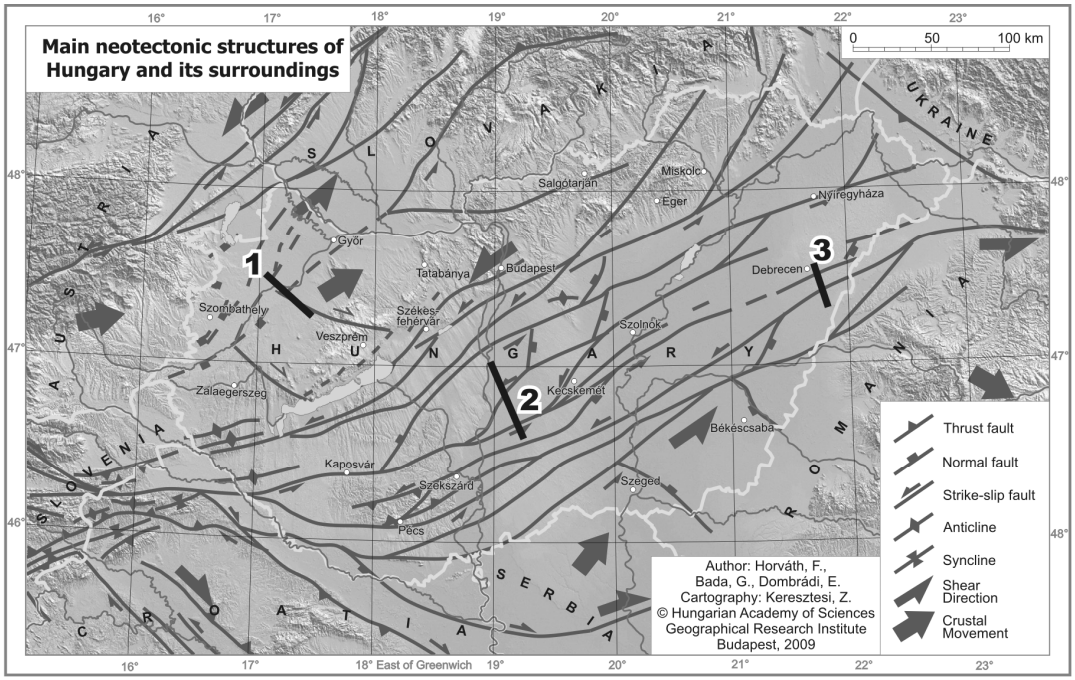

Figure 3.17 *Neotectonic structures mapped in Hungary and neighbouring countries (Horváth et al., 2009). In comparison with Fig. 3.11, more details are shown in the basin interior. Numbered lines represent the location of the interpreted seismic lines shown in Figs. 3.18-3.20.*

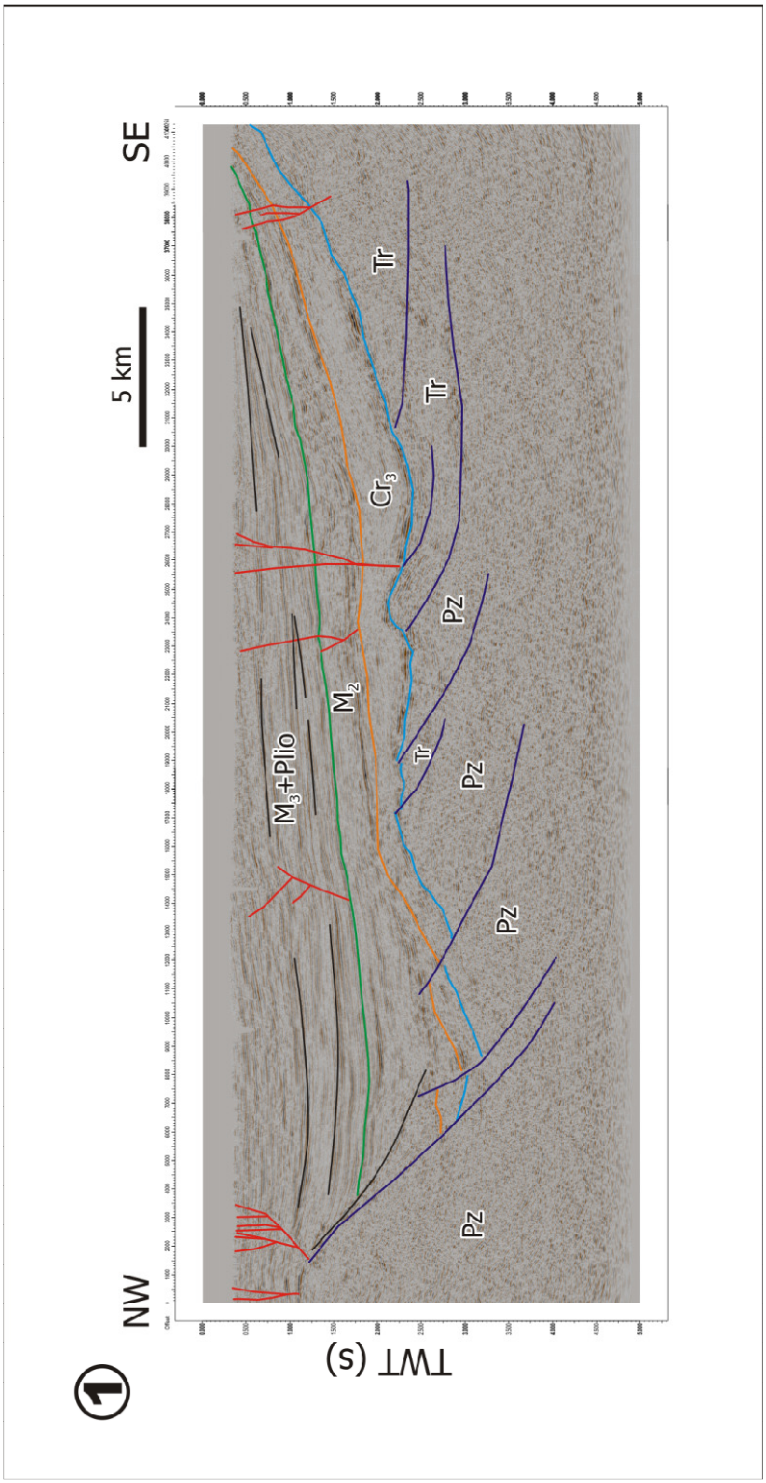

Figure 3.18 *Interpreted seismic time section from the Little Hungarian Plain (Transdanubia) in the foreland of the Eastern Alps (modified after Tari, 1994). Neotectonic faults are coloured in red. The seismic line has imaged numerous flower structures in the post-rift strata. Some are related to the pre-existing thrust planes (blue lines) in the basement, while others appear to detach at a shallower level. Used abbreviations: Pz = Palaeozoic, Tr = Triassic, C_3 = Upper Cretaceous, M_2 = Middle Miocene, M_3+Plio = Upper Miocene (Pannonian) and Pliocene.*

Figure 3.19 *Another example for strike-slip structures penetrating the post-rift sediments. The seismic time section is from the central part of the Pannonian basin, within the Danube-Tisza interfluves. The distribution of the young faults shows similar style as in Fig. 3.18. The used abbreviations stand for as follow: Pz = Palaeozoic, J_{1-2} = Lower to Middle Jurassic, J_3-Cr_1 = Upper Jurassic to Lower Cretaceous, M_{1-2}: Lower to Middle Miocene (syn-rift), M_3+Plio = Upper Miocene and Pliocene (post-rift).*

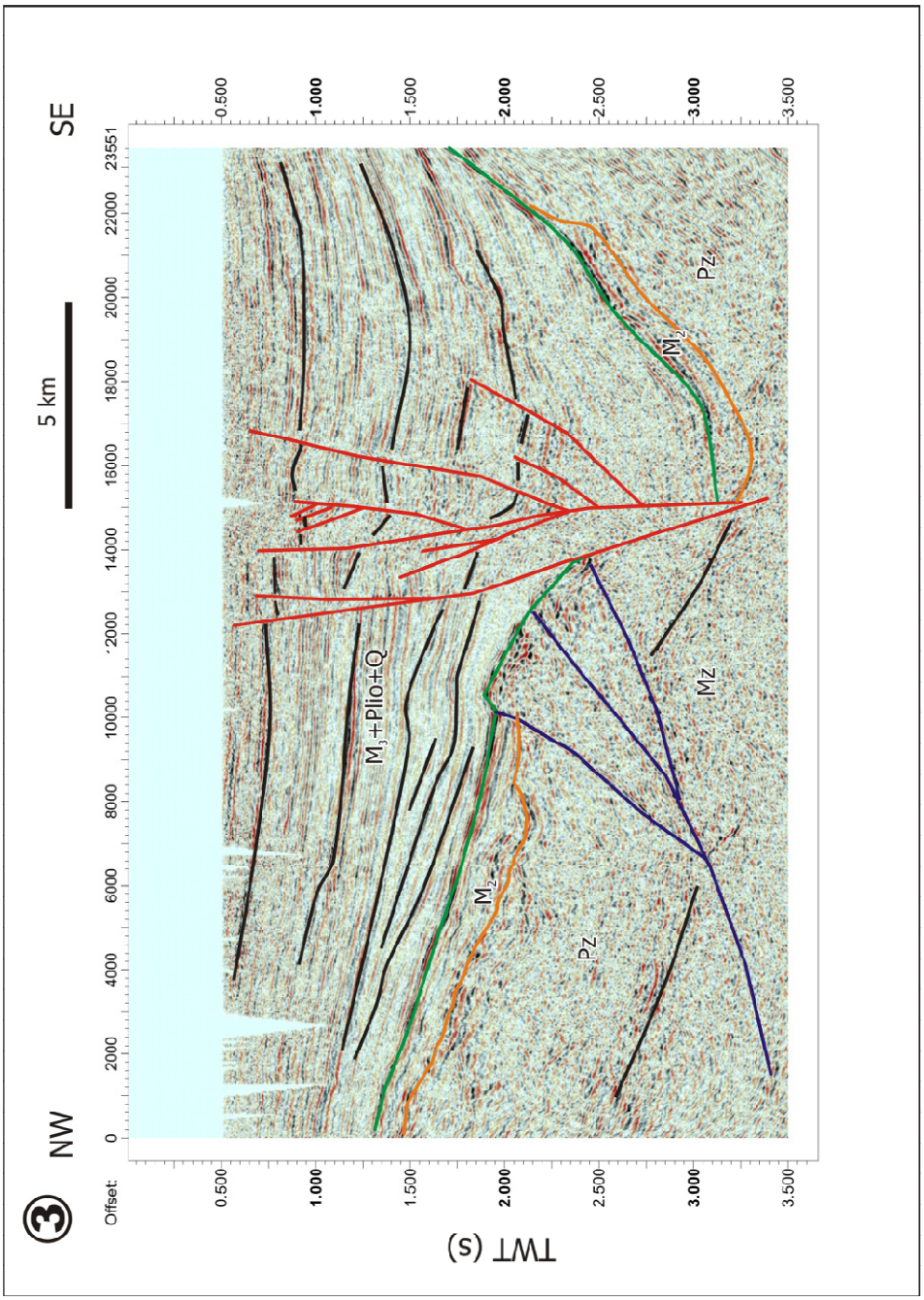

Figure 3.20 *Wrench zone in the eastern part of the Great Hungarian Plain. Seismic time section evidences a large negative flower structure and its young activity deducible from the geometry of the post-rift sediments. Used abbreviations: Pz = Palaeozoic, Mz = Mesozoic, M_2 = Middle Miocene (syn-rift), M_3+Plio+Q = Upper Miocene, Pliocene and Quaternary (post-rift).*

In most cases, the mapped strike-slip structures nucleate along inherited weak zones in the upper crust, usually normal faults of previous Miocene grabens. In Type-5 models multiple weak zones have been incorporated in the model crust to simulate these inherited structures (*Fig. 2.6*). Again the main focus was on the previously inferred folding of the weak Pannonian lithosphere and the activation of the crustal discontinuities.

The sketch in *Fig. 3.21* illustrates the set-up of Type-5 models from a plan view. The major change compared to previous series of experiments is the geometric boundary condition at the backstop. In order to facilitate differential horizontal movement, the rigid backstop representing the East European Platform was brought slightly forwards. The weak material adjacent to it was allowed to reach the glass wall. This boundary condition was to simulate the South Carpathian bend zone, where slab detachment is taking place and the foreland is the relatively weaker Moesian platform playing an essential role in the detachment process (e.g. Cloetingh et al., 2004). It is to be noted that another type of weak silicone putty was also tested to play the role of the soft backstop. However, no significantly weaker behaviour was experienced in comparison with the already weak material constituting the Pannonian experimental lithosphere. Five pieces of oblique weak zones were set in the brittle crust with similar angle than in Type-4 models. This time there was one single indenter applied to avoid complications in the interpretation.

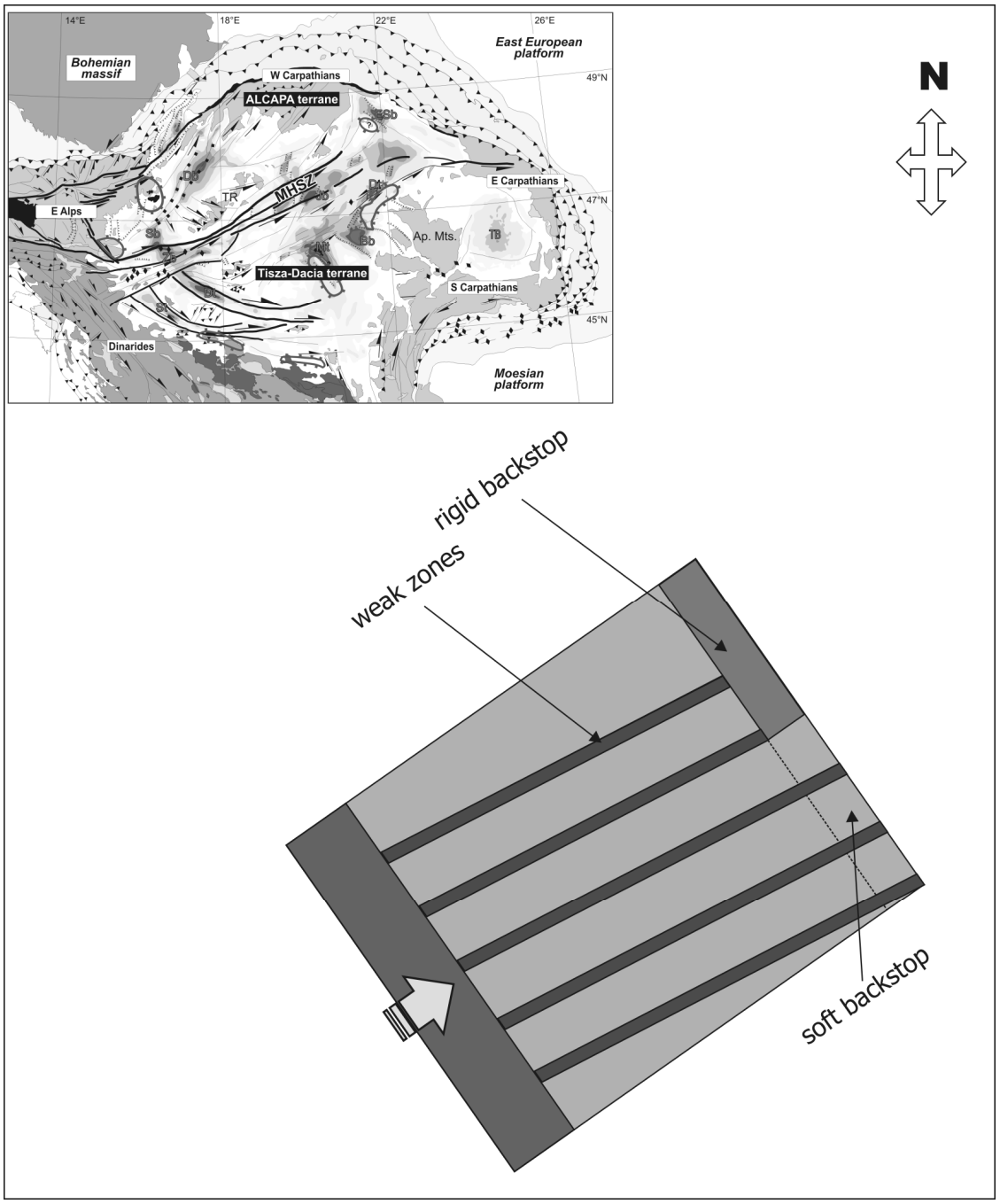

Figure 3.21 *Cartoon for Type-5 model set-up from top-view. As a change, different backstops have been applied and a set of weak zones incorporated in the brittle crust. Yellow arrow indicates the direction of the moving wall. The drawing is rotated to largely match the true north of the modelled area shown in the inset map. Major tectonic units are labelled. For the position of the inherited tectonic structures, see Figs. 2.6 & 3.17.*

The experiments of Type-5 have resulted in localised shortening along two structures. Between them and within the second zone observable sinistral strike-slip faults have developed controlled by the position of the pre-existing weak zones (*Fig. 3.22a*). Interpretation of the second thrust belt advancing more towards the centre of the model in

front of the rigid backstop is not straightforward. It is likely to be connected to the sharp corner of the backstop.

The model topography is dominated by the large pop-up systems (*Fig. 3.22b*). The recorded elevation of thrust located closer to the indenter is 2-3 times higher than in Type-4 models. Part of the second thrust belt, which occupies the central part of the model surface exhibits similar altitude (~1 mm in the model) as those in Type-4 series. In addition to these pronounced topographic features, examined uplift and subsidence trends calculated from the laser scan data along two representative profiles show gentle folding (A-A', *Fig. 3.22c*) or half-wavelengths of lithosphere folds (*Fig. 3.22d*). All in all, folding of the weak lithosphere is confirmed but heavily overprinted by the developed thrusts.

An alternative way of visualising horizontal displacements during the model run was possible owing to the fine grid made of sand on the top of the experimental brittle crust. Calculating the difference in the position of the individual grid nodes prior to (*Fig. 3.23a*) and after the deformation (*Fig. 3.23b*) provides an impression of the overall distribution of horizontal strain (*Fig. 3.23c*). In the proximity of the indenter the difference between the rigid and soft backstops is reflected by the displacement vectors. Displacement is larger in the domain with soft backstop and confirms the idea that Tisza-Dacia having more degree of freedom in terms of kinematic boundary conditions will create larger offset strike-slip faults and/or movements. Towards the distal region of the experimental lithosphere the difference between the two parts of the model diminishes. Recent studies by seismic interpretation and geomorphologic analysis of river terraces suggested ~5 km Quaternary shortening in the SE Carpathians (e.g., Necea et al., 2005; Leever et al., 2006). With regard to the displacements on strike-slip faults it is to be noted that if scaled to nature the trends in horizontal displacement are overestimated by the experiments.

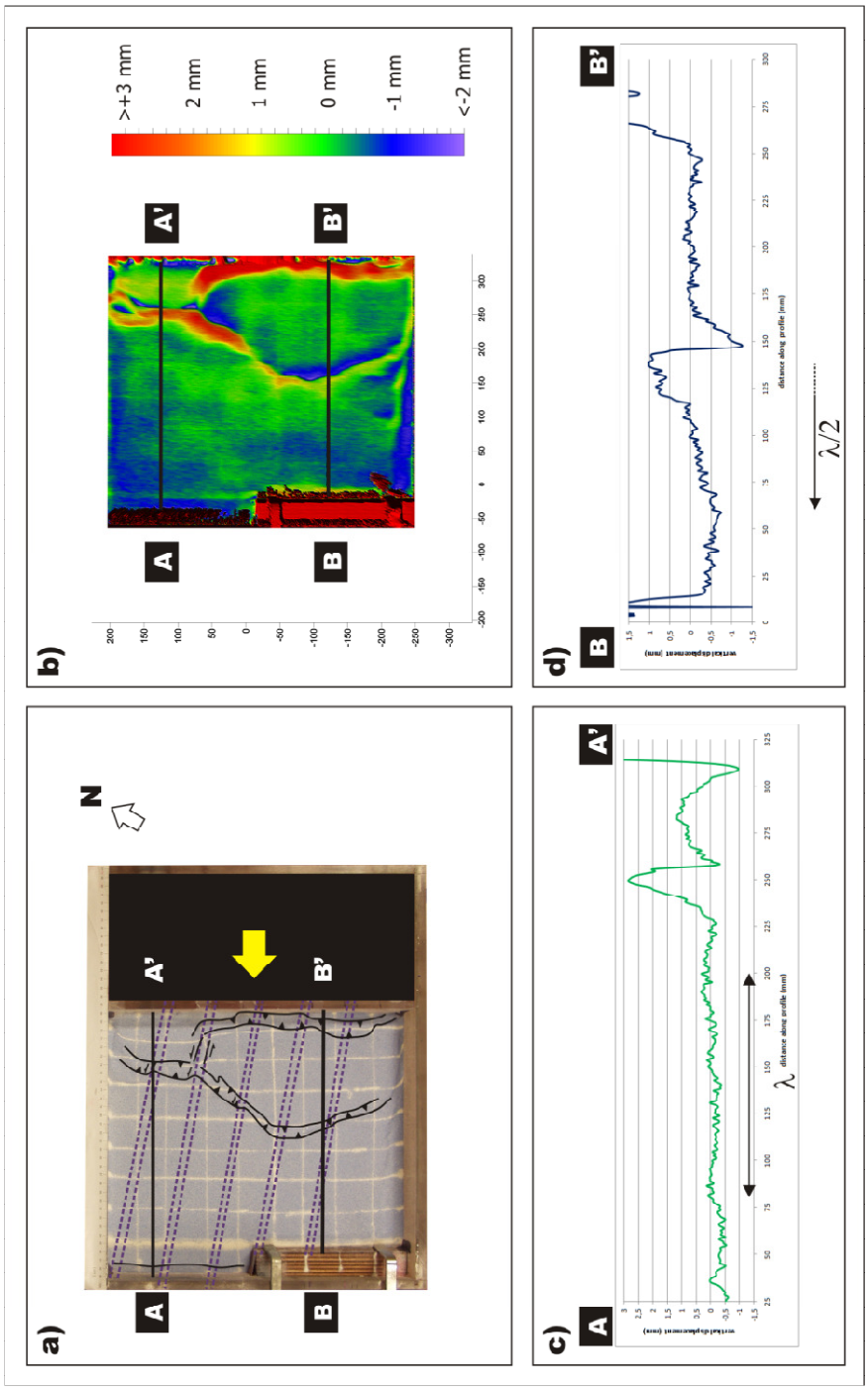

Figure 3.22 *Results of Type-5 models. a) Top-view photo of the model with structural interpretation. Purple dashed lines show the position of the weak zones. Yellow arrow points to the direction of shortening. b) DEM with the trends of relative vertical displacements. c-d) Vertical displacements along selected profiles A-A′ and B-B′, respectively, for each model region.*

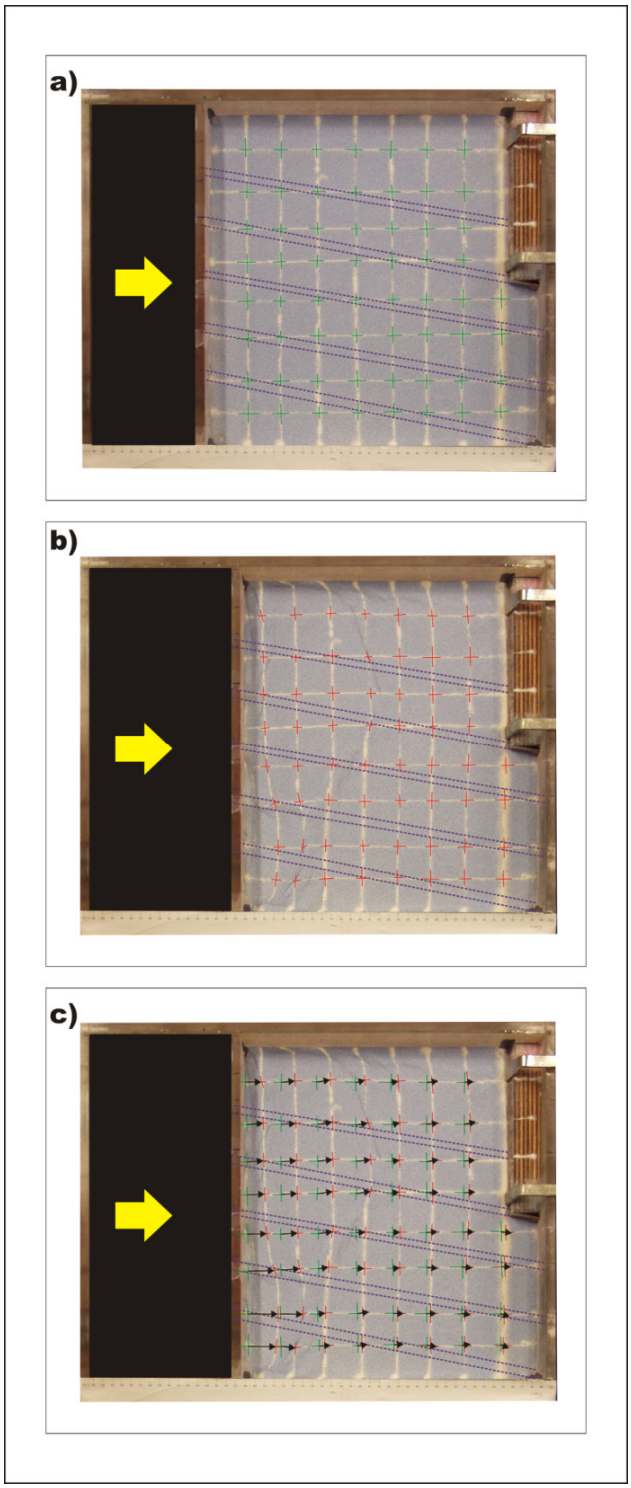

Figure 3.23 *Horizontal strain distribution deduced from the movements of the set of grid nodes on the surface. a) Model surface and grid points before the initiation of deformation and b) after deformation. c) Derived horizontal displacement vectors. For convenient comparison with the natural prototype, the plan-view of the model was mirrored compared to Fig. 3.22a.*

In case of Type-5 models, cross-sections from the frozen model were not taken parallel to the main direction of compression but perpendicular to it. The reason of doing so, was to investigate the very fine-scale deformation of the brittle crust above and around the weak zones. *Fig. 3.24* is an example of the observed structures. The small-scale offset within coloured sand layers modelling the upper crust is just around the limit of detection but the existence of the flower structures connected to the deformed weak zones can definitely be inferred.

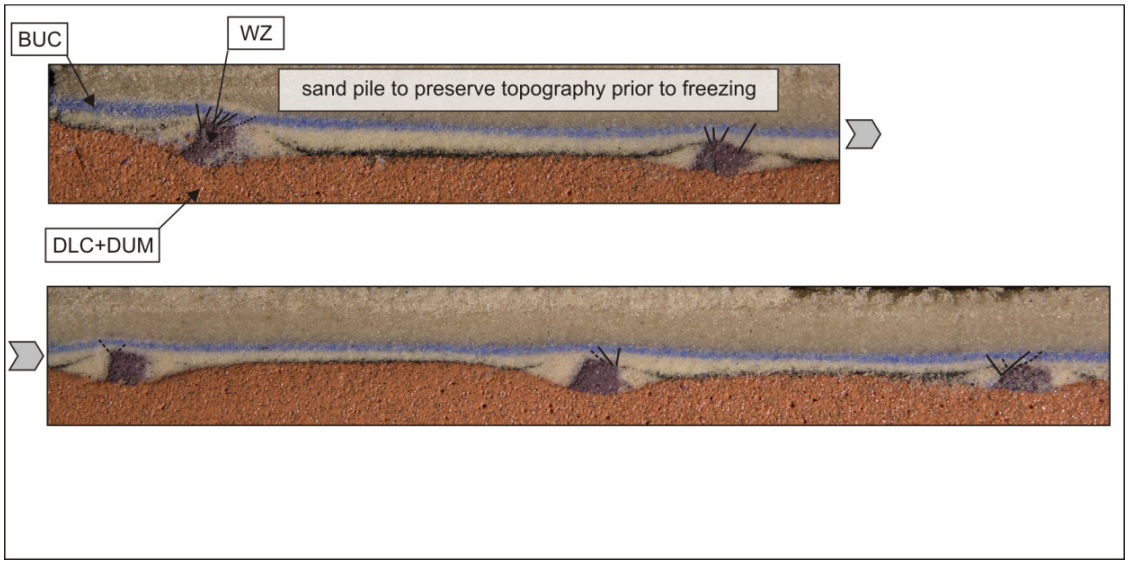

Figure 3.24 *High-resolution photo of a cross-section transecting the weak zones (purple patches) looking towards the indenter. The zoomed image is broken apart: left and right side of the cut in the top and bottom panel, respectively. Very fine-scale brittle deformation is reflected by the coloured sand layers above the deformed zones of weakness. Used abbreviations: BUC = brittle upper crust, WZ = weak zone, DLC+DUM = ductile lower crust and upper mantle.*

According to the findings of the quasi-3D, Type-4 & -5 models, the combination of lithosphere-scale folds and the activation of shear zones is a feasible mechanism to control inversion of the interior of the Pannonian basin. Type-5 models exhibited brittle deformation of the upper crust above the weak zones and the observed tectonic style is comparable to interpretation of neotectonic faults in seismic sections. Although there is still room for more complex modelling strategies, perhaps mostly on a crustal-scale, the results of this set of experiments are valuable. A large part of the strain was absorbed by the folding of the weak lithosphere. The rest of the horizontal displacement was distributed along several weak zones. It means that in this tectonic setting, slip rates along individual fault surfaces are expected to be low and due to the shallow brittle-ductile transition, the overall seismoactive surface to be reduced. In this way, the observed seismicity pattern within the basin can be explained and these findings also provide direct implications on seismic risk assessment.

3.7 Conclusions

The Pliocene to Quaternary tectonic evolution of the hot and weak Pannonian basin in response to compressional intraplate stresses was investigated by analogue experiments. The model of the Pannonian lithosphere was a two-layered system consisting of a thin sand layer overlying the ductile silicone layer, corresponding to the upper brittle crust and ductile lower crust and mantle, respectively. The entire system being deformed under relatively low strain rate, imitating the NE-directed indentation of Adria, produced a gentle large-scale folding.

Inferred from the experimental results scaled to nature, the far-field tectonic and additional gravitational stresses lead to the deflection of the weak Pannonian lithosphere manifested in an approximately 400 km wavelength folding. This is in agreement with previous numerical studies and correlates to the first-order vertical crustal motions in the area.

The subsidence and uplift pattern observed on the surface of Type-1 models was directly influenced by the wavelength and amplitude of lithospheric folding. In other words, a close link between landscape development and deep lithospheric processes in the Pannonian region has been demonstrated (*Fig. 3.25*). Apart from the pronounced uplift in the orogens, the amplitude of folding was able to produce a few hundred metres uplift and create depressions exceeding 1 km in depth in the basin interior during Quaternary times. These results are in line with the field observations and geophysical data.

Folding on various scales related to the ongoing basin inversion is reported from the basin interior, which implies the possibility of multi-wavelength mode of folding. By subtle analysis of the model surface, these modes were evidenced during the deformation of the initially homogeneous models. Crustal thickness variations built in the experiments prior to deformation profoundly changed the wavelength of the folds. The results of Type-2 models indicate that the heterogeneous basement morphology after the extension of the basin may account for the amplification of smaller wavelength deformations and the existence of irregular folds.

In Type-3 models, besides the push from the Adriatic indenter, the influence of the perpetual eastward escape of the northern Pannonian unit (ALCAPA) was also assumed. This change in the geometric boundary conditions resulted in strain localisation close to the indenter system in the form of thrusting and less pronounced uplift towards the central part of the basin. The uplifted areas within the model correlate well to the SW margin and W-SW part of the Pannonian basin (Dinarides, Sava fold belt, Mecsek hills and Fruska Gora Mts.).

Type-4 and -5 models complemented the interpretation with the aspect of activity of inherited weak zones. The quasi-3D conceptual models confirmed the possible co-activity of lithosphere folds and deformation along shear zones providing a reasonable reconstruction

of the first-order structural development of the natural prototype. Model results emphasise that low magnitude and intensity of earthquakes in the basin interior may be attributed to low strain rates, ductile deformation of the lithosphere and low slip rates along fault planes in the presence of multiple reactivated weak zones.

In summary, the large-scale folding of the hot and weak lithosphere can be considered as a viable mechanism controlling the inversion of the Pannonian basin to a major extent and together with other factors shaping the tectonic topography of the basin system.

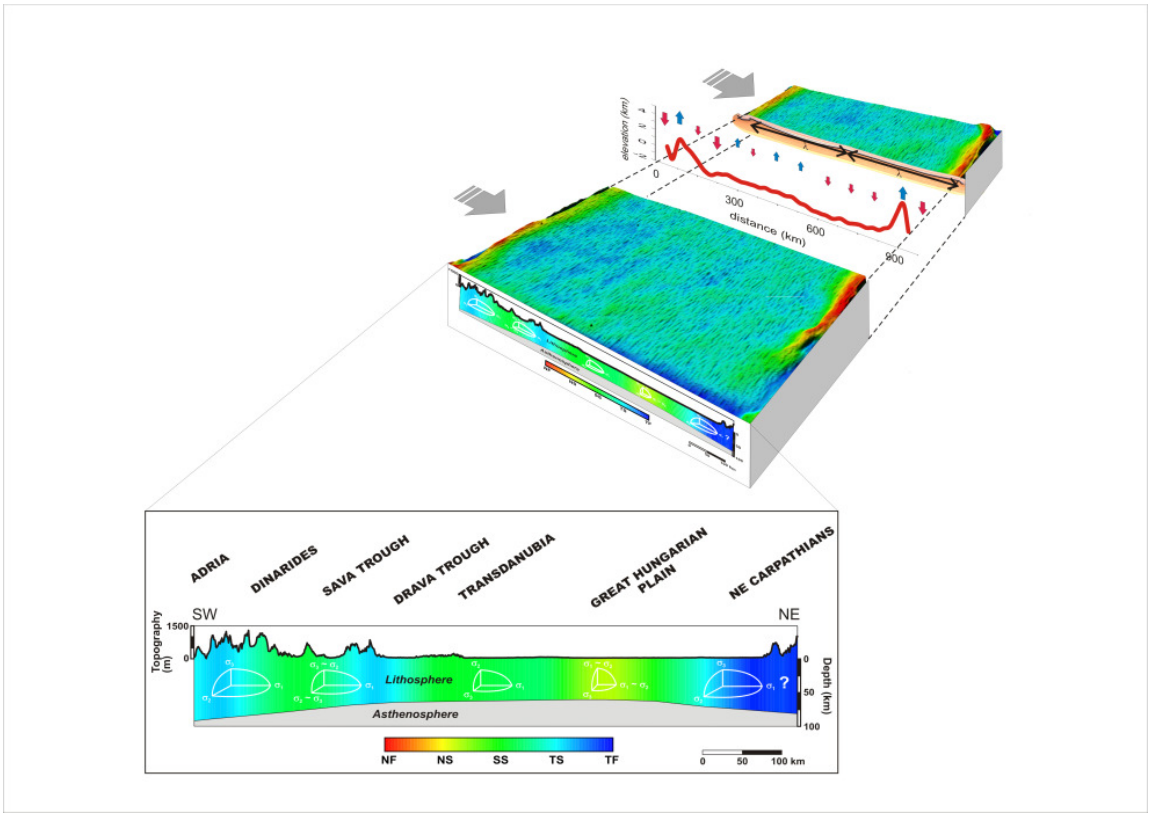

Figure 3.25 *A composite figure that summarises the inferences from the analogue experiments. Coupling between deep lithospheric and surface processes is emphasised. Changes of tectonic regimes across the Pannonian basin in SW-NE direction are draped on the frontal wall of the box and shown in the inset (Bada et al., 2007a, abbreviations and colour-code are same as in Fig. 3.9). Surface scan image of the Type-1 experiments covers the box with warm colours representing uplift and colder ones the subsidence. General trend of vertical motions is illustrated by the arrows in the middle of the box. The diagram shows the smoothed curve of vertical displacement derived from the model and up-scaled to the natural prototype. Inside the box the cross section demonstrates the long wavelength (λ) component of lithospheric folding controlling the basin inversion and related surface morphology.*

Chapter 4

Neotectonics versus surface processes in the western Pannonian basin: Inferences from interpretation of shallow geophysical data[3]

4.1 Introduction and problem statement

One of the most interesting research subjects on the evolution of the Pannonian basin is the mechanics of the Pliocene-Quaternary basin inversion and its impact on the present-day morphological development in terms of the evolution of the river drainage system and the response of landforms to tectonic and climatic events. The balance between the inherited Miocene rifting geometries and the Pliocene-Quaternary inversion structures and their role in shaping the morphological development of the Pannonian basin is of particular importance.

Two types of methodologies have approached this line of research so far. Basin evolution studies aided by the interpretation of industry seismic lines and exploration wells have detected the overall patterns of deformation and have demonstrated the major interplay between the inherited rifting and inversion geometries and regional development of topography. On the other end, geomorphological studies aided by modern technologies of quantification of the incision and/or exhumation rates, such as low-temperature isotope thermochronology or cosmogenic nuclides, have demonstrated that the morphology of the Pannonian basin is a dynamic one, active geodynamic processes shaping the topographic development. However, the direct link between the lithospheric and basin scale processes and the morphology is still missing in terms of direct quantification of structures responsible for the formation of, for instance, river deflection structures, conditioned incision of valleys or terrace development in response to specific deformational features. This link can be studied only at local scale on case studies situated in the most sensitive parts of the system. One critical method of this quantification is the deployment of high-resolution, shallow geophysical investigations. These methods are able to link directly the morphological development with the regional deformational or sedimentological patterns derived at the scale of the entire basin.

Two distinct state of the art methodologies, ultra high-resolution shallow seismics and geoelectric tomography were selected to link the subsurface structures to the morphological development. These methods can provide a detailed image of the near-surface domain beneath the analysed landforms. The advantage of these shallow geophysical surveys is not only the excellent resolution, but the fact that industrial seismic acquisitions generally cannot obtain information on the uppermost 50-100 m. Therefore,

[3] This chapter is based on the following published works: Horváth, F., Dombrádi, E. (Eds.), 2010. *Földtani Közlöny* (*Bulletin of the Hungarian Geological Society*), 140/4, special volume, 333-510. Particularly, Horváth, F., Dombrádi, E., 2010. Evolution of Hungarian tectonics: an overview of a century of research on and around the Lake Balaton. *Földtani Közlöny,* 140/4:335-354. and Horváth, F., Sacchi, M., Dombrádi, E., 2010. Seismic stratigraphy and tectonics of Late Miocene basin fill in southern Transdanubia and below the Lake Balaton. *Földtani Közlöny,* 140/4:391-418. Investigation of the Zala hills is published in: Dombrádi, E., Németh, K., Timár, G., 2012. Geoelectric investigation and morphologic interpretation of the valley system in the Zala hills (Hungary), *Geomorphology*, submitted

these geophysical data can be vital in the integration of deep structures with surface morphology.

The deformational geometries of the Pliocene-Quaternary inversion have been proven to be laterally highly variable across the Pannonian basin, changing from the large scale thrusting with variable offsets along its strike recorded near the Dinaridic margin, the late stage indentation of the Adria and Eastern Alps in the Pannonian basin, the large scale transcurrent features observed in the central part of the basin along the Transdanubian Central Range to the low-offset structures observed in the eastern part of the Great Hungarian Plain. This large variability is controlled by the counter-clockwise rotational kinematics of the Adriatic indentation into the highly curved Pannonian domain, which is affected by significant weakness zones along major inherited tectonic lineaments.

In this rather complex tectonic scenario, one area stands out in terms of Pliocene-Quaternary deformation, linking domains with contrasting proposed geodynamic history controlling topography evolution: the southern part of Transdanubia. Two critical case studies were selected in this area, where the deformational patterns linked to the Pliocene-Quaternary inversion are more pronounced. Basin and regional geological studies assume that the main control on the morphological development is related to the (re-)activation of the NE-SW oriented Mid-Hungarian Shear Zone, a major Miocene transcurrent system separating ALCAPA from the Tisza-Dacia continental units. On the opposite end, geomorphological studies assume that similar control must be given by NW-SE to N-S oriented fault systems that should mimic the main orientation of topographic features. The critical link between the two approaches is in the range of the high-resolution geophysical methodologies, i.e. the first couple of hundreds of metres.

The Lake Balaton and its recent sedimentation provides an excellent opportunity to discriminate between the long-term (i.e. Pliocene–Quaternary) deformational processes affecting the Transdanubia and the short-term neo-tectonic patterns affecting, potentially, not only the shallow sediments of the lake, but also the entire river drainage network situated in its neighbourhood. The ultra-high resolution seismic methodology is particularly suitable in these conditions as it is capable to detect not only rather discrete fault movements, but also the associated syn-kinematic sedimentation and other sedimentological-derived interpretations. Regional and/or local offsets and their associated expression in terms of vertical movements along faults prolonged from the margins of the lake should affect its sedimentary structure and, therefore, are easily depicted by the ultra-high resolution methodology. In particular interesting is the long-standing dispute in terms of the formation of the so-called meridional (NW-SE to N-S) and longitudinal (NE-SW) sets of valleys and adjacent ridges in Transdanubia (*Fig. 4.1*). Both research methodologies concluded that the topography of NE-SW oriented valleys is being controlled by re-activation of faults due to basin inversion. The problem addressed in this context is whether the other set of long lineaments (called meridional) have been formed due to direct fault control or purely as a consequence of denudation processes. This question has been the focus of an almost century-long debates and discussions. Beyond the review of

the hypotheses, the latest high-resolution geophysical data and interpretations are presented and also discussed in the context of the folding mechanics. The outcome of the study is highly relevant not only in terms of active tectonic processes shaping topography and influencing the river network, but has also a critical societal impact. The area of the Balaton Lake is a densely populated area in the western Pannonian basin with a number of recreational and industrial objectives with vital importance for the regional economy. Detection of active movements along young, near surface faults is essential in seismic risk mitigation in terms of the assessment of the probability ranges of the anticipated peak ground acceleration and the related hazard imposed on vulnerable industrial facilities in the region.

Basin evolution studies have inferred that the area of the Zala hills in SW Transdanubia is critical in terms of Pliocene-Quaternary deformational patterns. Here is the place where the most active part of the Mid-Hungarian Shear Zone transcurrent lineament meets a series of abnormal morphological features developed along long lineaments of topographic highs and lows. Their study does not have only local importance, but can, potentially, derive the neo-tectonic activity along the entire lineament. A similar discrepancy exists here between the NE-SW orientation of the lineament and the N-S orientation of the above-mentioned morphological features. This particular morphology has been explain by a numerous number of contrasting interpretations, such as (i) fault control implied by the length and linearity of the valleys, (ii) crustal-scale folding creating the alternating pattern of topographic highs and lows, (iii) incision and lateral migration of rivers due to differences in vertical crustal movements and (iv) wind erosion or the combination and interplay of these processes.

The key link in terms of imaging in the Zala hills is again in the first tens of metres beneath the surface, and therefore, perfectly suitable for high-resolution geophysical techniques. Overlying the same major lineament, the area provides also an excellent opportunity to test and apply the inferences from the area of Lake Balaton and to test the concept of tectonic-driven topography. The active fluvial sedimentation leaving abandoned morphological features at various altitudes provides here opportunity to examine the concept of active faulting bounding morphology. Classical geological and geomorphologic mapping have separated a terrace system that was, speculatively, considered of tectonic origin. The imaging derived from regional basin studies (i.e. seismic and well data) have proven to have insufficient resolution to provide the accuracy required to visualise these tectonic features.

In this context, the most appropriate high-resolution methodology in the area of the Zala hills is the geoelectric tomography. Interpretation of the numerous inverted 2D geoelectric profiles was carried out in order to detect deformational patterns and to link them with the neotectonic evolution of the broader region. The resistivity surveys have targeted the areas in which meridional valleys are still dominant in the topography, but the size of the valleys is smaller and their investigation is in the range of the proposed methodology. Geoelectric profiling was carried out in three localities within the study area, mostly concentrated on

the vicinity of valleys occupied by present-day drainage. Besides the detection of potential tectonic features, resistivity data gave valuable geological information from areas where only surface data was available and complemented subsurface data within a depth range, which is usually outside the range of standard industrial seismic surveys. The surveys focused on previously reported coarse-grained fluvial deposits that acted as markers for the geoelectric method. The expected contrast in the electric properties of the various Quaternary sediments enabled reconstruction of the subsurface distribution and geometry of these gravel layers along selected cross-sections. The representative sections served as a basis for further structural and morphological considerations to infer the viable deformation mechanisms or mass transport processes which have accounted for the formation of the ridge-and-valley system. The interpreted resistivity profiles provided the key to a high-resolution insight into the composition and structure of the shallow subsurface. The results evidence a young deformation phase, which in combination with aeolian processes is regarded as primary mechanism creating the present-day topography of the Zala region.

The high-resolution geophysical methodologies employed on this study are optimal to link the long-term and regional tectonic evolution to the short-term local morphological development. The range of these methodologies limits their application to case studies in spatially reduced areas. However, by choosing these cases studies in the two critical locations parts of the active tectonic system, the local inferences can be step-wise extrapolated at regional scale for a much larger area of Transdanubia. These inferences are the key in deriving the mechanical processes driving long-term tectonic inversion and short-term topographic evolution.

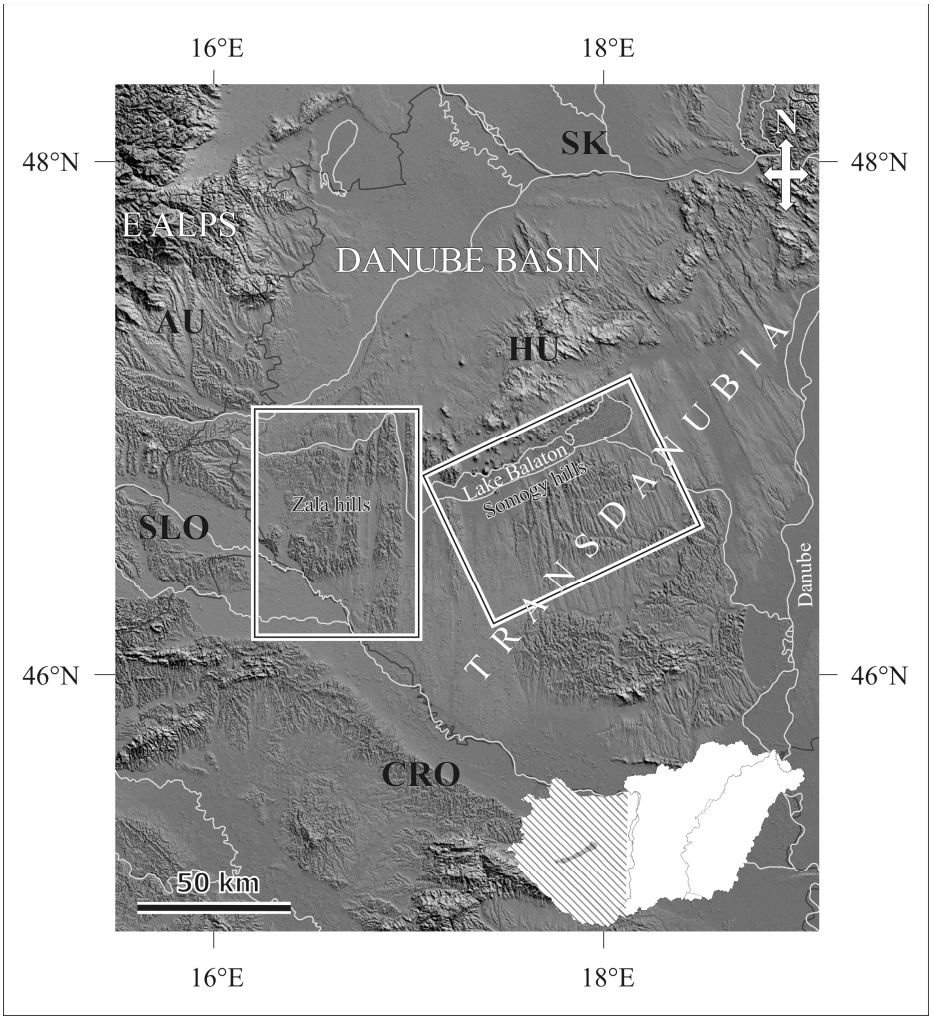

Figure 4.1 *Digital elevation model illustrating the morphology of the western Pannonian basin. Location of the case studies discussed in this chapter, the Lake Balaton together with the Somogy Zala hills south of it and the Zala hills in SW Hungary are indicated by rectangles.*

4.2 Qualitative inferences on the late-stage evolution of Transdanubia

In this section a look back is given on the evolution of the tectonic concepts explaining the structural and topographic elements present in Transdanubia. Early concepts in Hungarian tectonics were born about a century ago as a result of exploration of the Lake Balaton and its surroundings conducted by Lajos Lóczy. Therefore, the early tectonic concepts are considered necessary to be reviewed in the light of our contemporary knowledge in a comparative manner. An early concept explained the formation of the Pannonian basin in terms of subsidence of blocks bounded by a longitudinal and a meridional set of faults. It was also thought that the present surface morphology, particularly a meridional system of valleys and ridges was controlled by these faults. Even at that time alternative views emerged rejecting block faulting and, instead, suggested regional scale folding in the basin, and wind erosion as a primary mechanism of surface evolution.

4.2.1 The fixist median-mass model

Based on detailed field observations, the first most extensive studies regarding the longitudinal and meridional structures were published by Lóczy (1913) and Cholnoky (1911, 1918). Before introducing the various ideas on the formation of these valleys, a short overview is given on the fixist point of view on tectonics of the Pannonian basin (for further details see Horváth, 2007).

Lóczy's main idea on the tectonic evolution of the basin was centred on the 'median-mass' concept. It was to explain the special situation of the Pannonian basin within the Alpine orogenic belt, that is the branches of orogens depart and then reunite, meanwhile embracing an apparently hardly deformed central area covered by thick succession of young sediments. It was considered as a remnant of a rigid Altaid-Variscan massif, which had formerly been in connection with the Rhodope massif (Lóczy, 1913b, 1918, 1920b). From Palaeozoic times until Early Miocene, this massif was assumed to be continuously uplifting. Firths of sea during the Palaeozoic and the Mesozoic had intruded into the massif creating numerous bays. Thus, the massif became covered by alternating marine and terrestrial deposits due to the regressional and transgressional cycles. An essential element of this notion is that the median-mass remained intact from the young Alpine deformation phase. Sporadically some Mesozoic formations might have been gently folded, but the dominant structural units were thought to be the Tertiary longitudinal and meridional faults. These faults have dissected the massif into a chessboard-like pattern. Along the faults both vertical and horizontal displacements could have occurred. Finally, it was supposed that the formation of the Pannonian basin was directly controlled by these sets of faults such as the blocks bounded by the faults were downthrown forming several grabens during the Early and Middle Miocene.

4.2.2 Concepts on the formation of meridional and longitudinal valleys

According to the above-described evolution of the median-mass of the Pannonian region, it was concluded that the interior massif had retained its rigidity throughout the young deformation phases and thus brittle structures must prevail in the area. A quasi-orthogonal system of longitudinal and meridional faults was proposed several times, but only one sketch has been published on the surroundings of Lake Balaton (*Fig. 4.2*, Lóczy 1913b). It is to be noted that a similar map had been previously published by Cholnoky (1911) that covered a significantly larger area (*Fig. 4.3*).

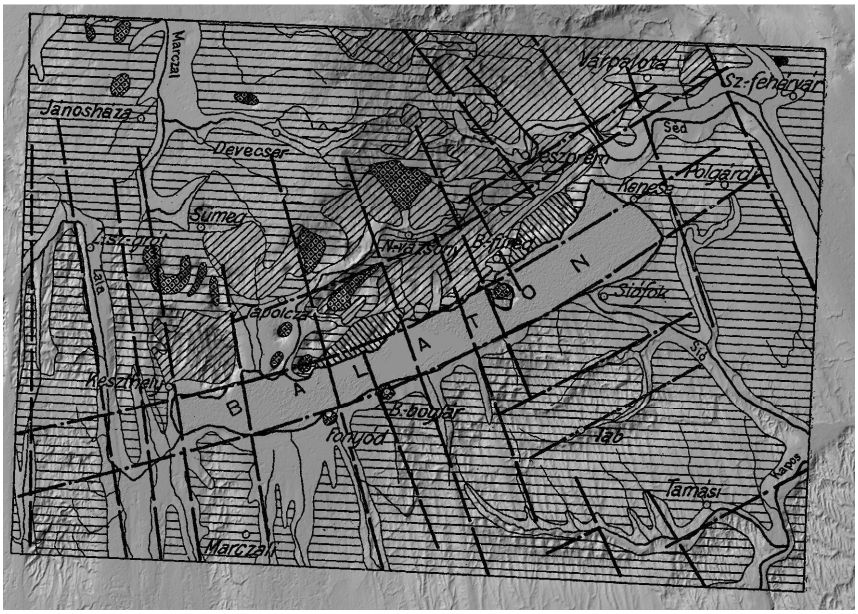

Figure 4.2 *Sketch of meridional (roughly N-S oriented) and longitudinal (NE-SW oriented) faults in the broad vicinity of Lake Balaton (dashed black lines after Lóczy, 1913) draped on a present-day DEM to correlate with the actual landforms (Horváth, 2007; Horváth & Dombrádi, 2010).*

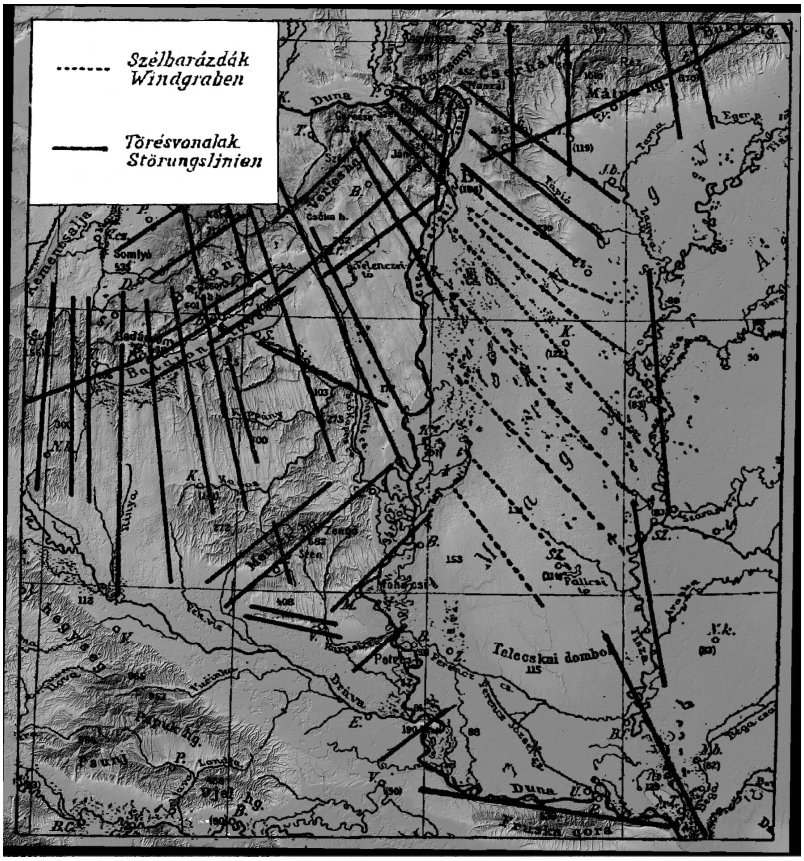

Figure 4.3 *Map of meridional and longitudinal faults (black solid lines) also displaying identified windgrabens in the central part of the basin (dashed black lines) according to Cholnoky (1911). They are visualised on a DEM such as in Fig. 4.2 (Horváth, 2007; Horváth & Dombrádi, 2010).*

However, he considered these remarkably linear valleys of purely aeolian origin, representing a set of wind channels or windgrabens. Based on the observation that between the rivers Danube and Tisza, the mapped windgrabens slightly, yet consistently deviate from the strike of meridional faults, he concluded that there is no connection between the faults and the system of ridges and valleys. Later he redefined the formation of the windchannels much emphasising the role of tectonic pre-formation (Cholnoky, 1918). In this sense, the two authors shared the common idea. Cholnoky excluded fluvial erosion and normal faulting from the processes to form the long (sometimes reaching 50 km in length) and narrow, elongated valleys. Instead he gave an elegant and straightforward explanation that comprised the contemporaneous knowledge on horizontal displacements in the crust. In modern geologic terms, the valleys in the broad environment of the Lake Balaton were regarded as fractures generated by strike-slip faults and subsequently turned into windgrabens by aeolian processes.

As for the longitudinal valleys such a definition was not given, yet they were of importance in the structural development of the median-mass. The Lake Balaton itself was assumed to

be a graben bounded by normal faults and shaped by subsequent aeolian and fluvial activity (Lóczy, 1913b).

A concurrent model at that time was proposed by Pávai Vajna (1925, 1943) denying brittle tectonics. In his concept, the tectonics of the young sediments was dominated by E-W trending folds. He observed, based on a vast number of field measurements, gently dipping layers in the Pannonian and Pleistocene deposits forming a series of folds with E-W oriented axes. Detailed gravity and seismic surveying of hydrocarbon exploration campaigns later revealed folds roughly parallel to the strike of those proposed by Pávai Vajna. However, the misfit between the proposed and the real location of the folds was found to be enormous (Papp, 1939). Nevertheless, since then several geological cross sections demonstrated folding of Quaternary sediments that in certain places are in close correlation to the observed surface morphology (Urbancsek, 1963, 1977).

In the middle of the 20th century, other hypotheses were put forward based on borehole data and geological sections emphasising the importance of thrusts as a result of NW-SE horizontal compression. The observed compressional structures in the longitudinal valleys showed that blocks of south-eastwards dip were pushed above their neighbours (Schmidt, 1952; Erdélyi, 1961, 1962). According to these authors, the surface manifestation of the basement-related fractures perpendicular or parallel to the fold axes is observed. The meridional ridge-and-valley system was interpreted as horst and graben structures pre-dating the development of the longitudinal valleys.

Effects of fluvial and aeolian activities are documented by terrace remnants on both sides of the valleys and by characteristic morphologic features such as ventifacts and wind polished surfaces (e.g. Bulla, 1943; Erdélyi, 1961; Marosi, 1962; Jámbor, 1992, 2002). Elongated, mostly loess ridges, situated between the valleys appear to be asymmetrical. Their northwestern margin is steeper compared to their southeastern boundary. In addition, the overlying Quaternary sediments also show a trend of thickening towards this direction.

As an ultimate reason for tectonic pre-formation the remarkable linearity is quoted (Jámbor, 1993; Síkhegyi, 2002), which does not point beyond the former hypotheses formulated by Lóczy and Cholnoky (Lóczy, 1913; Cholnoky, 1918, 1936).

4.3 Quantitative inferences on the late-stage evolution of Transdanubia

4.3.1 Tectonic interpretation of industrial seismic sections, borehole data and outcrop analyses

Recent studies established the neotectonic evolution and structural developement due to the ongoing basin inversion the Transdanubian part of the basin system on a regional scale as well as in particular locations on a local scale. Neotectonic deformation in the compressional stress field and the initiation of pronounced vertical movements commenced the latest Miocene or the earliest Pliocene in the southern part of the Pannonian basin. The gradual build-up of compression during the Pliocene and Quaternary times is manifested in folds across the western and central part of the basin that are mainly connected to reactivation of Miocene normal or strike-slip faults (Fodor et al., 2005; Bada et al., 2010; *Fig. 4.4*). Such deformation patterns have been derived in the area of the Zala hills (Fodor et al., 2005) and south of Lake Balaton, in the Somogy Hills (Csontos et al., 2005). Fault-related folds have been formed in facilitated by the reactivation of fault planes, which often remain to be blind faults or their continuation into the Upper Miocene post-rift sedimentary strata cannot be observed at least within the limits of the resolution of standard seismic acquisition methods. It is one of the major obstacles to ascertain that the observed trends in the arrangement of the valleys are primarily defined by active neotectonic structures.

Complementing the inferences from seismic interpretation, outcrop studies have been conducted in the Somogy hills with extensive tectono-morphological and sedimentological observations (Magyari et al., 2005). Based on these results, the Somogy hills were found to be an active scence of neotectonic deformation, with several episodes of compressional phases. In terms of the development of the two distinct sets of the valleys, also characterising the morphology of the Somogy hills, along the NE-SW trending valleys, left-lateral movements have been documented with an offset ranging between tens to maximum a few hundreds of metres. Concerning the NW-SE morphologic structures (meridional valleys) the analyses did not confirm the prevalent role of tectonics unambiguously. However, aeolian and fluvial activity was assumed to enhance the landforms already preformed by tectonic lines. Through this research approach an explicit explanation on the formation of the latter series of valleys could not be given and a direct link between the neotectonic fault activity and the observed morphology could not be confirmed.

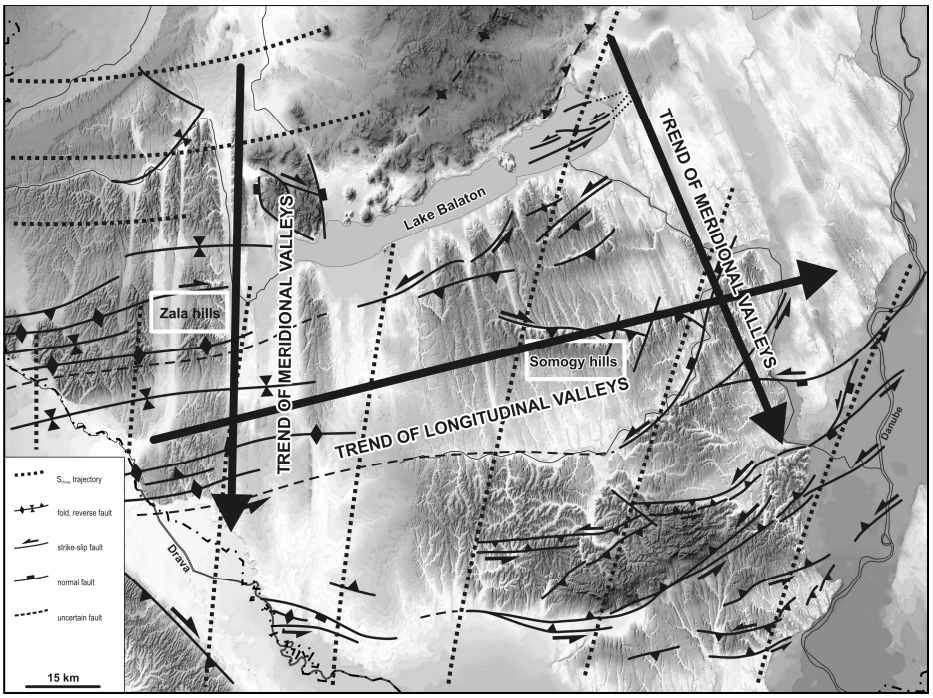

Figure 4.4 Overview map of the neotectonic structures in Transdanubia projected on a DEM showing the detailed topography (after Bada et al., 2010). Dotted lines indicated the smoothed trajectories of the present-day maximum horizontal stresses. The location of the case studies is labelled. General trends of both longitudinal (NE-SW) and meridional (N-S to NW-SE) valleys are given for reference.

4.3.2 Geomorphological constraints on the tectonic topography in Transdanubia

Discrimination between these morphologic expressions that have tectonic influence or developed due to fluvial or wind erosion was attempted in the central part of the Pannonian basin using geomorphologic methods and linking them with the neotectonic evolution constrained by the structural interpretation of seismic data and outcrop observations (Ruszkiczay-Rüdiger et al., 2007). Integration of these investigations successfully revealed a key role of tectonic control governing the late-stage landscape evolution in the case of NE-SW trending landforms. The NW-SE trending valleys and adjacent, moderately elevated, ridges showed no tectonic control according to the geomorphologic indicators. Instead, they were found to be shaped mostly by deflation and wind channels were identified acting during the Pleistocene glaciations, which represent the easternmost members of the fan-shaped, locally NW-SE oriented (meridional) valleys. The results have high level of relevance for the entire area of the Transdanubian hills, where resembling structural and topographic setting are observed.

In spite of the geomorphologic proxies supporting the fluvial or aeolian erosion representing the primary forces behind the formation of these landforms, there still remains a data and knowledge gap between the depth range where seismic data can provide

constraints for the structural control and the observed surface processes. To overcome this lack of information and create an efficient link between the two presented research methodologies, high-resolution, shallow geophysical techniques, seismic and electric methods are of particular importance in the context of this research line (*Fig. 4.5*).

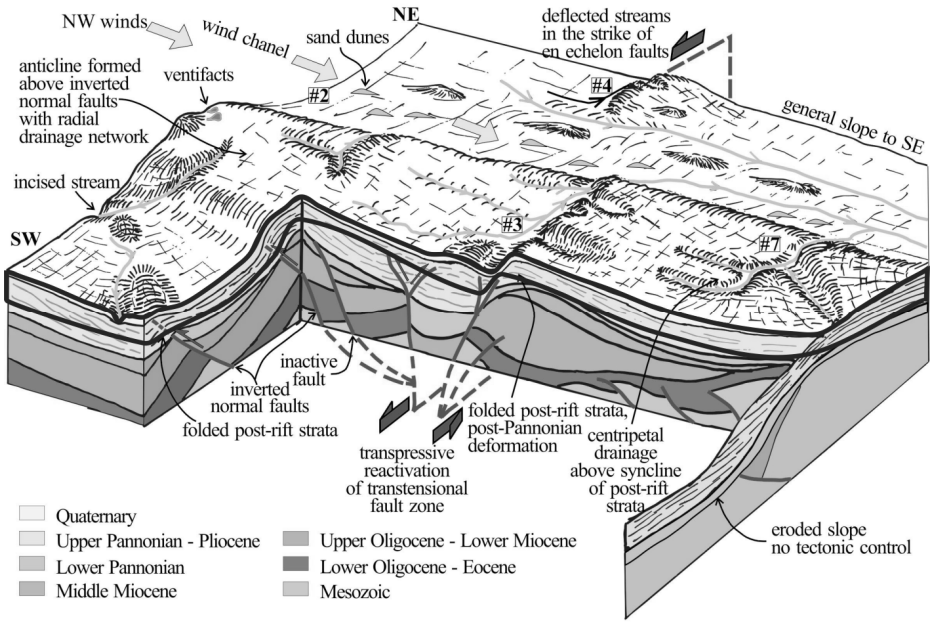

Figure 4.5 *Summary figure of the inferred morphotectonic development in the central part of the Pannonian basin (Gödöllő hills), which can generally be applicable to areas in Transdanubia in similar settings (Ruszkiczay-Rüdiger et al., 2007). Active neotectonic structures have been identified by seismic interpretation and available borehole data, while the associated landforms were analysed by geomorphologic tools. Although by the combination of the two methodologies, tectonic control could be proposed for various landforms in the particular study area, their direct interface, lying in the uppermost 100 m of the subsurface could not be studied by either of the methods. This is the interface (highlighted by thick black contour), where shallow geophysical methods can be applied successfully and provide valuable data for the complete interpretation.*

4.4 Interpretation of high resolution seismic data in the area of Lake Balaton

4.4.1 Data and methods

The resolution in case of standard industrial applications is a few tens of metres. Water seismic acquisition can provide two orders of enhancement in resolution. Therefore, the single- and multi-channel seismic data acquired on Lake Balaton are of key importance in the interpretation (Tóth et al., 2010; Bada et al., 2010). High resolution seismic reflection is a cost-effective method for mapping shallow and deeper structures beneath rivers and lakes. Propagation of seismic (or more precisely, acoustic) waves in water is almost exclusively attenuated by spherical dissipation. Therefore, the resolution of profiles recorded on water surfaces can even reach the centimetre scale. Due to this resolution, seismic images of the subsurface can be directly correlated to outcrops, thus, detailed stratigraphic studies can be carried out. Seismic acquisition in a riverine or lacustrine environment provides continuous imaging of the substrata down from the bedrock, unlike in land seismic sections, in which the upper 200-250 ms is usually muted. It is obvious that important information might also be found in these uppermost levels.

Since 1997 regular seismic surveying is carried out in the eastern part of Lake Balaton that resulted in about 700 km and 145 km long single- and multi-channel reflection seismic dataset, respectively. The different vertical resolution and depth penetration of the two methods complement each other. The integrated interpretation allows a quasi 3D structural analysis, correlation of tectonic elements and understanding the kinematic connection between deeper and shallow structures. *Fig. 4.6* demonstrates the capability of the single-channel reflection seismic method.

An extensive overview is given on the neotectonic consequences derived from the high-resolution seismic by Bada et al. (2010). Hereby, only the synthesis is referred to (*Fig. 4.7*) with a particular attention to the meridional geomorphologic features.

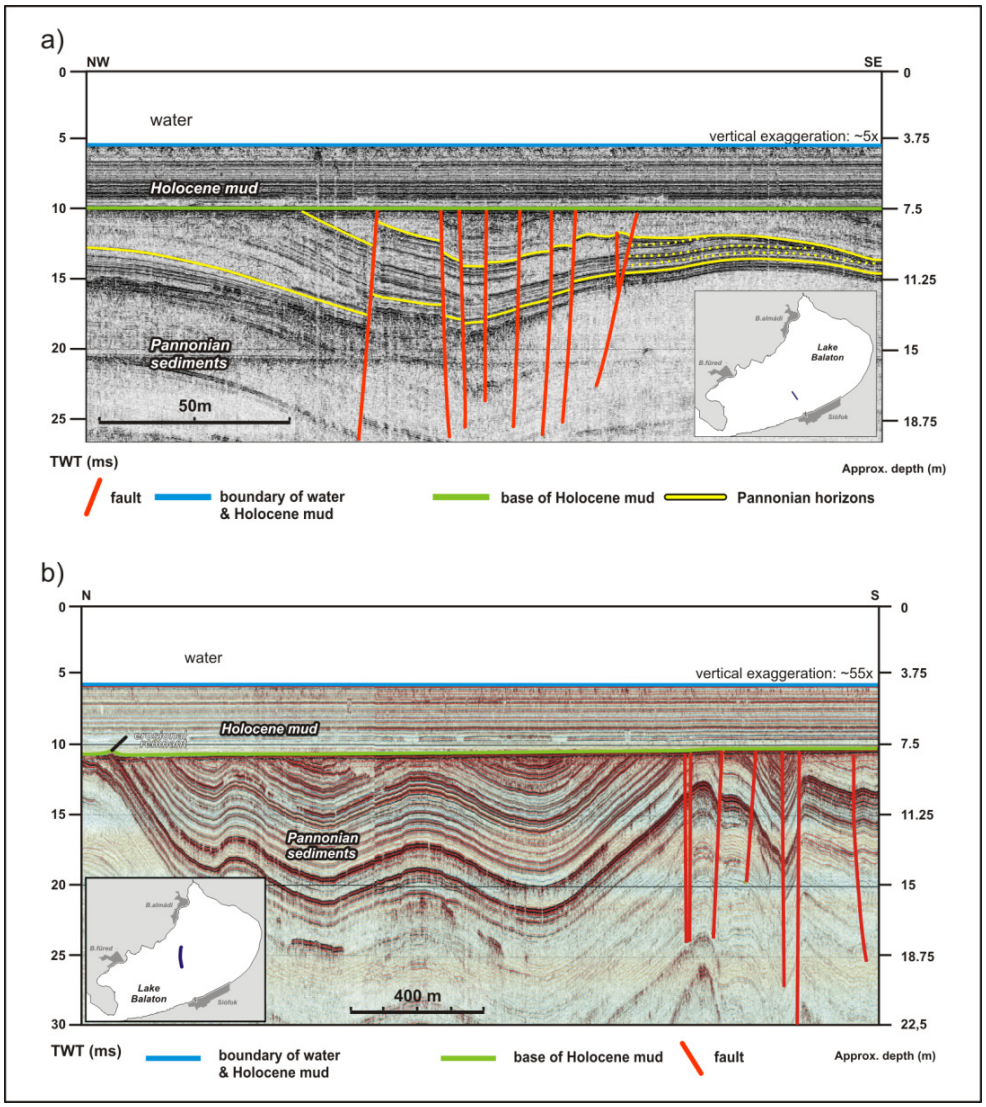

Figure 4.6 *Illustration for the technical capabilities of single-channel, high-resolution water seismic acquisition (Bada et al., 2010). Interpreted seismic sections from Lake Balaton have imaged a) small-offset faulting and b) gentle (max. 1-1.5°) folding of the Upper Miocene (Pannonian) strata. Note the two-way travel times and converted depth scales for the impression of the detailed images of the subsurface this type of seismic data provides.*

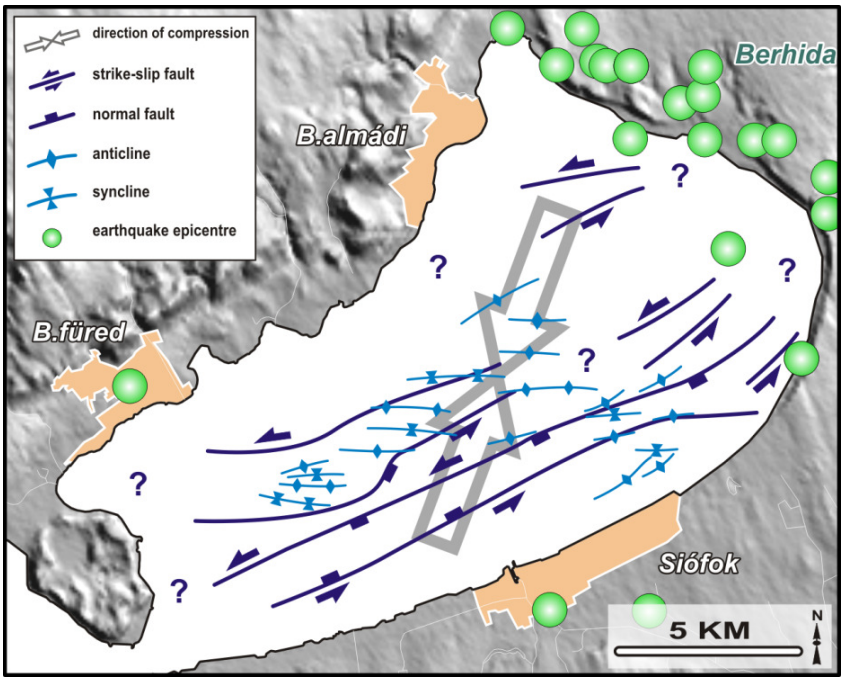

Figure 4.7 *Results of the seismic investigations in the eastern part of Lake Balaton. Generalised neotectonic map with major faults and folds derived from the multi- and single-channel seismic profiles (Bada et al., 2010).*

It is to be noted that formerly, due to the restricted vertical resolution of industrial seismic sections existence of faults with less than ca. 20 m offset could not be excluded. However, such small-scale faults could control the formation of only short sections of the valleys. It is highly unlikely that structural elements at this scale could have controlled the valley formation over their entire length, which is usually of several kilometres (Fodor et al. 2004). The high and ultra-high resolution (10 cm) seismic data from Lake Balaton did not show N-S oriented (meridional) faults at all, whereas in the longitudinal direction a marked fault zone has been imaged (*Fig. 4.7*). Therefore, control of brittle deformation, i.e. fault control on the meridional ridge-and-valley system is not confirmed by these results.

4.4.2 Relevance to the formation of the meridional valleys

The identified fold structures beneath the lake and the spatial configuration of the valleys onshore were correlated (Horváth & Dombrádi, 2010). A geologic cross section along the longer axis of Lake Balaton integrating water seismic, outcrop and shallow borehole data is presented in *Fig. 4.8*. The 45 km long profile visualises the stratigraphic setting and tectonic deformation ~30 times vertically exaggerated. In reality, the dip of the Pannonian strata does not exceed 1-6°. The gentle folding of 15-20 km wavelength and maximum 100 m amplitude is considered as typical for the Pannonian formations in Transdanubia (Lóczy 1913; Bada et al., 2010). The elevation difference between the outcrops of Tihany Fm. around Lake Balaton (e.g. at Tihany Peninsula) and the top of the formation imaged below the lake is around 60-100 m. According to the detailed seismic information, it is a consequence of neotectonic folding. Such amounts of differential erosion as well as graben

formation facilitated by normal faults can be ruled out. Few faults can be identified offsetting the strata found in onshore outcrops and the same formations beneath the lake but they all proved to be strike-slip faults (Novák et al., 2010). The former erosional surface (Pan-2, *Fig. 4.8*) was once a more continuous and even surface. After subaerial erosion occurred the sequences have most probably been entirely covered by the transgressional deposits of the subsequent sedimentary sequence (PAN-3). At present the overlying sequence unit (PAN-3) is completely missing owing to erosion related to neotectonic inversion but its remnants have been seismically imaged in a few patches preserved under the Holocene mud of Lake Balaton.

Fig. 4.8 clearly demonstrates that the alternation of meridional valleys and associated ridges south of the lake does not correlate to the folded structures identified by the interpretation of high-resolution seismic dataset. Neither the high in the vicinity of Tihany Peninsula nor the synclines at its flanks or subsequent anticlines manifest in surface morphology (Horváth et al., 2010; Horváth & Dombrádi, 2010). Faults pre-forming the meridional valley-and-ridge system around Lake Balaton, according to the vast amount of high-resolution seismic data, simply do not exist.

Figure 4.8 *Geological cross section traversing the Tihany Peninsula (modified after Sacchi, 2001). The compilation is based on water seismic profiles, field observations and borehole data. The Upper Pannonian Somló and Tihany Formations as well as the Tapolca Formations, which is interpreted to belong to the overlying TST sequence, can be found between the top Sarmatian and base Holocene unconformities across the lake. Basaltic intrusions occur below Lake Balaton, which are likely to be coeval with the basalts of the Tihany Peninsula and date the formation of the Pan-2 sequence boundary. In the eastern basin of the lake, buried travertine mounds can be seen on the top of the sequence boundary just like on the surface at Tihany peninsula. The original stratigraphic architecture has been folded and eroded due to the neotectonic structural inversion. During the latest Pleistocene the lake developed on this erosional surface and, in contrast with the classic theory, it is not a graben bounded by normal faults. However, roughly parallel to the longer axis of the lake, left-lateral strike-slip faults are well documented. The alternating pattern of anticlines (e.g. Tihany peninsula) and synclines shown by seismic data does not correlate to the series of meridional valleys and ridges to the south in the Somogy area (profile A-B). No tectonic control is evidenced by the high resolution seismics concerning the formation of these meridional landforms (Horváth et al., 2010; Horváth & Dombrádi, 2010).*

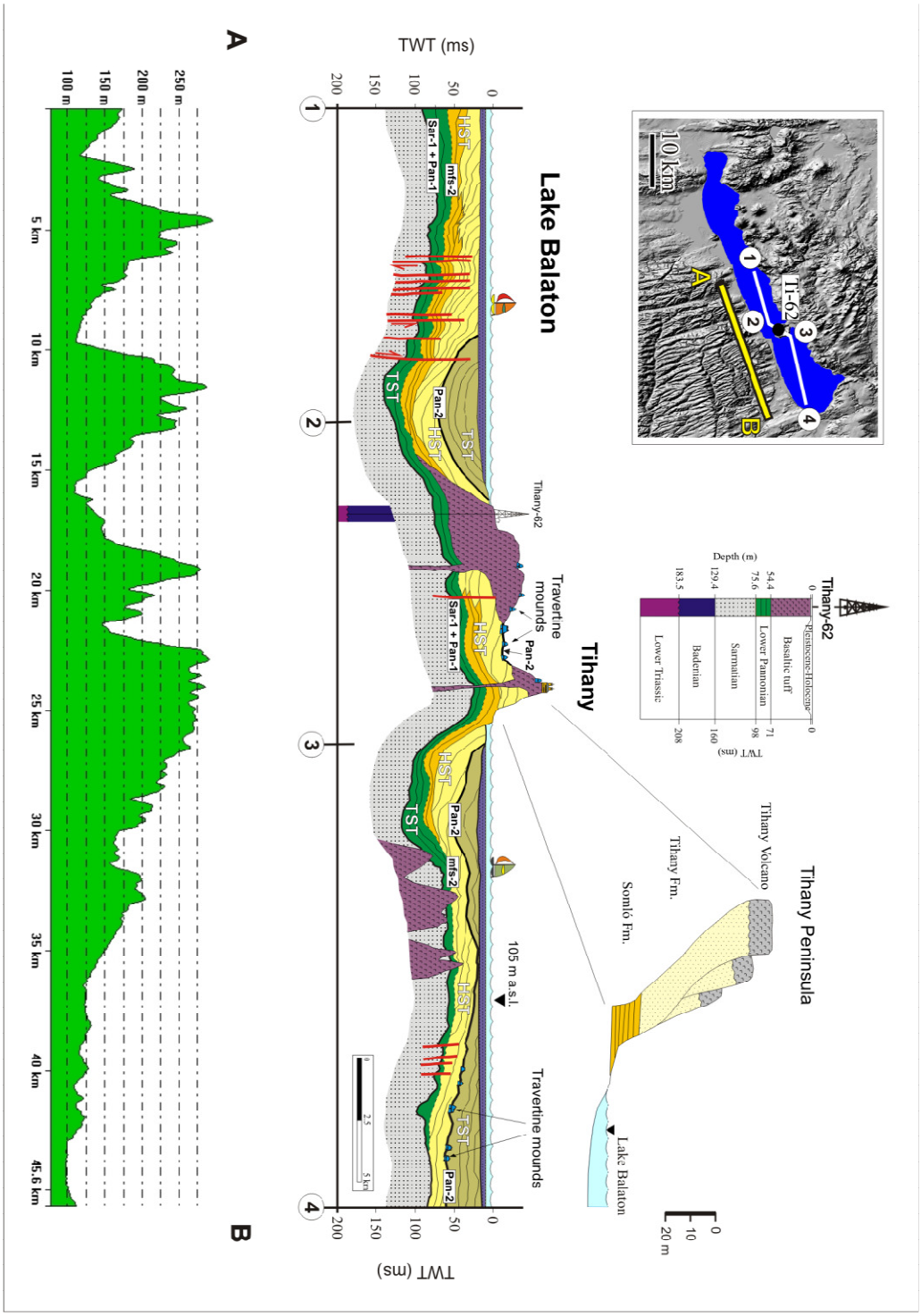
Ti-62
10 km
A
B
1
2
3
4
Tihany-62
Pleistocene-Holocene
Basaltic tuff
Lower Pannonian
Sarmatian
Badenian
Lower Triassic
Depth (m)
TWT (ms)
Tihany Peninsula
Tihany Volcano
Tihany Fm.
Somló Fm.
Lake Balaton
0
10
20 m
Lake Balaton
Tihany
Travertine mounds
Pan-2
Tihany-62
105 m a.s.l.
HST
TST
mfs-2
Sar-1 + Pan-1
Pan-2
TWT (ms)
0
2.5
5 km
A
B
250 m
200 m
150 m
100 m
5 km
10 km
15 km
20 km
25 km
30 km
35 km
40 km
45.6 km

4.5 Geophysical and geomorphologic investigations in the Zala hills

The integrated research philosophy applied in the case of the Lake Balaton area and its inferences on tectonic topography were extended to the Zala hills, in order to assess the link between neotectonic activity and topography development in an area, where much less geological constraints were available. In order to meet the requirements of joining the scales of the regional mechanisms and the local surface expressions, high-resolution geoelectric tomography was applied, which provided a shallow penetration, yet a detailed insight into the subsurface of the local ridge-and-valley system of the Zala region.

4.5.1 Geological background

4.5.1.1 Structural evolution of the Zala hills

The Zala hills are located in the southwestern part of the Pannonian basin close to the Slovanian border (*Figs. 4.1*). The basement is composed of series of Palaeozoic and Mesozoic nappes. During basin formation the NE-SW oriented former thrust planes have been reactivated as normal faults. Thus in Miocene times several halfgrabens have been formed, providing accommodation space for the synrift deposits of Lake Pannon (*Fig. 4.9*, Horváth et al., 2006a).

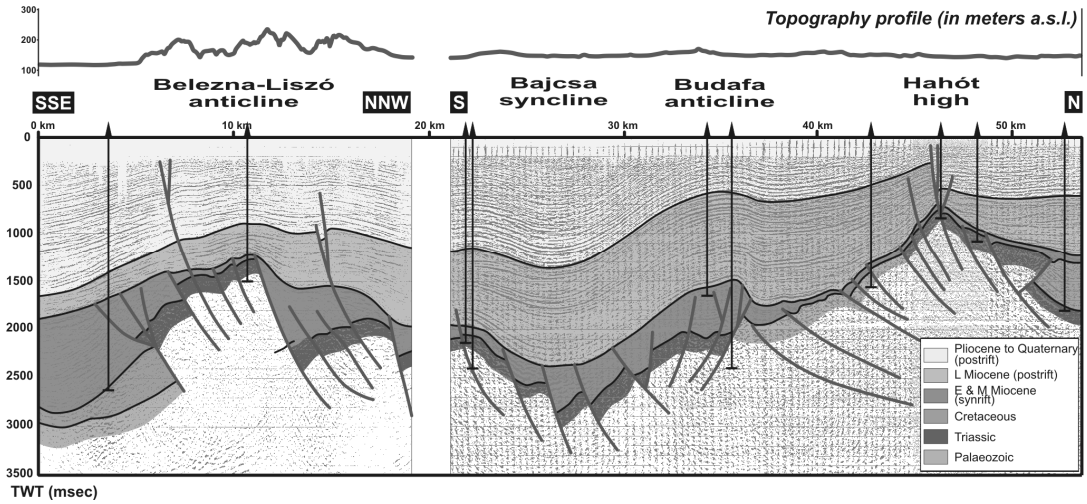

Figure 4.9 *Representative interpreted industrial seismic section from the Zala region. Mesozoic to neotectonic activity is imaged in the section. The latest phase of tectonic inversion has resulted in the build-up of anticlines and affected surface morphology as well (Bada et al., 2003; Horváth et al., 2006a).*

Basin inversion has affected the area of Zala hills in a relatively short time due to the proximity of the Adriatic microplate. Faults transecting the basement have again been reactivated in the form of blind thrust faults. The bulk part of the deformation is assumed to be ductile and the hot and weak Pannonian lithosphere with extremely soft rheology is likely to have been folded on various scales (as discussed in *Chapter 3*). The late-stage uplift has formed the roughly E-W striking anticlines (Budafa and Belezna-Liszó anticlines,

Fig. 4.9), which determine the overall landscape of the Zala hills. The series of these antiforms can be interpreted as small wavelength (20-30 km) folding controlled by the former (Palaeozoic and Mesozoic) thrust planes (Dombrádi et al., 2010, Jarosinski et al., 2011).

According to stratigraphic data from the Zala basin, the onset of uplift and formation of the anticlines could have initiated at around 8-7.5 Ma. It has forced the prograding delta systems to change direction and partly bypass the already elevated terrains (Uhrin et al., 2009). The various amplitudes of the relative vertical motion are also reflected in the topography. The amplitude and wavelength of the small-scale folding and the envelope of the topography align (Fodor et al., 2005). These observations point to the fact that influence of the young deformation must be taken into account in the examination of surface processes.

4.5.1.2 Palaeogeography of the Zala hills

A detailed and extensive description of the young geologic and geomorphic evolution of the Zala hills is given by Lovász (1970). From his research, in the light of recent studies, we extracted and briefly reviewed the lithology and origin of various sediments with special emphasis on deposits, which may be characterised by resistivity contrasts.

During the post rift subsidence, the gradual fill-up of the isolated Lake Pannon has taken place (9.5 Ma, Magyar et al., 1999). Terrestrial sediments, transported from the Alpine and Carpathian orogens have formed prograding delta systems. Thus, the northern shoreline of Lake Pannon was continuously retreating towards the south. By the Early Pliocene it remarkably shrank in size leaving only a small lake behind.

Accordingly, in the area of the present-day Zala hills, the deep water marls have been replaced by sandy-clayey sediments by the end of the Pannonian. During Pliocene times they were overlain by cross-bedded alluvial deposits consisting gravel and sand. At the time, two larger rivers appeared in the area, the palaeo-Rába (Raab) and the palaeo-Mura. The coarse grained sediments have already been deposited in the Styrian basin and, therefore, the Zala basin was covered by more fine grained, mostly sandy deposits.

In the Pleistocene the intensive fluvial sediment accumulation continued. However, the alluvial fans of the rivers (Rába and Mura), following the river course, migrated towards the southwest. Consequently, the fine grained sands became topped by coarse gravels. The deposition of the gravel was also intensified by the changing climate. As the average temperature became lower and dryer conditions prevailed, the discharge of the rivers dropped, thus, more coarse grained sediments were deposited by the palaeo-Rába and the palaeo-Mura in the N-NE and the W-SW part of the Zala hills, respectively (Lovász, 1970). These sediments are generally overlain by young loess strata (younger than 320 ky Paks Loess Fm., Gábris, 2007). The loess cover is widespread in the area and the boundary

between the pre-dating fluvial deposits and the loess is often marked by a sedimentary hiatus.

4.5.1.3 Terrace levels and terrace-like features

Observing the detailed morphology of the ridge-and-valley system of the Zala hills, several features resemble to fluvial terraces, although their fluvial origin is not always proven (Fodor et al., 2005). The sandy-gravel and gravel accumulations in the valleys and side-valleys were first mapped by Strausz (1949) and then classified into a uniform terrace system by Lovász (1970). They were divided into two groups upon assumed differences in their genetics. Classic terrace levels were considered to be formed by fluvial sediment deposition and erosion. The other category comprises terrace-like features, which exhibit similar geometry and were attributed to re-deposition and foothill accumulation. This analysis has pointed out the importance of differences in vertical surface movements. The origin of the differences remained an open question. The formation of the anticlines had favourably been attributed to folding but brittle tectonics had not been excluded either. As a consequence of changes in surface uplift, incision and lateral migration of the river courses were thought to contribute to climatic effects and together having built the observed terrace system.

Upon their elevation distribution, five terrace levels were identified in the Zala hills (Lovász, 1970).

- #5: The highest and oldest level at about 270-310 m altitude. It is interpreted as the remnant of an ancient alluvial fan from the end of Pliocene.
- #4: Between 250-270 m this level can be observed in the northern and central parts as a narrow ridge.
- #3: In contrast with the previous two levels, this terrace level is connected with valleys, which in certain cases form wider inter-valley crests. Their average elevation is between 220-240 m a.s.l.
- #2: The second terrace level is found at an elevation about 170-190 m and found at the periphery of even smaller valleys.
- #1: The youngest terrace level (155-165 m) is situated 3-5 metres above the floodplain.

It is to be noted that the spatial distribution of the mapped terrace levels was found to be rather heterogeneous in the territory of the Zala hills (*Fig. 4.10*). The classification system was founded on the scarce surface occurrences of gravel and morphological considerations and hence it reflects a generalised view on the dimensions of the terraces.

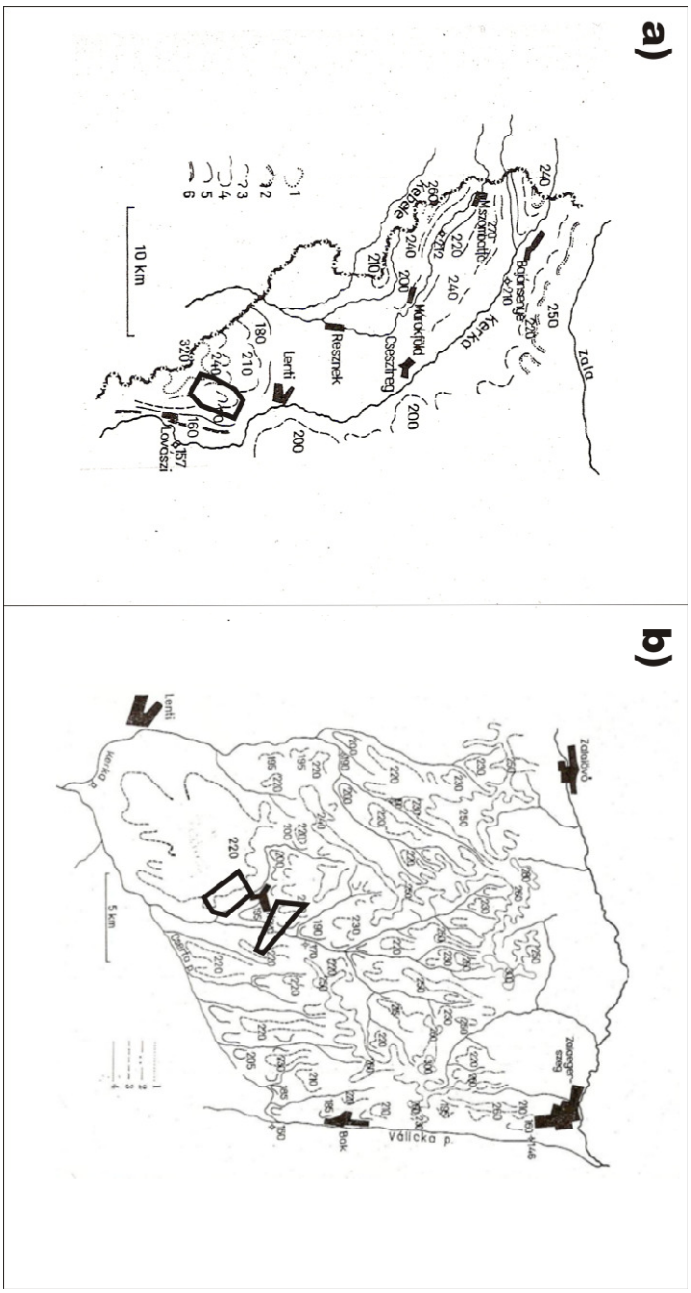

Figure 4.10 *Distribution of proposed terrace levels of various ages in the a) western and b) northern Zala hills. Based on mostly geomorphologic considerations, geologic ages were tentatively corresponded to the different levels for both areas as follow: a) 1-2. Late Pliocene (= level #5), 3. Early Pleistocene (= level #4), 4. Middle Pleistocene (= level #3), 5-6. Late Pleistocene (= levels #2 & #1) b) 1. Late Pliocene (= level #5), 2. Early Pleistocene (= level #4), 3. Middle Pleistocene (= level #3), 4. Late Pleistocene (= level #2). Black boxes outline location of resistivity measurements shown in Fig. 4.13. The presented maps are not to precise scale, they are mainly for illustration purposes. Modified after Lovász (1970).*

An alternative explanation for the elevated position of the gravel bodies is given by Fodor et al. (2005). According to the authors the present-day gravel patches on the surface could all belong to a single, continuous gravel carpet forming the alluvial fan of a larger river in the Pliocene to Pleistocene times. The gradual uplift of the anticlines led to the rise and massive erosion of these gravel beds. In that sense the remnants of the alluvial fan would demonstrate a young deformation phase of the ongoing inversion.

4.5.2 Methods

4.5.2.1 Brief theory of DC geoelectric tomography

With the surface geoelectric methods, using natural or artificial sources, the electromagnetic field properties of the subsurface layers are determined. The geometry and lithology of near surface layers is then defined upon their different electric characteristics. Direct current geoelectric surveys aim at the determination of resistivity. Resistivity is primarily dependent upon the amount and ion composition of the pore fluids within the rock but other factors such as temperature and pore structure also affect the measurable resistivity values. The best conductors, which are characterised by the lowest values, are clays and marls containing considerable amount of bonded water within the rock matrix. The range of resistivity varies over orders of magnitudes (*Table 4.1*) and thus is not a specific value for certain rock types. However, where *a priori* geologic information suggests a significant contrast in the resistivities, geoelectric methods provide a suitable tool to delineate different lithological formations. For the theoretical background see *Appendix A.4.*

Gravel (dry)	100-10000	Clay	2-20	Granite	200-10000
Sand (dry)	50-1000	Claymarl, marl	5-50	Gneiss	200-10000
Gravel (wet)	50-1000	Limestone, dolomite	100-5000	Diorite	500-10000
Sand (wet)	15-100	Sandstone, conglomerate	100-2000	Basalt	200-10000

Table 4.1 *Representative resistivity values (in ohmms) of various rock types (Salát & Szabadváry, 1970)*

4.5.2.2 Resistivity tomography

Resistivity profiling is carried out by laying out several electrodes along a straight line. The electrodes are attached to cables and connected to the control unit. Resistivity values are systematically measured according to the given array in all possible electrode configurations. Several standard electrode arrays exist and the choice is determined by the geophysical target. We used the combined Wenner-Schlumberger array (Pazdirek & Blaha, 1996).

In the Wenner array the distance between adjacent electrodes *(a)* is constant (*Fig. 4.10*). It is usually employed for horizontal profiling to gain a qualitative image of the lateral changes in apparent resistivity. In the Schlumberger array, the two potential electrodes are located between the current electrodes symmetrically. The MN distance *(b)* is significantly

smaller than the AM or BN distance *(a)*. It is the typical configuration used during sounding (VES). In this case, gradually deeper penetration is achieved by systematic increase of distance *a* (*Fig. 4.11*). The multielectrode Wenner-Schlumberger array welds these two standard arrays and changes the parameters in both manners.

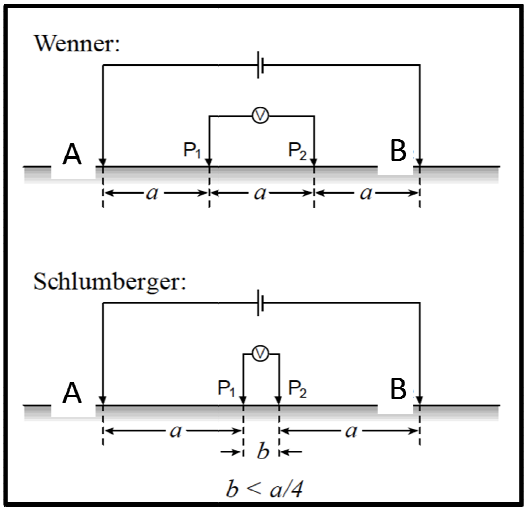

Figure 4.11 *Scheme of the commonly used Wenner and Schlumberger electrode arrays. A and B denote current electrodes that feed DC current into the ground. P_1 and P_2 are the potential electrodes through which the resultant voltage is measured. In the Wenner configuration the distance between each neighbouring electrode is equal (a). In case of the Schlumberger array, the distance between the two potential electrodes (b) is shorter than the distance between a current and a potential electrode (a, usually b<a/4, Lowrie, 2007).*

The combination of the two arrays is advantageous. Both horizontal and vertical sensitivity is slightly increased, while of course the number of data points is also increased compared to the individual electrode configurations. It is also to be noted that the depth penetration is theoretically the half of the current electrode spacing *(AB/2)*. Practically, when measuring above inhomogeneous subsurface the depth penetration reduces to *AB/4* or *AB/5*.

4.5.2.3 Data acquisition and processing

Data was collected by using an ARES-G (GF Instruments) multielectrode resistivity metre. 4 m electrode spacing was used providing sufficient horizontal resolution. For the sake of fast and effective data acquisition, we employed the combined Wenner-Schlumberger array in all cases. The maximum depth penetration was about 50 m. The depth penetration is proportional to the distance between the current electrodes. Hence, the maximum depth of investigation is determined by the cable length. The relation between the apparent and real resistivity values is fairly complex hence, inversion of the measured apparent values is necessary. Measured apparent resistivity values were inverted by Res2DInv inversion software (Loke, 2010). Quality control of the input data and adjustment of the inversion parameters resulted in a standard error less than 5% in the presented results. Topographic data were also included in the inversion, since the elevation was a key element to correlate the geoelectric tomography results with the proposed terrace level classification system.

Surface elevation was extracted from DEMs and also measured by high-precision differential GPS.

4.5.3 Results and interpretation of 2D geoelectric tomography

Resistivity profiles were taken in present day valleys, in the vicinity of Cserta and Kerta creeks and around Lovászi village (*Fig. 4.12*). The location of the study areas was selected to fulfil a two-fold purpose: i) test the hypothesis of the proposed river terrace levels and ii) since these areas are also transected by meridional valleys, though somewhat subdued in size compared to the eastern side, to draw a general conclusion on their formations. Measurements were attempted to target both the valleys and the adjacent ridges. However, rough terrain conditions, vegetation and private estates hindered the optimal choice of the profile locations.

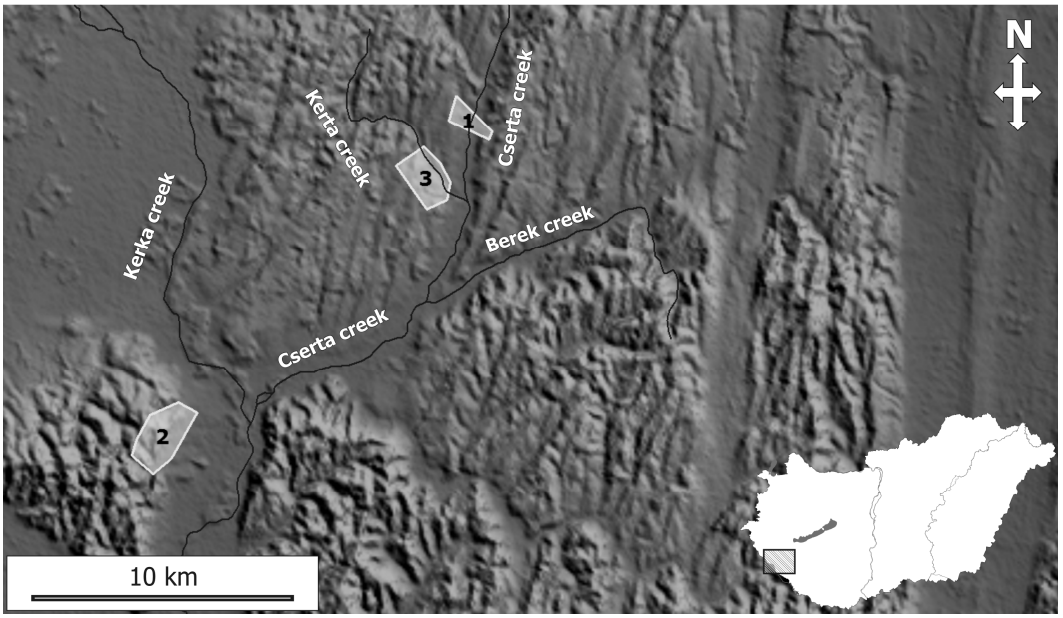

Figure 4.12 *Direct vicinity of the selected study areas is outlined by numbered boxes. For reference, present-day drainage is also indicated.*

In the following subchapters results of the geoelectric surveys are presented and interpreted. All resistivity sections shown were colour-coded in the same manner for the sake of easy comparison. Though extremities were not experienced, the selected interval does not always represent the maximum measured values. Zones of interest were denoted sequentially from left to right and low and high resistivity domains were highlighted with distinctive labels.

4.5.3.1 Study area #1: Cserta valley

The valley of the Cserta creek provided an excellent area to image the subsurface beneath both flanks and the valley itself. Small offset faults, fingerprints of young deformation or erosional and depositional processes manifested in the sedimentary architecture were sought via the geometry and composition of sediments with various electric properties. The valley was traversed by two sections (Cserta-01 & Cserta-02), while a third, control profile was measured north of them (Cserta-03, see *Fig. 4.13a*).

On the western flank of the valley, the 1000 m long Cserta-01 profile showed several distinct resistivity anomalies (*Fig. 4.13b*). Beneath the valley, a roughly 10 m thick, characteristically low resistivity body (10-20 Ωm) was seen (E) corresponding to the recent fine grained alluvial sediments of the creek. The vertical high resistivity blob intersecting this low resistivity zone was an artefact representing lack of data due to dummy electrodes laid out on the bridge over the creek. On the western bank of the valley two significant, high resistivity regions (over 100 Ωm, A & C) were imaged alternating with moderate resistivity bodies of most probably finer grained composition (B & D). The high resistivity layers were apparently dipping to W with approximately 10°. Exact geometry of anomaly A may be burdened by uncertainties as it is on the edge of the profile, where data coverage is less and thus the inversion results may be biased by the edge effect. The observed geometry can hardly be indicative of an eastward migration and gradual incision of the precedent Cserta creek. Assuming that the two high resistivity bodies are remnants of terraces of various ages, their lower boundary indicates significant post-depositional tilting to the W, which contradicts the observed morphology.

The continuation of this profile, on the eastern side of the valley showed a remarkably different geometry (Cserta-02, *Fig. 4.13c*). In contrast to the Cserta-01 section to W (*Fig. 4.13b*), where two separate high resistivity layers could be identified, the geoelectric image of the eastern flank depicted a single massive high resistivity body (A). It exposed to the surface in the proximity of the valley. Eastward, it gradually became overlain by lower resistivity deposits (B). The depth of the high resistivity layer increased in this direction, while its top approximately remained at the same absolute elevation (see envelope surface, *Fig. 4.13c*), contouring an overall curved shape of the observed anomaly.

A third section, a few hundred metres offset towards the north is presented (Cserta-03, *Fig. 4.13d*) to complement the interpretation of this study area. High resistivity values formed a laterally extended anomaly again close to the surface below the topographic high (A). This anomaly then became slightly disintegrated and had been replaced by lower values (B) towards the valley reflecting a more heterogeneous lithology. The easternmost edge of the profile revealed another high resistivity anomaly in ca. 5-6 m depth (C). The most obvious difference between the Cserta-01 and Cserta-03 profiles (*Fig. 4.13b & d*) was the lack of apparently dipping layers from the latter one. Instead, similar to the E side, the high values seemed to form a single rock mass. As significant amount of gravel was found

on the surface along this section and in its proximity, the highest resistivity values definitely represent coarse grained fluvial sediments and, predominantly, gravel composition. The slight decrease in the resistivity at the eastern shoulder of the river bank is most probably related to increase of relatively finer grained sediments. In summary, no step-wise character could be detected in the anomaly pattern, which could correspond to two different levels of river terraces.

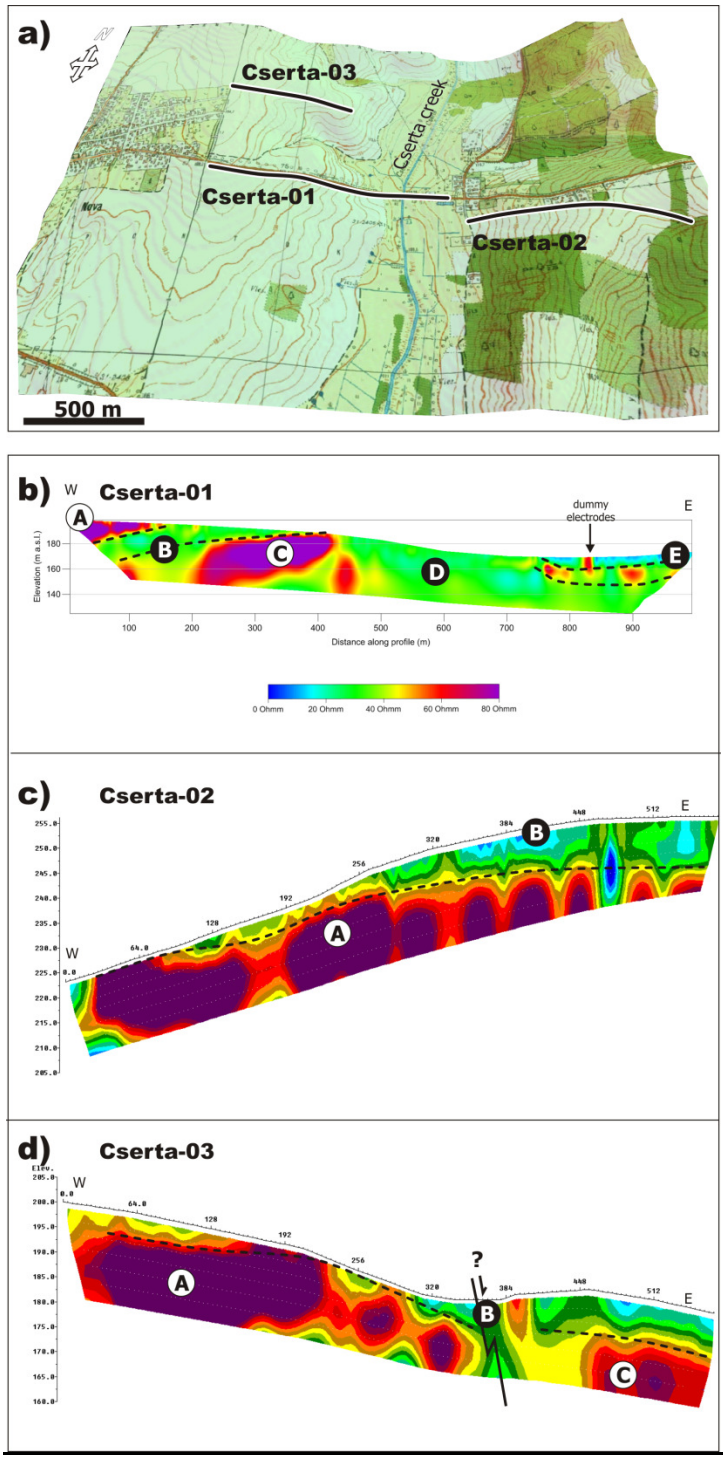

Figure 4.13 *Resistivity tomography results in study area #1 (Cserta creek). a) Topographic map draped on digital elevation model with the location of the presented geoelectric profiles. b)-d) Inverted resistivity sections. Major anomalies referred to in the interpretation are labelled from left to right (A, B, C, etc.) in all cases. Note that the letters used do not intend to express correlation of individual resistivity domains from one profile to another High and lower resistivity anomalies are denoted by black letters in white circle and white letters in black circle, respectively. Dashed lines mark the inferred outlines (top and bottom) of high resistivity anomalies. Fig. 4.13c & d is modified after Kovács & Marinov (2009).*

4.5.3.2 Study area #2: Resistivity profiles around Lentihegy and their interpretation

Profiles of the second study area represent the foot of the Lentihegy and the adjacent valley (*Fig. 4.15a*). The morphology of the Lentihegy displays step-like features (see photo, *Fig. 4.14a & b*) and thus was regarded one of the most perspective to identify various terrace levels. A sketch of the proposed terraces is shown in *Fig. 4.10a*, which displays densely spaced members of the terrace system in the given study area.

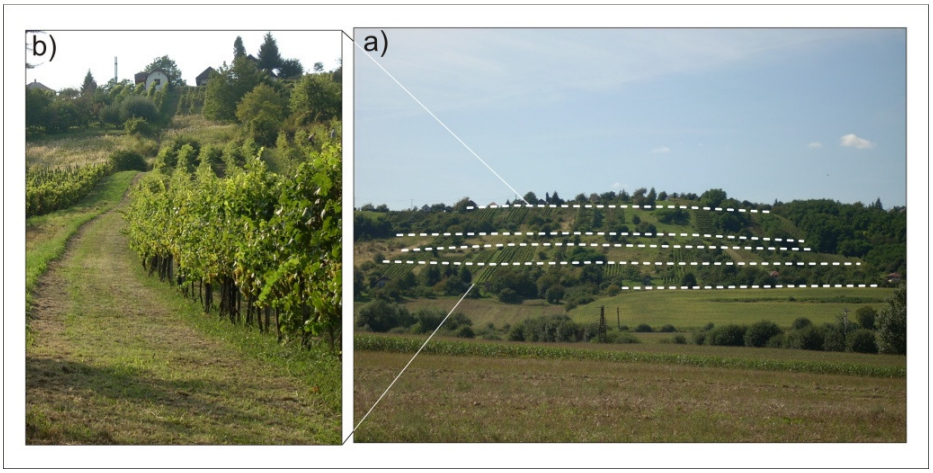

Figure 4.14 *Photo of the Lentihegy, considered as the most promising study area to detect fluvial terraces. a) White dashed lines indicate step-like changes in the terrain tentatively attributed to different terrace levels sketched in Fig. 4.10a. b) Close up on the observed morphology along one of the resistivity profiles.*

Although significant variations in the subsurface resistivities were expected, the profiles measured in the second study area had not much variability in the values. On the crest itself, there was only one spot, where relatively higher values were recorded than the average. However, it is to be emphasised that the maximum measured resistivity (~60 Ωm) was significantly lower than those of the Cserta valley. As a matter of fact, this higher resistivity body appeared to be exposed on the surface where there was a small step in the relief (Lenti-02 profile, *Fig. 4.15f, A*). According to the measurements, which documented rather monotonous resistivity data, there is no indication of remnants of fluvial terraces beneath the step-like morphology within the depth of investigation (ca. 25-30 m).

The majority of the resistivity tomography data from the valley adjacent to Lentihegy was of low values in the range of 10-40 Ωm (*Fig. 4.15c-e*). The single exception is the N-S oriented Lenti-05 profile in the northern part of the study area, which yielded high resistivity values, exceeding 100 Ωm, both on the surface and below (*Fig. 4.15b*, C & B).
In this particular site, gravel occurred on the surface in several patches. Furthermore, close to the Lenti-05 profile an outcrop was found exposing 80-100 cm thick gravel layer and hard sandstone streak interbedded between sandy deposits (*Fig. 4.16*). Geometry of the

imaged high resistivity body was continuous over more than 100 m, followed the dip of the surface and seemed to wedge out to the N-NE.

Compared to the results of Lenti-05 profile in the northern periphery of the area, the measured values on the ridge are profoundly lower (see *Fig. 4.15f & b*). Since the high resistivity body imaged in the Lenti-05 profile can unambiguously be related to gravel deposits based on the field observations, it is concluded that the composition of the uppermost subsurface (20-30 m) of the ridge of Lentihegy does not contain gravels at all. In the absence of gravel or at least more compacted sandy fluvial sediments close to the surface, it is difficult to explain the observed morphology of the Lentihegy as a series of fluvial terrace levels of various ages, unless we assume that a thick loess cover is blanketing the entire hill.

The most obvious answer to the lack of the fluvial sediments is that the Lentihegy had already been in an elevated position when the rivers originating from the Alpine region arrived to this location. Therefore the river course was diverted and no deposition took place. This idea well explains why coarse grained fluvial sediments were only found at the foot of the hill. It is in line with the observations that already during the deposition of the Late Miocene basin-fill sediments, the Belezna-Liszó anticline could have been a topographic high forcing a lateral migration of the prograding lobes. This fact also points towards the onset of inversion in the Zala hills predating Pliocene times. All in all, the interpreted geoelectric profiles transecting the Lentihegy favour aeolian origin of the observed morphology.

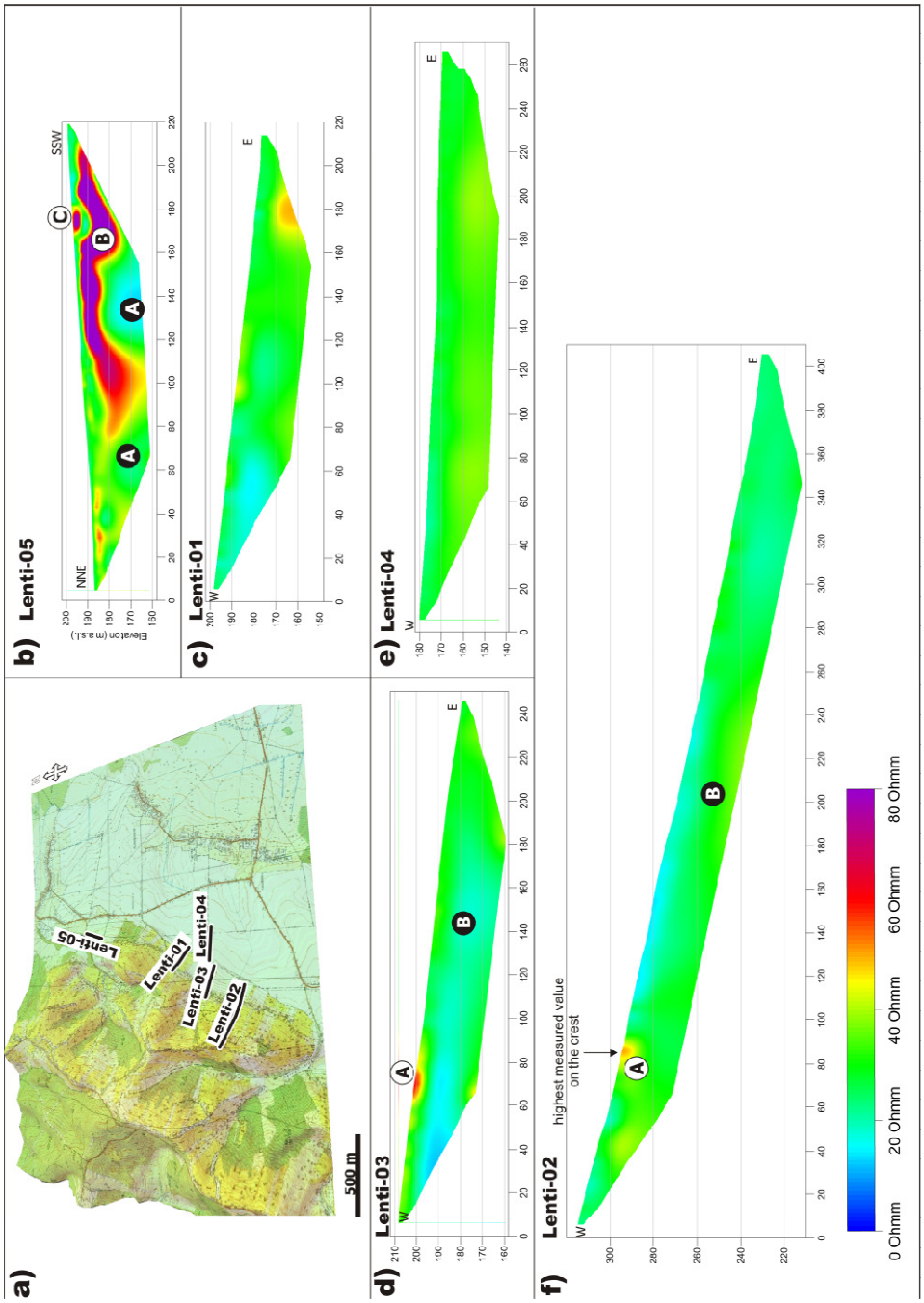

Figure 4.15 *a) Location map of the geoelectric profiles in study area #2, at the foot of the Lentihegy. b-f) Inverted resistivity sections. Same labelling convention was used for the anomalies as in Fig. 4.13.*

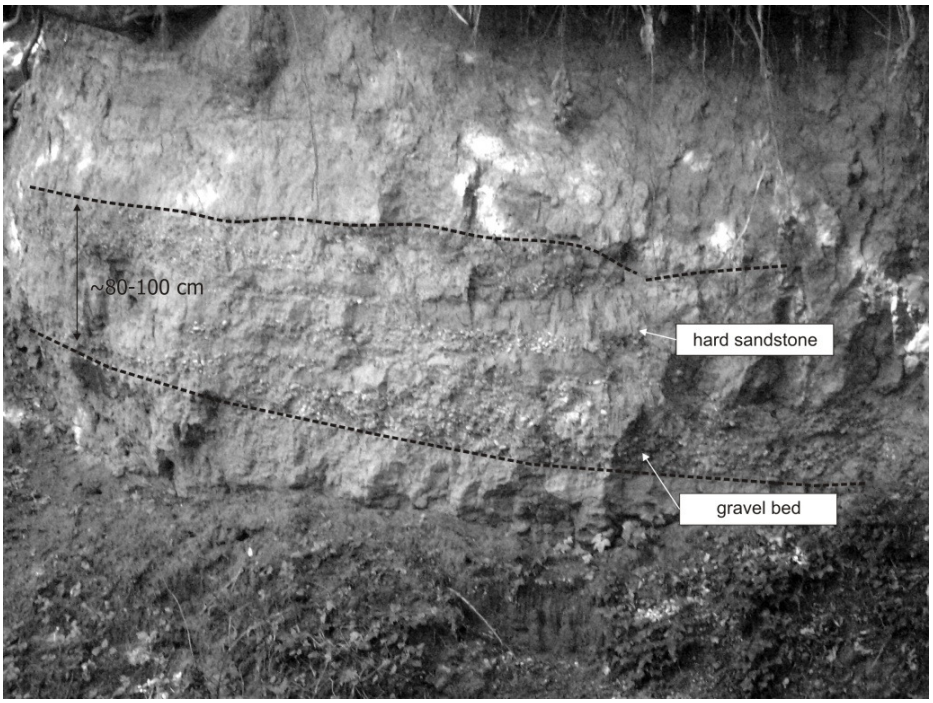

Figure 4.16 *Sandpit close to Lenti exposing coarse grained fluvial sediments (gravel and compacted sandstone) embedded into finer grained cross-bedded sandstone. The black dashed lines contour the gravel bed which has most likely been imaged by means of geoelectric tomography in Lenti-05 profile.*

4.5.3.3 Study area #3: Kerta valley

The greatest number of measurements was taken in the valley-and-ridge system surrounding the small Kerta creek (*Fig. 4.17a*). According to the terrace classification and the surface map (*Fig. 4.10b*) the topographic highs between the valleys are described as broad, plateau-like morphologic features, which all belong to the same terrace class. The characteristic resistivity image inferred for this study area is well illustrated by the Kerta-07 profile *(Fig. 4.17c*). The profile portrayed a high resistivity zone in the valley with values ranging between 100-240 Ωm (B). In up-dip direction it became capped by a significantly low resistivity anomalies (15-30 Ωm, A). The resistivity pattern on the W side was similar to that of Kerta-07 though in certain profiles discontinuity of the highest resistivity domain was recorded. In case of Kerta-03 and -09 sections a moderately resistive body (30-40 Ωm) interrupted the highest resistivity layer (*Fig. 4.17b & d*, layers C). The lowest resistivity was always found in the topmost part of the profiles. As for Kerta-10, which has a lower altitude, the low resistivity layer was much thicker (*Fig. 4.17e*, layer A). High resistivity values were encountered exclusively at the lowermost edges of the profile (*Fig. 4.17e*, B). It suggests a deeper position of the coarser grained sediments.

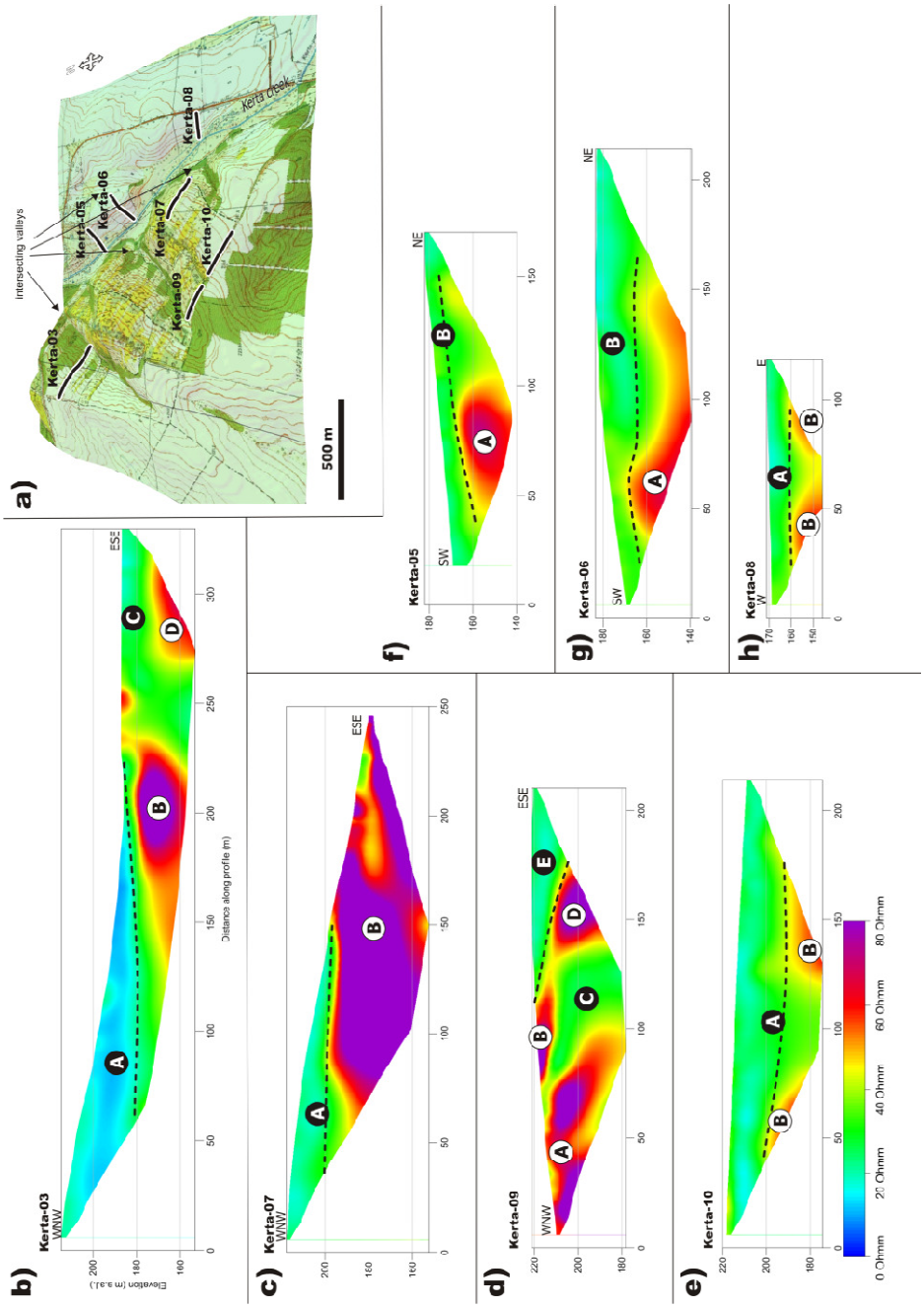

Figure 4.17 *a) Location map of the geoelectric profiles in study area #3 (Kerta creek). b-h) Inverted resistivity sections. Same labelling convention was used for the anomalies as in Fig. 4.13.*

The corresponding lithology could be determined based on the few outcrops found in the study area. On the crests sand layers were found, sometimes in quite compacted form, which were overlain by thinner clayey material. Another nearby outcrop revealed water saturated loess on top of the sand, which corresponds to the widespread Paks Loess Fm. (*Fig. 4.18*).

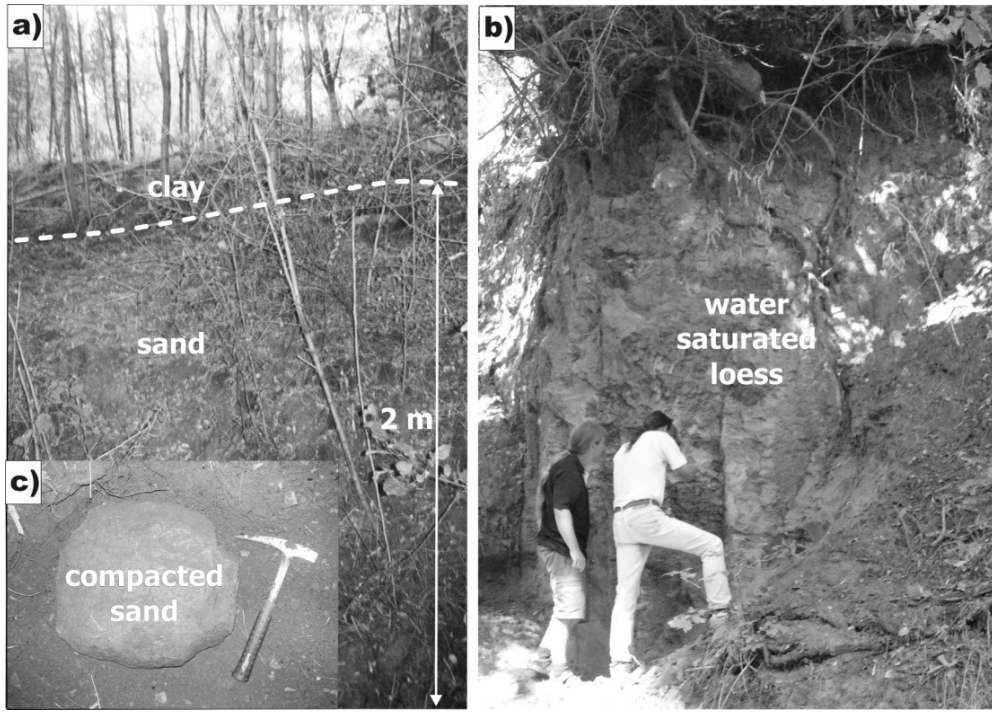

Figure 4.18 *Field observations in the vicinity of Kerta creek. a) Clay capped sand layers as well as b) water saturated loess column were observed in outcrops close to the location of geoelectric profiles. c) Well compacted sandstone was also found in surface exposure, which contributed to high resistivity anomalies.*

Examination of the inverted resistivity profiles from the Kerta creek area and topographic variations led to the following inferences on the spatial distribution of the sediments. E of the creek the area is characterised by low relief changes, while the W part exhibits more marked topographic variations. The total difference in elevation along the profiles in the eastern part is ca. 5-10 m, whereas the maximum difference in the profiles on the other side of the creek reached 40 m. On either side of the creek, the profiles showed high values in the deeper subsurface (*Fig. 4.17b-h*). The contrast between these high resistivity beds and the overlying deposits forms a marked boundary in the western profiles (*Fig. 4.17b-e*) and appears less pronounced in the eastern part (*Fig. 4.17f-h*). The imaged boundary is in line with the reported unconformity between the fluvial deposits and the loess cover. Field observations suggest that the high resistivity values originate from compacted sand bodies and/or gravel beds, while the low resistivity cap on top of them may correspond to clays and loess infiltrated by water.

Interpreted resistivity profiles around the Kerta creek demonstrate gravel or coarser sand layers over a relatively large area. At first glance, the results are not in contradiction with the existence of the laterally extensive terrace level #3 as it is indicated in *Fig. 4.10b*. Again, the fit of the imaged gravel beds into the classification scheme is discussed in detail in *Section 4.2.5.2*. Morphology, however, varies over relatively short distances in the study area, where several valleys have been traversed during the measurements. One may not

exclude that differential uplift of the ridges adjacent to the valleys might have caused lateral migration and consequent episodes of incision of the former drainage in the area resulting in small-scale step-like changes in the topography. In any case of this latter scenario, the continuous high resistivity anomalies, which appear undisrupted, do not imply formation of separate terraces.

On the other hand, the geometry of the imaged gravel layers documents that the wavelength of their deformation is comparable to the topography of the entire anticline and the intersecting valleys are much closely spaced. Therefore, the imaged fluvial sediments belong rather to the proposed, most probably Pleistocene alluvial fan, which has been deformed and eroded. In addition, the interpretation and comparison of geophysical surveys on Lake Balaton with the pattern of the meridional valleys onshore revealed no correlation (see *Section 4.4*). The results inferred from the resistivity sections around the Kerta creek favour that aeolian erosion must have played the most important role in the formation of the meridional valleys.

The top of the gravel layers at the highest positions often appears to be near horizontal, which indicates an erosional unconformity overlain by wind-transported and re-deposited loess. As a remark, the upper part of Kerta-03 profile over the entire depth section is interpreted as loess. This fact points to the possibility that the monotonous near subsurface lithology observed for the Lentihegy (*Fig. 4.15*) is of a thick loess sequence indeed. If the loess is assumed to be deposited on a sequence of fluvial terraces, then the palaeo-morphology would either be completely filled up and no steps in the relief could be observed or remnants of the terraces should have been found near the surface where changes in topography occur. This is again strong evidence supporting that the meridional valleys have been carved into the ridges post-dating deposition of the gravel or, as it is most likely the case at Lentihegy, gravels could not deposit at all.

4.5.4 Discussion

4.5.4.1 Fault control of the valleys

Subsurface gravel bodies have been identified as large, generally continuous regions associated with high resistivity values. The large horizontal extent and deepest achieved penetration enabled the profiles in study area #1 (Cserta creek) to trace disturbances in the boundaries of sedimentary beds caused by offsetting faults, if there were any. No significant lateral variation or disturbed zone in the imaged lithology was inferred, which could be related to either strike-slip or small offset vertical fault activity (e.g. Kelevitz et al., 2010).

4.5.4.2 Correlation of assumed terrace levels to the geoelectric results

Even though the results appear to favour aeolian processes, owing to the great number of identified coarse grained deposits on the resistivity sections correlation to the members of

the classified terrace system proposed by Lovász (1970) has been attempted. First, only those sections of the measured profiles were taken into account, where the high resistivity layer reached the surface. The reason of doing so is that the classification of the assumed terraces was mainly based on surface mapping and thus the subsurface lithology could not be investigated. The comparison for the selected profiles is given in *Table 4.2*. Hereby the correlation is overviewed in each study area.

Profile/anomaly	Elevation of surface gravel occurrence (m a.s.l.)	Position in the terrace classification scheme
Cserta-01/A+(C)	180-200	between #2 & #3
Cserta-02/A	180-185	#2
Cserta-03/A	190-195	above #2
Lenti-02/A	290*	#5
Lenti-03/A	200*	between #2 & #3
Lenti-05/C	185-190	#2
Kerta-03/B	175-180	#2
Kerta-07/B	180-195	#2
Kerta-09/A+B	210-220	between #2 & #3

**only moderately high resistivity, much less than measured elsewhere*

Table 4.2 *Gravel occurrences identified in resistivity profiles in the study areas (profile name and label of the anomaly are indicated) with the corresponding elevation values of their surface exposure and correlation with the generalised terrace classification system.*

In the morphologically most interesting area, Lentihegy, the tomography profiles did not prove presence of coarse grained fluvial sediments at the given altitudes. Although two sections have been categorised within the frame of the terrace system and one of them may correspond to level #5, it is to be taken into account that their measured resistivity is significantly lower than any of other anomalies in the rest of the study areas interpreted as gravel or compacted sand deposition. In comparison with *Fig. 4.10a*, the closely spaced terrace levels could not be inferred from the resistivity profiles.

In case of the Cserta study area, profiles on the right bank of Cserta creek should have encountered two terrace levels, #2 and #3. Easternmost part of the Cserta-02 profile was to traverse terrace #3 (*Fig. 4.10b*). High resistivity anomalies close to the surface seem to conform to the generalised classification scheme. However, it is again to be emphasised that the tomography images evidence large, several hundreds of metres, continuous bodies in the subsurface, which also extend to the slopes and do not terminate. Disruption of high resistivity layers on the flank could only be observed in profile Cserta-01 but the geological interpretation has not concluded fluvial terraces (see explanation in *Section 4.5.3.1*).

The Kerta study area has been traversed with several resistivity lines. The whole area is described as a broad topographic high between the valleys, which belongs to terrace level #3. Three profiles have depicted gravel on the surface. They correlate rather to terrace level #2, though not fitting perfectly. However, below the surface a fairly continuous

transition is inferred from the altitude of terrace level #1 to #3 as evidenced by the rest of the profiles. Kerta-03, -07 and -09 profiles are separated by valleys. Their presence across the investigated area may be explained by intermediate stages of incision partly due to differential uplift. Since the terrace level classes represent a generalised view, there would be room for their existence but such steps in the subsurface data were not evidenced. As a conclusion, the intersecting valleys are unlikely to have been formed by fluvial processes. In the light of the inversion results, the geometry of the gravel layers supports the hypothesis that they all belong to a large alluvial fan (Fodor et al., 2005). The age of the alluvial fan gravel is poorly constrained, between Late Pliocene and Early Quaternary (Strausz, 1949). The present-day lateral and vertical distribution of the gravel bodies in the Zala hills can be interpreted as remnants of the old alluvial fan which has undergone deformation and erosion during the latest, still ongoing, tectonic phase (*Fig. 4.19*) and later became dissected by valleys formed by wind erosion. It is to be noted that in spite of the limitations of the data collected by surface mapping, Lovász (1970) also considered the existence of a former alluvial fan but restricted its deposits to the oldest (#5) terrace level.

Unambiguous evidence for the continuity of the assumed 'gravel carpet' over a large area and its exact 3D geometry below the surface could be constrained by a dense grid of geoelectric profiles preferably with even deeper penetration capability. Unfortunately, such a systematic survey could not be performed due to the terrain conditions but the presented resistivity profiles are indicative of the existence of the deformed and eroded alluvial fan.

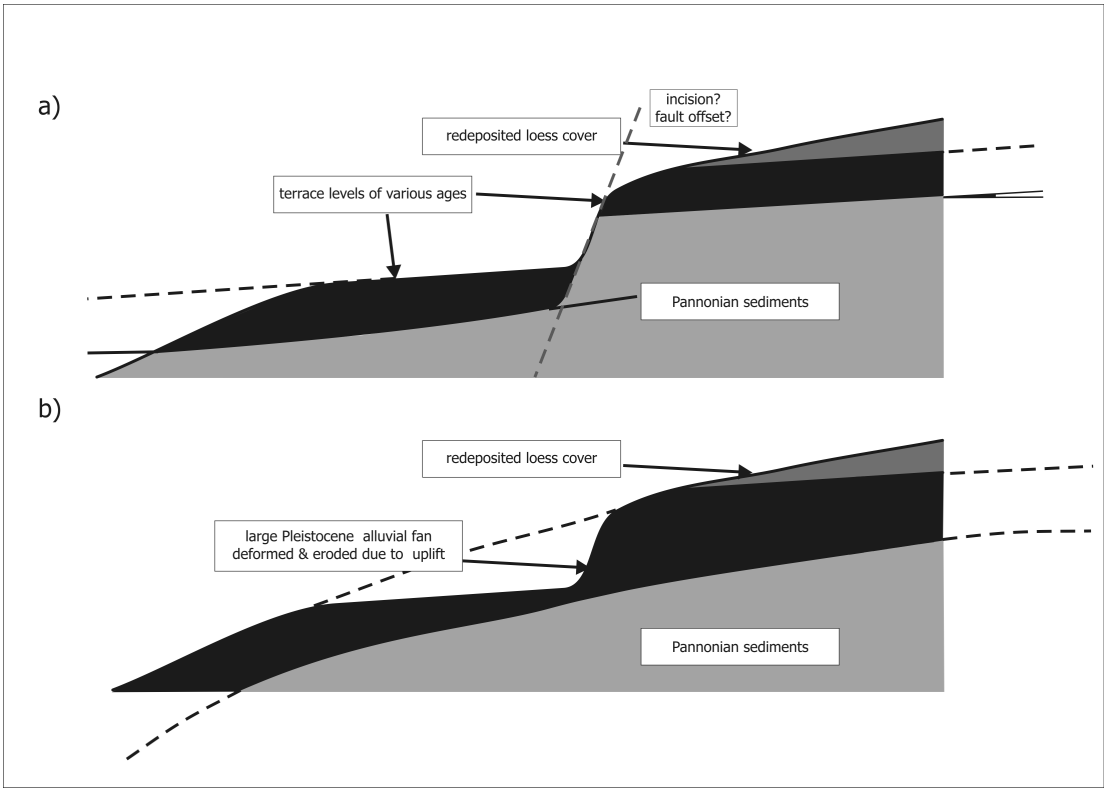

Figure 4.19 *Simplified cartoon illustrating two alternative explanations for the occurrence of gravel layers. a) Fluvial sediments arranged into terrace levels of various ages. b) A single alluvial fan, which has been being continuously deformed according to the rise of the anticline. Interpretation of the collected resistivity data supports the latter case. Actual geometry of the gravel beds is highly simplified in the cartoon.*

4.6 Conclusions

The quantitative analysis linking basin-scale interpretations with morphological analysis by the means of high-resolution geophysical measurements generally confirm the qualitative hypothesis that links the wind erosion in landscape forming processes in the Transdanubian region (e.g. Jámbor, 2002). According to the presented results, it can explicitly be stated that in case of the NW-SE oriented (meridional) valleys around Lake Balaton (area of Somogy hills, see *Fig. 4.1*) direct fault control is absent (Horváth & Dombrádi, 2010). Our results are further correlated by morphological studies in the Balaton region that corroborated the dominance of aeolian processes (Csillag et al., 2010). These inferences demonstrate ventifacts all pointing to the significance of deflation processes in the central part of Transdanubia. According to these results, the NW-SE to N-S trending ridges can be considered as yardangs, while the valleys between them are wind channels. Under conditions similar to the Holocene climate, fluvial erosion and wave abrasion were also important factors in forming the present-day topography. Chronological data indicated that in Transdanubia deflation must have caused considerable denudation in several phases at least during the last 1.2 million years and mass re-distribution took place as late as the early Holocene.

In contrast to the NW-SE (meridional) valleys, the NE-SW (longitudinal) ones are controlled by neotectonic fault activity as several other studies have inferred. Regional tectonic analyses using seismic profiles, outcrop studies and borehole data (Bada et al., 2003, 2005; Wórum & Hámori, 2004; Csontos et al., 2005; Fodor et al., 2005; Némedi Varga, 1977) have suggested the trace of the active faults that should be responsible for the observed morphotectonic studies features. This link between these faults and the surface topography has been confirmed by this study. Furthermore, the observed strike of neotectonic faults (NE-SW and ENE-WSW) is in agreement with the main Cretaceous and Miocene structural lineaments of the basin. These lineaments functioned as mechanical weakness zones and therefore have been repeatedly reactivated.
These findings have been also confirmed by 2D geoelectric surveys conducted in the SW corner of Zala hills that has successfully linked shallow subsurface data to the formation of the strikingly linear valleys, and, therefore, have provided critical information for deriving a mechanical model. The novelty of these results lies in the fact that they efficiently bridge the gap between surface derived geologic, geomorphologic information and standard industrial seismic data available for the broader study area. The interpreted resistivity sections have imaged marked high resistivity anomalies, which could be correlated directly to surface exposures and outcrops of Pliocene to Pleistocene coarse grained fluvial sediments, mostly gravels, previously mapped in details. The distribution and the geometry of these gravel layers below the valleys and their flanks provided valuable complementary information, which could be tested against various hypotheses of the valley formation.

The theory of tectonic pre-formation of the meridional valleys, already questioned by industrial seismic sections and high-resolution water seismic data from Lake Balaton, has

been furthermore rejected by the geoelectric profiling (*Section 4.4*). The top of the gravel layers, being easy to map based on the resistivity contrast, did not reveal even small vertical components of faults. A strike-slip zone could have been manifested as a disturbed zone in the inverted resistivity sections due to its higher conductivity, which was not observed either. All these findings demonstrate that recent (i.e. Pliocene-Quaternary) faults has not played an active role in the development of N-S striking ridges and valleys.

Multi-scale folding during the basin inversion and its contribution to the build-up of the anticlines, already inferred by the analogue modelling at basin scale in *Chapter 3,* has been furthermore confirmed by the high-resolution geophysical measurements. The geometry and the continuity of the imaged gravel bodies are representative of the scale of folding comparable to the anticlines themselves. In fact, these fluvial deposits, which are assumed to be remnants of a Pliocene or Pleistocene alluvial fan are distributed at more regional scale, demonstrate an episode of the on-going deformation by folding. The position of the intersecting N-S (meridional) valleys does not correlate with the wavelength of this folding. This means that the rate of incision by wind erosion is higher than the rate of creating topography by folding, i.e. erosion beats tectonics. Therefore, the concept of pure aeolian processes generating the meridional valleys is rather clearly demonstrated by the geophysical measurements. Using the interpreted resistivity data, lack of near-surface fault control, inconsistency within the fluvial terrace model, closer spacing between the valleys than the wavelength of folding have been inferred, which indirectly imply that the valleys are actually wind-grabens carved into the continuously uplifting anticlines.

A system of fluvial terraces with several members has been speculated by previous studies based on the description of the surface occurrences of the gravel deposits and their elevations complemented by scarce outcrop and borehole data. Apart from climatic effects, this idea has invoked a gradual river incision and lateral migration due to uplift. The quantitative high-resolution geophysical data have not imaged terraces beneath what at the surface is an apparent step-like morphology. At the extreme, in case of study area 2 (Lentihegy) fluvial sediments are even completely missing. Outside this area, the straightforward continuity of the gravels below the surface supports the existence of a larger-scale alluvial fan system, as opposed to the presumed evolution of a terrace-like morphology.

The presented data and their interpretation provided examples for smaller-scale folding in Transdanubia manifested in near surface sediments. In addition, effects of surface processes in the form of wind erosion are superimposed on the overall folded character of the topography in Transdanubia. The collected evidence excludes the fault control of the examined N-S to NW-SE set of valleys in the studied area. However, NE-SW striking Pliocene-Quaternary fault activity is rather significant both at the scale of Transdanubia and at a larger scale in the Pannonian basin outside the Dinarides margin (for instance the interpreted industrial seismic sections in *Chapter 3, Figs. 3.18-3.20,* see also Bada et al., 2010; Csontos et al., 2005; Magyari et al., 2005). Outside the study area, movements along these neotectonic lineaments are clearly reflected in morphology and river drainage

evolution, such as deflection or river patterns, stability of river profiles or channel migration (e.g. Timár et al., 2003; Magyari et al., 2005; Nádor et al., 2007; Petrovszki & Timár, 2010).

By having a direct link with surface morphology, the advantage of high-resolution geophysical methods examining the few metres to hundred metres sub-surface has been clearly demonstrated. The use of such techniques provides valuable information, which can complement deeper penetration geophysical data and surface observations and bridge the gap between them (see an example in Cloetingh et al., 2005b). The studied case shows that interpretations relying on such methods can successfully decrease or eliminate geologic ambiguities or occasionally, as shown, solve a century-long tectonic enigma. Beyond the local interest of landscape evolution these methods are generally applicable to study areas, where integration of multi-scale geological information is demanded.

Appendix A.4

Theoretical background of the DC resistivity measurements is summarised below (e.g. Lowrie, 2007).
During operation, direct current is fed into the ground through current electrodes (denoted as A & B) and the generated potential difference (voltage) is measured by the potential electrodes (M & N).

Let us consider a point source above a homogeneous, isotropic half-space. In this case the potential field (V) of the point source is:

$$V(r) = \frac{I\rho}{2\pi}\frac{1}{r}, \tag{A.4.1}$$

where r is the distance from the point source, I is the strength of the current and ρ is the resistivity of the medium. Hence, the potential difference in case of two point sources measured at the potential electrodes is the following:

$$\Delta V = V_M - V_N = \frac{I\rho}{2\pi}\left(\frac{1}{r_{AM}} - \frac{1}{r_{BM}} - \frac{1}{r_{AN}} + \frac{1}{r_{BN}}\right) \tag{A.4.2}$$

If the strength of the current *(I)*, the array of electrodes are known and the potential difference *(ΔV)* is measured, the resistivity can be easily calculated.

$$\rho = K\frac{\Delta V}{I} = \frac{2\pi}{\frac{1}{r_{AM}} - \frac{1}{r_{BM}} - \frac{1}{r_{AN}} + \frac{1}{r_{BN}}}\frac{\Delta V}{I}, \tag{A.4.3}$$

where K stands for the geometric coefficient.

In inhomogeneous media, this equation yields the apparent resistivity *(ρ_a)*:

$$\rho_a = K\frac{\Delta V}{I}, \tag{A.4.4}$$

The apparent resistivity represents the resistivity of a substituting homogeneous rock mass, above which we would measure the same potential difference with the same array. It is somehow an average of the resistivity of different layers and is very much dependent on the properties of the medium, in which the current flows. The real resistivity values can be evaluated via inversion algorithms.

Chapter 5

Drainage network evolution due to differential vertical motions from the perspective of multifractal analyses[4]

5.1 Introduction and research objective

Fractal geometry describes irregular patterns in nature that do not obey the rules of classic or Euclidean geometry but have fractional dimensions. Fractals, at least in a statistical sense, are self-similar. Zooming on a part of a fractal object, the magnified piece resembles to the whole object. Complex branching architecture and dendritic shape of drainage systems makes the impression of fractal-like structure. Superimposition of different physical and geological processes governing the evolution of rivers, including also random components, produces fractal river networks. The development of drainage network in the intra-Carpathian realm is influenced by tectonic topography primarily manifested in differential vertical surface motions. An excellent dataset on the present-day configuration of the left-hand side tributary system of the Tisza River (*Fig. 5.1*) was studied by means of fractal analysis in order to detect effects of different amounts of uplift. Boundary conditions set by tectonic topography were assumed to affect the self-organisation capability of the rivers and streams draining the surface.

[4] This chapter is largely based on the publication: Dombrádi, E., Timár, G., Bada, G., Cloetingh, S., Horváth, F., 2007. Fractal dimension estimations of drainage network in the Carpathian-Pannonian system. *Global and Planetary Change*, 58:197-213.

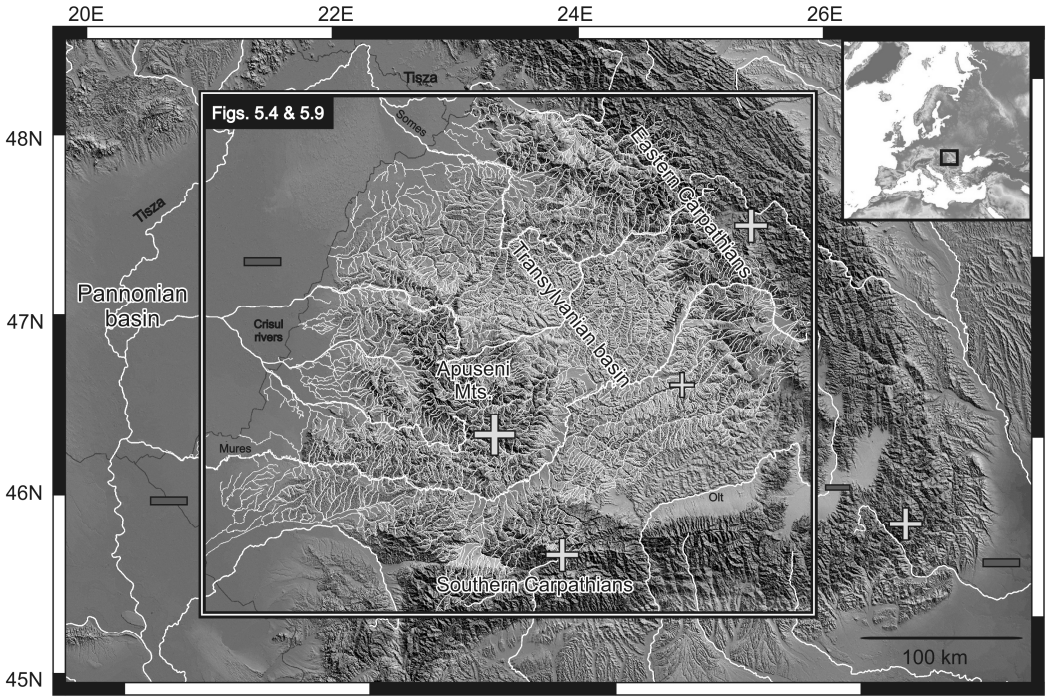

Figure 5.1 *Digital elevation model of the Carpathian-Pannonian system and the analysed drainage network (in white for a better contrast). Larger rivers are indicated by thicker solid line and main tributaries of the Tisza River are also labelled. Differential vertical motions are illustrated by the (+) and (-) symbols, uplift and subsidence, respectively (out of scale). Location of the study area is indicated on the inset map of Europe (top right corner).*

Fractal analysis of the rivers in this area has not been carried out previously. Therefore, various methods were tested to describe the complexity of the network by sets of fractal dimensions. These included the early estimations based on stream ordering hierarchy and the application of the box-counting and sandbox algorithms representing fixed-size algorithms considered as efficient tools in fractal set analysis. The calculations were applied to the entire drainage system and also on three distinct subdivisions of the region characterised by different Quaternary uplift history. These are the Apuseni Mts., the Transylvanian basin and a part of the eastern Carpathians, investigated separately (*Fig. 5.1*). The concept of multifractality was also taken into consideration and dimensions of both higher and lower orders were determined along with the corresponding singularity spectra. The study aimed at finding a possible link between the different amount of relative uplift and the space-filling ability of the river network (i.e. how evenly or unevenly they occupy the available surface) represented by the fractal attributes.

5.2 Overview of fractal characteristics of river networks

5.2.1 Fractal nature of drainage systems: Horton's laws

Scaling properties of river networks were early investigated and empirical scaling laws have been proposed by Horton (1932, 1945). These statistical calculations are based upon hierarchical classification of the tributary system starting from streams lacking upstream tributaries and giving increasing order numbers towards the outlet (see *Fig. 5.2a*). Number of river sections and their mean length in each class are compared to streams in an order higher class. Proportions of the above parameters are called the bifurcation (i.e. branching properties) and length ratios. Complemented with the area ratio (Schumm, 1956), these three ratios are referred to as Horton's laws or Horton ratios, and were found to be approximately constant through a wide range of drainage basins.

Fractal dimension (D_0) quantifies the complexity of a river system and the ability of the network to fill a plane. In this sense, a drainage network represented by a fractal dimension equal to 2 implies that the river channels are randomly distributed over the plane. The idea of plane-filling drainage evolution by random processes had long been under debate. Using the Horton ratios, the network fractal dimension was first derived by La Barbera and Rosso (1987, 1989) and D_0 was found less than 2. Modifications were considered by Tarboton et al. (1990) as the individual streams building up the network also exhibit fractal characteristics. This is due to their sinuosity and, thus, contributes to the fractal dimension of the whole network (see Rodriguez-Iturbe & Rinaldo 1997, Schuller et al. 2001 for a review). Incorporating the effect of sinuosity, results for network fractal dimensions became closer to 2, exhibiting a space-filling behaviour according to the assumptions of topologically random development of channels (Shreve, 1966). However, studies of other natural basins (e.g. Veltri et al., 1996; Claps & Oliveto, 1996) frequently evidenced dimensions being non space-filling, indicating that geological constraints prevent channels from developing as a pure branching process. Results of Monte Carlo tests demonstrated (Kirchener, 1993) that Horton's laws hold for almost all possible channel networks and cannot distinguish between random and non-random ones. Since Horton ratios require the statistical self-similarity of drainage networks, the applicability of the method was questioned (e.g. Tarboton, 1996; Beauvais & Montgomery, 1997). According to Tarboton (1996), the structure of Horton laws does not admit space-filling, whilst an alternative configuration of stream orders introduced by Tokunaga (1978) allows for a fractal dimension equal to 2.

5.2.2 Multifractal approach

Parallel to these studies, the concept of multifractals was also applied to river basins examining distribution of various hydrological parameters (Ijjasz-Vasquez et al., 1992; Rinaldo et al., 1992; Rodriguez-Iturbe & Rinaldo, 1997). While a single fractal dimension describes the complexity of a fractal set, multifractal theory (Mandelbrot, 1974; Frisch &

Parisi, 1985; Halsey et al., 1986, for a detailed description see Mandelbrot, 1990) accounts for the distribution of a measure over the fractal set and enables separate investigations of regions with low and high intensity of the given measure (Ijjasz-Vasquez et al., 1992). In other words, multifractals are compound of a series of fractals, each having its own scaling exponent (Lipschitz-Hölder or singularity exponent, α), and the corresponding monofractal dimensions (Aharony, 1989). Multifractals can be represented in two ways, either by an infinite number of generalised fractal dimensions (D_q) or via the singularity or multifractal spectrum ($f(\alpha)$). This spectrum yields the dimensions of the fractals with the same Lipschitz-Hölder exponent. Interpretation of the subsequent generalised fractal dimensions is fairly difficult. In this study the focus is on the spatial variations of the support dimension (D_0), i.e. the network fractal dimension of the rivers. Instead of correlating fractal dimensions of higher and lower orders directly, the shape of the evaluated curves was used to compare the multifractal characteristics of the different regions. In our case, Lipschitz-Hölder exponents express how the probability of finding neighbouring points belonging to the river network changes with distance. Thus, the singularity spectrum describes the fractal behaviour of dense and sparse clusters of the drainage network.

5.3 Brief geological and tectonic overview

Geodynamic evolution of the Pannonian basin from the Early Miocene onwards has already been overviewed in *Chapter 2*. In the following sections more attention is paid to the tectonic history of the Carpathians and particularly to the latest inferences on its hinterland, the Apuseni Mts. and Transylvanian basin (see latest review by Merten, 2011). Here, a brief overview is given on the formation of the orogenic belt and the post-collisional deformation of the Carpathian realm, which are necessary to understand the context of the results of this study. For an extensive and detailed review of the pre-collisional tectonic setting, see e.g. Schmid et al. (2008) or Matenco et al. (2010).

5.3.1 Formation of the Carpathian orogen system

The Carpathian orogenic belt was formed due to subduction and subsequent collision events between the European plate and the intra-Carpathian terranes during Cretaceous and Neogene times (Săndulescu, 1988; Royden & Horváth, 1988; Csontos & Vörös, 2004). Subduction beneath the contemporaneous Carpathian chains occurred partly coeval with the gravitational collapse of the Eastern Alps and lateral extrusion of crustal wedges towards the east (Ratschbacher et al., 1991).

First phase of contraction in the Eastern Carpathian due to continental collision between the European Foreland and the Tisza-Dacia terrane took place in early Burdigalian and the main period of thrusting lasted until Late Miocene times (~Middle Sarmatian, e.g. Matenco & Bertotti, 2000). Evolution of the thrust belt was characterised by temporal and spatial variation of the stress and strain fields (Huismans et al., 1997; Linzer et al., 1998). The overall trend in space and time reflects a gradual shift towards the foreland. The non-cylindrical shape of the orogen was most likely controlled by the geometry of plate boundaries, the variations in thickness of the propagating sedimentary wedges, and the major contrasts in the thermomechanical character of the foreland units (Matenco & Bertotti, 2000; Matenco et al., 2003; Tarapoanca et al., 2003). As a matter of fact, the different mechanical properties of the underplated blocks not only influenced the architecture of the thrust-belt but also account for the present-day stress field (Bada et al., 2001). It is to be noted that in contrast to previous thermochronological interpretations (e.g. Sanders, 1998), latest apatite fission track and (U-Th)/He data do not confirm a widespread exhumation in the South Carpathians, nor in the area of the Apuseni Mts. (Merten et al., 2010)

Starting from Late Miocene, following the cessation of collision, general exhumation and erosion commenced in the Eastern Carpathians, except for the SE bend zone, which is characterised by a different late-stage evolution (e.g. Cloetingh et al., 2004).

5.3.2 Post-collisional evolution of the Carpathians and its fore- and hinterland

After the collision a general exhumation has affected the units of the Tisza-Dacia plate, according to the most recent data, to an extent of 1-2 km. Synchronous subsidence has been recorded in the external thrust belt and in the Focsani foredeep basin (e.g. Leever et al., 2006; Matenco et al., 2007). Late-stage uplift is considered to be concentrated to the collision zone based on thermochronological data and no significant uplift is assumed further away from it, for instance in the Apuseni Mts. (Merten, 2011), at least below the resolution of these methods (1-1.5 km). This fact appears to lessen the possibility of late-stage uplift of in the Apuseni Mts., which is generally attributed to intraplate folding (e.g. Horváth & Cloetingh, 1996, Ciulavu et al., 2002). However, youngest sediments being of Miocene age at high elevation in the Apuseni Mts., while in the adjacent parts of the Pannonian basin situated at several kilometres of depth, tilted strata at the western part of the Transylvanian basin, and 300-400 m incision recorded by the hydrography in certain parts of the mountain chain together may refer to a few hundred metres uplift during Pliocene-Quaternary times.

Significant deep seismic activity in the Vrancea zone, SE Carpathians suggests the presence of a subducted lithospheric slab near the Vrancea zone (Oncescu, 1984; Sperner et al., 2001, 2002). Seismic tomography studies depicted the high-velocity body to a depth of 300-350 km (Wortel & Spakman 2000; Martin et al., 2006) and results of extended seismic campaigns corroborate the existence of the nearly vertical slab (Wenzel et al. 1998, 2002). This data set suggests that the Vrancea slab is the only existing relict of the subducted slab beneath the Carpathians. Inferred from basin analysis studies, accelerated subsidence in the Focsani Depression in the Carpathian foredeep was continuous from the Badenian throughout Quaternary times and more than 10 km of sediments accumulated (Matenco et al., 2003, 2007), which can be a result of the pull of the downgoing slab.

New thermochronological results suggest that the SE part of the Carpathian belt has undergone two young exhumation events during Pliocene-Quaternary times with a continuous advance of the core of uplift and erosion towards the foreland with a range of uplift between 1.6-1.7 mmy^{-1} (Merten et al., 2010). It is also documented by the deformed, eastward tilted Pliocene-Quaternary sedimentary sequences in the foredeep (Hippolyte & Sandulescu, 1996; Tarapoanca et al., 2003; Leever et al., 2006). Among the various geodynamic scenarios proposed to explain the observed uplift, one possible mechanism is lithospheric-/crustal-scale folding.

As a result of the tectonic evolution of the Carpathian orogen, considerable topography relief has been formed due to the differential vertical motions taking place in the area (*Fig. 5.1*).

5.4 Data and methods

Extraction of the natural drainage network using remote sensing techniques and high-resolution digital elevation models was performed in the framework of Tisza River Project (Müschen & Hochschild, 2002; Kardeván, 2002; Jolánkai, 2005). The selected area was further divided to three sub-regions: 1) the Transylvanian basin, 2) the entire Apuseni Mts. and 3) the western slopes of Eastern Carpathians. The latter two sub-regions, uplifted and exposed considerably, represent the source areas of the Transylvanian basin as well as the eastern part of the Pannonian basin.

Left-hand side tributaries of the Tisza River constitute the backbone of the analysed river network (*Fig. 5.1*). In spite of the close connection, streams in the adjacent Hungarian territories could not be utilised due to different resolution and the abundant artificial channels in the available dataset. The value of performing similar analysis on the subsiding area was tempting, therefore an attempt has been made to filter the accessible GIS data and retain only those segments that belong to natural flows. Unfortunately, the remaining, fairly incomplete data set proved to be insufficient and could have generated intolerable bias from a fractal characterisation point of view. Therefore, analysis was decided to be kept in the originally selected study area.

Spacing between the vertices of the polylines of the original digitised river network was not uniform. In order to obtain a homogeneous set of points representing the drainage system for the multifractal analyses, vertices were redistributed in the data set with equidistant 50 m spacing, resulting in a total number of more than 500,000 points.

5.4.1 Stream ordering and fractal dimensions

The empirical bifurcation and length laws of river networks were established by Horton (1932, 1945) using a simple stream ordering pattern, which was later developed by Strahler (1957). The commonly used Horton-Strahler scheme classifies the streams so that from sources to outlets they are assigned with increasing order numbers as the confluence of two streams of the same order makes up an order higher stream (*Fig. 5.2a*). Branching ratio can be calculated from the number of streams of each order:

$$R_B = N(\omega)/N(\omega+1) \tag{5.1}$$

and the length law is obtained from the average stream lengths using the following formula

$$R_L = L(\omega+1)/L(\omega), \tag{5.2}$$

where R_B and R_L is the branching ratio and length ratio respectively, $N(\omega)$ is the number of streams of order ω, and $L(\omega)$ is the average stream length of order ω. Fractal dimension of

the network based on the branching hierarchy (D_b, which is equivalent to D_0 support dimension) was first derived by La Barbera and Rosso (1987):

$$D_b = \ln R_B / \ln R_L \tag{5.3}$$

Plotting $N(\omega)$ versus $L(\omega)$ on a log-log scale, tangent of the line fitted through linear regression yields the ratio of R_B and R_L and consequently D_b (see *Fig. 5.6*).

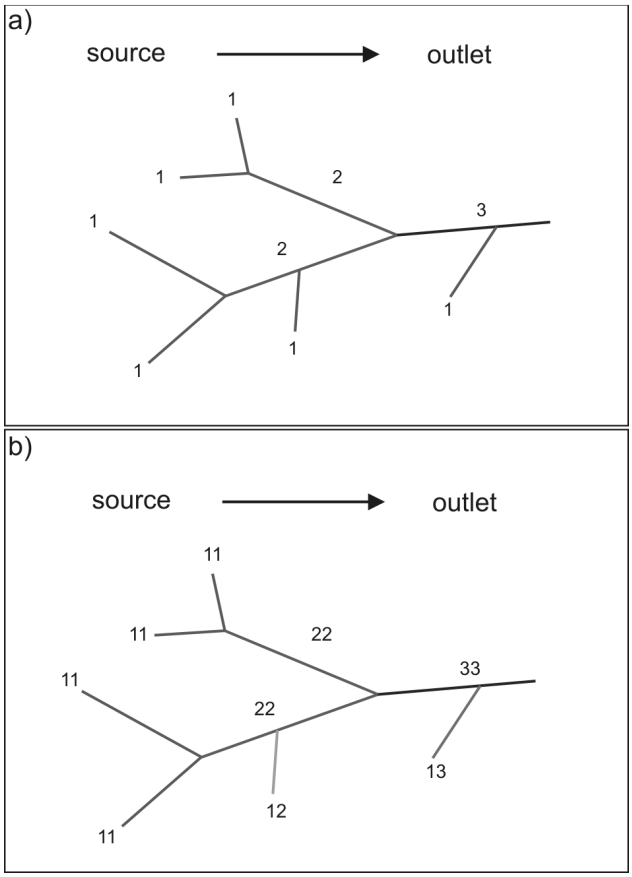

Figure 5.2 *Illustration of hierarchical stream ordering following a) Horton-Strahler scheme and b) Tokunaga rules. Streams are indexed with increasing numbers from source to outlet. River sections in the Tokunaga system are assigned with two digits and side branches are also classified (after Turcotte, 1997).*

The construction of the Horton-Strahler ordering system does not account for side tributaries as lower order tributaries flowing into higher ones do not alter the order number of the latter. To avoid this deficiency an alternative ordering scheme was developed (Tokunaga, 1978) which denotes streams with two digits. The first digit gives the order of the side branch in the sense of Horton-Strahler indexing while the second one refers to the order of the stream it flows into (*Fig. 5.2b*). Streams that are not side tributaries are denoted with the same digits such as 11, 22, etc. Branching ratios of real drainage basin dataset have shown good correlation with the concept of Tokunaga fractal trees and suggested the self similar structure of natural rivers and their tributaries in a statistical

sense (for details see e.g. Peckham 1995, Turcotte 1997). Quantitative analysis of the branching rules in a Tokunaga fractal tree also leads to the estimation of the fractal dimension and D_0 can be obtained by

$$D_0=\ln Q/\ln R_L, \tag{5.4}$$

where Q contains the branching ratios (for a detailed description see Tarboton, 1996). Following the Horton-Strahler classification rules, in case of the Romanian data set the highest order was 6, which is a long section of the river Mureş and correspondingly there were 21 groups according to the Tokunaga indexing. The associated fractal dimensions were assessed through the best linear fit (*Fig. 5.6*).

5.4.2 Generalised box-counting method

The generalised box-counting method is a member of the family of fixed-size algorithms (FSA). Application of the algorithm is also possible on river basins (De Bartolo et al., 2000, 2004). Besides the estimation of D_0 support dimension, further positive generalised fractal dimensions can be evaluated as well. Although with limitations, the technique enables multifractal analysis of river networks. In this case the measure (μ_i) gives the number of points in the ith cell of a given size (δ), i.e. the probability of finding neighbouring points that belong to the fractal set.

$$\mu_i=N_i/N, \tag{5.5}$$

where N is the total number of points. The fractal set, that is the assemblage of the points representing the river system, is covered by cells of side size δ, where δ is adjusted in each step and the points of each cells are counted (*Fig. 5.3*). The generalised fractal dimensions can be expressed using the partition function (Halsey et al., 1986). For the corresponding formulae see Appendix. Practically, the series of fractal dimension is assessed by means of linear regression over the values of $\ln(Z_q(\delta))/(q-1)$ versus $\ln(\delta)$ if $q\neq1$, and $\sum_{i}^{N_c(\delta)} \mu_i(\delta)\ln\mu_i(\delta)$ for q=1 (see De Bartolo et al., 2000). To avoid both over- and the underestimation of fractal dimensions by large and very small box sizes respectively, the obtained curve is truncated between upper and lower limits of δ (δ_{lower}, δ_{upper}). The excluded values are determined by the best fit parameters. Employing this procedure, usually only the left side of the multifractal spectrum ($f(\alpha)$) can be reconstructed properly as for negative values it often becomes divergent. An additional disadvantage is that cells containing too few points, particularly at the borders of the fractal set, also cause bias in the estimations for positive values of q.

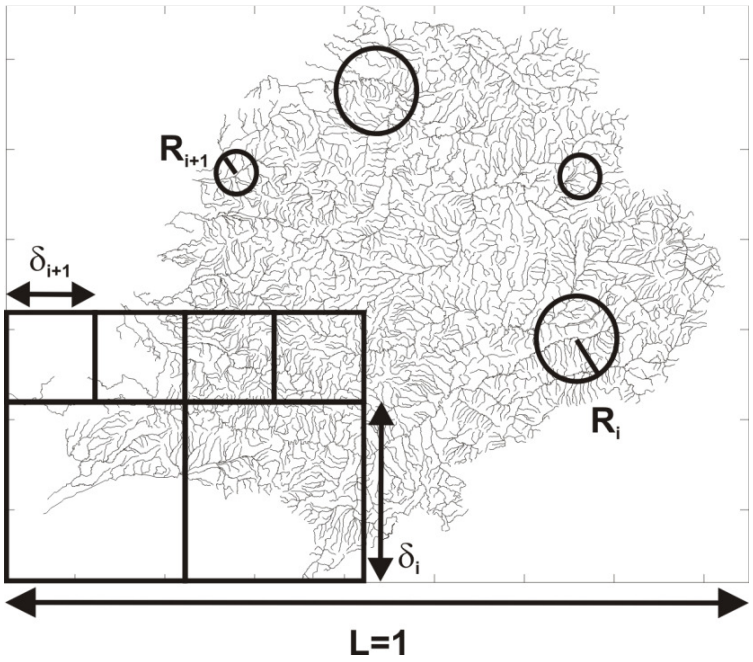

Figure 5.3 *Schematic illustration of the cells and circles used in the fixed-size algorithms. In case of generalised box-counting method, the fractal set is systematically covered by tiles of different size.* δ_i *and* δ_{i+1} *refer to the size of the cells in two subsequent steps. During sandbox algorithm circles of randomly distributed centres are placed on the points. Radius of the circles is also decreased step by step (*R_i*,* R_{i+1}*).*

5.4.3 Sandbox method

The sandbox approach was introduced by Tél et al. (1989), developed by Vicsek (1990) and Vicsek et al. (1990) and was applied in the analysis of river networks by De Bartolo et al. (2004). It offers an efficient tool to overcome border effects distorting the results of box-counting algorithm and to evaluate the right side of the singularity spectrum (f(α)) at the same time. Instead of covering the whole drainage system with grids, a number of circles with given radius (R) are placed on the fractal set with randomly distributed centres. The number of points within the circles, also considered as the mass (M(R)), and their qth moments are then averaged over the number of circles (Tél et al., 1989). Similar to the box-counting technique, values of D_q are obtained by linear regression between the truncation limits of R/L, where L is the lattice size (*Fig. 5.3*). In this case, quantities plotted against each other are $\ln\left\langle [M(R)/M_0]^{q-1}\right\rangle/(q-1)$, referred to as the scaling curve and ln(R/L) for q≠1 and $\ln\left\langle M(R)/M_0\right\rangle$ versus ln(R/L) for q=1. By eliminating the undesired effects of data scarcity, i.e. the divergence for negative orders, completion of the multifractal spectrum becomes possible.

5.4.4 Application of FSAs on the drainage system

The above two fixed-size algorithms, namely the box-counting and sandbox procedures were applied on the natural water flows of the Transylvanian basin, the Apuseni Mts. and the western slopes of the Eastern Carpathians (see *Fig. 5.1*). For the sake of comparison with the results based upon stream ordering, the same procedure was also carried out for the entire river network. Another possible technique of multifractal analysis is the method of generalised correlation integral (Pawelzik & Schuster, 1987). However, numerical treatment of large datasets is rather complicated (Füchslin et al., 2001). Therefore this method was not involved in the fractal analysis.

The box-counting procedure is carried out within rectangular boundaries because the cells are square shaped. The largest possible square portions of the sub-regions were extracted to minimise the number of blank cells or cells with insufficient number of points causing border effects. The Apuseni Mts. were represented by a single 100 km by 100 km square (Ap), the Transylvanian basin with three squares of the same size (Tb1, Tb2, Tb3). Two smaller squares (EC1 and EC2 with side size of 50 km) were extracted from the narrow and elongated chains of the eastern Carpathians. The overall network (referred to as ALL) was covered with a square of 350 km by 350 km (*Fig. 5.4*).

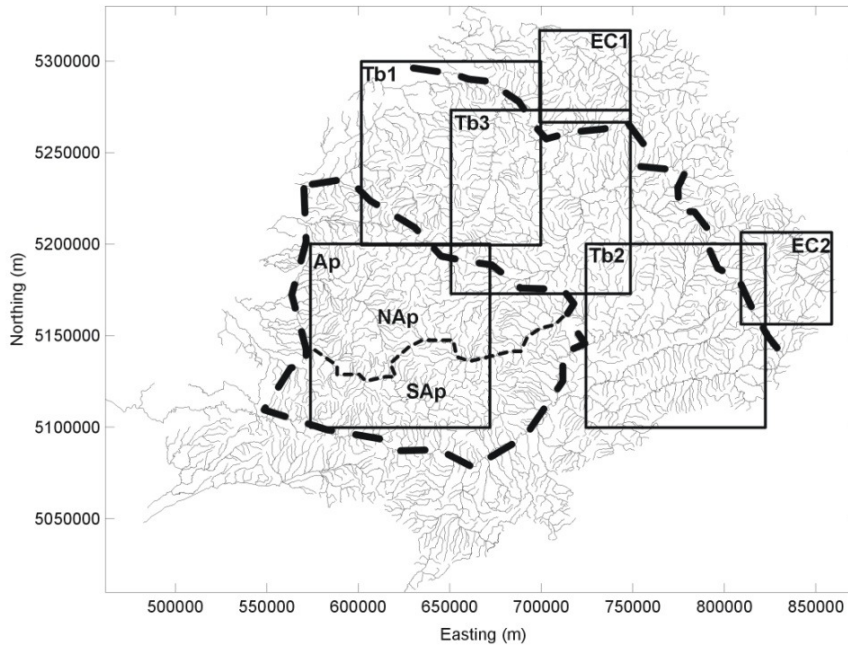

Figure 5.4 *Digitised net-points of the intra-Carpathian drainage system. Dashed lines indicate borders of the three regions analysed separately. Solid squares illustrate the square portions representing the drainage network of the Apuseni Mts. (Ap), Transylvanian basin (Tb1, Tb2, Tb3) and Eastern Carpathians (EC1, EC2) in the computations with box-counting method. Apuseni Mts. are further divided to northern (NAp) and southern parts (SAp). Coordinates are given in UTM projection. For location see Fig. 5.1.*

Naturally, the sandbox method could readily be applied for the irregularly shaped areas. Nevertheless, fractal dimensions and multifractal spectra of the square portions were also estimated in order to study the consistency of the fractal characteristics within a given region. Grid sizes and radii used in the subsequent steps of the numerical codes were normalised with the length of the side of the squares. In case of the sandbox method, the lattice size was determined as the possible minimum size of a square enclosing the studied drainage network. This kind of normalisation meets the criteria of geometrical invariance (Falconer, 1990). In the box counting procedure grid sizes were decreased from 1 to 0.01, radii of circles used in the sandbox analysis were logarithmically decreasing operating with a maximum number of 100 circles. Scaling curves were calculated for the moment orders from q=-10 to q=10 and linear fits were performed to obtain the generalised fractal dimensions. An example of the scaling curves for different q orders in the sandbox algorithm is illustrated in *Fig. 5.5*. Lower and upper cuts were adjusted to maximise goodness of the fit (R^2). Owing to the fewer data points in the box-counting method, it means that only the first and last points of the fractal curves had to be excluded from the analysis. Related mass exponents ($\tau(q)$) could be then calculated and by means of Legendre transform the Lipschitz-Hölder exponents (α) and the singularity spectra were evaluated (see Appendix A.5).

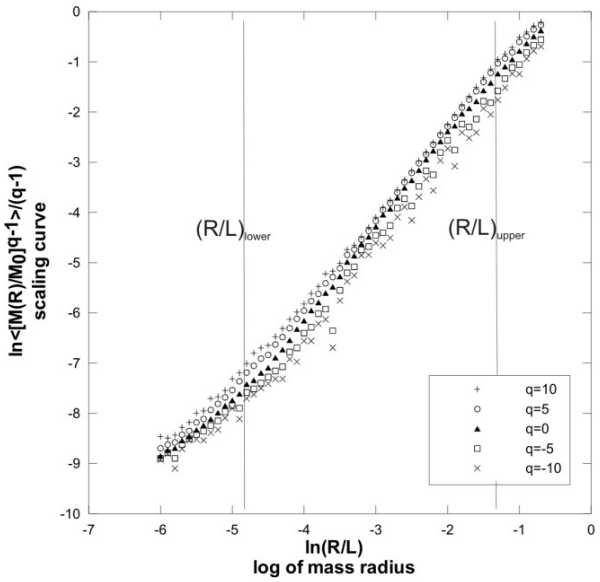

Figure 5.5 *Example of scaling curves for different moment orders obtained through sandbox algorithms. Note the few outliers for negative orders. Linear regression was performed between the lower (R/L_{lower}) and upper (R/L_{upper}) clip limits.*

5.5 Results

5.5.1 Results of stream ordering

First, the network fractal dimensions calculated from branching and length ratios obeying the Horton-Strahler and Tokunaga ordering rules are overviewed. In case of the Horton-Strahler method, the number of streams was plotted against the average stream length for the orders 1 to 6 on a doubly logarithmic scale (*Fig. 5.6*). Linear fit on these values directly yields the estimation of the fractal dimension ($D_b=D_0$). The slope of the line gives 1.89 for D_b. A significant scatter of the values around the regression line is well visible. As the selected area is not a single closed drainage basin, the overrepresentation of first order streams is expected, while the highest order is represented by only one value. Exclusion of these two outliers results in a decrease of the uncertainty and a slightly better estimation, $D_b=1.83$.

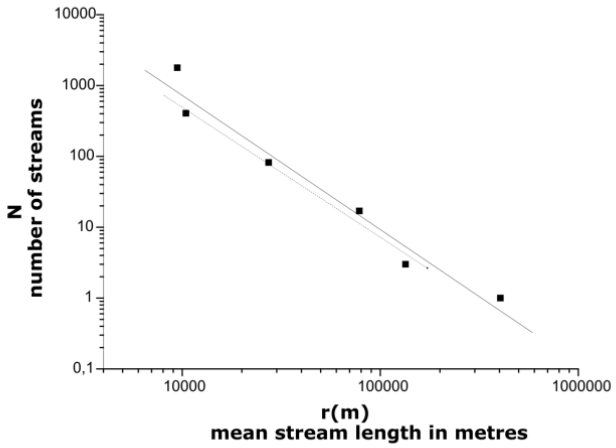

Figure 5.6 *Number of streams plot versus average stream length according to the Horton-Strahler ordering. Solid and dashed lines show best linear fits without omitting values and after the removal of values related to lowest and highest orders, respectively.*

The difference in the orders of two confluent streams forms the base of the Tokunaga classification. For instance, a first order stream joining a third order one and a third order stream flowing into a fifth order river section are in the same group as the difference in the orders is two in both cases (Tokunaga, 1978, 1984). In doing so, a more precise ordering of the side branches becomes possible. On the other hand, the fractal dimension cannot be deduced directly. It is determined by weighted averages of number of streams in each of these groups (Tarboton, 1996). Fractal dimension of the analysed catchment of Tisza River was found to be 1.91 according to the Tokunaga stream ordering rule. The estimated

network fractal dimensions were below two, indicating non-space filling behaviour of the rivers. As a first order inference, the investigated drainage network cannot be developed by purely random erosional processes.

5.5.2 Results of box-counting method

Whilst the previous methods were only capable of monofractal characterisation, analysis by means of fixed-size algorithms revealed multifractality in the scaling relations of the drainage network. Results of box-counting technique were supposed to be biased by border effect, but were regarded as appropriate for a qualitative analysis. Accordingly, the right-hand side of the multifractal spectra could not be resolved because even small errors are significantly magnified by large negative moment orders. The generalised fractal dimensions for positive values of q of the overall region and the selected square portions are illustrated in *Fig. 5.7a* and the results are summarised in *Table 5.1*.

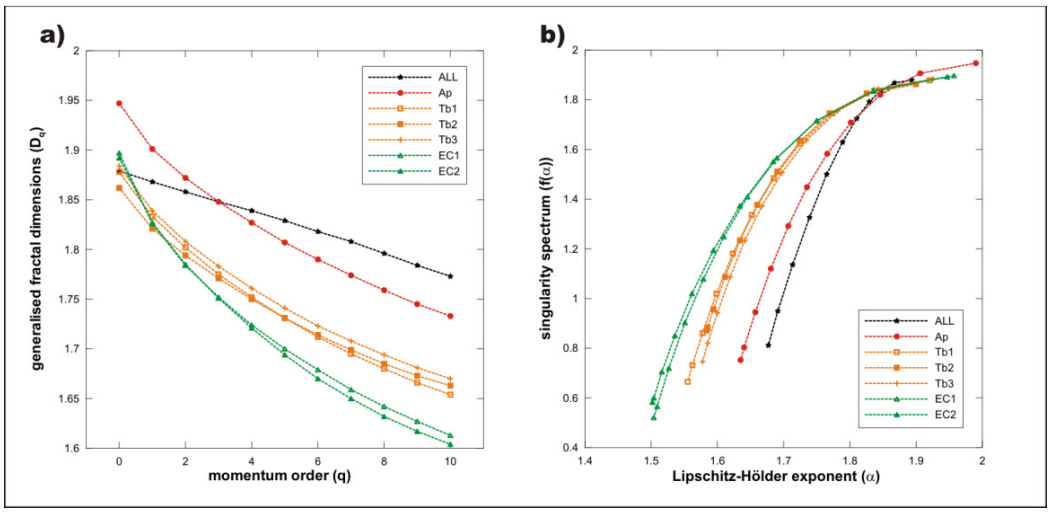

Figure 5.7 *a) Generalised fractal dimensions of square portions and the entire network (ALL) estimated through box-counting method. b) Left side of the corresponding multifractal spectra. For legend see Fig. 5.4.*

	N	D_0	R^2	δ_{lower}	δ_{upper}	α_{min}	α_0
Whole network (ALL)	511,124	**1.879**	0.9998	0.02	0.502	1.677	1.893
Ap	90,654	**1.947**	0.9993	0.02	0.502	1.635	1.99
Tb1	72,050	**1.878**	0.9995	0.02	0.502	1.555	1.92
Tb2	69,219	**1.862**	0.9997	0.02	0.502	1.585	1.9
Tb3	71,428	**1.884**	0.9994	0.02	0.502	1.578	1.926
EC1	20,601	**1.897**	0.999	0.02	0.502	1.504	1.957
EC2	22,262	**1.892**	0.999	0.02	0.502	1.502	1.947

Table 5.1 *Results of box-counting method. For meaning of abbreviations and symbols, see text.*

In the comparison of the sub-regions the support dimension was selected for quantitative analysis as it gives the network fractal dimension. Rest of the generalised fractal dimensions was not investigated in detail. Instead, the whole sequence of the generalised dimensions and the shape of the multifractal spectra were in the correlation of square portions. The highest value of the fractal dimensions (D_0) is from the Apuseni Mts., followed by square portions in the Eastern Carpathians (EC1 and EC2). The lowest values characterise the three extracted set of points from the Transylvanian basin (Tb1, Tb2, Tb3). The overall fractal dimension of the area is 1.879, lower than the first results of the Horton-Strahler and Tokunaga stream ordering.

Fig. 5.7a & b demonstrate that both the graphs of generalised fractal dimensions and the multifractal spectra of the three sub-regions are clearly separable. Conversely, the spectra of the extracted square portions in the Transylvanian basin tend to follow a narrow band as well as the curves of the Eastern Carpathians. This observation implies that any of the square portions fully represents the scaling properties of the sub-regions. Furthermore, variation of the fractal dimensions suggests the influence of the different tectonic background in the evolution of the river system.

5.5.3 Results of sandbox algorithm

Due to the structure of its algorithm, the sandbox method is less sensitive to border effects. Consequently, it is an appropriate tool to investigate the fractal dimensions for negative moment orders. However, below a certain extent, insufficient number of net-points results in distortion and divergence. This was experienced for all the cases in the Eastern Carpathians, which prevented the completion of the multifractal spectra. Otherwise the procedure provided reliable results for the whole Apuseni Mts. and the semi-circular shaped Transylvanian basin. Results of the sandbox analysis are summarised in *Table 5.2*. For the sake of clarity, generalised dimensions and associated multifractal spectra are illustrated in separate panels (*Fig. 5.8a-f*).

	N	D_0	R^2	$(R/L)_{lower}$	$(R/L)_{upper}$	α_{min}	α_0	α_{max}
Whole network (ALL)	511,124	**1.853**	0.9992	0.005	0.497	1.776	1.86	1.913
Apuseni Mts.	153,376	**1.833**	0.9991	0.012	0.333	1.728	1.835	1.854
Nap	85,286	**1.832**	0.9996	0.011	0.183	1.674	1.837	-
Sap	68,132	**1.831**	0.9991	0.007	0.223	1.745	1.846	-
Transylvanian basin	216,108	**1.808**	0.9994	0.006	0.333	1.722	1.819	1.868
Tb1	72,050	**1.814**	0.9991	0.018	0.497	1.723	1.823	1.901
Tb2	69,219	**1.801**	0.999	0.027	0.497	1.752	1.804	1.852
Tb3	71,428	**1.813**	0.9991	0.018	0.497	1.699	1.826	1.909
Eastern Carpathians	105,884	**1.821**	0.9994	0.011	0.135	1.656	1.826	-
EC1	20,601	**1.765**	0.9992	0.041	0.497	1.627	1.764	-
EC2	22,262	**1.823**	0.9992	0.041	0.273	1.631	1.849	-

Table 5.2 *Results of sandbox method. For meaning of abbreviations and symbols, see text.*

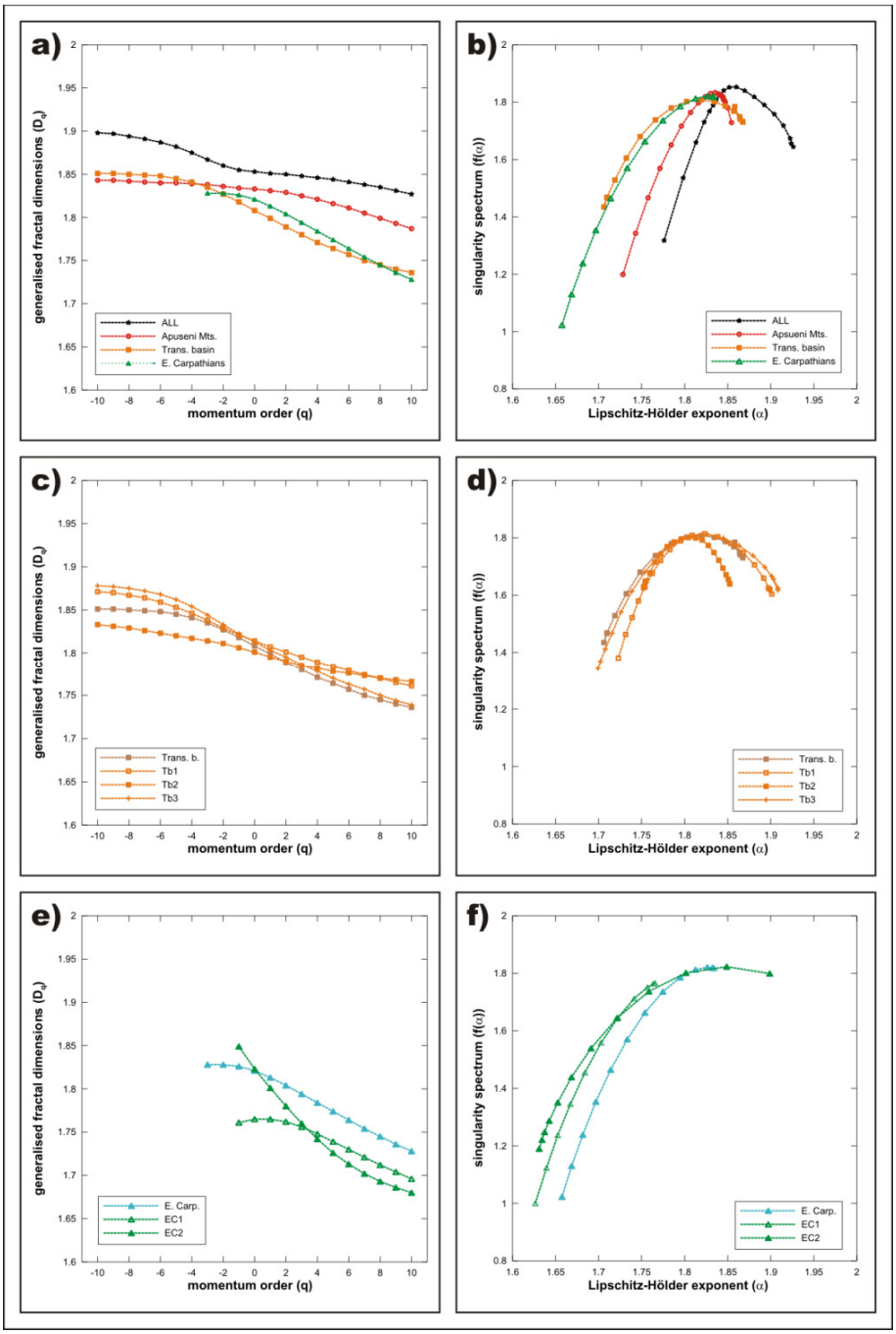

Figure 5.8 *a) Generalised fractal dimensions of the whole river network (ALL) and the three sub-regions obtained by sandbox method. b) Multifractal spectra of the whole river network and the three sub-regions. c) Generalised fractal dimensions of the Transylvanian basin and square portions by sandbox method. d) Multifractal spectra of the Transylvanian basin and square portions. e) Generalised fractal dimensions of the Eastern Carpathians and square portions. f) Multifractal spectra of the Eastern Carpathians and square portions. For legend see Fig. 5.4.*

As a first order conclusion, the results are qualitatively similar to the outcome of the box-counting procedure but lower support dimensions and less pronounced variations were obtained (*Tables 5.1 & 5.2*). *Fig. 5.8a & b* present the generalised fractal dimensions and the corresponding multifractal spectra of the whole network and the sub-regions. The separation of the curves is still well visible. The square portions and the entire Transylvanian basin are characterised by very similar curves without significant deviation (*Fig. 5.8c & d*). Due to the errors, the consistency of the fractal parameters of the streams draining the Eastern Carpathians is less obvious (*Fig. 5.8e & f*). However, the difference in the support dimensions of EC2 and the total East Carpathian area appears only in the third digit. It is also noteworthy that most of the curves are left skewed. Asymmetry of multifractal curves expresses dominancy of low or high fractal exponents with respect to the other (e.g. Telesca et al., 2004). It implies that dense parts of the river network tend to occupy the space in a similar way, while the sparse regions are much more inhomogeneous.

5.6 Discussion

In the framework of this study, fractal properties were investigated by means of different numerical calculations. With respect to the entire intra-Carpathian network, each method corroborated non space-filling configuration of the tributary system, as the obtained network fractal dimensions were all below D_0=2. These results are in accordance with the findings of analyses of other drainage basins and exclude the possibility of a totally random evolution of the streams.

5.6.1 Mono- and multifractal description of the drainage network

Fractal dimension estimations carried out following the rules of stream ordering, employing either the Horton-Strahler or the Tokunaga method, yielded relatively high values. However, absolute errors of the linear fit and weighted averaging are in the order of ±0.1. The high level of errors primarily suggests that scale invariance of the fractal structure of the rivers in the selected region of the Carpathian-Pannonian system is violated and cannot be locally characterised by a single fractal dimension.

Expectations concerning the non-invariant scaling of the selected drainage network were confirmed by the application of multifractal analysis. In case of a statistically self-similar fractal set, fractal dimensions for different moment orders (q) would be the same and, consequently, the multifractal spectrum would consist merely a single point (e.g. Ijjasz-Vasquez et al., 1992). Multifractal behaviour and inhomogeneous scaling properties were evidenced through both the generalised box-counting and the sandbox algorithms, with the latter approach being more reliable. Both methods automatically incorporate fractal dimensions of individual streams into the network fractal dimension. During the analysis, the focus was on the selected three sub-regions with different tectonic history and behaviour.

In order to reduce border effects during runs of box-counting algorithm, square portions were extracted from the drainage network. It means that the total fractal set was approximated with subsets of it. Such substitution may result in different support dimensions (D_0). Normally, the dimension of the union of subsets could not be exceeded by any of the subsets for a countable sequence of sets. Unfortunately, the so-called countable stability does not hold for the box-counting procedure (see De Bartolo et al., 2000 and references therein). Accordingly, analysing a square portion of the river network may produce higher fractal dimensions than for the network itself. *Fig. 5.7a & b* shows that the support dimension of the overall network is lower than those of the Apuseni Mts. and Eastern Carpathians. Hence, the obtained fractal dimensions appear to be overestimated. Nevertheless, the tendency of higher and lower values for each sub-region is similar to the results of the sandbox approach. Therefore the evolution of the drainage network is assumed to be controlled by recent geological processes.

Sandbox algorithm is less influenced by border effects and free of deficiency concerning the countable stability rule. Therefore, the values obtained by this method can be considered more certain. The support dimension of the entire river system is the highest value in this case (*Table 5.2*). Moreover, reconstruction of the right side of singularity spectra could be accomplished in most cases. In general, the estimations are of good quality in a statistical sense which is also demonstrated by the goodness of the linear fits presented in *Tables 5.1 & 5.2*.

5.6.2 Discussion in the context of vertical movements

The support dimensions of the fractal sets are close to each other but show a slight, yet important variation across the investigated territories and a particularly strong consistency within the Transylvanian basin. The highest value was obtained for the Apuseni Mts. followed by the Eastern Carpathians, disregarding value for EC1. The lowest values were obtained for the Transylvanian basin. As the sub-regions are characterised by different tectonic habitat, these values imply a likely correlation between the complex scaling properties of the evolved river network and the different vertical motions each territory has undergone.

Originally, a tentative correlation was set between inferred Quaternary uplift rates and the fractal dimensions (Dombrádi et al., 2007). Considering numerical model calculations for surface uplift due to isostatic rebound, the Transylvanian basin has attained a 0.1 mmy^{-1} uplift rate (Sanders, 1998, Sanders et al., 2002). Apuseni Mts. were considered to be characterised by an accelerated Quaternary uplift based on the lithospheric folding model. An average rate of 0.25 mmy^{-1} Quaternary uplift was set on the basis of this model complemented by field observations and geological maps. As for the Eastern Carpathians region, previous fission track data suggested 0.5-1 mmy^{-1} long-term surface uplift but on geomorphological analogues (Radulescu et al., 1996; Necea et al., 2005) a 0.3 mmy^{-1} rate was assumed for the Quaternary period.

According to new thermochronological data from the region (Merten et al., 2010; Merten, 2011), exhumation during the Pliocene-Quaternary was restricted to the SE Carpathians and neither the East Carpathians, nor the Apuseni Mts. have significantly uplifted. Particularly, the Apuseni Mts. are believed to have gained their overall topography during the Late Cretaceous, or the subsequent Palaeogene exhumation phases. In the light of these new results, such a quantitative comparison cannot be justified.

However, surface uplift and erosion below 1-1.5 km cannot be detected by the combined AFT and (U-Th)/He methods. Based on the arguments lined up in *Section 5.3.2* for the case of Apuseni Mts. an uplift of up to 1000 m in consequence of intraplate folding is likely, which is compatible with the amount of Pliocene-Quaternary uplift in the western Pannonian basin (Transdanubia) and the predictions of the analogue models and has definitely added extra relief compared to the Transylvanian basin.

The lowest fractal dimensions were found in the Transylvanian basin with both methods, while the East Carpathian orogen and the Apuseni mountain belt have higher support dimensions. Qualitatively, these fractal measures suggest that the river network of the Transylvanian basin has been subject to geologic factors, which forced a more non-space filling character in comparison to the drainage of the bounding mountains. Either the Pliocene-Quaternary processes or the earlier phases of deformation have determined the bulk topography of the investigated area, the Transylvanian basin has always been enclosed by higher topography regions, which situation may have pre-set conditions for the space-filling ability of the drainage located in its interior.

5.6.3 Morphology of the catchments

The morphology of the river network in the intra-Carpathian area is clearly affected by the relative vertical movements (Gábris, 1998; Timár, 2003; Timár et al., 2005). Associated geomorphologic features such as reorganisation of local drainage divides, river diversions and captures, changes in drainage pattern and several levels of uplifted river terraces are reported from the SE Carpathians (e.g. Fielitz & Seghedi, 2005; Necea et al., 2005). Rose diagrams in *Fig. 5.9* display the angular distribution of present-day river reaches of the three study areas approximated by polyline sections between two neighbouring vertices.

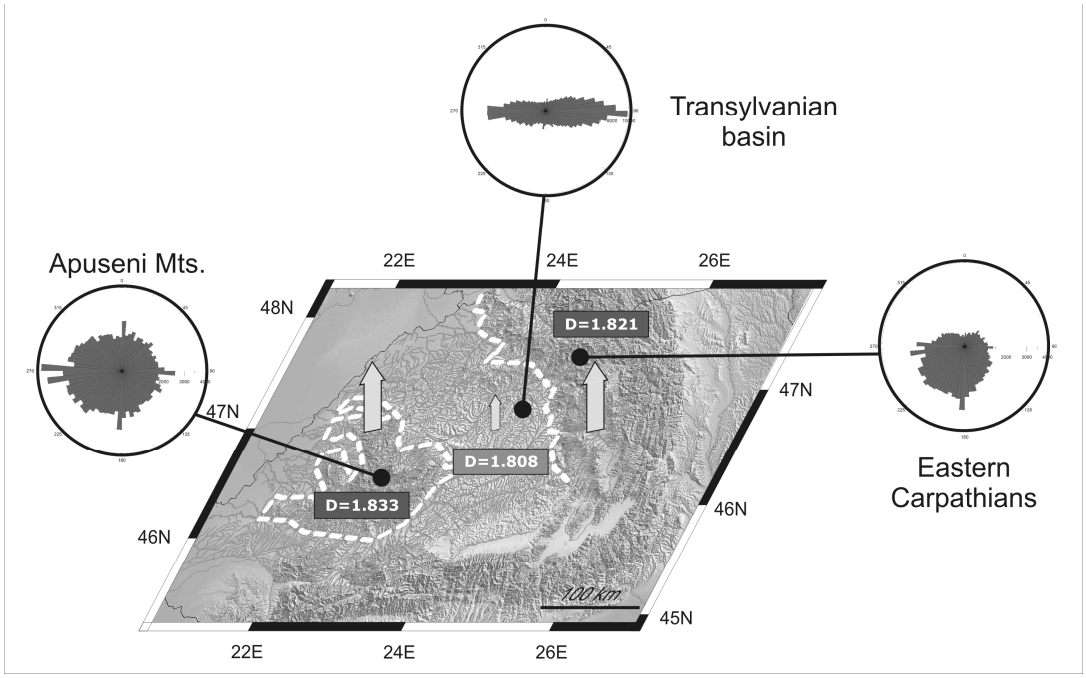

Figure 5.9 *Arrows illustrate relative differences in the amount of uplift (out of scale). Rose diagrams represent distribution of river reach orientations in the three sub-regions of the study area (separated by white dashed lines). For location see Fig. 5.1.*

The distribution seems to be uniform in the Apuseni Mts. In the Eastern Carpathians a SW direction is dominant, due to the fact that only the western slopes of the Eastern

Carpathians were analysed. Uniform distribution of channels implies adaptation of the rivers to ongoing uplift with concentric drainage patterns around the highest elevations. However, the least uplifting, bowl shaped Transylvanian basin bounded by the two mountainous areas exhibits the clear dominance of E-W orientation. The E-W oriented drainage in the central parts of the basin is assumed to reflect an older drainage network which evolved in a typical hinterland-orogen setting along the main Carpathian drainage divide (Fielitz & Seghedi, 2005). On the basin flanks the drainage system was modified by the more rapidly uplifting source areas. Fractal dimensions do not provide information on the shape and directions of river networks. However, such a geometrical constraint caused by the different velocity of vertical movements may prohibit the formation of a more space-filling configuration in the basin.

5.6.4 Comparison to other river basins

Recent studies focused on the multifractal characterisation of spatial organisation of Calabrian rivers through various techniques (De Bartolo et al., 2000, 2004, 2006). Streams were digitised from topographic maps and represented by a set of points called as 'net-points' (De Bartolo et al., 2000). Analyses through a range of fixed-size algorithms confirmed multifractal scaling properties with support dimensions all below two. Observed variations in the fractal dimensions in these river basins were attributed to different type of source rock lithologies (De Bartolo et al., 2004; Gaudio et al., 2006) or spatial heterogeneity of lithology (De Bartolo et al., 2004).

Gaudio et al. (2006) studied square portions with an area of 100 km^2 via the methods of sandbox algorithm and generalised correlation integral. Consistently higher fractal dimensions and singularity exponents were found in areas of plutonic-metamorphic source rocks than in those of coherent sedimentary rocks. However, previous analysis of these river basins with the sandbox approach (De Bartolo et al., 2004) provided contradicting results as river basins underlined by crystalline rocks have higher fractal dimensions compared to networks that drain siliciclastic sedimentary rocks. De Bartolo et al. (2004) also pointed out that the observed variations are likely to be linked to the spatial heterogeneity of source rocks as the studied catchment was considered to be tectonically unaffected.

To test lithologic control on fractal dimensions in the study area, the Apuseni Mts. were selected as they can be divided into two units of different origin and rock properties (*Fig. 5.4*). The North Apuseni Mts. consist of mainly crystalline basement covered with Permo-Mesozoic sediments, while the Southern Apuseni Mts. are characterised by Jurassic volcanic rocks (ophiolites) and Cretaceous molasse and flysch type sediments (e.g. Patrascu et al., 1994; Dallmeyer et al., 1998). The corresponding fractal dimensions and multifractal spectra (*Fig. 5.10a & b*) show that support dimension for both units and the entire Apuseni Mts. are essentially the same (*Table 5.2*). However, multifractal spectra of the two units show deviation from the curve for the whole Apuseni Mts.

On the other hand, Neogene calk-alkaline magmatism also accompanied the subduction in the Carpathian orogen and rivers of the Eastern Carpathians drain these volcanic rocks. Multifractal estimators of this region definitely differ from the values characterising the Southern Apuseni unit. Consequently, it is supposed that rock properties may be of far less significance concerning the fractal dimensions of the drainage network in the Carpathian-Pannonian system. Instead, as has been already pointed out, differences in the rate of vertical motions (uplift) play a much more essential role controlling fractal properties in the region.

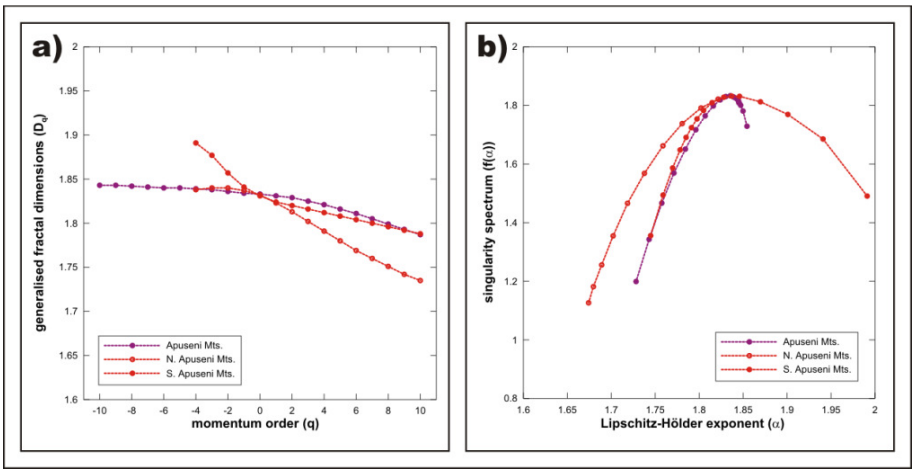

Figure 5.10 *Fractal dimension and reconstructed multifractal spectra for the a) northern and b) southern parts of the Apuseni Mts. to test the influence of lithology on fractal dimensions.*

5.7 Conclusions

The landscape development of the Carpathian-Pannonian realm has been influenced by a poly-phase deformation history, which resulted in significant differential crustal movements. Among various aspects of the complex tectonic processes, this study focussed on the effect of crustal movements on drainage network development as rivers are sensitive recorders of differences in subsidence or uplift rates. Left-hand side tributary system of the Tisza River was selected for analyses. The catchment area covered the Apuseni Mts, Transylvanian basin and the western slopes of the East Carpathians. The Transylvanian basin itself has been uplifted but with a slower rate than the bordering mountain belts. Thus, differences in the topographic evolution were expected to be reflected by large-scale spatial organisation of the drainage network.

Description of the topology of rivers via fractal dimensions is a well-known method. However, the major challenge is to attribute the underlying physical and geological process to the fractal characteristics. To arrive to such interpretation, traditional and novel methods of fractal theory have been applied. Since it was the first time that such examination of the area has been done, several algorithms have been tested and in that sense it can also be considered as a feasibility study.

Even preliminary techniques, mainly based on the branching properties of the river network, have clearly demonstrated the long-lasting influence of geological processes reflected by non-space filling architecture of the river reaches. Multifractal spectra yield fractal dimensions of the subsets of a given geometrical formation. Multifractal spectra of river networks, beyond the examination of the space-filling behaviour, enables representation of sparsely and densely populated parts of the surface water flows. Among the tested methods, the advanced sandbox algorithm proved to be the most reliable to generate these spectra for all three above-mentioned geological units and their smaller compartments as well.

Comparison of the determined fractal dimensions and spectra showed coherent values for the streams draining the Transylvanian basin, while the adjacent mountain chains (Apuseni Mts. and Eastern Carpathians) exhibited slight, yet systematic deviations from these trends. Consequently, stochastic behaviour of erosional processes has been overprinted by alterations related to crustal deformation to such an extent that is detectable in the spatial organisation of the drainage network. Differences in the uplift history of the three areas are likely to have set such topographic boundary conditions, which hinder the evolution of a space-filling river network in the basin. This scenario is supported by the trends in the statistics of the directions of stream segments. Azimuthal distributions in case of the mountains are fairly homogeneous, whereas the river network of the Transylvanian basin exhibits a clear E-W trend.

It is to be emphasised that fractal dimensions and spectra reflect the spatial organisation and the evolution of the large-scale structure of the entire drainage network. Information on the individual river pattern types cannot be derived from these mathematical measures and hence conclusions on the climatic and tectonic factors influencing the smaller-scale morphology cannot be drawn either.

An additional important aspect was highlighted by the results in the Apuseni Mts, which exhibited uniform properties in terms of fractal characteristics. This fact supports that differences in bedrock lithology play only a secondary role and, thus, areal variations in the multifractal dimensions reflect the varying rates of surface uplift independent of the types of rocks exposed on the surface.

In summary, the presented techniques are essential geomorphologic tools and can readily be employed to detect active tectonic processes affecting spatial evolution of river networks. Examples of successful application, especially when combined with other analyses, are reported in several recent studies (e.g. Shahzad et al., 2010; Mahmood & Gloaguen, 2011, 2012).

Appendix A.5

The generalised fractal dimensions in the box-counting method are computed for q≠1 as follows:

$$D_q = \frac{1}{q-1} \lim_{\delta \to 0} \frac{\ln Z_q(\delta)}{\ln \delta}, \tag{A.5.1}$$

where Z_q is the partition function,

$$Z_q(\delta) = \sum_{i=1}^{N_c(\delta)} [\mu_i(\delta)]^q \tag{A.5.2}$$

summing the qth momentum of the number of points (normalised with the total number of points, $\mu_i=N_i/N$) through the $N_c(\delta)$ number of cells covering the studied area at δ resolution.

For the special case of q=1

$$D_1 = \lim_{\delta \to 0} \frac{\sum_{i}^{N_c(\delta)} \mu_i(\delta) \ln \mu_i(\delta)}{\ln \delta} \tag{A.5.3}$$

The Lipschitz-Hölder exponent and the multifractal spectrum can be expressed from the generalised fractal dimensions by introducing the mass exponent $\tau(q)$:

$$\tau(q) = (1-q) \cdot D_q \tag{A.5.4}$$

through a Legendre transform

$$\begin{aligned} \alpha(q) &= -\frac{d\tau(q)}{dq} \\ f(\alpha(q)) &= \tau(q) + q\alpha(q) \end{aligned} \tag{A.5.5}$$

Similarly, the sandbox dimensions of momentum orders q≠1

$$D_q(R/L) = \frac{1}{q-1} \lim_{R/L \to 0} \frac{\ln \left\langle [M(R)/M_0]^{q-1} \right\rangle}{\ln(R/L)}, \tag{A.5.6}$$

where R is the radius of circles, L is the lattice size, while M(R) is the number of points within the circle and M_0 is the total number of points. Using Taylor's formula De Bartolo et al. (2004) expanded the relation to q=1

$$D_1(R/L) = \lim_{R/L \to 0} \frac{\ln\langle M(R)/M_0 \rangle}{\ln(R/L)} \qquad \text{(A.5.7)}$$

In case of the sandbox procedure the multifractal spectrum is also obtained by the equations A.5.4 and A.5.5.

Chapter 6

Main conclusions and forward look

The objective of this thesis was to investigate for possible coupling between late-stage deformation of the Pannonian basin and development of the topography across various horizontal and vertical scales. The importance of tectonic topography in the Pannonian-Carpathian system has already been underlined by research activities during the last two decades. The research presented in this thesis aimed at unravelling some further aspects of the interplay among lithospheric-, crustal-scale and surface processes acting on orogen-to-basin, regional or local scale. For this purpose, several new research methodologies have been introduced, which assisted a more complete interpretation. Below, the main results of this investigation, following a depth to surface order, are summarised, together with an outlook on the possible follow-up of the presented work.

6.1 Inferences from lithospheric-scale analogue modelling

6.1.1 Concept of lithospheric folding in the Pannonian basin

During the last compressional phase of the basin evolution, deformation due to the accumulation of intraplate stress has been assumed to be manifested in the form of lithospheric folding. Surface as well as subsurface evidence for young folded strata and significant opposite sense vertical movements documented across the basin all support this concept. The idea became more established by 2D numerical models performed in order to simulate the formerly extended Pannonian lithosphere under compression (Horváth & Cloetingh, 1996). These models proved that the mechanically weak lithosphere is able to fold and create alternating series of subsiding and uplifting regions. The wavelength of the folding (~400 km) correlated well to the observed periodicity of this series in the basin system. In terms of the amplitude of the folding, however, only limited amount of Pliocene-Quaternary subsidence and uplift could be derived from the models adopting a uniform elastic rheology of the lithosphere, totalling maximum 200 m. Based on basin analyses 3-5 times larger subsidence and, although less constrained, mostly by indirect evidence, often two times larger uplift was observed. In addition, tectonic and stratigraphic studies documented existence of shorter wavelength folding (e.g. Sacchi et al., 1999; Fodor et al., 2005). These unresolved questions gave motivation to investigate the deformation of the Pannonian basin by analogue models.

6.1.2 Mechanism and quantification of folding

Application of the 2D analogue tectonic modelling approach provided an independent method, which confirmed the viability that the weak Pannonian lithosphere of "crème brûlée" type of rheological stratification (Burov & Watts, 2006) can be folded (Type-1 experiments). The primary source of compression driving lithospheric folding is the far-field

stress exerted by the indentation of the Adriatic microplate. However, the modelling results clearly show that in the case of the weak Pannonian lithosphere, gravitational stresses originating from the elevated orogens can have a considerable contribution to trigger the folding as proposed by numerical stress field modelling by Bada et al. (2001). It may be a general mechanism for the intraplate deformation of lithospheres with weak rheology.

The reconstructed subsidence and uplift pattern is in accordance with the field data and predictions of the previous numerical models. It invokes that large scale folding of the lithosphere could indeed play a major role in the Pliocene-Quaternary vertical crustal movements. If the amplitude of the folded model lithosphere is scaled back to nature, it corresponds to 500-700 m and subsidence larger than 1 km in the basin interior.

Surface derived estimation from 2D analogue models suggest a Pliocene-Quaternary inversion phase as generally assumed for the Pannonian basin. However, the onset of the inversion dates to Late Miocene times in the Dinarides and few subsurface data from the basin interior also point towards an earlier occurrence of inversion. Similarly larger period was inferred from 3D analogue models with more complex geometric boundaries, suggesting that strain localisation has taken place.

6.1.3 Multi-wavelength folding

Existence of shorter wavelength folding at upper crustal level during the inversion of the Pannonian basin is supported by ample geological and geophysical data. Initiation of these shorter modes was observed during the deformation of the initially homogeneous models. Subtle analysis of the surface in the spatial frequency domain revealed peaks at the following wavelengths: ~400 km, ~100 km, ~20-30 km. However, they were not accompanied by pronounced surface deformation. Conceptual 2D analogue models incorporating initial thickness and thus strength variations in the brittle upper crust (Type-2) documented amplification of shorter wavelength folding and deformation on a great variety of wavelengths. These multiple modes of folding were highly dependent on the position of the different crustal blocks. This fact emphasises the substantial role of lateral changes in the upper crust in the intraplate deformation of overall weak lithospheres. This is a likely scenario in the Pannonian basin as well. The uneven basement morphology beneath the basin is indicative of such lateral changes at the upper crustal level, which could intensify folding at a smaller scale. Folding observed at shorter than 20 km wavelength can be best explained as fault related folds.

6.1.4 Inferences from 3D analogue models

Analogue models with 3D set-up allowed the investigation of a few more aspects of lithospheric folding in the Pannonian basin system in a simplified manner. The primary source of the compressional stresses is attributed to the motion of the Adriatic microplate. In addition, seismotectonic data and GPS measurements of the horizontal velocity field imply that lateral escape of the ALCAPA unit from the Eastern Alps has not yet terminated.

This geodynamic scenario was tested by the first series of 3D analogue models (Type-3). Even this simple setting has shown strain localisation in front of the indenter and resulted in a more complicated structural development. In the proximity of the indenter small-scale strike-slip faults developed, which certainly could not be achieved by the 2D analogue models. Despite the significant simplifications, the localised shortening controlled by the folding with ~100 km wavelength could be well correlated to thrust-and-fold structures of the natural laboratory.

The Mid-Hungarian Shear Zone separating the ALCAPA and Tisza-Dacia units has accommodated significant deformation since Early Miocene times. Several present-day active strike-slip structures constitute this fault corridor. The offset along these faults is fairly small and thus are below the achievable resolution of lithospheric-scale physical tectonic models. Yet, the concept of lithospheric folding in the presence of a zone of weakness at upper crustal level was worth to be tested. In the present-day landlocked position of the basin there is not much room for differential horizontal movements. The East European Platform and the Moesian Platform exhibit significant differences in their rheological properties. They act as the backstops of the ALCAPA and Tisza-Dacia blocks, respectively. In this respect, some degree of freedom for differential horizontal movements does exist, though very limited. In 3D analogue models designed according to the aforementioned boundary conditions (Type-4) the weak zone could be activated in a left-lateral sense. However, lithospheric folding remained the primary mode of deformation.

The last series of the 3D analogue experiments (Type-5) comprised multiple weak zones in the upper crust with an oblique position relative to the indenter. These models simulated the shear zones in the basin with documented neotectonic activity. The main objective of this model series was to examine the strain partitioning between the weak zones and the folding of the entire lithosphere. Similar to Type-4 models with a single zone of weakness the bulk part of the deformation was realised in large-scale lithospheric folding. These results have implication on the occurrence of earthquake events in the basin interior. Admittedly, several upper crustal structures were ignored in this modelling strategy. However, the model results call for a low to moderate seismic activity based on the following observations. The majority of the shortening is absorbed by the folding of the lithosphere. The low strain rate of shortening is distributed among a number of reactivated fault zones, thus only low slip rates can occur along the individual fault planes. These inferences are well reflected by the seismicity pattern of the basin.

It is to be emphasised that none of the two latter types of analogue experiments (Type-4 and -5) were expected to be directly comparable to the actual structural evolution during basin inversion owing to the applied simplifications. To achieve such a goal, very complicated set-up of the models would be demanded, which are beyond the limitations of the lithospheric-scale models. To address such problems with complex kinematic, geometric boundary conditions crustal-scale models are to be employed. Local studies at this scale have already been done in the Pannonian basin (Windhoffer et al., 2005; Windhoffer & Bada, 2005).

6.2 Inferences from interpretation of shallow geophysical data

The presented analogue models have demonstrated the evolution of topography in response to lithospheric folding in absence of sedimentation and erosion. In the subsiding areas of the Pannonian basin alluvial deposition is taking place and thus no marked topography change can be associated with them. Obviously, differences in the subsidence rates, activity of near-surface faults are recorded by the rivers draining these areas. These are usually manifested in continuous migration of the river channels, captures or changes in the river pattern. Regions of uplift, on the other hand, provide opportunity to study the combined effect of the tectonic processes and erosion (and re-deposition) in the topography. Therefore the focus of this study was in the western part of the Pannonian basin.

An integrated research effort has recently been dedicated to gain new inferences on the Late Pleistocene through Holocene environmental conditions, palaeoclimatic changes, tectonics and landscape evolution of the area around Lake Balaton, central Transdanubia. These investigations used basin-scale tectonic models, interpretations derived from industrial seismic data and boreholes from the broader environment, outcrop studies, shallow geophysical data and morphological analyses. Integration of this diverse set of methods and disciplines of earth sciences led to numerous new results in terms of neotectonics, stratigraphy and geomorphology and successfully accomplished a depth-to-surface research strategy.

As one of the outcome of the research programme, more constraints could be provided for the formation of long, linear valleys transecting Transdanubia with a fan-shaped pattern. These valleys, among other theories, had long been thought to be pre-formed by faults. Interpretation of the data collected in the framework of this research, however, favour their purely aeolian origin.

These valleys extend to the southwestern part of Transdanubia and cross-cut the elevated terrain of the Zala hills. The Zala hills are one of the most prominent areas, where small-scale folding during tectonic reactivation can be detected in the form of the build-up of series of anticlines. Unlike the Lake Balaton, the selected study area was rather unexplored. There were hardly any available subsurface geological data from this ridge-and-valley system. Incision of the valleys due to fault activity was mainly proposed based on morphological characteristics. Building on the results obtained on and around the lake by shallow geophysical methods, 2D resistivity tomography was applied to image the near-surface sediments. These data were used to investigate the connection between the mechanism of folding investigated by the analogue modelling study presented in this thesis and its expression in terms of geomorphologic observations.

The interpreted geoelectric profiles well documented the ongoing process of inversion. Identified fluvial deposits of most probably Late Pliocene-Pleistocene age clearly showed a

deformed geometry being parallel to the topography of the anticlines. On the other hand, the analysis of the collected data excluded tectonic pre-formation of the valleys and supported the key role of wind erosion similar to their northeastern continuation.

6.3 Inferences from fractal analysis of river networks

As previously discussed, the landscape development of the Carpathian-Pannonian realm is characterised by significant differential crustal movements. This study focused on the effect of crustal movements on drainage network development as rivers are sensitive recorders of differences in subsidence or uplift rates. As demonstrated by numerical and analogue modelling studies, lithosphere folding during Pliocene to recent times has been a major contributor to vertical movements in the Pannonian-Carpathian system with testable predictions for differential motions at the surface directly influencing the organisation of the drainage system.

The catchment area, which comprised the Apuseni Mts., Transylvanian basin and the western margin of the Eastern Carpathians, was analysed by fractal dimension estimators. The three tectonic domains of the intra-Carpathian region bear varying uplift history that were expected to influence the computable characteristics of scaling invariance. The ultimate goal of this exploratory work was to ascertain whether these types of geomorphologic or geostatistical tools are usable indicators of tectonic influences. Several algorithms have been tested in a comparative manner and in that sense it can be considered as a feasibility study.

Coherent values of multifractal dimensions were obtained for the Transylvanian basin, which were smaller than those of the adjacent mountains. These trends of the fractal dimensions are explained by the dominantly E-W orientation of the drainage determined by the bounding topographic highs. The results also show that fractal properties of the drainage are rather controlled by the vertical movements of the surface than the bedrock lithology. The presented technique links on the present-day fractal dimensions with the uplift history of various tectonic domains, extracting a signal compatible with the predictions of models for lithospheric folding. Recent studies also document fractal dimension changes due to the spatial reorganisation of river sections being a good indicator of tectonic topography.

6.4 Forward look

The coupling between lithospheric and surface processes has been addressed by means of analogue tectonic models, near-surface geophysical interpretation and analyses of the drainage development in the Pannonian region. Apart from their relevance to the deformation of the Pannonian lithosphere and the evolution of the related tectonic topography, the described research methodologies may be applicable to other natural laboratories and move forward such investigations.

The reconstructed subsidence and uplift pattern by means of analogue modelling is in accordance with the field data and predictions of previous numerical models. It demonstrates that large scale folding of the lithosphere plays a major role in the recent vertical crustal movements in the Pannonian basin. The predicted (scaled) values for tectonic subsidence and uplift inferred from the modelling experiments with typical magnitudes of up to 1 km will be magnified the effects of surface erosion and sedimentation (Cloetingh & Burov, 2011). Therefore the present research should be complemented by studies that take into account surface processes in terms of sedimentation and/or erosion. In order to account for the mass transport during deformation, coupled analogue and numerical models could offer a solution (see Persson et al., 2004). This coupling is of particular importance because the estimation of the differential vertical movements in analogue models is based on changes in the model topography and the cross sections of the final deformation stage. These experiments cannot provide a continuous insight into the internal deformation of the individual layers of the lithosphere. In order to complete a full 4D deformation history, it is advised to utilise alternative visualisation techniques such as computer tomography. 4D analogue models with parallel numerical models could allow for achieving a fully coupled scenario.

The deployment of high-resolution shallow geophysical methods has demonstrated that in a well chosen test area the interplay between topographic response of the small-scale folding and erosion can be successfully studied. The case study provided a prominent example that knowing the tectonic topography controlled by deep-seated dynamics and exploring the shallow subsurface with high-resolution geophysical methods can give a better insight into the factors controlling landscape development. Beyond the scientific results, the research strategy bears significant societal importance. For instance, seismic risk mitigation in highly vulnerable industrial areas already benefits from using such an approach to discriminate landforms that were created by young fault activity. This type of methodologies combined with very good existing knowledge of basin evolution can be easily applied to other natural scenarios located either in the Pannonian–Carpathians system or elsewhere. For instance, the large expression of neotectonic activity in the entire Pannonian basin is recorded at the SW Dinaridic margin, where basin evolution and surface kinematic studies have successfully determined the regional patterns, but a detailed quantification of timing and geometries at depth is still missing. Case studies such as the Medvenica and Papuk Mountains of Croatia where the amplitude of vertical movements is in the order of 2 km can be excellent case studies complemented by the ready availability of detailed basin imaging.

The fractal analysis study has demonstrated that such an analysis can be very successful in predicting relief development and localisation of recent deformation in relationship with the long-term evolution of a sedimentary basin. This type of study can be complemented by detailed analysis of industrial seismic lines and high resolution geophysical measurements, which can provide critical constraints on the long wavelength patterns of tectonic movements versus their localisation in morphology and influence on the river network system. Such an analysis cumulates multi-scale and multi-temporal tectonic and climatic

effects on topography. A more clear differentiation between temporal tectonic events and climatic versus kinematic multi-scale events is likely to be achieved by a step-wise implementation of regional to local kinematic and sedimentological response to these processes, discriminating time and wavelengths. In this context, coupled experimental tectonic and sedimentological studies (e.g. Athmer et al., 2010) and the integrated use of experimental research infrastructure provided by the ISES TecLab and the EuroTank laboratory for sedimentary processes at Utrecht University hold a great potential.

References

Ádám, A., Wesztergom, V., 2001. An attempt to map the depth of the electrical asthensophere by deep magnetotelluric measurements in the Pannonian Basin (Hungary). *Acta Geologica Hungarica*, **44**:167-192.

Aharony, A., 1989. Measuring multifractals. *Physica D*, **38**:1-4.

Athmer, W., Groenenberg, R.M., Luthi, S.M., Donselaar, M.E., Soukoutis, D., Willingshofer, E., 2010. Relay ramps as pathways for turbidity currents: A study combining analogue sandbox experiments and numerical flow simulations. *Sedimentology*, **57**:806-823.

Bada, G., Fodor, L., Windhoffer, G., Ruszkiczay-Rüdiger, Zs., Sacchi, M., Dunai, T., Tóth, L., Cloetingh, S., Horváth, F., 2003. Lithosphere dynamics and present-day deformation pattern in the Pannonian basin. *Geophysical Research Abstracts*, **5**:05772.

Bada, G., Gerner, P., Cloetingh, S., Horváth, F., 1998. Sources of recent tectonic stress in the Pannonian region: inferences from finite element modelling. *Geophysical Journal International*, **134**:87-102.

Bada, G., Grenerczy, Gy., Tóth, L., Horváth, F., Stein, S., Cloetingh, S., Windhoffer, G., Fodor, L., Pinter, N., Fejes, I., 2007b. Motion of Adria and ongoing inversion of the Pannonian basin: Seismicity, GPS velocities and stress transfer. In: Stein, S., Mazzotti, S., (Eds.), Continental Intraplate Earthquakes: Science, Hazard, and Policy Issues. *Geological Society of America Special Paper*, **425**:243-262.

Bada, G., Horváth, F., 2001. On the structure and tectonic evolution of the Pannonian basin and surrounding orogens. *Acta Geologica Hungarica*, **44**:301-327.

Bada, G., Horváth, F., Cloetingh, S., Coblentz, D.D., Tóth, T., 2001. The role of topography induced gravitational stresses in basin inversion: The case study of the Pannonian basin. *Tectonics*, **20**:343-363.

Bada, G., Horváth, F., Dövényi, P., Szafián, P., Windhoffer, G., Cloetingh, S., 2007a. Present-day stress field and tectonic inversion in the Pannonian basin. *Global and Planetary Change*, **58(1-4)**:165-180.

Bada, G., Horváth, F., Fejes, I., Gerner, P., 1999. Review of the present-day geodynamics of the Pannonian basin: progress and problems. *Journal of Geodynamics*, **27**:501-527.

Bada, G., Horváth, F., Tóth, L., Fodor, L., Timár, G., Cloetingh, S., 2006. Societal aspects of ongoing deformation in the Pannonian region. In: Pinter, N., Grenerczy, Gy., Weber, J., Stein, S., Medak, D., (Eds.), *The Adria Microplate: GPS Geodesy, Tectonics, and Hazards*. NATO Science Series: IV: Earth and Environmental Sciences, Springer-Verlag, **61**:385-402.

Bada, G., Szafián, P., Vincze, O., Tóth, T., Fodor, L., Spiess, V., Horváth, F., 2010. The neotectonic habitat of the eastern part of Lake Balaton and its broader environs: inferences from high-resolution seismic profiling. *Földtani Közlöny*, **140(4)**:367–390. (in Hungarian with English abstract)

Beauvais, A.A., Montgomery, D.R., 1997. Are channel networks statistically self-similar? *Geology*, **25**:1063-1066.

Biot, M. A., 1961. Theory of folding of stratified viscoelastic media and its implications in tectonics and orogenesis. *Geological Society of America Bulletin*, **72**:1595-1620.

Bulla, B., 1943. Geomorphologic observations in the Balaton highlands. *Földrajzi Közlemények*, **71**:18-45. (in Hungarian)

Burg, J.-P., Davy, P., Martinod, J., 1994. Shortening of analogous models of the continental lithosphere: New hypothesis for the formation of the Tibetan plateau. *Tectonics*, **13**:475-483.

Burg, J.-P., Podladchikov, Y., 2000. From buckling to asymmetric folding of the continental lithosphere: numerical modelling and application to the Himalayan syntaxes. In: Asif Khan, M., Qasim Jan, M., Treloar, P.J., Searle, M.P. (Eds.), Tectonics of the Nanga Parbat Syntexis and the Western Himalaya and Karakoram. *Geological Society, London, Special Publication*, **170**:219-236.

Burov, E., 2009. The equivalent elastic thickness (Te), seismicity and the long-term rheology of continental lithosphere: Time to burn-out "crème brûlée"?: Insights from large-scale geodynamic modelling. *Tectonophysics*, **484**:4-26.

Burov, E., Cloetingh, S., 2009. Controls of mantle plumes and lithospheric folding on modes of intraplate continental tectonics: differences and similarities. *Geophysical Journal International*, **178(3)**:1691-1722.

Burov, E., Lobkovsky, L., Cloetingh, S., Nikishin, A., 1993. Continental lithosphere folding in Central Asia. Part 2: constraints from gravity and topography. *Tectonophysics*, **226**:73-87.

Burov, E., Molnar, P., 1998. Gravity anomalies over the Ferghana Valley (central Asia), and intracontinental deformation. *Journal of Geophysical Research*, **103**:18137-18152.

Burov, E., Watts, A.B., 2006. The long-term strength of continental lithosphere: "jelly sandwich" or "crème brûlée"? *GSA Today*, **16(1)**:4-10.

Cagnard, F., Brun, J-P., Gapais, D., 2006. Modes of thickening of analogue weak lithospheres. *Tectonophysics*, **421**:145-160.

Carter, N.L., Tsenn, N.C., 1987. Flow properties of continental lithosphere. *Tectonophysics*, **136**:27-64.

Cholnoky J., 1911. Earthquake at Kecskemét. Földrajzi Közlemények, **39(9-10)**:373-391. (in Hungarian)

Cholnoky J., 1918. Hydrogeology of Lake Balaton. *Report on results of the scientific investigations of Lake Balaton*, vol. 1, part 2. Hungarian Geographical Association, Lake Balaton Committee, Budapest, 316p. (in Hungarian)

Cholnoky J., 1936. Geography of Hungary. *The Life of Earth*, vol. 6., Franklin Társulat kiadó, Budapest, 1-530. (in Hungarian)

Ciulavu, D., Dinu, C., Cloetingh, S.A.P.L., 2002. Late Cenozoic tectonic evolution of the Transylvanian basin and northeastern part of the Pannonian basin (Romania): Constraints from seismic profiling and numerical modelling. In: Cloetingh, S., Horváth, F., Bada, G., Lankreijer, A. (Eds.), Neotectonics and surface processes: the Pannonian basin and Alpine/Carpathian system. *EGU Stephan Mueller Special Publication Series*, **3**:105-120.

Claps, P., Oliveto, G., 1996. Reexamining the determination of the fractal dimension of river networks. Water Resources Research, **32**:3123–3135.

Cloetingh, S. and TOPO-EUROPE Working Group, 2007. Editorial: 4-D topography evolution in Europe: Uplift, subsidence and sea level change (TOPO-EUROPE). *Global and Planetary Change*, **58**:viii-xii

Cloetingh, S., Bada, G., Matenco, L., Lankreijer, A., Horváth, F., Dinu, C., 2006. Modes of basin (de)formation, lithospheric strength and vertical motions in the Pannonian–Carpathian system: inferences from thermo-mechanical modelling. In: Gee, D.G., Stephenson, R.A. (Eds.), European Lithosphere Dynamics. *Geological Society, London, Memoirs*, **32**:207–221.

Cloetingh, S., Burov, E., 2011. Lithospheric folding and sedimentary basin evolution: a review and analysis of formation mechanisms. *Basin Research*, **23(3)**:257-290.

Cloetingh, S., Burov, E., Beekman, F., Andeweg, B., Andriessen, P.A.M., Garcia Castellanos, D., de Vicente, G., Vegas, R., 2002. Lithospheric folding in Iberia, *Tectonics*, **21(5)**:1-26.

Cloetingh, S., Burov, E., Matenco, L., Toussaint, G., Bertotti, G., Andriessen, P.A.M., Wortel, M.J.R., Spakman, W., 2004. Thermo-mechanical controls on the mode of continental collision in the SE Carpathians (Romania). *Earth and Planetary Science Letters*, **218(1-2)**:57-76.

Cloetingh, S., Burov, E., Poliakov, A., 1999. Lithosphere folding: Primary response to compression? (from central Asia to Paris basin). *Tectonics*, **18**:1064-1083.

Cloetingh, S., Kooi, H., Groenewoud, W., 1989. Intraplate stress and sedimentary basin evolution. In: Price, R.A. (ed.), Origin and Evolution of Sedimentary Basins and their Energy and Mineral Resources. *American Geophysical Union, Geophysical Monograph*, **48**:1-16.

Cloetingh, S., Lankreijer, A., 2001. Lithospheric memory and stress field controls on polyphase deformation of the Pannonian basin–Carpathian system. *Marine and Petroleum Geology*, **18**:3–11.

Cloetingh, S., Matenco, L., Bada, G., Dinu, C., Mocanu, V., 2005a. The evolution of the Carpathians-Pannonian system: Interaction between neotectonics, deep structure, polyphase orogeny and sedimentary basins in a source to sink natural laboratory. *Tectonophysics*, **410**:1-14.

Cloetingh, S., Ziegler, P., Beekman, F., Andriessen, P., Matenco, L., Bada, G., Garcia-Castellanos, D., Hardebol, N., Dezes, P., Sokoutis, D., 2005b. Lithospheric memory, state of stress and rheology: neotectonic controls on Europe's intraplate continental topography. *Quaternary Science Reviews*, **24**:241–304.

Crittenden, M.D., Coney, P.J., Davies, G.H. (Eds.), 1980. Tectonic significance of metamorphic core complexes of the North American Cordillera. *Memoirs of Geological Society America*, **153**:350p.

Csillag, G., Fodor, L., Sebe, K., Müller, P., Ruszkiczay-Rüdiger, Zs., Thamóné Bozsó, E., Bada, G., 2010. The role of wind erosion in the surface development of Transdanubia during the Quarternary. *Földtani Közlöny*, **140(4)**:463-482. (in Hungarian with English abstract)

Csontos, L., Magyari, Á., Van Vliet-Lanoë, B., Musitz, B., 2005. Neotectonics of the Somogy hills (Part II): Evidence from seismic sections. *Tectonophysics*, **410**:63-80.

Csontos, L., Nagymarosy, A., 1998. The Mid-Hungarian line: a zone of repeated tectonic inversions. *Tectonophysics*, **297**:51-71.

Csontos, L., Nagymarosy, A., Horváth, F., Kovac, M., 1992. Tertiary evolution of the Intra-Carpathian area: a model. *Tectonophysics*, **208**:221-241.

Csontos, L., Vörös, A., 2004. Mesozoic plate tectonic reconstruction of the Carpathian region. *Palaeogeography Palaeoclimatology Palaeoecology*, **210**:1-56.

Dallmeyer, R.D., Pană, D.I., Neubauer, F., Erdmer, P., 1999. Tectonothermal evolution of the Apuseni Mountains, Romania: Resolution of Variscan versus Alpine events with 40 Ar/39 Ar ages. *Journal of Geology*, **107**:329-352.

Davy, P., Cobbold, P.R., 1988. Indentation tectonics in nature and experiments: 1. Experiments scaled for gravity. *Bulletin of the Geological Institutions of the University of Uppsala*, **14**:129-141.

Davy, P., Cobbold, P.R., 1991. Experiments on shortening of a 4-layer continental lithosphere. In: Cobbold, P.R. (Ed.), Experimental and Numerical Modelling of Continental Deformation, *Tectonophysics*, **188**:1-25.

De Bartolo, S.G., Gabriele, S., Gaudio, R., 2000. Multifractal behaviour of river networks. *Hydrology and Earth System Sciences*, **4**:105-112.

De Bartolo, S.G., Gaudio, R., Gabriele, S., 2004. Multifractal analysis of river networks: sandbox approach. *Water Resources Research*, **40**:W02201.

De Bartolo, S.G., Veltri, M., Primavera, L., 2006. Estimated generalized dimensions of river networks. *Journal of Hydrology*, **322**:181-191.

Del Ventisette, C., Montanari, D., Sani, F., Bonini, M., Corti, G., 2007. Reply to comment by J. Wickham on "Basin inversion and fault reactivation in laboratory experiments". *Journal of Structural Geology*, **29**:1417-1418.

Dombrádi, E., Sokoutis, D., Bada, G., Cloetingh, S., Horváth, F., 2008. Quaternary inversion of the Pannonian lithosphere: large-scale lithospheric folding controlling active deformation and topography development. *Bolletino di Geofisica Teorica ed Applicata*, **49**:38-42.

Dombrádi, E., Sokoutis, D., Bada, G., Cloetingh, S., Horváth, F., 2010. Modelling deformation of the Pannonian lithosphere: lithospheric folding and tectonic topography. *Tectonophysics*, **484**:103-118.

Dombrádi, E., Timár, G., Bada, G., Cloetingh, S., Horváth, F., 2007. Fractal dimension estimations of drainage network in the Carpathian-Pannonian system. *Global and Planetary Change*, **58**:197-213.

Dövényi, P., Horváth, F., 1988. A review of temperature, thermal conductivity and heat flow data from the Pannonian basin. In: Royden, L.H., Horváth, F. (Eds.), The Pannonian Basin. *American Association of Petroleum Geologists Memoirs*, **45**:195-233.

Dunkl, I. Grasemann, B., Frisch, W., 1998. Thermal effects of exhumation of a metamorphic core complex on hanging wall synrift sediments – an example from the Rechnitz Window, Eastern Alps. *Tectonophysics*, **297**:31-50.

Dunkl, I., Demény, A., 1997. Exhumation of Rechnitz Window at the border of the Eastern Alps an Pannonian Basin during Neogene extension. *Tectonophysics*, **272**:197-211.

Erdélyi, M., 1961. Hydrogeology of Internal Somogy Hills. *Hidrológiai Közlöny*, **41**:445-458. (in Hungarian).

Erdélyi, M., 1962. Hydrogeology of External Somogy Hills. *Hidrológiai Közlöny*, **42**:56-65 (in Hungarian).

Faccenda, M., Minelli, G., Gerya, T.V., 2009. Coupled and decoupled regimes of continental collision: Numerical modeling. *Earth and Planetary Science Letters*, **278**:337-349.

Falconer, K. J., 1990. *Fractal Geometry: Mathematical Foundations and Applications*, John Wiley, Hoboken, N. J.

Fernandez-Lozano, J., 2012. *Cainozoic deformation of Iberia: A model for intraplate mountain building and basin development based on analogue modelling*. PhD thesis, Utrecht Studies in Earth Sciences No. 013, 173p.

Fielitz, W., Seghedi, I., 2005. Late Miocene-Quaternary volcanism, tectonics and drainage system evolution in the East Carpathians, Romania. *Tectonophysics*, **410**:111-136.

Fleitout, L., Froidevaux, C, 1982. Tectonics and topography for a lithosphere containing density heterogeneities. *Tectonics*, **2**:21-56.

Fodor, L., Bada, G., Csillag, G., Horváth, E., Ruszkiczay-Rüdiger, Zs., Horváth, F., Cloetingh, S., Palotás, K., Síkhegyi, F., Timár, G., 2005. An outline of neotectonic structures and morphotectonics of the western and central Pannonian basin. *Tectonophysics*, **410**:15-41.

Fodor, L., Bada, G., Csillag, G., Horváth, E., Ruszkiczay-Rüdiger, Zs., Síkhegyi, F., 2004. New data on neotectonic structures and morphotectonics of the western and central Pannonian Basin. *Occasional Papers of the Geological Institute of Hungary*, **204**:35-44. (in Hungarian)

Fodor, L., Csontos, L., Bada, G., Györfi, I., Benkovics, L., 1999. Tertiary tectonic evolution of the Pannonian basin system and neighbouring orogens: a new synthesis of paleostress data. In: Durand, B., Jolivet, L., Horváth, F., Séranne, M. (Eds.), The Mediteranean Basins: Tertiary Extension Within the Alpine Orogen. *Geological Society Special Publications*, **156**:295-334.

Frisch, U., Parisi, G., 1985. Fully developed turbulence and intermittency. In: Ghil, M., Benzi, R., Parisi, G. (Eds.), *Turbulence and Predictability in Geophysical Fluid Dynamics*, North Holland, New York, pp. 84-92.

Füchslin, R.M., Shen, Y., Meier, P.F., 2001. An efficient algorithm to determine fractal dimensions of points sets. *Physics Letters A*, **285**:69-75.

Gábris, Gy., 1998. Late glacial and post glacial development of drainage network and the paleohydrology in the Great Hungarian Plain. In: Bassa, L., Kertész, Á. (Eds.), Windows on Hungarian Geography. FKI, Budapest, pp. 23-36.

Gábris, Gy., 2007. Relation between the time scale of Quaternary surface processes and Oxygen Isotope Stratigraphy - loess-palaeosoil sequences and river terraces in Hungary. *Földtani Közlöny*, **137(4)**:515-540. (in Hungarian with English abstract)

Gaudio, R., De Bartolo, S.G., Primavera, L., Gabriele, S., Veltri, M., 2006. Lithologic control on the multifractal spectrum of river networks. *Journal of Hydrology*, **327**:365-375.

Gerbault, M., Burov, E., Poliakov, A., Dagnieres, M., 1999. Do faults trigger folding in the asthenosphere? *Geophysical Research Letters*, **26(2)**:271-274.

Gerner, P., 1992. Recent stress field in Transdanubia. *Földtani Közlöny*, **122**:89-105. (in Hungarian with English abstract).

Gerner, P., Bada, G., Dövényi, P., Müller, B., Oncescu, M.C., Cloetingh, S., Horváth, F., 1999. Recent tectonic stress and crustal deformation in and around the Pannonian Basin: data and models. In: Durand, B., Jolivet, L., Horváth, F., Séranne, M. (Eds.), The Mediterranean Basins: Tertiary Extension within the Alpine Orogen. *Geological Society, London, Special Publications*, **156**:269-294.

Gölke, M., Coblentz, D., 1996. Origins of the European regional stress field. *Tectonophysics*, **266**:11-24.

Grenerczy, Gy., Bada, G., 2005. GPS baseline length changes and their tectonic interpretation in the Pannonian Basin. *Geophysical Research Abstracts*, **7**:04808.

Grenerczy, Gy., Sella, G.F., Stein, S., Kenyeres, A., 2005. Tectonic implications of the GPS velocity field in the northern Adriatic region. *Geophysical Research Letters*, **32**:L16311.

Halsey, T.C., Jensen, M.H., Kadanoff, L.P., Procaccia, I., Shraiman, B.I., 1986. Fractal measures and their singularities: The characterization of strange sets. *Physics Review A*, **33(2)**:1141–1151.

Hetényi, Gy., Stuart, G.W., Houseman, G.A., Horváth, F., Hegedűs, E., Brückl, E., 2009. Anomalously deep mantle transition zone below Central Europe: Evidence of lithospheric instability. *Geophysical Research Letters*, **36**:L21307. doi:10.1029/2009GL040171

Hippolyte, J.-C., Săndulescu, M., 1996. Paleostress characterization of the "Wallachian"-phase in its type area (southeastern Carpathians, Romania). *Tectonophysics*, **263**:235-248.

Horton, R.E., 1932. Drainage basin characteristics. *American Geophysical Union Transactions*, **13**:350-361.

Horton, R.E., 1945. Erosional development of streams and their drainage basins: Hydrophysical approach to quantitative morphology. *Geological Society America, Bulletin*, **56**:275-370.

Horváth, F. 1988. Neotectonic behavior of the Alpine-Mediterranean Region. In: Royden, L.H., Horváth, F. (Eds.), The Pannonian Basin: A case study in basin evolution. *American Association of Petroleum Geologists Memoirs*, **45**:49-55.

Horváth, F., 1993. Towards a mechanical model for the formation of the Pannonian basin. *Tectonophysics*, **225**:333-358.

Horváth, F., 1995. Phases of compression during the evolution of the Pannonian basin and its bearing on hydrocarbon exploration. *Marine and Petroleum Geology*, **12**:837–844.

Horváth, F., 2007. *Geodynamics of the Pannonian basin: history of ideas and geophysical synthesis*. DSc thesis, Hungarian Academy of Sciences, Budapest, 238p. (in Hungarian)

Horváth, F., Bada, G., Szafián, P., Tari, G., Ádám, A., Cloetingh, S., 2006a. Formation and deformation of the Pannonian basin: Constraints from observational data. In: Gee, D.G., Stephenson, R.A., (Eds.), European Lithosphere Dynamics, *Geological Society, London, Memoirs*, **32:**191-206.

Horváth, F., Cloetingh, S., 1996. Stress-induced late-stage subsidence anomalies in the Pannonian basin. *Tectonophysics*, **266**:287-300.

Horváth, F., Dombrádi, E., 2010. Evolution of Hungarian tectonics: an overview of a century of research on and around Lake Balaton. *Földtani Közlöny*, **140(4)**:335-354. (in Hungarian with English abstract)

Horváth, F., Dombrádi, E., Tóth, L., 2009. Natural conditions, Geophysics. In: Kocsis, K., Schweitzer, F., (Eds.), *Hungary in Maps*, Geographical Research Institute, Hungarian Academy of Sciences, 29-33.

Horváth, F., Dövényi, P., Szalay, Á., Royden, L.H., 1988. Subsidence, thermal and maturation history of the Great Hungarian Plain. In: Royden, L.H., Horváth, F. (Eds.), The Pannonian Basin. *American Association of Petroleum Geologists Memoirs*, **45**:355-372.

Horváth, F., Dunkl, I., Tóth, T.M., Tari, G., Bada, G., 2006b. Surface vs. Moho topography and the core complex mode of extension in the Pannonian basin. *Geophysical Research Abstracts*, **8**:04290

Horváth, F., Faccenna, C., 2011. Central Mediterranean mantle flow system and the formation of the Pannonian basin. *Geophysical Research Abstracts*, **13**:EGU2011-8894-2

Horváth, F., Faccenna, C., Husson, L., Dombrádi, E., 2011. Dynamic subsidence and uplift history of the Pannonian backarc basin, *Dynamic Topography: A key surface record of deep Earth processes*, Geolgical Society, London, conference abstract.

Horváth, F., Royden, L., 1981. Mechanism for formation of the intra-Carpathian basins: a review. *Earth Evolution Sciences*, **1**:307-316.

Horváth, F., Rumpler, J., 1984. The Pannonian basement: extension and subsidence of an Alpine orogene. *Acta Geologica Hungarica*, **27**:222-236.

Horváth, F., Sacchi, M., Dombrádi, E., 2010. Seismic stratigraphy and tectonics of Late Miocene basin fill in southern Transdanubia and below Lake Balaton. *Földtani Közlöny*, **140(4)**:391-418. (in Hungarian with English abstract)

Horváth, F., Sztanó, O., Uhrin, A., Fodor, L., Balázs, A., Kóbor, M., Wórum, G., 2012. Towards a dynamic model for the formation of the Pannonian basin. *Geophysical Research Abstracts*, **14**:EGU2012-10178-1.

Houseman, G.A., Gemmer, L., 2007. Intra-orogenic extension driven by gravitational instability: Carpathian-Pannonian orogeny. *Geology*, **35**:1135-1138

Hubbert, M.K., 1937. Theory of scaled models as applied to the study of geological structures. *Geological Society of America Bulletin*, **48**:1459-1520.

Huismans, R. S., Bertotti, G., Ciulavu, D., Sanders, C.A.E., Cloetingh, S.A.P.L., Dinu, C., 1997. Structural evolution of the Transylvanian Basin (Romania): a sedimentary basin in the bend zone of the Carpathians, *Tectonophysics*, **272**:249-268.

Ijjasz-Vasquez, E.J., Rodriguez-Iturbe, I., Bras, R.L., 1992. On the multifractal characterization of river basins. *Geomorphology*, **5**:297-310.

Ilić, A., Neubauer, F., 2005. Tertiary to recent oblique convergence and wrenching of the Central Dinarides: constraints from a paleostress study. *Tectonophysics*, **410**:465-484.

Jackson, J., 2002. Strength of the continental lithosphere: Time to abandon the jelly sandwich? *GSA Today*, **12 (9)**:4-10, doi: 10.1130/1052-5173(2002)012 <0004:SOTCLT>2.0.CO;2.

Jackson, J., McKenzie, D., Priestley, K., Emmerson, B., 2008. New views on the structure and rheology of the lithosphere. *Journal of the Geological Society*, **165**:453-465.

Jámbor, Á., 1992. Pleistocene ventifact occurences in Hungary. *Acta Geologica Hungarica*, **35**:407-436.

Jámbor, Á., 1993. *Explanatory text for 1:500,000 Pleistocene fault map of Hungary*. Manuscript, Data repository of the Geological Institute of Hungary, Budapest, 42p. (in Hungarian)

Jámbor, Á., 2002. Occurrences and importance of the Pleistocene ventifacts in Hungary. *Földtani Közlöny*, **132**:101-116. (in Hungarian with English abstract)

Jarosinski, M., Beekman, F., Matenco, L., Cloetingh, S., 2011. Mechanics of basin inversion: Finite element modelling of the Pannonian Basin System. *Tectonophysics*, **502(1-2)**:196-220.

Jolánkai, G., 2005. The Tisza River Project. Real-life scale integrated catchment models for supporting water- and environmental management decisions. Final report, manuscript, available on the Internet,

Juhász, Gy., Pogácsás, Gy., Magyar, I., Vakarcs, G., 2006. Integrated stratigraphy and sedimentary evolution of the Late Neogene sediments of the Hungarian Plain, Pannonian Basin. *Földtani Közlöny*, **136**:51-86. (in Hungarian with English abstract)

Kardeván, P., 2002. The Tisza River Project. 2nd MINEO Workshop, Orleans, France, 11-13 Dec, 2002. URL: http://www2.brgm.fr/mineo/workshop/ 2ndWorkshop/12th%20Dec /Session%203/Tisza%20River.pdf

Kelevitz, K., Raáb, D., Dombrádi, E., Spahic, D., 2010. Geoelectric survey of a roll-over anticline (Austria). SEG - 72nd EAGE conference & exhibition. **7**:5341-5343.

Kirby, R.H., 1983. Rheology of the lithosphere. *Reviews of Geophysics and Space Physics*, **21**:1458-1487.

Kirby, R.H., 1985. Rock mechanic observations pertinent to the rheology of the continental lithosphere and the localization of strain along shear zones. *Tectonophysics*, **119**:1-27.

Kirchener, J.W., 1993. Statistical inevitability of Horton's laws and the apparent randomness of stream channel networks. *Geology*, **21**:591-594.

Kovács, A., Marinov, E., 2009. Structure and genesis of Cserta and Kerta creeks. Field report. Dept. of Geophysics & Space Sciences, Eötvös University, Budapest, 16p. (in Hungarian)

Kummerow, J., Kind, R., Oncken, O., Giese, P., Ryberg, T., Wylegalla, K., Scherbaum, F. and TRANSALP Working Group, 2004. A natural and controlled source seismic profile through the Eastern Alps: TRANSALP. *Earth and Planetary Science Letters*, **225**:115-129

La Barbera, P., Rosso, R., 1987. Fractal geometry of river networks. *American Geophysical Union Transactions*, **68**:1276.

La Barbera, P., Rosso, R., 1989. On the fractal dimension of stream networks. *Water Resources Research*, **25**:735-741.

Lankreijer, A., Mocanu, V., Cloetingh, S., 1997. Lateral variations in lithospheric strength in the Romanian Carpathians, constraints on basin evolution. *Tectonophysics*, **272**:433-451.

Lankreijer, A., Bielik, M., Cloetingh, S., Majcin, D. 1999. Rheology predictions across the western Carpathians, Bohemian massif, and the Pannonian basin: Implications for tectonic scenarios. *Tectonics*, **18**:1139-1153.

Leever, K.A., Matenco, L., Bertotti, G., Cloetingh, S., Drijkoningen, K.G., 2006. Late orogenic vertical movements in the Carpathian bend zone – seismic constraints on the transition zone from orogen to foredeep. *Basin Research*, **18(4)**:521-545.

Lenkey, L., 1999. *Geothermics of the Pannonian basin and its bearing on the tectonics of basin evolution*. PhD thesis, Vrije Universiteit, Amsterdam, 215p.

Lenkey, L., Dövényi, P., Horváth, F., Cloetingh, S., 2002. Geothermics of the Pannonian basin and its bearing on the neotectonics. In: Cloetingh, S., Horváth, F., Bada, G., Lankreijer, A. (Eds.) Neotectonics and Surface Processes: the Pannonian Basin and Alpine/Carpathian System. European Geosciences Union, *Stephen Mueller Special Publication Series*, **3**:29-40.

Linzer, H-G., Frisch, W., Zweigel, P., Girbacea, R., Hann, H-P., Moser, F., 1998. Kinematic evolution of the Romanian Carpathians. *Tectonophysics*, **297**:133-156.

Lister, G.S., Banga, G., Feenstra, A., 1984. Metamorphic core complexes of the Cordilleran type in the Cyclades, Aegean Sea. *Geology*, **12**:221-225.

Lister, G.S., Davies, G.A., 1989. The origin of metamorphic core complexes and detachment faults formed during Tertiary continental extension in the northern Colorado River region U.S.A. *Journal of Structural Geology*, **11**:65-94.

Lóczy L., 1913. Geological formations and their distribution around Lake Balaton, Report on results of the scientific investigations of Lake Balaton, vol. 1, part 2. Hungarian Geographical Association, Lake Balaton Committee, Budapest, 617p. (in Hungarian)

Lóczy, L., 1918. Structural geology of Hungary. In: Lóczy, L. (Ed.): *Geographical, social, educational and economical description of the countries of the Hungarian saint crown*, vol. 1. Hungarian Geographical Association, Budapest, 5-43. (in Hungarian)

Lóczy, L., 1920. Field visit in Western Serbia. *Földrajzi Közlemények*, **48**:82-84. (in Hungarian)

Loke, M.H., 2010. Tutorial: 2-D and 3-D electrical imaging surveys. Online course notes, 154p. http:\\ www.geoelectrical.com

Lovász, Gy., 1970. Main morphological problems of the Zala hills. In: *Geographical studies in the area of Southern Transdanubia*. Budapest, Akadémiai Kiadó, pp. 11-85. (in Hungarian)

Lowrie, W., 2007. *Fundamentals of Geophysics*, Cambridge University Press. 381p.

Magyar, I., Fogarasi, A., Vakarcs, G., Buko, L., Tari, G., 2006. The Largest Hydrocarbon Field Discovered to Date in Hungary: Algyő. In: Golonka, J., Picha, F.J. (Eds.), The Carpathians and their foreland: Geology and hydrocarbon resources, *American Association of Petroleum Geologists Memoirs*, **84**:619-632.

Magyar, I., Geary, D. H. and P. Müller, 1999. Paleogeographic evolution of the Late Miocene Lake Pannon in Central Europe. *Paleogeography Paleoclimatology Paleoecology*, **147**:151-167.

Magyari, Á., Musitz, B., Csontos, L., Van Vliet- Lanoë, 2005. Quaternary neotectonics of the Somogy Hills, Hungary (part I): Evidence from field observations. *Tectonophysics*, **410**:43-62.

Mahmood, S.A., Gloaguen, R., 2011. Fractal Measures of Drainage Network to Investigate Surface Deformation from Remote Sensing Data: A Paradigm from Hindukush (NE-Afghanistan). *Journal of Mountain Sciences*, **8**:641-654.

Mahmood, S.A., Gloaguen, R., 2012. Appraisal of active tectonics in Hindu Kush: Insights from DEM derived geomorphic indices and drainage analysis. Geoscience Frontiers, in press.

Mandelbrot, B.B., 1974. Intermittent turbulence in self-similar cascades: Divergence of high moments and dimension of the carrier, *Journal of Fluid Mechanics*, **62**:331-358.

Mandelbrot, B.B., 1990. Multifractal measures, especially for the geophysicist. *Pure and Applied Geophysics*, **131**:5-42.

Marosi, S, 1962. Internal Somogy Hills. Földrajzi Értesítő, **11**:61-81. (in Hungarian)

Marovic, M., Djokovic, I., Pesic, L., Radovanovic, S., Toljic, M., Gerzina, N., 2003. Neotectonics and seismicity of the southern margin of the Pannonian basin in Serbia. *EGU Stephan Mueller Special Publication Series*, **3**:277-295.

Marques, F.O., Podladchikov, Y.Y., 2009. A thin elastic core can control large-scale patterns of lithosphere shortening. *Earth and Planetary Science Letters*, **277**:80-85.

Martin, M., Wenzel, F., and CALIXTO working group, 2006. High-resolution teleseismic body wave tomography beneath SE-Romania – II. Imaging of a slab detachment scenario. *Geophysical Journal International*, **164**:579-595.

Martinod, J., Davy, P., 1992. Periodic instabilities during compression or extension of the lithosphere, 1, Deformation modes from an analytical perturbation method. *Journal of Geophysical Research*, **97**:1999-2014.

Martinod, J., Davy, P., 1994. Periodic instabilities during compression of the lithosphere, 2, Analogue experiments. *Journal of Geophysical Research*, **99**:12057-12069.

Márton, E., 2001. Tectonic implications of Tertiary paleomagnetic results from the PANCARDI area (Hungarian contribution). *Acta Geologica Hungarica*, **44**:135-144.

Matenco, L. and Bertotti, G., 2000. Tertiary tectonic evolution of the external Eastern Carpathians (Romania). *Tectonophysics*, **316**:255-286.

Maţenco, L., Bertotti, G., Cloetingh, S., Dinu, C., 2003. Subsidence analysis and tectonic evolution of the external Carpathian–Moesian Platform region during Neogene times. *Sedimentary Geology*, **156**:71-94.

Matenco, L., Bertotti, G., Leever, K., Cloetingh, S., Schmid, S.M., Tărăpoancă, M., Dinu, C., 2007. Large-scale deformation in a locked collisional boundary: Interplay between subsidence and uplift, intraplate stress, and inherited lithospheric structure in the late stage of the SE Carpathians evolution. *Tectonics*, **26**:TC4011.

Matenco, L., Krézsek, C., Merten, S., Schmid, S., Cloetingh, S., Andriessen, P., 2010. Characteristics of collisional orogens with low topographic build-up: an example from the Carpathians. *Terra Nova*, **22**:155-165.

Matenco, L.C., Radivojević, D., 2012. On the formation and evolution of the Pannonian basin: constraints derived from the orogenic collapse recorded at the junction between Carpathians and Dinarides. *Geophysical Research Abstracts*, **14**:EGU2012-6939.

Mattick, R.E., Phillips, R.L., Rumpler, J., 1988. Seismic stratigraphy and depositional framework of sedimentary the Pannonian basin in sortheastern Hungary. In: Royden, L.H., Horváth, F. (Eds.), The Pannonian Basin: A case study in basin evolution. *American Association of Petroleum Geologists Memoirs*, **45**:117-146.

McKenzie, D., 1978. Some remarks on the development of sedimentary basins. *Earth and Planetary Science Letters*, **40**:25-32.

Merten, S., 2011. *Thermo-tectonic evolution of a convergent orogen with low topographic build-up: Exhumation and kinematic patterns in the Romanian Carpathians derived from thermochronology*. PhD thesis. Vrije Universiteit, Amsterdam, 202p.

Merten, S., Matenco, L., Foeken, J.P.T., Stuart, F.M., Andriessen, P.A.M., 2010. From nappe stacking to out-of-sequence postcollisional deformations: Cretaceous to Quaternary exhumation history of the SE Carpathians assessed by low-temperature thermochronology. *Tectonics*, **29**:TC3013.

Michon, L., Merle, O., 2000. Crustal structures of the Rhinegraben and the Massif Central grabens: an experimental approach, *Tectonics*, **19**:896-904.

Michon, L., Sokoutis, D., 2005. Interaction between structural inheritance and extension direction during graben and depocentre formation: An experimental approach. *Tectonophysics*, **409**:125-146.

Molnar, P., England, P., Martinod, J., 1993. Mantle dynamics, uplift of the Tibetan plateau and the Indian monsoon. *Reviews of Geophysics*, **31**:357-396.

Müschen, B., Hochschild, V., 2002. Development of a Hybrid Data Base for the Tisza River Project. *29th International Symposium on Remore Sensing of Environment*, Buenos Aires, Argentina, April 8-12, 2002. Proceeding on CD-ROM. URL: http://www.tiszariver.com/public/publication_29isrse.pdf

Nádor, A., Lantos, M., Tóth-Makk, Á ., Thamó-Bozsó , E., 2003. Milankovich-scale multi-proxy records from fluvial sediments of the last 2.6 Ma, Pannonian basin, Hungary. *Quaternary Science Reviews*, **22**:2157-2175.

Nádor, A., Thamó-Bozsó, E., Magyari, Á., Babinszki, E., 2007. Fluvial responses to tectonics and climate change during the Late Weichselian in the eastern part of the Pannonian Basin (Hungary). *Sedimentary Geology*, **202**:174-192.

Necea, D., Fielitz, W, Maţenco, L., 2005. Late Pliocene-Quaternary tectonics in the frontal part of the SE Carpathians: Insights from tectonic geomorphology. *Tectonophysics*, **410**:137-156.

Némedi Varga, Z., 1977. The Kapos Line. *Földtani Közlöny*, 107:313-328. (in Hungarian with English abstract).

Novák, D., Koncz, D., Horváth, A., Szafián, P., Sztanó, O., 2010. A Pleistocene meander loop near Fonyód: remnants of channels on ultra-high resolution seismic images, Lake Balaton, *Földtani Közlöny*, **140(4)**:419-428. (in Hungarian with English abstract)

Oncescu, M.C., 1984. Deep structure of the Vrancea region, Romania, inferred from simultaneous inversion for hypocenters and 3-D velocity structure. *Annales Geophysicae*, **2**:23-28.

Papp, S., 1939. Oil and gas exploration of the Hungarian-American Oil Trust in Transdanubia. *Bányászati és Kohászati Lapok*, **72**:200-241. (in Hungarian)

Pascal, C., Cloetingh, S., 2009. Gravitational potential stresses and stress field of passive continental margins: Insights from the south-Norway shelf. *Earth and Planetary Science Letters*, **277**:464-473.

Patrascu, S., Panaiotu, C., Şeclăman, M., Panaiotu, C.E., 1994. Timing of rotational motion of Apuseni Mountains (Romania): paleomagnetic data from Tertiary magmatic rocks. *Tectonophysics*, **233**:163-176.

Pávai Vajna F., 1925. On the youngest tectonic movements of Earth's crust. *Földtani Közlöny*, **55(1)**:63-85. (in Hungarian)

Pávai Vajna, F., 1943. Structure of the Transdanubian Range. *Appendix of the Annual Report of the Hungarian Royal Geological Institute on 1943.*, vol. 5., pp. 212-223, Comments and reply, pp. 224-238. (in Hungarian)

Pavelic, D., 2001. Tectonostratigraphic model for the North Croatian and North Bosnian sector of the Miocene Pannonian Basin System. *Basin Research*, **12**:359-376.

Pawelzik, K., Schuster, H.G., 1987. Generalized dimensions and entropies from a measured time series. *Physical Review A*, **35**:481-484.

Pazdirek, O., Blaha, V., 1996. Examples of resistivity imaging using ME-100 resistivity field acquisition system. EAGE 58th Conference and Technical Exhibition Extended Abstracts, Amsterdam.

Peckham, S.D., 1995. New results for self-similar trees with applications to river networks. *Water Resources Research*, **31**:1023-1029.

Pécsi, M., 1959. *Evolution of the Hungarian Danube valley*. Akadémiai Kiadó, Budapest, 346p. (in Hungarian)

Persson, K.S., Garcia-Castellanos, D., Sokoutis, D., 2004. River transport effects on compressional belts: First results from an integrated analogue-numerical model. *Journal of Geophysical Research*, **109**: B01409.

Petrovszki, J., Timár, G., 2010. Channel sinuosity of the Körös River system, Hungary/Romania, as possible indicator of the neotectonic activity. *Geomorphology*, **122(3-4)**:223-230.

Popescu, M.N., Lazarescu, V., 1988. Recent vertical crsutal movements in Romania: spatial and temporal variations. *Journal of Geodynamics*, **9**:187-197.

Posgay, K., Bodoky, T., Hegedűs, E., Kovácsvölgyi, S., Lenkey, L., Szafián, P., Takács, E., Timár, Z., Varga, G., 1995. Asthenospheric structure beneath a Neogene basin in southeast Hungary. *Tectonophysics*, **252**:467-484.

Posgay, K., Hajnal, Z., Mueller, St., Ansorge, J., Asudeh, I., Bérczi, I., Bodoky, T., Deiaco, R., Hegedűs, E., Jánváriné, K. I., Nagy, Z., Pápa, A., Reilkoff, B., Szalay, Á., Takács, E., Timár, Z., Varga, G., 1996. International deep reflection survey along the Hungarian Geotraverse. *Geophysical Transactions*, **40**:1-44.

Prelogović, E., Saftić, B., Kuk, V., Velić, J., Dragaš, M., Lučić, D., 1997. Tectonic activity in the Croatian part of the Pannonian basin. *Tectonophysics*, **297**:283-293.

Radulescu, F., Mocanu, V., Nacu, V., Diaconescu, C., 1996. Study of recent crustal movements in Romania: a review. *Journal of Geodynamics*, **22**:33-50.

Ramberg, H., 1961. Contact strain and folding instability of multilayered body under compression. *Geologische Rundschau*, **51**:405-439.

Ramberg, H., 1967. *Gravity, Deformation and the Earth's Crust as Studied by Centrifuged Models*. Academic Press, London, 214p.

Ramberg, H., 1981. *Gravity, Deformation and the Earth's Crust*. 2nd ed., Academic Press, London. 452p.

Ranalli, G., 1995. *Rheology of the Earth*. 2nd ed., Chapman and Hall, London. 413p.

Ranalli, G., 1997. Rheology of the lithosphere in space and time. In: Burg, J.P., Ford, M. (Eds.), Orogeny Through Time, *Geological Society, London, Special Publications*, **121**:19-37.

Ratschbacher, L., Behrmann, J.H., Pahr, A., 1990. Penninic windows at the eastern end of the Alps and their relation to the intra-Carpathian basins. *Tectonophysics*, **172**:91-105.

Ratschbacher, L., Frisch, W., Linzer, H.-G., Marle, O., 1991. Lateral extrusion in the Eastern Alps, part 2: Structural analysis. *Tectonics*, **10**:257-271.

Richardson, R.M., Coblentz, D.D, 1994. Stress modelling in the Andes: Constraints on the South American intraplate stress magnitudes. *Journal of Geophysical Research*, **99**:22015-22025.

Rinaldo, A., Rodriguez-Iturbe, I., Rigon, R., Bras, R.L., Ijjasz-Vasquez, E.J., Marani, A., 1992. Minimum energy and fractal structures of drainage networks. *Water Resources Research*, **28**:2183-2195.

Rodriguez-Iturbe, I., Rinaldo, A., 1997. *Fractal River Basins: Change and Self-Organization*, Cambridge Univ. Press, New York.

Rosenberg, C.L., Brun, J-P., Gapais, D., 2004. Indentation model of the Eastern Alps and the origin of the Tauern Window. *Geology*, **32**:997-1000.

Royden, L.H., Horváth, F. (Eds.), 1988. The Pannonian Basin: A case study in basin evolution. *AAPG Memoir*, **45**:394p.

Rumpler, J., Horváth, F., 1988. Some representative seismic reflection lines from the Pannonian basin and their structural interpretation. In: Royden, L.H., Horváth, F. (Eds.), The Pannonian Basin: A case study in basin evolution. *American Association of Petroleum Geologists Memoirs*, **45**:153-169.

Ruszkiczay-Rüdiger, Zs., Dunai, T., Bada, G., Fodor, L. and Horváth, E., 2005b. Middle to late Pleistocene uplift rate of the Hungarian Mountain Range at the Danube Bend (Pannonian Basin), using in situ produced 3He. *Tectonophysics*, **410**:173-187.

Ruszkiczay-Rüdiger, Zs., Fodor, L., Bada, G., Leél-Össy, Sz., Horváth, E., Dunai, T., 2005a. Quantification of Quaternary vertical movements in the central Pannonian Basin: review of chronologic data along the Danube river, Hungary. *Tectonophysics*, **410**:157-172.

Ruszkiczay-Rüdiger, Zs., Fodor, L.I., Horváth, E., 2007. Neotectonics and Quaternary landscape evolution of the Gödöllő Hills, Central Pannonian Basin, Hungary. *Global and Planetary Change*, **58**:181-196.

Sacchi, M., 2001. *Late Miocene evolution of the western Pannonian basin, Hungary*. PhD thesis, Eötvös Loránd University, Budapest, Hungary, 193p.

Sachsenhofer, R.F., Lankreijer, A., Cloetingh, S., Ebner, F. 1997. Subsidence analysis and quantitative basin modelling in the Styrian basin (Pannonian Basin System, Austria). *Tectonophysics*, **272**:175-196.

Salát, P., Szabadváry, L., 1970. *Geophysical survey methods: surface geophysics*, Tankönyvkiadó, Budapest.

Sanders, C., 1998. *Tectonics and Erosion, Competitive forces in a compressive orogen. A fission track study of the Romanian Carpathians*. Published PhD thesis, Vrije Universiteit, Amsterdam, 204p.

Sanders, C., Huismans, R., van Wees, J.D., Andriessen, P., 2002. The Neogene history of the Transylvanian basin in relation to its surrounding mountains. In: Cloetingh, S., Horváth, F., Bada, G., Lankreijer, A. (Eds.), Neotectonics and surface processes: the Pannonian basin and Alpine/Carpathian system. *EGU Stephan Mueller Special Publication Series*, **3**:29-40.

Sanders, C.A.E., Andriessen, P.A.M., Cloetingh, S.A.P.L., 1999. Life cycle of the East Carpathian orogen: Erosion history of a doubly vergent critical wedge assessed by fission track thermochronology. *Journal of Geophysical Research*, **104(B12)**:29095–29112.

Sandulescu, M., 1988. Cenozoic tectonic history of the Carpathians. In: Royden, L.H., Horváth, F. (Eds), The Pannonian Basin. *AAPG Memoir*, **45**:17-25.

Scheuer, Gy., Schweitzer, F., 1988. Travertines in the Gerecse and Buda hills. *Földrajzi Tanulmányok*, **20**:129p. (in Hungarian)

Schmid, S.M., Bernoulli, D., Fügenschuh, B., Matenco, L., Schefer, S., Schuster, R., Tischler, M., Ustaszewski, K., 2008. The Alpine-Carpathian-Dinaridic orogenic system: Correlation and evolution of tectonic units. *Swiss Journal of Geosciences*, **101(1)**:139-183.

Schmidt, E.R., 1952. Geomechanical explanations of development and structural framework of northeastern part of Transdanubian Central Range. *Bányászati és Kohászati Lapok*, **85**:31-36 (in Hungarian).

Schuller, D.J., Rao, A.R., Jeong, G.D., 2001. Fractal characteristics of dense stream networks. *Journal of Hydrology*, **243**:1-16.

Schumm, S.A., 1956. Evolution of drainage systems and slopes in Badlands at Perth Amboy, New Jersey. *Geological Society America Bulletin*, **67**:597-646.

Shahzad, F., Mahmood, S.A., Gloaguen, R., 2010. Nonlinear analysis of drainage systems to examine surface deformation: an example from Potwar Plateau (Northern Pakistan). *Nonlinear Processes in Geophysics*, **17**:137-147.

Shreve R.L., 1966. Statistical law of stream numbers. *Journal of Geology*, **74**:17-37.

Síkhegyi, F., 2002. Active structural evolution of the western and central part of the Pannonian basin: A geomorphologic approach. In: Cloetingh, S., Horváth, F., Bada, G., Lankreijer, A., (Eds.), Neotectonics and surface processes: the Pannonian basin and Alpine/Carpathian system. *European Geosciences Union, St. Mueller Special Publication Series*, **3**:203-216.

Sokoutis D., Corti G., Bonini M., Brun J. P., Cloetingh S., Mauduit T., Manetti P., 2007. Modelling the extension of heterogeneous hot lithosphere. *Tectonophysics*, **444**:63-79.

Sokoutis, D., Bonini, M., Medvedev, S., Boccaletti, M., Talbot, C.J., Koyi, H., 2000. Indentation of a continent with a built-in thickness change: experiment and nature. In: Cloetingh, S., Podladchikov, Y., Y. (Eds.), Perspectives on Tectonic Modelling, *Tectonophysics*, **320**:243-270.

Sokoutis, D., Burg, J-P., Bonini, M., Corti, G., Cloetingh, S., 2005. Lithospheric-scale structures from the perspective of analogue continental collision. *Tectonophysics*, **406**:1-15.

Sokoutis, D., Willingshofer, E., 2011. Decoupling during continental collision and intra-plate deformation. *Earth and Planetary Science Letters*, **311**:197-198.

Somogyi, S., 1961. Evolution of the Hungarian river network. *Földrajzi Közlemények*, **9**:25-50. (in Hungarian)

Sperner, B., Lorenz, F., Bonjer, K., Hettel, S., Müller, B., Wenzel, F., 2001. Slab break-off - abrupt cut or gradual detachment? New insights from the Vrancea Region (SE Carpathians, Romania). *Terra Nova*, **13**:172-179.

Sperner, B., Ratschbacher, L., Nemčok, M., 2002. Interplay between subduction retreat and lateral extrusion: tectonics of the Western Carpathians. *Tectonics*, **21**:1051.

Stephenson, R., Lambeck, K., 1985. Isostatic response of the lithosphere with in-plane stress: application to Central Australia. *Journal of Geophysical Research*, **90(B10)**:8581-8588.

Strahler, A.N, 1957. Quantitative analysis of watershed geomorphology. *American Geophysical Union Transactions*, **38**:913-920.

Strausz, L., 1949. Gravel formations in the southwestern part of Transdanubia. *Földtani Közlöny*, **79**:8-64. (in Hungarian)

Szafián, P., Horváth, F., 2006. Lithospheric structure in the Carpatho-Pannonian region: New constraints from three-dimensional gravity modelling and their geodynamic significance. *International Journal of Earth Sciences*, **95**:50-67.

Szafián, P., Tari, G., Horváth, F, Cloetingh, S., 1999. Crustal structure of the Alpine-Pannonian transition zone: a combined seismic and gravity study. *International Journal of Earth Sciences*, **88**:98-110.

Szanyi, Gy., Bada, G., Surányi, G., Leél-Őssy, Sz., Varga, Zs., 2009. Pleistocene uplift rate of the Buda Hills (Hungary), using uranium-series dating of cave rafts. *Földtani Közlöny*, **139(4)**:353-365. (in Hungarian with English abstract).

Tarapoanca, M., Bertotti, G., Matenco, L., Dinu, C., Cloetingh, S.A.P.L., 2003. Architecture of the Focsani Depression: a 13 km deep basin in the Carpathians bend zone (Romania). *Tectonics*, **22**:1074.

Tarboton, D.G, 1996. Fractal river networks, Horton's laws and Tokunaga cyclicity. *Journal of Hydrology*, **187**:105-117.

Tarboton, D.G., Bras, R.L. and Rodriguez-lturbe, I., 1990. Comment on "On the Fractal Dimension of Stream Networks" by Paolo La Barbera and Renzo Rosso. *Water Resources Research*, **26**:2243-2244.

Tari, G., 1994. *Alpine tectonics of the Pannonian Basin*. PhD thesis, Rice University, Houston TX, 501p.

Tari, G., Dövényi, P., Dunkl, I., Horváth, F., Lenkey, L., Stefanescu, M., Szafián, P., Tóth, T., 1999. Lithospheric structure of the Pannonian basin derived from seismic, gravity and geothermal data. In: Durand, B., Jolivet, L., Horváth, F., Séranne, M. (Eds.), The Mediteranean Basins: Tertiary Extension within the Alpine Orogen. *Geological Society, London, Special Publications*, **156**:215-250.

Tari, G., Horváth, F., Rumpler, J., 1992. Styles of extension in the Pannonian basin. *Tectonophysics*, **208**:203-219.

Tari, V., Pamic, J., 1998. Geodynamic evolution of the northern Dinarides and the southern part of the Pannonian Basin. *Tectonophysics*, **297**:269-281.

Tél, T., Fülöp, Á., Vicsek, T., 1989. Determination of fractal dimensions for geometrical multifractals. *Physica A*, **159**:155-166.

Telesca, L., Lapenna, V., Macchiato, M., 2004. Mono- and multifractal investigation of scaling properties in temporal patterns of seismic sequences. *Chaos, Solitons and Fractals*, **19**:1-15.

Tesauro, M., Kaban, M., Cloetingh, S., 2009. How rigid is Europe's lithosphere? *Geophysical Research Letters*, **36**: L16303.

Timár, G., 2003. Controls on channel sinuosity changes – a case study on the Tisza River, the Great Hungarian Plain. *Quaternary Science Reviews*, **22**:2199-2207.

Timár, G., Sümegi, P., Horváth, F., 2005. Late Quaternary dynamics of the Tisza River: Evidence of climatic and tectonic controls. *Tectonophysics*, **410**:97-110.

Tokunaga, E., 1978. Consideration on the composition of drainage networks and their evolution. *Geographical Reports Tokyo Metropolitan University*, **13**:1-27.

Tokunaga, E., 1984. Ordering of divide segments and law of divide segment numbers. *Japenese Geomorphological Union*, **5**:71-77.

Tomljenović, B., Csontos, L., 2001. Neogene–Quaternary structures in the border zone between Alps, Dinarides and Pannonian basin (Hrvatsko zagorje and Karlovac basin, Croatia). *International Journal of Earth Sciences*, **90**:560-578.

Tóth, L., Mónus, P., Zsíros, T. and Kiszely, M., 2002. Seismicity in the Pannonian Region – earthquake data. In: Cloetingh, S., Horváth, F., Bada, G. and Lankreijer, A., (Eds.), Neotectonics and surface processes: the Pannonian basin and Alpine/Carpathian system. *EGU Stephan Mueller Special Publication Series*, **3**:9-28.

Tóth, L., Mónus, P., Zsíros, T., Kiszely, M., Czifra, T., 2004. *Hungarian Earthquake Bulletin 2003*. GeoRisk - MTA GGKI, Budapest, 138p.

Tóth, Zs., Tóth, T., Szafián, P., Horváth, A., Hámori, Z., Dombrádi, E., Fekete, N., Spiess, V., Horváth, F., 2010. Seismic investigations of Lake Balaton. *Földtani Közlöny*, **140(4)**:355-366. (in Hungarian with English abstract)

Turcotte, D.L., 1997. *Fractals and Chaos in Geology and Geophysics*, 2nd ed., Cambridge University Press, Cambridge.

Uhrin, A., Magyar, I., Sztanó, O., 2009. Control of the Late Neogene (Pannonian s.l.) sedimentation by basement deformation in the Zala Basin. *Földtani Közlöny*, **139(3)**:273-282. (in Hungarian with English abstract)

Urbancsek, J., 1963. New possibilities of geological synthesis of Pliocene and Pleistocene sediments in geological research. *Hidrológiai Közlöny*, 43:392-400. (in Hungarian)

Urbancsek, J., 1977. Abyssal water reservoirs of the Pannonian Basin. In: Urbancsek, J. (Ed.), *Cadastres of wells in Hungary*, vol. 7, OHV Water Resources Institute, Budapest, 546p. (in Hungarian)

Ustaszewski, K., Schmid, S.M., Fügenschuh, B., Tischler, M., Kissling, E., Spakman, W., 2008. A map-view restoration of the Alpine-Carpathian-Dinaridic system for the Early Miocene. *Swiss Journal of Geosciences*, **101**, Supplement 1:S273–S294

van Gelder, I.E., 2010, *The effect of slab-pulling forces on lateral extrusion in the Eastern Alps: insights from analogue crustal scale models*. MSc thesis, Vrije Universiteit, Amsterdam, 56p.

Vasiliev, I., Krijgsman, W., Langereis, C.G., Panaiotu, C.E., Matenco, L., Bertotti, G., 2004, Magnetostratigraphic dating and astronomical forcing of the Mio-Pliocene sedimentary sequences of the Focsani basin (eastern Paratethys-Romania), *Earth and Planetary Science Letters*, **227(1-2)**:231-247.

Veltri, M., Veltri, P., Maiolo, M., 1996. On the fractal description of natural channel networks. *Journal of Hydrology*, **187**:137-144.

Vicsek, T., 1990. Mass multifractals. *Physica A*, **168**:490-497.

Vicsek, T., Family, F., Meakin, P., 1990 Multifractal geometry of diffusion-limited aggregates. *Europhysics Letters*, **12**:217-222.

Weijermars, R., Schmeling, H., 1986. Scaling of Newtonian and non-Newtonian fluid dynamics without inertia for quantitative modelling of rock flow due to gravity (including the concept of rheological similarity. *Physics of the Earth and Planetary Interiors*, **43**:316-330.

Wenzel, F., Achauer, U., Enescu, D., Kissling, E., Russo, R., Mocanu, V., Musacchio, G., 1998. Detailed look at final stage of plate break-off is target study in Romania. *EOS, AGU Transactions*, **79(48)**:592-594.

Wenzel, F., Sperner, B., Lorenz, F., Mocanu, V., 2002. Geodynamics, tomographic images and seismicity of the Vrancea region (SE-Carpathians, Romania). In: Cloetingh, S.A.P.L., Horváth, F., Bada, G., Lankreijer, A.C. (Eds) Neotectonics and Surface processes: the Pannonian basin and the Alpine/Carpathian system. *European Geosciences Union, Stephan Mueller Special Publiaction Series*, **3**:95-104.

Wickham, J., 2007. Comment on "Basin inversion and fault reactivation in laboratory experiments". *Journal of Structural Geology*, **29**:1414-1416.

Willingshofer, E., Cloetingh, S., 2003. Present-day lithospheric strength of the Eastern Alps and its relationship to neotectonics. *Tectonics*, **22**:1075, doi:10.1029/ 2002TC001463.

Willingshofer, E., Sokoutis, D., 2009. Decoupling along plate boundaries: Key variable controlling the mode of deformation and the geometry of collisional mountain belts. *Geology*, **37**:39-42.

Willingshofer, E., Sokoutis, D., Burg, J.-P., 2005. Lithospheric-scale analogue modelling of collision zones with a pre-existing weak zone. In: Gapais, D., Brun, J.P., Cobbold, P.R. (Eds.), Deformation Mechanisms, Rheology and Tectonics: from Minerals to the Lithosphere, *Geological Society, London, Special Publications*, **243**:277-294.

Windhoffer, G., Bada, G., 2005. Analogue modelling of the formation and deformation of the Derecske trough. *Acta Geologica Hungarica*, **48**:351-369.

Windhoffer, G., Bada, G., Nieuwland, D., Wórum, G., Horváth, F., Cloetingh, S., 2005. On the mechanics of basin formation in the Pannonian basin: inferences from analogue and numerical modelling. *Tectonophysics*, **410**:389-415.

Wortel, M.J.R., Spakman, W., 2000. Subduction and slab detachment in the Mediterranean-Carpathian region. *Science*, **209**:1910-1917.

Wórum, G., Hámori, Z., 2004. *Reprocessing of vintage seismic sections of MOL relevant for BAF research programme*. Manuscript, Mecsekérc Ltd., Pécs, 39p. (in Hungarian)

Wórum, G., Horváth, F., 2005. *3D geological-hydrogeological model for the vicinity of Paks Nuclear Power Plant*. Manuscript, Paks NPP archive, Paks, 65p. (in Hungarian)

Ziegler, P.A., Bertotti, G., Cloetingh, S., 2002. Dynamic processes controlling foreland development — the role of mechanical (de)coupling of orogenic wedges and forelands. In: Bertotti, G., Schulmann, K., Cloetingh, S. (Eds.), Continental Collision and the Tectono-Sedimentary Evolution of Forelands. *EGU St. Mueller Special Publication Series*, **vol. 1**:17-56.

Ziegler, P.A., Cloetingh, S., van Wees, J.D., 1995. Dynamics of intraplate compressional deformation: the Alpine foreland and other examples. *Tectonophysics*, **252**:7-59.